Terms and Conditions of Use of Digitised Theses from Trinity College Library Dublin

Copyright statement

All material supplied by Trinity College Library is protected by copyright (under the Copyright and Related Rights Act, 2000 as amended) and other relevant Intellectual Property Rights. By accessing and using a Digitised Thesis from Trinity College Library you acknowledge that all Intellectual Property Rights in any Works supplied are the sole and exclusive property of the copyright and/or other IPR holder. Specific copyright holders may not be explicitly identified. Use of materials from other sources within a thesis should not be construed as a claim over them.

A non-exclusive, non-transferable licence is hereby granted to those using or reproducing, in whole or in part, the material for valid purposes, providing the copyright owners are acknowledged using the normal conventions. Where specific permission to use material is required, this is identified and such permission must be sought from the copyright holder or agency cited.

Liability statement

By using a Digitised Thesis, I accept that Trinity College Dublin bears no legal responsibility for the accuracy, legality or comprehensiveness of materials contained within the thesis, and that Trinity College Dublin accepts no liability for indirect, consequential, or incidental, damages or losses arising from use of the thesis for whatever reason. Information located in a thesis may be subject to specific use constraints, details of which may not be explicitly described. It is the responsibility of potential and actual users to be aware of such constraints and to abide by them. By making use of material from a digitised thesis, you accept these copyright and disclaimer provisions. Where it is brought to the attention of Trinity College Library that there may be a breach of copyright or other restraint, it is the policy to withdraw or take down access to a thesis while the issue is being resolved.

Access Agreement

By using a Digitised Thesis from Trinity College Library you are bound by the following Terms & Conditions. Please read them carefully.

I have read and I understand the following statement: All material supplied via a Digitised Thesis from Trinity College Library is protected by copyright and other intellectual property rights, and duplication or sale of all or part of any of a thesis is not permitted, except that material may be duplicated by you for your research use or for educational purposes in electronic or print form providing the copyright owners are acknowledged using the normal conventions. You must obtain permission for any other use. Electronic or print copies may not be offered, whether for sale or otherwise to anyone. This copy has been supplied on the understanding that it is copyright material and that no quotation from the thesis may be published without proper acknowledgement.

The glycosylphosphatidylinositol - phospholipase C (GPI-PLC) in bloodstream forms of *Trypanosoma brucei*

Being a thesis submitted by Orla Hanrahan B.A. (Mod.) in fulfilment of a Ph.D.

School of Biochemistry and Immunology

Trinity College Dublin

2007

Dedicated to my family for all their support and encouragement through the years.

DECLARATION

This thesis has not been submitted as an exercise for a degree at any other university. Except where stated, the work described therein was carried out by me alone.

I give permission for the Library to lend or copy this thesis upon request.

Signed: Orla Hanrahan

Declaration

I certify that none of the work described in this thesis has been submitted for any degree or diploma at this or any other university and that all of the work reported in this thesis is entirely my own. I also grant powers of discretion to the library to allow this thesis to be copied in whole or in part.

Orla Hanrahan

Orla Hanrahan

The glycosylphosphatidylinositol-phopholipase C in bloodstream forms of *Trypanosoma brucei*

Summary

The localization of the GPI-PLC in bloodstream form trypanosomes was investigated using confocal microscopy and surface labelling techniques, namely biotinylation and iodination. The confocal data indicate that the GPI-PLC is exclusively located on the flagellar membrane rather than the pelicular membrane of the cell body or the flagellar pocket membrane. This location places the GPI-PLC and the VSG on the same side of the plasma membrane bilayer covering the flagellum, thereby indicating that both enzyme and substrate reside in close proximity making the cleavage reaction of the GPI-PLC on the GPI anchor a much more feasible process than previously thought. The GPI-PLC did not co-localize with the para-flagellar rod, a large structure found within the flagellum of bloodstream form trypanosomes. The GPI-PLC was found to lie closer to the cell body than the para-flagellar rod. In addition, the GPI-PLC was found not to lie in the same compartment as the flagellar attachment zone (FAZ). When the GPI-PLC was activated to release the VSG from the surface of *T. brucei* by incubating trypanosomes with 2-deoxyglucose (10 mM) the GPI-PLC remained associated with the flagellar membrane. Consequently, for VSG release to occur the VSG must have diffused within the plane of the membrane to the position of the GPI-PLC; and the GPI-PLC did not move to the position of each molecule of VSG in turn. Surface labelling of trypanosomes with Iodine-125 revealed that the GPI-PLC is at least partially exposed to the outer surface of bloodstream form trypanosomes. Surface biotinylation assays failed to detect the GPI-PLC on the surface of bloodstream forms of *T. brucei*. Further studies on the biotinylation technique revealed that the GPI-PLC was unable to react with the sulfo-NHS-biotin. The amino acid sequence of the GPI-PLC was then analysed by mass spectrometry to determine whether any of the lysine residues were modified. This analysis suggested that a minimum of 67 % of the lysine residues in the recombinant GPI-PLC are not modified and hence one would expect these to be reactive unless they are folded into the hydrophobic core of the protein or exist as salt bridges.

The GPI-PLC was found not to be involved in the disaggregation of trypanosomes or the cycle of endocytosis and exocytosis of either transferrin or

surface immune complexes. The sulfydryl blocking reagent, iodoacetamide, inhibited the process of disaggregation completely. Consequently, this result implies that an essential thiol group is involved in the disaggregation of bloodstream form trypanosomes. The specific location of this thiol group is as yet unknown but from the preliminary results presented here it is on the cell and not on the immunoglobulin that is binding the two cells together.

Acknowledgements

I am totally indebted to my supervisor Dr. H. P Voorheis, who has been such a great help to me throughout this whole project. I am grateful for his constant advice, encouragement, patience and ideas throughout this project. He motivated me and made me persist when I was ready to give up. I would also like to thank Dr. Derek Nolan for his help and advice and for the occasional story of past happenings in the department (a great story teller)! Thanks are extended to Dr. Mark Carrington and Dr. Helena Webb for supplying the GPI-PLC $^{-}$ mutant trypanosomes and the supply of anti-GPI-PLC antibody when I ran out. In addition, I would like to thank Kyran in stores and Brian in the prep room for giving me all the chemicals I needed when I needed them (enjoyed the banter with both of you). I would also like to thank everyone in the animal house.

I owe a huge thanks to all the people I have had the pleasure to work with throughout my project. Thanks to Elaine Brabazon for her help in introducing me to the world of Biochemistry in Lab 1.3, I would have been lost without you. To Uns (wiggy) and Mary-Jo who I started my project with in the lab. We used to have such a laugh and I really did miss our "girly chats" when you both left. I only had Conor to talk girly stuff to and I don't think he really appreciated that! We used to have great sessions in Mahaffeys (in the early days with the Biochem Soc), then the Pav in the Summer months followed by O'Neills when we matured slightly!! I will never forget the first time we had to "do the rats", poor Uns nearly passed out!! We always had the radio on (which we know used to drive some people up the wall) and we would all sing thinking we were the best singers ever!! Conor tried to keep me sane when the girls left and he did an OK job of it (at least I think I am not mad!!). I learnt to appreciate a different type of music with Conor in the lab, from Classical to heavy metal.... I can't say I loved all of it, but I did put up with it! "Oh my God" "Saponin", a couple of phrases that used to crack Conor up!!! What me with my DORT accent from SWARDS!!! Conor has been my coffee buddy recently and we have enjoyed plenty of Cappucinos discussing the wonders of Science and the ever-changing colours of the leaves on the trees!!

I would like to thank Katherine for rescuing Conor from becoming my agony aunt when the "girls" left. I miss your visits especially now that you are in New Zealand. Thanks also to Noirin and Diana for listening to my moans and helping me out with the techniques I didn't have a clue of!

A huge thanks go to Tommy. Your mind is so full of wisdom and knowledge; I would have been lost without all of your help and advice throughout the project. I enjoyed our trips to 'Little Italy' where the pesto pasta was only delicious.... I will keep getting my coffee there and maybe one day I will take your advice and go to the country itself!! I will try and learn the language first though!!

A special thanks to Pearl and Cos (the 'Greek God' or so he thinks anyway!!!! joke...) from the O'Neill lab who kept me sane and whom I enjoyed many a drinky with!! I am dying to visit LA and get a ride in your 'Thunderbird' Pearl. The builders have been looking for their 'Maureen O' Hara' .....they are missing you loads!

Finally, I want to express my gratitude to my family, Ted, Judy, Lisa and Elaine. You have all been a great support and thanks for having such a great interest in my work. Thanks to all of you for listening to my tails of woe and uplifting my spirits when I was down in the dumps. I am looking forward to having lots of nights out with my two best friends, Lisa and Elaine and lots of quality time with Mum and Dad. I will have a lot more time on my hands now and I won't be saying "I will do that when I am finished". Thank you all so much.

Abbreviations

DEAE-52: Diethylaminoethyl cellulose

DMSO: Dimetylsulphoxide

DTT: Dithioreitol

EDTA: Ethylene-diamine-tetra-acetic acid

FITC: Fluorescein isothiocyanate

GPI-PLC: Glycosylphosphatidyl inositol phospholipase C

IgG: Immunoglobulin G

IgM: Immunoglobulin M

MBP: Maltose binding protein

MBP-TbGPI-PLC: Maltose binding protein fused with GPI-PLC from T. brucei

Nog: N-octylglucoside detergent

PBS: Phosphate buffered saline

PAGE: Polyacrylamide gel electrophoresis

PMSF: Phenylmethylsulfonyl fluoride

MfVSG: membrane bound VSG

sVSG: Soluble or released form of the VSG

SDS: Sodium Dodecyl sulphate

TEMED: (N,N,N',N')-Tetra-methyl-ethylene-diamine

TBST: Tris buffered saline containing Tween

TES: **2**-{[2-hydroxy-1,1-bis(hydroxymethyl)ethyl]amino}ethanesulphonic acid

TLCK: Tosyl-lysine-chloromethyl-ketone

Tris: 2-amino-2-hydroxymethylpropane-1,3-diol

V/V: Volume per volume

VSG: Variant Surface Glycoprotein

W/V: Weight per volume

Table of Contents

Chapter 1

Introduction

1.1 Introduction to Trypanosomes

Trypanosomes are eukaryotic, flagellated, digenetic parasitic protozoons. The family Trypanosomatidae consists of a large variety of genera that infect birds, mammals, fish, insects and plants. The African trypanosomes of the brucei subgroup are transmitted from host to host by the tsetse fly (Glossina species) in which they undergo cyclical development. The mammalian trypanosomes have been classified and divided by Hoare (1972) into seven subgenera, which are grouped into two sections, the sterocoria and salivaria, based on the site of production of infective metacyclic trypanosomes in the invertebrate host. The sterocoraria are those in which the developmental cycle in the insect vector is completed in the hind-gut; metacyclic form trypanosomes are present in the faeces and transmission is indirect by contamination of the wound formed by the bite of the insect. The salivarian trypanosomes are those in which the developmental cycle in the tsetse fly vector is completed in the mouthparts or salivary glands so that metacyclic trypanomastigotes are transmitted directly by inoculation during a blood meal.

The parasites of medical importance all belong to the genera *Leishmania* and *Trypanosoma* of which *Trypanosoma brucei* is a member. There are three distinct subspecies of *T. brucei* that are virtually identical biochemically and morphologically but differ in their host range and virulence. *T. brucei rhodesiense* and *T. brucei gambiense* cause acute and chronic forms of African sleeping sickness respectively. The subspecies *T. brucei brucei* used in this study is not pathogenic to man and can easily be cultivated in laboratory animals such as mice, rats and rabbits and hence, has been extensively studied due to the ease and safety of its maintenance in the laboratory. Figure 1.1 shows the taxonomic position of *T. brucei brucei* in the Family Trypanosomitidae.

1.1.2 Discovery of trypanosomes and *T. brucei brucei*

The discovery of the first bloodstream form trypanosomes was attributed to Valentine of Berne (1841) who saw free-swimming parasites in the blood of a trout, *Salmo fario*. However, it is more likely these parasites are from the Genus, Trypanoplasma, judging by the morphology of the organisms drawn by Valentine Brumpt, 1906. During 1842 and 1843, trypanosomes were seen in the blood of a pike (Remak, 1842) and there also appeared papers by Gluge of Brussels, Mayer of Bonn and Gruby of Paris, who saw trypanosomes in frogs. It was for these frog parasites that Gruby introduced the name *Trypanosoma* from *trupanon* meaning "borer" and soma meaning "body". Our knowledge

of trypanosomes was greatly enriched by Lewis in 1878 who studied the parasites in the blood of rats in India, which was followed by the description by Evans in 1880 of trypanosomes in horses and cattle again in India. Both of these men gave their names to species of trypanosomes (*Trypanosoma lewisi* and *Trypanosoma evansi* respectively).

In 1893, Smith and Kilborne demonstrated for the first time that disease causing protozoan parasites could be transmitted *via* arthropod vectors. The following year Major David Bruce was appointed by the British Army Medical Service to Zululand to investigate outbreaks of Nagana, a fatal disease of unknown aetiology that was affecting local cattle. After his arrival in Ubombo, Bruce began examining the blood of infected cattle microscopically and found in films stained with Carbol-fuchsin 'a curiously-shaped object', while in fresh blood preparations he saw actively motile bodies. After consulting the literature, he recognised these organisms as trypanosomes, which he likened to *Trypanosoma evansi* and which were later ascribed the name *Trypanosoma brucei brucei.* The relation of these parasites to Nagana was then demonstrated by inoculating the blood of infected bovines into horses and dogs, which developed the disease in acute form. Following this, the role of insects in the transmission of the infection was demonstrated experimentally by allowing "wild" tsetse-flies to feed on healthy animals. Thus, Bruce had discovered that the causative agent of Nagana was a blood parasite transmitted *via* a blood sucking arthropod. Indeed by demonstrating the intricate connection between trypanosomes, the tsetse fly and disease, a whole new era on trypanosome research began. Subsequently, Bruce sent a dog infected with the Nagana trypanosome to England. In London, Kanthak *et al.*, (1898) showed that the parasite gave rise to acute, heavy and uniformly fatal infections in laboratory animals, including rabbits, mice and rats. However, it was not until 1909 that Kleine observed transmission of the disease to healthy animals by *Glossina fuscipes* (which had fed on mammals infected with trypanosomes) after a non-infectious prepatent period of 18-20 days. This research substantiated that trypanosomes underwent a definite cycle of development in the insect vector before they again became infective. In total, these observations laid the foundation for all subsequent studies on the life cycle and metabolism of the tsetse-borne trypanosomes.

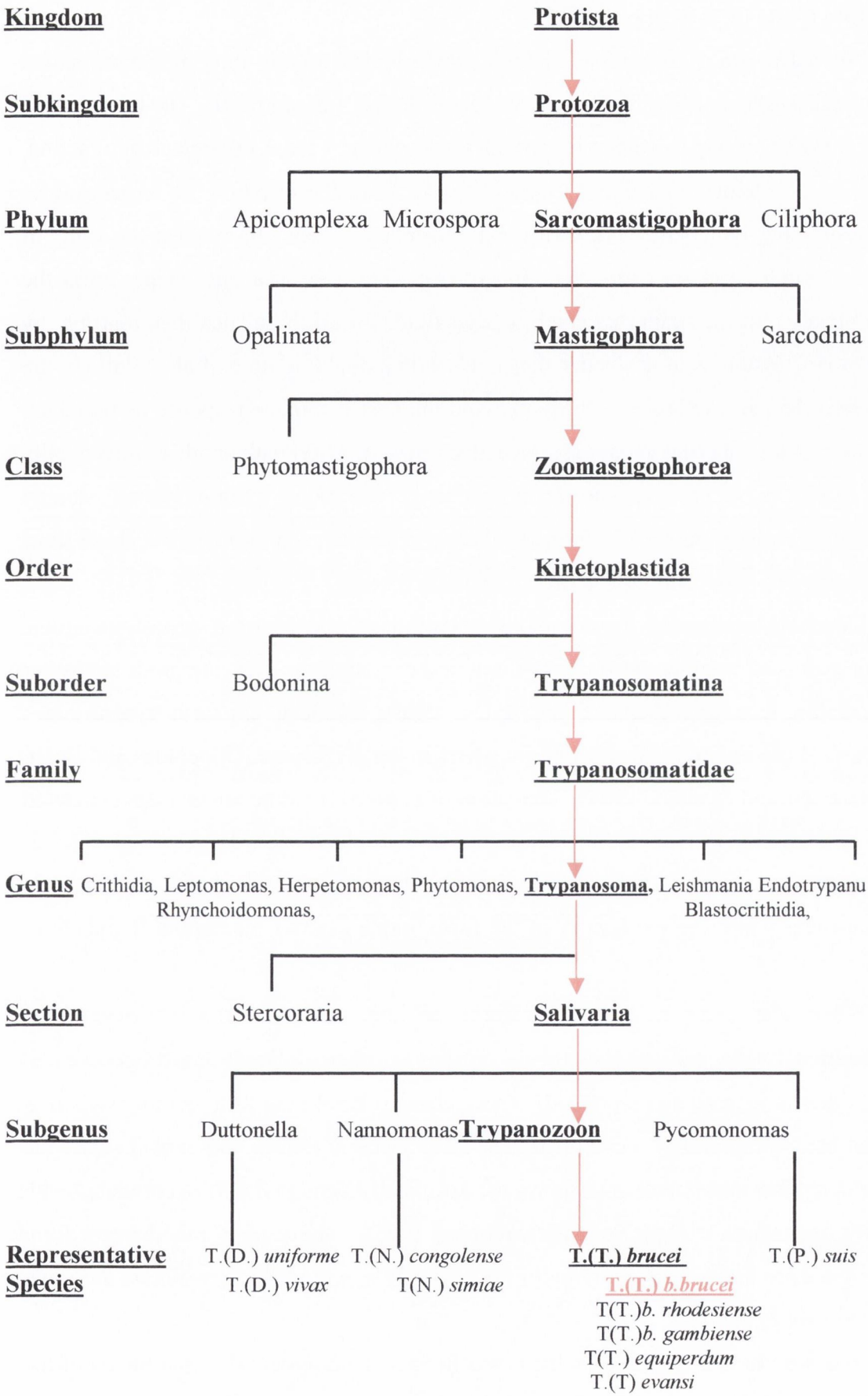

Fig 1.1. The current taxonomic position of *T. brucei brucei* in the Kingdom Protista. The classification of *T. brucei brucei* is shown in red. Adapted from Molyneux & Ashford (1983).

1.1.3 Life Cycle of *T. brucei*

The Salivarian trypanosomes, as their name implies, usually enter their mammalian host in the discharged saliva of their insect vector during a blood meal. The biting tsetse deposits metacyclic trypanosomes in dermal tissue where a local inflammatory reaction, the 'chancre', develops (Barry and Emergy, 1984). From the chancre, the trypanosomes enter the draining lymphatics and then the bloodstream. They can traverse the walls of blood and lymph capillaries into the connective tissues and, at a later stage, cross the choroid plexus into the brain and cerebrospinal fluid. In all these sites they multiply by asexual binary fission as long slender flagellates with a doubling time of 6h. While in the bloodstream the parasite has the ability to avoid the host's immune response by replacing its surface protein coat (the variable surface glycoprotein, VSG) with another antigenically distinct VSG, in a process known as antigenic variation. Non-dividing, stumpy trypanosomes replace the slender forms as the parasitaemia goes into decline; these short stumpy forms can only continue the life cycle in the vector.

Slender bloodstream trypanosomes obtain their energy from glycolysis alone, consuming glucose from the host's body fluids and excreting the pyruvate produced rather than oxidizing it in the mitochondrion (Ryley, 1956). Bloodstream form trypanosomes house most of the enzymes involved in glycolysis in the glycosome (Opperdoes and Borst, 1977; Hannaert and Michels, 1994). Oxidation of reduced pyridine nucleotides generated in the glycosome is *via* a linked glycerol-3-phosphate dehydrogenase-glycerol-3-phosphate-oxidase system (Opperdoes and Borst, 1977). The dehydrogenase is located in the glycosome, while the oxidase is in the inner mitochondrial membrane (Opperdoes, 1985).

When the slender forms transform to the stumpy forms, however, the mitochondrion swells and develops tubular cristae as α-ketoglutarate dehydrogenase and succinate dehydrogenase are expressed. These changes herald the forth coming switch to an amino acid-based energy metabolism that takes place in the fly and explains why the ability of a trypanosome stock to be transmitted cyclically through the fly is correlated with its ability to produce stumpy forms (Vickerman, 1965). The stumpy bloodstream form trypanosomes are capable of surviving in the tsetse fly's gut, where they initiate the cycle of development in the fly.

Infected blood is ingested by the tsetse fly into the crop and then the lumen of the midgut where the stumpy trypanosomes transform into the so-called procyclic stage; slender bloodstream forms either die or change into stumpy forms in the anterior midgut.

Transformation to procyclic trypomastigote takes place in the posterior part of the midgut in the endoperitrophic space. Morphological transformation is accompanied by an increase in body length, including noticeable elongation of the post-kinetoplastic proportion of the body as the simple mitochondrion expands into a branched network with discoid rather than tubular cristae. The coat of variable antigen is progressively lost (Vickerman, 1969) during transformation to the procyclic form but is replaced by a predominant set of proline-rich surface glycoproteins, the procyclins (Roditi *et al.*, 1987; Richardson *et al.*, 1988). These changes occur over a 16 h period in the tsetse gut and are accompanied by active division of the flagellates. In the next 7 days the ectoperitrophic space becomes crowded with dividing trypanosomes. The parasites then migrate to the proventriculus, increase in length, cease to divide and a decrease in mitochondrial volume occurs. Migration to the fly's salivary gland is across the walls of the midgut and gland *via* the haemocoel, as the haemolymph contains trypanocidal factors.

The salivary gland population contains four different developmental stages in the life cycle. The main proliferative stage is the epimastigote, which is attached by the flagellum to the microvilli of the epithelial cells lining the gland lumen, by use of dendritic outgrowths of the flagellum creating elaborate junctional complexes. These attached epimastigote stages differentiate, through two intermediate stages, the premetacyclic and nascent metacyclic stages, into the non-multiplicative metacyclic trypanomastigote, acquiring a VSG coat that pre-adapts them for life in the mammalian host, and are liberated into the fly's saliva to be discharged during feeding, thus completing the life cycle of *T. brucei* (see Fig 1.2).

A characteristic feature of all trypanosomes is the possession of a kinetoplast (Alexeieff, 1917). The kinetoplast is situated at the base of the flagellum and is conserved throughout the life cycle of the parasite. It consists of a mass of mitochondrial DNA, unusual because it is composed of a single network of interlocked circular molecules of two class sizes. The maxi circles (Kleisen *et al.*, 1976) with a contour length of 22μm in *T. brucei* are present as 25-50 copies per network and the mini circles (Kleisen and Borst, 1975) with a contour length of 1μm in *T. brucei* are present as 5000-10,000 copies. Maxi circle DNA contains genetic information analogous to that of other mitochondrial DNAs and maxi circle gene products seem to be necessary for activation of the mitochondrion.

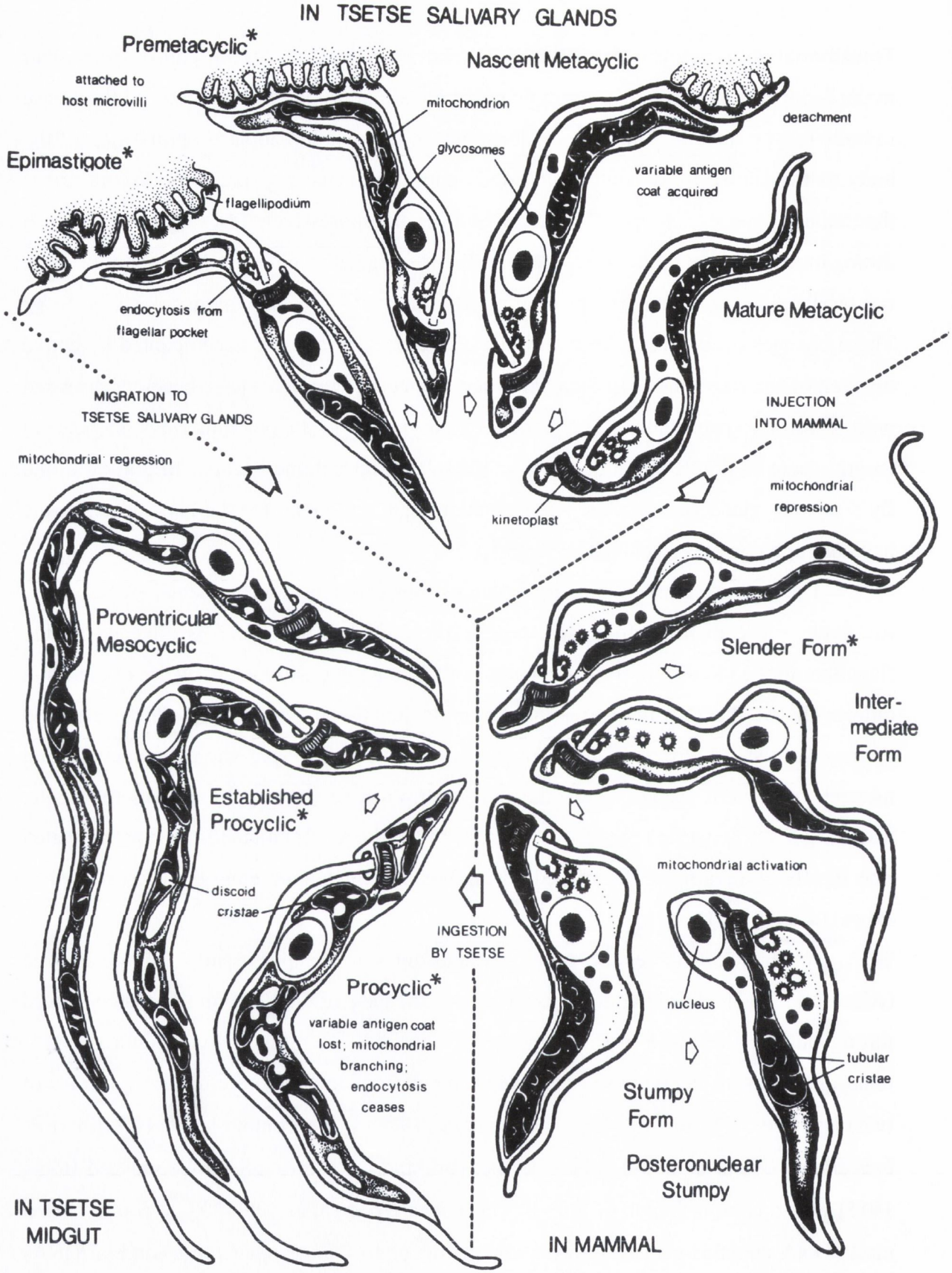

Fig.1.2. Life cycle of *Trypansoma brucei brucei* (reproduced from Vickerman 1985).

Hence a role for the kinetoplast in mitochondrial changes during the initial development of procyclic trypanomastigotes in the insect vector would seem plausible. Mini circles are heterogenous in sequence and evolve exceedingly rapidly. It has been postulated that the role of mini circles was merely to hold the maxi circles together in a network however, it has become apparent in recent years that mini circles can be transcribed into small RNA molecules (guide RNAs) that serve as templates for editing transcripts of maxi circle genes (Benne *et al.*, 1986; Simpson *et al.*, 1989). In one of the most extreme examples, synthesis of the mature 969 nucleotide cytochrome oxidase III mRNA of *T. brucei* requires the addition of 547 and the deletion of 41 uridine residues (Abraham *et al.*, 1988). Thus, RNA editing and the kinetoplast itself may play a pivotal role in the developmental cycle of the trypanosome.

1.1.4 Sleeping Sickness – A Brief Synopsis

Human African trypanosomiasis (sleeping sickness) occurs in 36 sub-Saharan countries, within the area of distribution of the tsetse fly. Recent estimates indicate that over 60 million people living in some 250 foci are at risk of contracting the disease, and there are about 300,000 new cases each year (WHO, 1998). However, less than 4 million people are under surveillance and only about 40,000 are diagnosed and treated, due to the difficulty of diagnosis and remoteness of some affected areas. These figures are relatively small compared to other tropical diseases, but African trypanosomiasis, without intervention, has the propensity to develop into epidemics, making it a major public health problem.

The disease occurs in two forms: a chronic one caused by *Trypanosoma brucei gambiense*, which occurs in west and central Africa; and an acute form, caused by *T. b. rhodesiense*, which occurs in eastern and southern Africa. The chronic infection lasts for years, whilst the acute disease may last only for weeks before death occurs, if treatment is not administered. The early phase entails bouts of fever, headaches, pains in the joints and itching. The second, known as the neurological phase, begins when the parasite crosses the blood-brain barrier and infests the central nervous system. This is when the characteristic signs and symptoms of the disease appear: confusion, sensory disturbances and poor coordination. Disturbance of the sleep cycle, which gives the disease its name, is the most important feature. Without treatment, the disease is fatal. If the patient does not

receive treatment before the onset of the second phase, neurological damage is irreversible even after treatment.

The current treatment of human African trypanosomiasis is based on four main drugs, namely suramin, pentamidine, melarsoprol, and eflornithine (difluoromethylornithine, or DFMO), with nifurtimox undergoing evaluation. It should be noted that most of these drugs were developed in the first half of the twentieth century and some of them would probably not pass current high safety standards (Fairlamb, 1990). Early-stage disease is treated with i.v. suramin in rhodesiense disease and with intramuscular (i.m.) pentamidine in gambiense disease according to established protocols. Treatment is effective and prevents disease progression. The trivalent organic arsenical melarsoprol (discovered in 1949) is the only effective drug for late-stage disease in both forms of human African trypanosomiasis, as the drug crosses the blood-brain barrier (Legros *et al.*, 2002). The undesired effects are drastic; they include reactive encephalopathy, often fatal, in 3 % to 10 % of cases; those who survive the encephalopathy suffer serious neurological sequelae. Futhermore, there is considerable resistance to the drug, rising to 30 % in parts of central Africa (WHO, 2001).

The unacceptable toxicity of the currently available drugs for human African sleeping sickness underpins the urgency of developing more effective and safer drug regimes. A safe drug that is effective in the treatment of the second phase of the disease would dramatically change the control and management of sleeping sickness. However, in reality no new drugs are likely to appear within the next five years, and even that may be overly optimistic.

1.1.5 Nagana

Nagana (derived from a Zulu term meaning "to be in low or depressed spirits"), also called Animal African Trypanosomiasis, is a disease of vertebrate animals caused by *T. brucei brucei* and particularly by *T. congolense.* It has a wide geographical distribution throughout tropical Africa wherever tsetse-flies are present. This disease affects all domestic mammals; cattle, sheep, goats, horses, donkeys, pigs, dogs and cats. The trypanosomes infect the blood of the vertebrate host, resulting in subacute, acute, or chronic disease characterized by intermittent fever, anaemia, occasional diarrhoea, and rapid loss of condition and often terminates in death. The marked immunosuppression, resulting from the trypanosomal infection, lowers the host's resistance to other infections

and causes secondary disease, which greatly complicates both the clinical and pathological features of trypanosomiasis.

1.2 The variable surface glycoprotein (VSG)

The bloodstream forms of *Trypanosoma brucei*, in common with the other African trypanosomes, express a smooth and compact surface coat composed of about 10 million copies of a variant surface glycoprotein (VSG). This VSG coat is 12-15nm thick and covers the entire surface membrane of the body and the flagellum (Vickerman, 1969)(Fig 1.3). Each VSG dimer is separated from an adjacent dimer by a mean distance of about 40Å (Cross, 1975, Auffret, 1981, Freymann, 1984, Jackson, 1985). The VSG coat acts as a macromolecular diffusion barrier that prevents the approach of macromolecules, such as the components of the alternative complement pathway, to the plasma membrane while allowing the free diffusion of small nutrient molecules to underlying transmembrane transporter systems.

Each VSG monomer has a molecular weight of 45-55 kDa and is 400 – 500 amino acids long (Carrington *et al.*, 1991). VSGs are dimeric molecules approximately 100 Å long (Auffret and Turner, 1981, Strickler, 1982) and are anchored in the plasma membrane by a glycosylphosphatidyl inositol (GPI) moiety linked *via* an ethanolamine to the mature C terminus of the protein (Holder, 1983, Ferguson, 1984, Ferguson, 1985, Jackson, 1985). It is assumed that the dimerization of the native VSG is by interactions with the N-terminal domain of the monomers. The N-terminal domain is a rod-shaped hairpin structure that exposes a few variable loops on the surface of the parasite, containing the only epitopes recognised by the host. The N-terminal domain of the VSGs represent about 75 % of the mature polypeptide sequences and show little primary sequence homology (Carrington *et al.*, 1991). The N-terminal domain is elongated and constitutes 60 – 84% of the total length of the protein sequence. It is composed of seven α- helices, which make up about 47% of the structure. Two major α-helices, each of ~ 70 Å, form a coiled coil that acts as a scaffold for the remaining smaller helices and loops.

Fig 1.3. Model of the complete VSG MITat1.2 dimer.

The two N-terminal domains are shown in *green* and *pink* and the two C-terminal domains in *blue*. The *dashed white line* in one of the monomers represents the 15-residue protease-sensitive linker between the two domains. There are an additional 16 residues containing an *N*-linked glycosylation site between the C terminus of the model and the ethanolamine of the glycosylphosphatidylinositol anchor. Adapted from (Chattopadhyay *et al.*, 2005)

Fig 1.3. Model of the complete VSG MITat1.2 dimer.

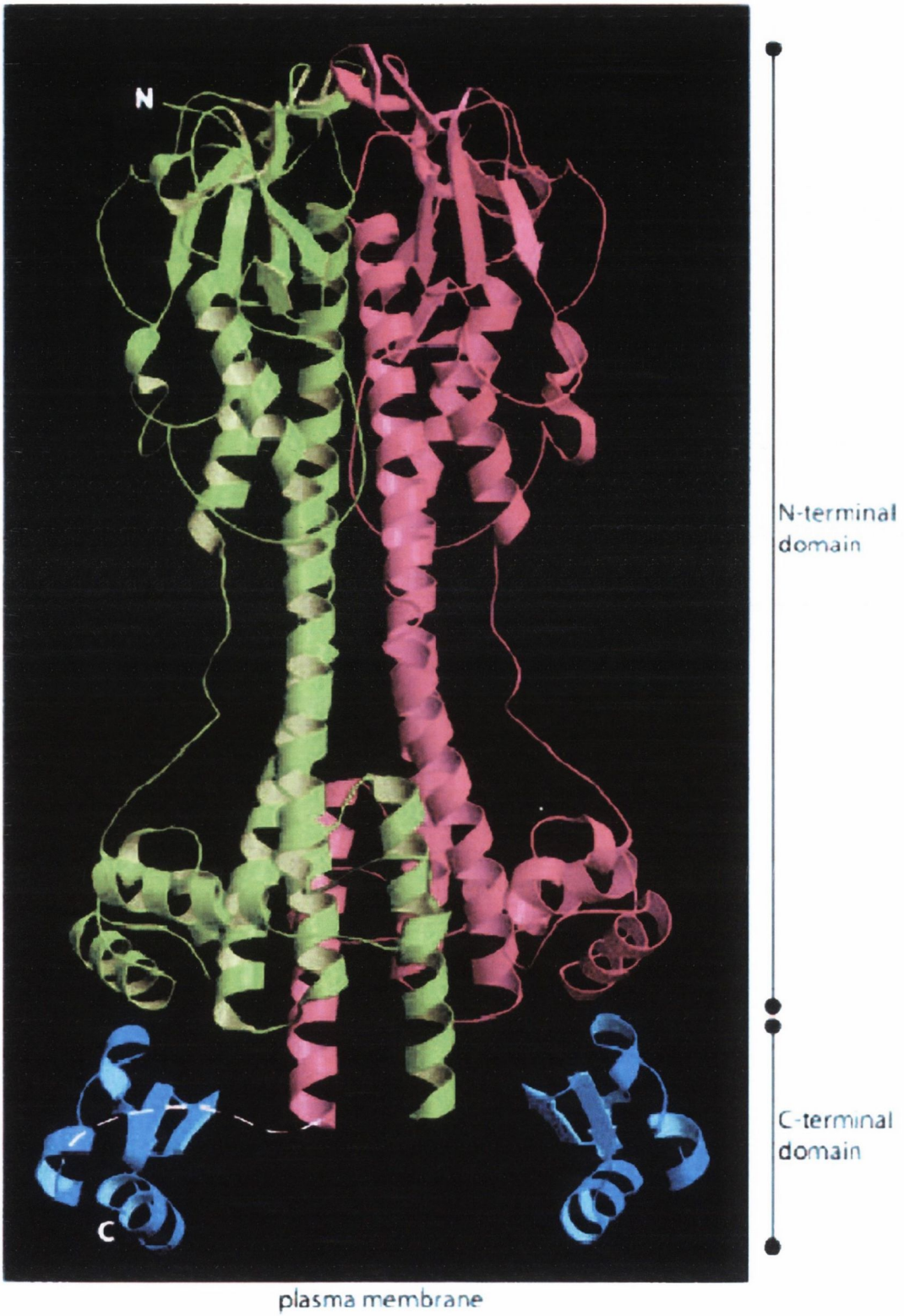

The tertiary structures of the N-terminal domains for two different VSGs (MITat 1.2 & ILTat 1.24) have been solved and are 60 % identical despite only 16 % sequence identity. This striking conservation of tertiary structure is believed to be necessary for the protective function of the VSG although this assertion has yet to be proven. (Freymann *et al.*, 1984, Blum, 1993). The elongated form of this domain, as well as the tight interactions between adjacent antigens appears to be important to protect the parasite membrane against lytic components in the blood.

The solution structure of the C — terminal domain of VSG MITat 1.2 was completed in 2005 thereby presenting the first structure of both domains of a VSG (Chattopadhyay *et al.*, 2005). The isolated C — terminal domain is a monomer in dilute solution (Chattopadhyay *et al.*, 2005) and forms a compact fold of 42 residues. The core of this domain is composed of two disulphide bonds and two conserved hydrophobic residues. These disulphide bonds are required to form its structure because in the absence of either pair of cysteines the structure does not fold correctly (Chattopadhyay *et al.*, 2005). The C — terminal domain is attached to the plasma membrane by a GPI — anchor and is linked to the N — terminal domain through a hinge region that is sensitive to proteolytic cleavage. The C — terminal domains from *T. brucei* like VSGs are related to one another but can be split into four types based on sequence homology (Carrington *et al.*, 1991). The C — terminal domain from MITat 1.2 VSG is a type 2 domain and these are characterised by four conserved cysteine residues. There is little sequence conservation between different type 2 C — terminal domains other than the cysteines, a conserved hydrophobic residue after the third cysteine and an N — linked glycosylation site very close to the C terminus (Chattopadhyay *et al.*, 2005). However, as is the case with the VSG N — terminal domain, the tertiary structure is conserved among different type 2 VSG C — terminal domains despite the sequence variation. The C — terminal domain of the VSG contributes to a region densely packed with polypeptide adjacent to the plasma membrane.

1.3 The GPI anchor of the VSG

The VSG is linked to the cell surface by a glycosyl phosphatidylinositol (GPI) anchor (Fig 1.4 & 1.5). The term GPI was introduced in 1985 for the membrane anchor of the VSG of *T. brucei* in order to facilitate a description of its biosynthesis in *T. brucei* (Ferguson *et al.*, 1985). The complete structure of the GPI anchor of a VSG in *T. brucei* was reported in 1988 (Ferguson *et al.*, 1988).

Biosynthesis of the GPI moiety of the VSG is a stepwise process: sugars and phosphoethanolamine are sequentially added to phosphatidylinositol. The complete GPI precursor, known as glycolipid A is then linked to the nascent VSG in a transamidase reaction (Masterson, 1990). The main difference in the GPI biosynthetic pathway between *T. brucei* and its mammalian host is that trypanosomes replace each of the two glyceryl fatty acids of the GPI with myristate, a 14-carbon saturated fatty acid. Following the fatty acid remodelling reactions where myristate is added, there are a number of myristate exchange reactions which serve as a proofreading mechanism to ensure that myristate is the only fatty acid in the VSG GPI anchor (Buxbaum, 1994, Buxbaum, 1996).

The conversion of the membrane bound form of the VSG (mfVSG) to the soluble form (sVSG), observed during lysis of trypanosomes, is accompanied by the removal of sn-1,2-dimyristylglycerol (Ferguson and Cross, 1984). This conversion is brought about by the action of the GPI specific phospholipase C on the GPI anchor of the VSG (Ferguson *et al.*, 1985). The difference between the mfVSG and the sVSG lies in the C — terminal domain. This domain in sVSGs contains an immunogenic oligosaccharide known as the cross-reacting determinant (CRD), attached to the C — terminal amino acid (Holder and Cross, 1981). This cross-reacting determinant is exposed only after conversion of the amphiphilic mfVSG to sVSG (Cardoso de Almeida and Turner, 1983).

It has been shown experimentally that GPI is essential for the growth of bloodstream forms of *T. brucei* (Nagamune *et al.*, 2000). Furthermore, procyclic form cells lacking the surface coat proteins because of disruption of TbGPI10 (trypanosomal gene involved in the biosynthesis of GPI) were less competent for establishment of infection in the tsetse fly midgut demonstrating the importance of GPI anchors in trypanosomes.

1.4 Antigenic Variation

The molecular mechanisms used by African trypanosomes to evade the immune system of their mammalian hosts have been an object of interest for most of the century. As early as 1907, the Italian scientist, A. Massaglia, concluded that African trypanosomes

VSG - Ethanolamine - Phosphate --- Glycan ---- Phosphatidylinositol

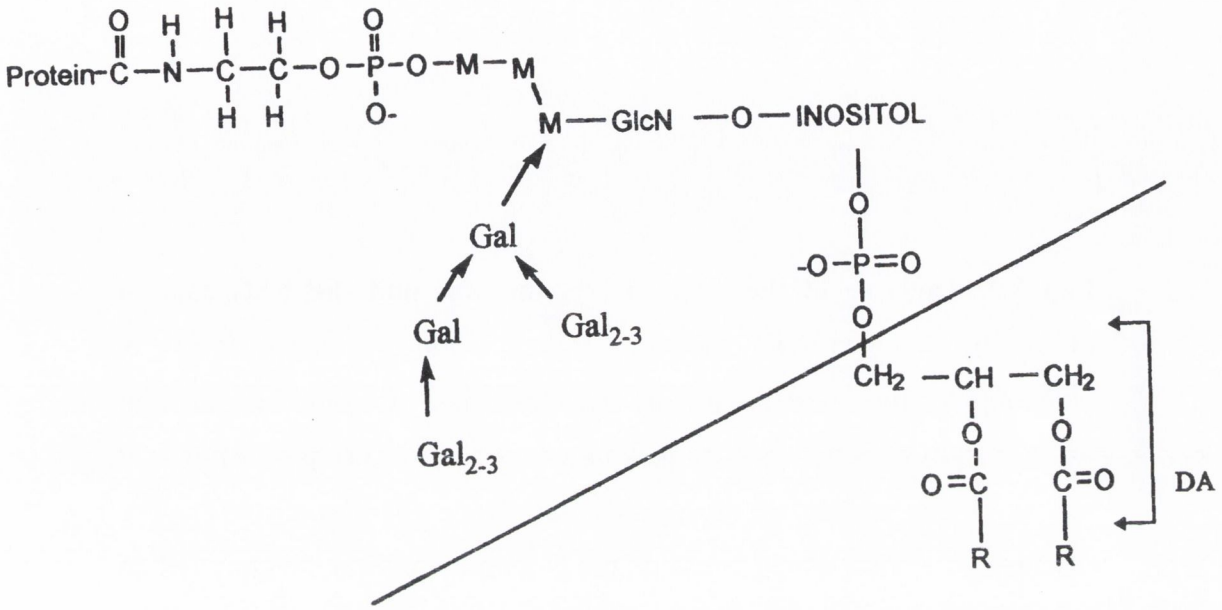

Fig 1.4. The glycosylphosphatidylinositol (GPI) anchor of the VSG of *T. brucei.*

Adapted from Ferguson *et at.*, 1988 where:

M =mannose

Gal = galacotse

GlcN = glucosamine

DA = diacylglycerol

R = myristate side chain, $(CH_2)_{12}CH_3$

And the line represents the outer face of the plasma membrane and the bond cleaved by the GPI-specific phospholipase C.

Fig. 1.5. The role of the African trypanosome and the VSG coat in providing the first GPI structure, taken from (Ferguson, 1999). A scanning electron micrograph (Michael Duszenko) of a bloodstream form of *T. brucei* (top left) is shown next to a cartoon model (top right) of a 20 nm x 20 nm section of the plasma membrane (Ferguson, 1997). The structure of a VSG dimer, based on the N-terminal crystal structure (Blum et al., 1993), is shown (bottom right) next to the primary structure of the GPI anchor (Ferguson *et al.*, 1988) (bottom left). The section of the GPI anchor structure shown in blue is conserved throughout the eukaryotes. The galactose side-chain (shown in green) and the fatty acids of the PI moiety, which are both myristate (shown in pink), are unique to VSGs.

Fig. 1.5. The role of the African trypanosome and the VSG coat in providing the first GPI structure, taken from (Ferguson, 1999).

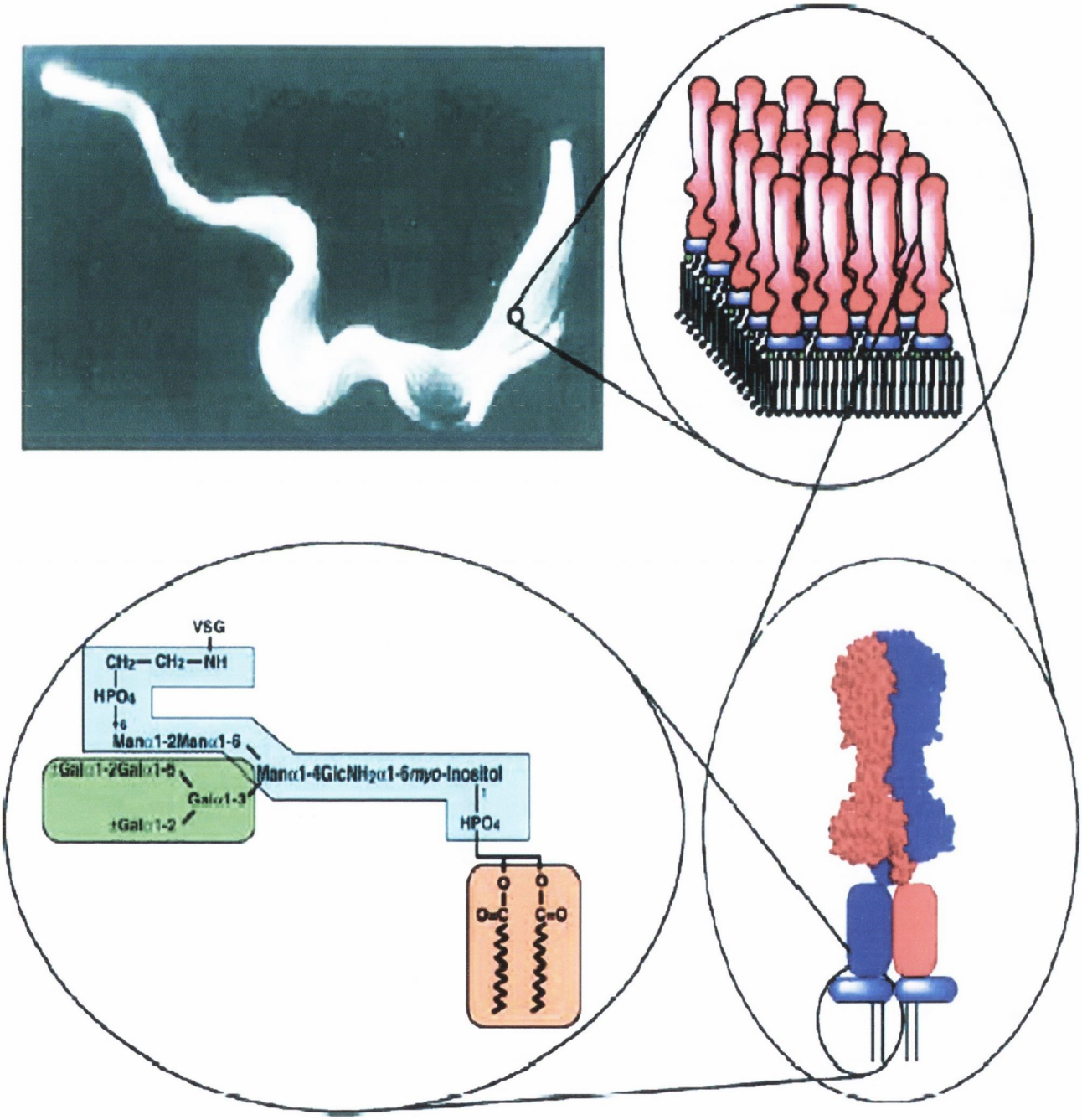

in the bloodstream 'escape destruction because they become used or habituated to the action of antibodies' (quoted in Ross *et al;* 1910). The discovery in 1967 that different populations of trypanosomes in the mammalian bloodstream possess different proteins on their surface (Bridgen *et al.*, 1976) drew attention to the phenonomen of antigenic variation in African trypanosomes, the process whereby these organisms periodically change the major protein on their surface enabling them to potentially keep one step ahead of the immune system's response.

The process of antigenic variation allows trypanosomes to cause prolonged chronic infections due to their ability to successively express different antigenic variants of the variant surface glycoprotein (VSG). During the bloodstream stage of the life cycle, the parasite surface is covered with a monolayer made of 1×10^7 copies of the VSG, whose antigenic specificity continuously changes. This process allows the development of sustained infections, since exposure of this dominant antigen triggers an efficient immune response that rapidly reduces the parasite number, thereby preventing rapid death of the host. However, the appearance of new variants permits the prolongation of infection by parasites transiently escaping the antibody response directed against the previous VSG. This variation of the VSG coat together with the host immune response gives rise to the regular cyclical peaks and remission of parasitemia every 8-10 days associated with the infection. The switching from one VSG on the surface to another occurs at a rate of 10^{-2} to 10^{-7} switches per doubling time of 5-10 h (Turner and Barry, 1989, Davies, 1997, Turner, 1997).

The almost complete sequencing of the *T. brucei* genome has revealed the presence of as many as 1700 VSGs, most of which are pseudogenes (Berriman *et al.*, 2005). The vast majority of these sequences are clustered in subtelomeric arrays. Many VSGs are also found at the extremity of telomeres, particularly in minichromosomes of around 50-150 kilobases, but also at the end of larger chromosomes (Van der Ploeg *et al.*, 1984). Transcription of the VSG occurs in one of the telomeres of the large chromosomes, which contain the VSG expression sites, or VSG ES's (Pays *et al.*, 2001). There are approximately 15 telomeres that contain VSG ESs (Pays *et al.*, 2001; Becker *et al.*, 2004) and these sites all harbour polycistronic transcription units containing a variable collection of expression site-associated genes (ESAGs) upstream from the VSG. It seems that two of these ESAGs (ESAG 6 and ESAG 7) are conserved between the ESs, but most ESAGs are shared between the different sites. The transcription promoters of the different VSG ESs are highly conserved and they can be present as one or two copies separated by around 15

kilobases. The VSG ESs are insulated between two arrays of repeats, upstream 70 bp repeats and downstream telomeric repeats.

An essential rule of the antigenic variation system in *T. brucei* is that only a single VSG expression site (VSG ES) is fully active at any one time ("mono-allelic" expression) and only in the bloodstream form of the parasite. Transcription starts in different VSG ESs simultaneously, but is abortive in all but the "active" one (Vanhamme *et al.*, 2000). The transcriptional machinery of the active site can be detected as an "ES body" that is distinct from the nucleolus despite the presence of RNA Pol I (Navarro and Gull, 2001). At present it is a mystery as to the linkage between the mono-allelic control of VSG ES activity and the selective recruitment of the RNA elongation and processing machinery at a single site at a time. What is clear is that the choice of active site can suddenly change from time to time, indicating that the ES body can accommodate different telomeres.

Trypanosomes have two possible mechanisms to change the VSG expressed and therefore perform antigenic variation (Fig 1.6). They can either switch expression between VSG ESs (in-situ switching) or replace the VSG gene within the active VSG ES (DNA recombination). For most VSG genes, the only way to become active is to replace the gene in the active VSG ES. There are a number of mechanisms whereby this can be achieved and they all involve homologous recombination. By contrast, *in-situ* switching applies only to genes that occupy a VSG ES. Although there are at least 20 VSG ESs, each of which contains a VSG gene, there are thought to be ~ 1000 VSG genes elsewhere in the genome. Most of these are in chromosome-internal arrays or at the telomeres of 100 or more specialized minichromosomes, and in neither location can they be expressed. Instead, they must be copied into the VSG ES, normally deleting the resident VSG by a gene conversion mechanism termed duplicative transposition. Occasionally the replacement of the resident VSG gene involves the generation of a mosaic gene from segments of more than one silent gene (generally seen late in trypanosome infections). Less commonly, telomeres can be exchanged by reciprocal recombination, moving a silent VSG gene into the VSG ES and the transcribed VSG gene into a silent telomere. It has never been entirely clear which mechanisms are used most frequently by trypanosomes to switch from expressing one VSG gene to an antigenically distinct variant. However, it does seem to be likely that trypanosomes are geared primarily for recombinational, rather than in-situ switching (Robinson *et al.*, 1999).

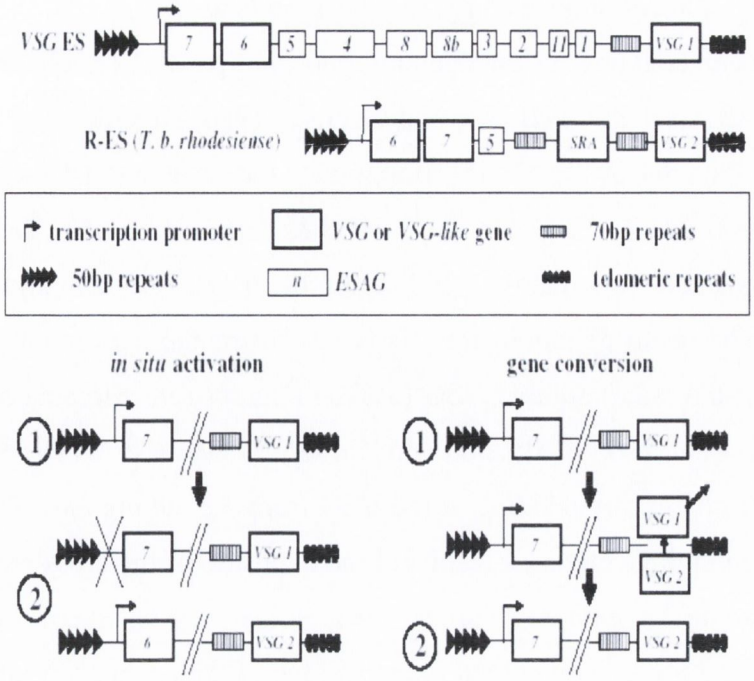

Figure 1.6. The antigenic variation system of *T. brucei* (taken from Pays, E 2006, Microbes and Infection).

From a very large repertoire, a single VSG is expressed at any one time, and this occurs in one of multiple telomeric VSG ESs, which contain polycistronic transcription units with several expression site-associated genes (ESAGs) ESAG 6 and ESAG7 are VSG-like genes encoding the heterodimeric receptor for the host transferrin. A partcular VSG ES specific to T.b. rhodesiense, termed R_ES, contains the VSG-like SRA genes that confers resistance to the trypanolytic factor apo-L-I of human serum. VSG variation (here, 1 to 2) can occur following transcriptional switching between VSG ESs (in situ (in) activation), or following homologous DNA recombination targeted to the active VSG ES, such as gene conversion.

1.5 The GPI-Phospholipase C of *Trypanosoma brucei*

T. brucei contains an endogenous phospholipase C (PLC) known as the GPI-phospholipase C (GPI—PLC) (Bulow and Overath, 1986, Hereld, 1986 & Fox, 1986) that cleaves the GPI-anchor of the VSG, forming diacylglycerol and a 1,2-cyclic phosphate on the inositol ring (Fig 1.7) (Ferguson *et al.*, 1988 & Ferguson, 1985). This enzyme behaves as a non-glycosylated amphipathic membrane protein of 37-40 kDa and is specific for the GPI moiety. The result of this hydrolysis is to convert the hydrophobic membrane form VSG (mfVSG) to a water soluble VSG (sVSG) (Cardoso de Almeida and Turner, 1983). Hypotonic lysis (Cardoso de Almeida and Turner, 1983) or stress (Voorheis *et al.*, 1982, Rolin, 1996) results in the shedding of the VSG from the membrane. This conversion can be detected immunologically as it results in the exposure of the cross-reacting determinant (CRD) (Cardoso de Almeida and Turner, 1983, Holder, 1981), an epitope with the inositol 1,2-cyclic phosphate group contained in the residue of the anchor left attached to the VSG after phospholipase hydrolysis. As well as the VSG, the majority of the precursors of the GPI — anchor are also substrates for the GPI—PLC in vitro. It has been shown that the GPI—PLC in *T. brucei* can hydrolyse phosphatidylinositol (PI) under certain assay conditions (Butikofer *et al.*, 1996). However, the enzyme is active against GPI under a wider range of assay conditions, and the Km for PI (37μM) is one to two orders of magnitude higher than that for GPI — linked proteins (0.4-0.7 μM for VSG (Bulow and Overath, 1986, Mensa-Wilmot, 1992), 0.8μM for acetylcholine esterase (Butikofer *et al.*, 1996). The Km values are significant as the number of VSG and PI molecules per trypanosome is roughly equivalent; 1.1 x 10^7 molecules of the VSG (Jackson and Voorheis, 1985) and approximately 2.7 x 10^7 molecules of PI (Carroll and McCrorie, 1986, Voorheis, 1980), so under most conditions of cell lysis the PLC would first act on the endogenous GPI-linked protein.

If the GPI—PLC acts on a single GPI — anchored protein, then the VSG is the most obvious candidate. The VSG is by orders of magnitude the most abundant GPI — anchored protein in bloodstream trypanosomes, yet at 3 x 10^4 molecules of GPI—PLC/trypanosome (Hereld *et al.*, 1986) and at an estimated turnover rate of 100 to 700 mfVSG molecules/min under assay conditions (Hereld *et al.*, 1986, Mensa-Wilmot, 1992), there is sufficient GPI—PLC to release the entire coat in a few minutes, as occurs on hypotonic or detergent lysis of trypanosomes. The stress conditions that induce VSG shedding cover a range of different treatments from a reduction in pH to 5.5 (Rolin *et al.*, 1996) to local anaesthetics (Jackson and Voorheis, 1985). The cell remains intact during shedding and there is no

release of cytoplasmic contents. Furthermore, VSG and GPI—PLC show the same developmentally regulated expression and are both found only in bloodstream forms in the mammalian host and the metacyclic forms in the salivary glands of the tsetse fly (Lamont *et al.*, 1987, Ross, 1987 & Grab, 1987) but not in procyclic trypanosomes, *i.e.*, the form that is present in the insect midgut (Bulow and Overath, 1986, Carrington, 1989 & Mensa-Wilmot, 1990). GPI—PLC expression also coincides with GPI-anchor sensitivity to GPI—PLC cleavage; all GPI-anchors analysed to date in procyclic trypanosomes are GPI—PLC resistant (Field *et al.*, 1991 & Engstler, 1992). In the case of the major surface protein, procyclin, this resistance to cleavage is due to palmitoylation of the inositol ring in the 2-position (Field *et al.*, 1991).

The GPI—PLC in *T. brucei* has some sequence identity with bacterial Pi — specific PLCs in the N — terminal half of the polypeptide (Carrington *et al.*, 1991). An alignment of the GPI—PLC from *T. brucei* and PI—PLC from *B. cereus* and *L. monocytogenes* (Fig 1.8) showed that the majority of the residues that interact with myo—inositol in *B. cereus* PI—PLC are conserved. This observation suggested that the reaction mechanism is the same for all three enzymes and, therefore would be dependent on a histidine (Heinz *et al.*, 1995). This histidine was altered to a glutamic acid by site—directed mutagenesis in the *T. brucei* GPI—PLC and like the same mutation in *B. cereus* PI—PLC (Heinz *et al.*, 1995); this mutation resulted in a totally inactive enzyme (Carnall *et al.*, 1997). This result indicates that the *T. brucei* GPI—PLC is related to the bacterial PI—PLC in catalytic mechanism and is consistent with the observation that it can also catalyse the hydrolysis of PI (Butikofer *et al.*, 1996) as the bacterial PI—PLCs also have dual substrate specificity (Ikeda *et al.*, 1991). However, bacterial PI—PLCs and *T. brucei* GPI—PLC have been distinguished by a number of characteristics. Most noticeable amongst these is the inhibition of GPI—PLC, but not bacterial PI—PLCs, by some sulphydryl reagents, most effectively by Zn^{2+} and *p*—chloromercurylphenylsulphonic acid (*p*CMPSA) (Voorheis *et al.*, 1982) (Bulow and Overath, 1985). The bacterial enzymes have been classified as type II PLCs and the *T. brucei* GPI—PLC as a type III (Low *et al.*, 1988; Mengaud *et al.*, 1991).

The GPI—PLC possesses several rather curious features that deserve further comment. Firstly, there is no easily recognisable N—terminal signal sequence, indicating that the mRNA is translated on free cytoplasmic polysomes and is not co—translationally secreted into the endoplasmic reticulum. Secondly, the polypeptide is not particularly

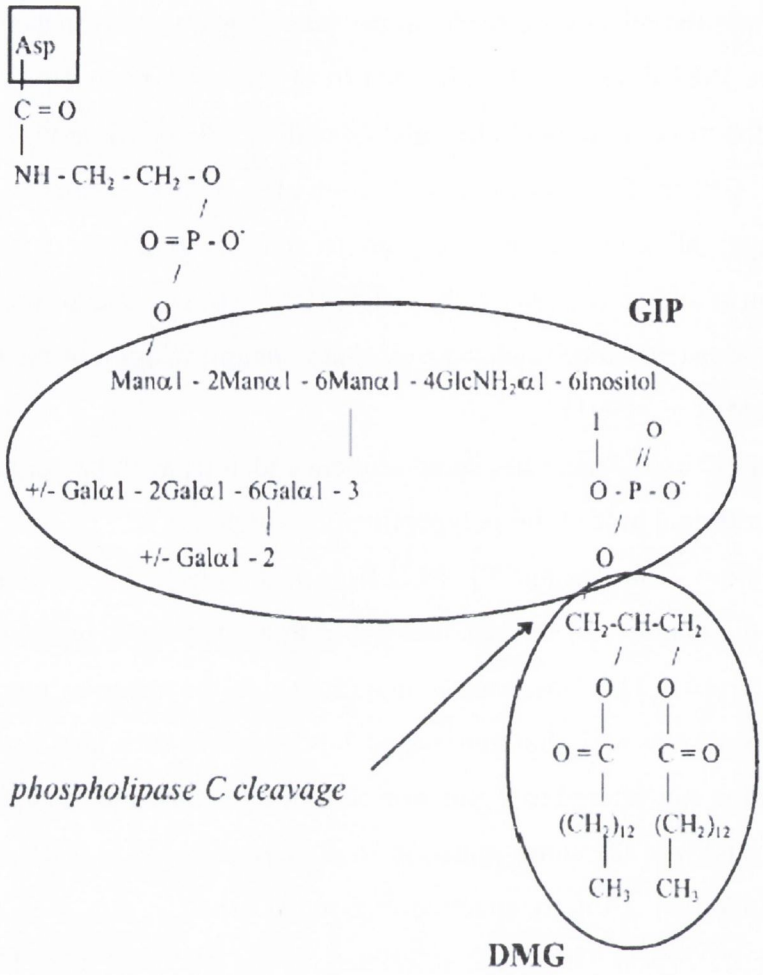

Fig 1.7. Diagram of the GPI anchor of the VSG, taken from Ferguson *et al.*, 1985. The boxed ASP is the C-terminal residue of the protein. The molecular bond cleaved by the GPI-PLC is indicated. This cleavage causes sVSG to be released.

DMG – Dimyristylglcerol

GIP-Glycosyl-inositol-phosphate

hydrophilic or hydrophobic, it contains 69 acidic and basic residues (R,K,D and E) evenly distributed throughout the sequence and 87 hydrophobic amino acids (I,L,W,F and Y) also distributed evenly throughout the sequence. There are no extended runs of hydrophobic amino acids and no regions of high potential for forming amphipathic α-helices. Thirdly, the regions of the α-helix, turn or β—sheet potential are evenly distributed. Fourthly, there is no hydrophobic sequence at the C—terminus and so GPI—PLC is unlikely to be modified by the addition of a GPI—anchor. The primary sequence does not contain any obvious features to indicate how the protein is associated with the membrane. However, the experimental observation is that the enzyme is membrane associated, requires detergent for solubilisation and can be reconstituted into liposomes (Bulow and Overath, 1986; Fox *et al.*, 1986; Hereld *et al.*, 1986). Therefore, either some part of the sequence must be folded in such a way that it penetrates the lipid bilayer, or the protein is covalently modified with a hydrophobic component.

The ability of the GPI—PLC to catalyse the shedding of the VSG coat *in vitro*, and the co-temporal expression of the two proteins, has led to models that suggest an important role for the enzyme in the developmental changes that involve alterations in expression of cell surface proteins (Carrington *et al.*, 1991). There are three circumstances when a trypanosome must replace its surface VSG and therefore when a specific VSG shedding activity, such as GPI—PLC, might be invoked. The first occurs within a few days after entry into a mammalian host when all cells exchange the metacyclic VSG, expressed in the insect salivary gland, for a bloodstream form VSG (Esser and Schoenbechler, 1985). The second occasion may arise in the individual trypanosomes undergoing antigenic variation. In both cases, a passive change of new for old VSG, based on measurements of VSG turnover (Bulow *et al.*, 1989) in combination with growth and dilution, would take several generations, so a process for more rapid exchange has obvious advantages in a host that is mounting an immune response to the old VSG. The third is on the differentiation of bloodstream to procyclic trypanosomes that occurs on ingestion by the insect vector and involves the replacement of surface VSG with procyclin (Roditi *et al.*, 1989).

The successful transmission of the GPI—PLC$^-$ trypanosomes through to bloodstream forms indicated that GPI—PLC activity is not necessary for these life cycle transmissions (Webb *et al.*, 1997). The GPI—PLC$^-$ trypanosomes were also grown in immunosuppressed mice and induced to differentiate to procyclic forms both *in vitro* (Ziegelbauer and Overath, 1990) and by feeding tsetse flies with blood from the mice. In

Fig. 1.8. Alignment of the PI-PLC from *Bacillus cereus* with GPI-PLC from *Trypanosoma brucei* and the PI-PLC from *Listeria monocytogenes*, taken from (Carrington *et al.*, 1998).

The six residues that interact with the myo-inositol in the *B. cereus* PI-PLC and the additional histidine proposed to be involved in catalysis are shown in bold. The proposed homologous residues are also shown in bold and all identities are marked by an asterisk. Tb, *Trypanosoma brucei* GPI-PLC; Bc, *Bacillus cereus* PI-PLC; Lm, *Listeria monocytogenes* PI-PLC.

Fig. 1.8. Alignment of the PI-PLC from *Bacillus cereus* with GPI-PLC from *Trypanosoma brucei* and the PI-PLC from *Listeria monocytogenes*, taken from (Carrington *et al.*, 1998).

```
Tb      MFGGVKWSPQSWMSDTRSSIEKKCIGQVYMVGAHNAGTHGIQMFSPFGL  49
Bc      ASSVNELENWSKWMQPIPDSIPLARIS...IPGTHDSGTFKLQN......  41
Lm      NKPIKNSVTTKQWMSALPDTTNLAALS...IPGTHDTMSYNGDI......  41

Tb      DAPEKLRSLPPYVTFLLRFLTVGVSSRWGRCQNLSIRQLLDHGVRYLDLR  99
Bc      .....................PIKQVWGMTQEYDFRYQMDHGARIFDIR  69
Lm      ...................TWTLTKPLAQTQTMSLYQQLEAGIRYIDIR  71

Tb      MNISPDQENKIYTTHFH..ISVPLQEVLKDVKDFLTTPASANEFVILDFL 147
Bc      GRLTDDNT..IVLHHGPLYLYVTLHEFINEAKQFLKDNPSETIIMSLKKE 117
Lm      ...AKDNL...NIYHGPIFLNASLSGVLETITQFLKKNPKETIIMRLKDE 115

Tb      ....HFYGFNESHTMKRFVEELQALEEFYIPTTVSLTTPLCNLWQSTRRI 193
Bc      ...YEDMKGAEDSFSSTFEKKYFVDPIFLKTEGNIKLGDARGKIVLLKRY 164
Lm      QMSNDSFDYRIQPLINIYKDYFYTTPRTDTSNKIPTLKDVRGKILLLSEN 165

Tb      FLVVRPYVEYPYARLRSVALKSIWVNQMELNDLLDRLEELMTRDLEDVSI 243
Bc      SGSNEPGGYNNFYWPDNETFT.TTVNQNANVTVQDKYKV.SYDEKVKSIK 212
Lm      .....HTKKPLVINSRKFGMQFGAPNQV....IQDDYNGPSVKTKFKEIV 206

Tb      GGVPSKMYVTQAIGTPRNNDFAVAACCGACPGSHPDLYSAAKHKNPHLLK 293
Bc      DTMDETMNNSEDLNHLYINFTSLSSGGTA..WNSPYYYASYI..NPEIAN 258
Lm      ...QTAYQASKADNKLFLNHISATSLTFTPRQYAAA..........LNN 242

Tb      WFYDLNVNGVMRGERVTIRRGNNTHGNILLLDFVQEGTCTVKGVDKPMNA 343
Bc      YIKQKNPARVGWVIQDYINEKWSPLLYQEVIRANKSLIKE           298
Lm      KVEQFVLNSTSEKVRGLGILIMDFPEKQTIKNIIKNNKFN           282

Tb      VALCVHLNTNQTARS                                    358
```

both cases differentiation to procyclic forms occurred and *in vitro* the kinetics of VSG loss, procyclin appearance and cell division was indistinguishable from wild type (Webb *et al.*, 1997). This result showed that the GPI—PLC$^-$ trypanosomes could complete the life cycle and that the GPI—PLC was not needed for the differentiation of bloodstream form to procyclic trypanosomes. It has been reported that a specific zinc metalloprotease is involved in the shedding of the VSG during differentiation (Gruszynski *et al.*, 2003). Finally, it was shown that GPI—PLC$^-$ trypanosomes were able to maintain a persistent infection in immunologically competent mice and undergo antigenic variation (Webb *et al.*, 1997). This result clearly showed that the GPI—PLC was not needed for either the switch from metacyclic to bloodstream form VSG or for subsequent antigenic variation. However, the mice infected with the GPI—PLC$^-$ trypanosomes lived for more than twice as long and the first peak of parasitemia of GPI—PLC$^-$ trypanosomes was significantly lower than in, mice infected with control trypanosomes (Webb *et al.*, 1997). This result is consistent with the proposal that the altered growth characteristics of the GPI—PLC$^-$ trypanosomes were due to the absence of the GPI—PLC gene. The reduction in parasitemia at the first peak can only be explained by a reduced rate of growth of the GPI—PLC$^-$ trypanosomes or a more efficient clearance of PLC$^-$ trypanosomes by the host immune system, or both.

Other biological substrates have been suggested for the GPI—PLC. The enzyme appears to be responsible for the majority of the degradation of the GPI precursor glycolipid A' that occurs during lipid remodelling *in-vitro* (Morita *et al.*, 2000). It was shown that the glycolipid A' released from the membrane binds to anti—CRD antibodies, indicating that it has the inositol 1,2-cyclic phosphate group. This species is produced when GPIs are cleaved by GPI—PLC. When mutant trypanosomes deficient in GPI—PLC were used for similar studies the GPI degradation rate was substantially reduced. However it is not immediately obvious why a general role in GPI metabolism, or homeostasis, unlike expression of GPI—PLC and VSG, would be confined to the bloodstream stage of the life cycle.

The activity of the GPI-PLC must be controlled. Otherwise the VSG would be shed from the membrane continuously. One possibility is that the enzyme is normally inactive, however, the regulatory factor(s) remains elusive. The GPI-PLC is an abundant protein, present at approximately 3×10^4 copies / cell, which represents 0.04 % of the total cellular protein (Hereld *et al.*, 1986). With an estimated turnover rate of 100-700 mf VSG molecules/min the VSG can be released (1.12×10^7 molecules/cell, 16 % total cellular

protein) within a few minutes (Hereld *et al.*, 1986). It is difficult to accept that a parasite, particularly one as parsimonious as *T. brucei* harbours an abundant enzyme on its surface that at least according to the literature is not required for any of the life cycle processes where the VSG is shed from the cell.

There have been a number of conflicting reports regarding the location of the GPI—PLC in bloodstream forms of *T. brucei*. Firstly, on the basis of cell fractionation experiments, it was concluded that the GPI—PLC resides in the part of the plasma membrane lining the flagellar pocket as well as intracellular membranes such as the Golgi apparatus, coated vesicles and endocytic organelles (Grab *et al.*, 1987). The principal evidence for the flagellar pocket localization of the enzyme was based on the finding that the fraction with the most GPI—PLC activity was high in two flagellar pocket markers, namely acid phosphatase and adenyl cyclase.

Following this report, another group demonstrated that the GPI—PLC is localized to the cytoplasmic face of intracellular vesicles (Bulow *et al.*, 1989), sequestering the enzyme away from extracellular VSG. Three different approaches were used to elucidate in greater detail the intracellular localization of GPI—PLC (cell fractionation, Immunofluoresence and Immunoelectron microscopy). All three experiments showed that the enzyme is not detectable on the plasma membrane and is associated with the cytoplasmic side of intracellular vesicles. This group did however confirm the previous observation of the GPI—PLC in the flagellar pocket membrane (Grab *et al.*, 1987) by also co-localizing the GPI—PLC with the flagellar pocket marker, acid phosphatase (Bulow *et al.*, 1989). This indicates a discrepancy in the results between the immuno-electron data and sub-cellular fractionation data. There are two possibilities to explain this discrepancy: first, disruption of trypanosomes may lead to fusion of GPI—PLC containing membranes with the flagellar pocket membrane; therefore the co-localization of the GPI—PLC and acid phosphatase may be an artefact. Also, acid phosphatase may be mainly associated with similar intracellular organelles to which the GPI—PLC is associated, rather than residing predominantly in the flagellar pocket membrane. Although the cytochemical staining experiments of Langreth and Balber (1975) and the hydrolysis of phosphatase substrates in live cells (Steiger *et al.*, 1980) suggest that some enzyme activity is located in the lumen or at the surface of the pocket, a quantitative evaluation of these experiments in terms of the molar ratio of surface versus intracellular phosphatase is not possible until the permeability of the substrates employed has been independently assessed (Bulow *et al.*, 1989).

Both the immunofluoresence and immuno-electron-microscopic results suggest that the GPI—PLC is associated preferentially with the peripheral face of intracellular vesicles whose function remains obscure. It was proposed that since the enzyme is likely to be formed on ribosomes (Carrington *et al.*, 1991), it may insert post-translationally into the membrane of several organelles such as glycosomes or part of the endocytic pathway. The above locations do, however, propose a topological problem for the enzyme and its substrate; how does the GPI—PLC gain access to the VSG on the outside of the cell, for example during the shedding of the VSG under stress conditions (Voorheis *et al.*, 1982); as the two would be on opposite sides of the membrane if conventional membrane fusion occurred. Since it has been established that the VSG and GPI—PLC have to be in the same membrane for catalysis to occur (Bulow and Overath, 1986), and presumably on the same face then it can only be concluded that something unusual is taking place.

GPI—PLC from *T. brucei* is post-translationally modified by thioacylation (Paturiaux-Hanocq *et al.*, 2000). This thioacylation involves a group of three closely clustered cysteine residues located in the C—terminal region of the polypeptide. It has been proposed that reversible thioacylation of GPI—PLC might modulate access of the enzyme to the GPI anchor of the VSG in trypanosomes (Paturiaux-Hanocq *et al.*, 2000) since the acylated form of the enzyme dominates the non—acylated form under conditions known to lead to cleavage of the GPI—anchor of the VSG, *e.g.* osmotic shock, detergent lysis or acid stress.

The most recent report regarding the location of GPI—PLC demonstrated the presence of the enzyme on the extracellular side of the plasma membrane in intact stumpy trypanosomes (Gruszynski *et al.*, 2003). Since the extracellular localization cannot be due to classic secretion, because the enzyme does not have an N—terminal signal sequence or any other hydrophobic domains (Hereld *et al.*, 1986) it has been suggested by (Gruszynski *et al.*, 2003) that reversible thioacylation of the enzyme regulates topological translocation in a manner similar to that demonstrated for Leishmania hydrophilic acylated surface protein B (Denny *et al.*, 2000).

There are still a lot of unanswered questions relating to the true localisation of the GPI—PLC in the bloodstream form of *T. brucei* and its biological function *in-vivo.* It is the aim of this thesis to attempt to answer these questions and shed some light on this unusual enzyme.

1.6 The paraflagellar rod (PFR) of bloodstream form trypanosomes.

All trypanosomatid flagellate parasites are characterised by the presence of a very particular cytoskeleton responsible both for maintaining the shape and form of the cell and the modulation of cell shape between the different life cycle stages (Sherwin and Gull, 1989). In order to complete their life cycle, these parasites need to migrate between different organs in the insect vector and different tissues in the mammalian host. Motility and mediation of attachment to host cell surfaces are likely additional functions of the cytoskeleton. The most obvious cytoskeletal components (Fig 1.9) are the microtubular subpellicular core, the axoneme, the basal body, the parafagellar rod, the flagellar attachment zone and the filaments responsible for the attachment to insect tissues.

The paraflagellar rod (PFR), also called the paraxial rod (Fig 1.10, B) is present from the point where the flagellum exits the flagellar pocket and runs alongside the axoneme right to the distal tip. Longitudinal sections reveal an elegant organisation of filaments crossing each other at defined angles (Fig 1.10, B). Cross-sections reveal that the PFR in *T. brucei* has a crescent shape and a diameter of ~ 150 nm. On these sections three domains can be defined by their position relative to the axoneme; a short proximal domain, an intermediate domain and a more developed distal domain (Fig 1.11). The PFR is connected to the axoneme *via* fibres attaching the proximal domain to the microtubule doublets 4 through 7. This connection is extremely strong and resistant to a variety of treatments, making PFR purification difficult. In addition, other filaments connect the proximal domain of the PFR to the FAZ (Fig 1.11). A PFR has so far only been seen in three groups of protists; the kinetoplastids, the euglenoids and the dinoflagellates (Cachon and Cosson, 1988). It is therefore not restricted to parasitic species and has not been seen in multicellular orgainisms.

For the last three decades scientists have tried to understand the composition and function of the PFR. Biochemical studies identified a doublet of proteins found in all orgainisms with a PFR: PFRA and PFRC (Bastin *et al.*, 1996). By immunofluoresence, anti-PFR antibodies exclusively recognise the flagellum. The sequences of PFRA and PFRC in *T. brucei* display extensive identity throughout their length (60 %). PFRA and PFRC are well conserved between species and only the ends show significant diversity. A few less abundant PFR proteins have been identified. Three different antigens were localised to distinct regions of the PFR of *T. brucei*: (1) in the distal domain of the PFR (Woods *et al.*, 1989 & Woodward, 1994); (2) throughout the PFR; and (3) on the connections between the PFR and the axoneme (Imboden *et al.*, 1995).

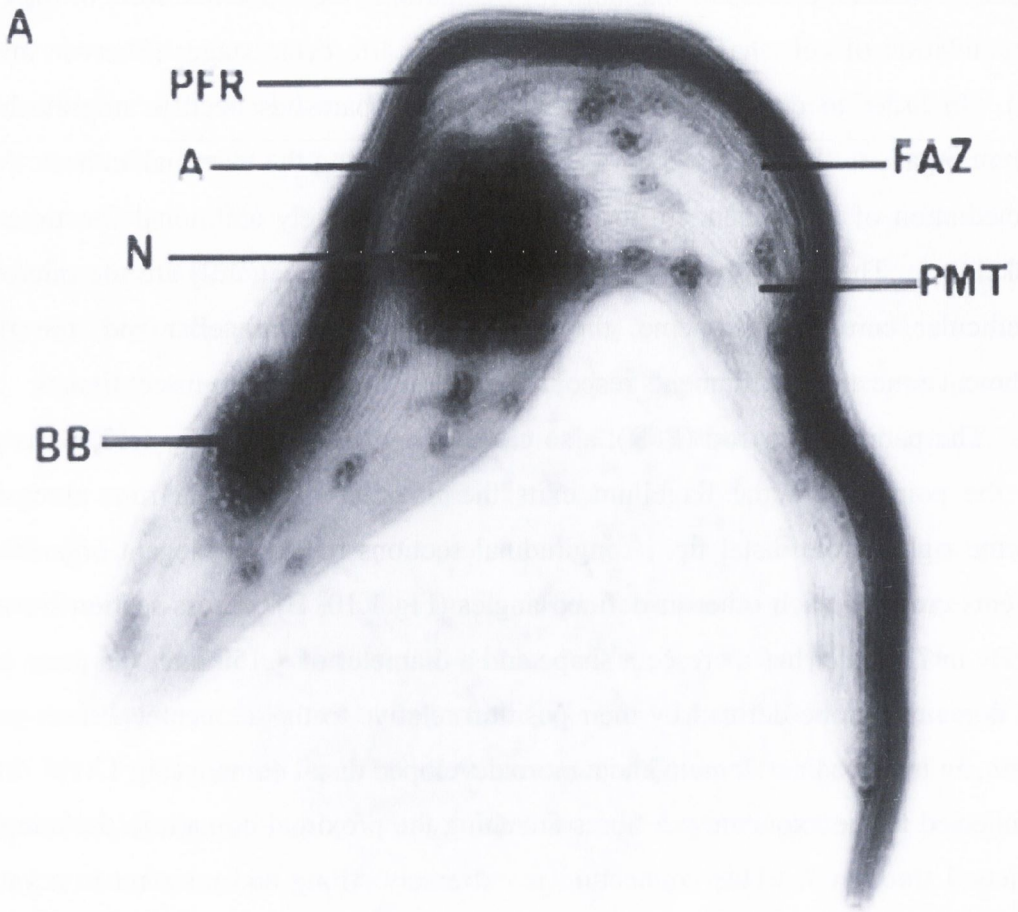

Fig 1.9. Negative stained procyclic cytoskeleton from *T. brucei* after detergent extraction, adapted from (Kohl and Gull, 1998).

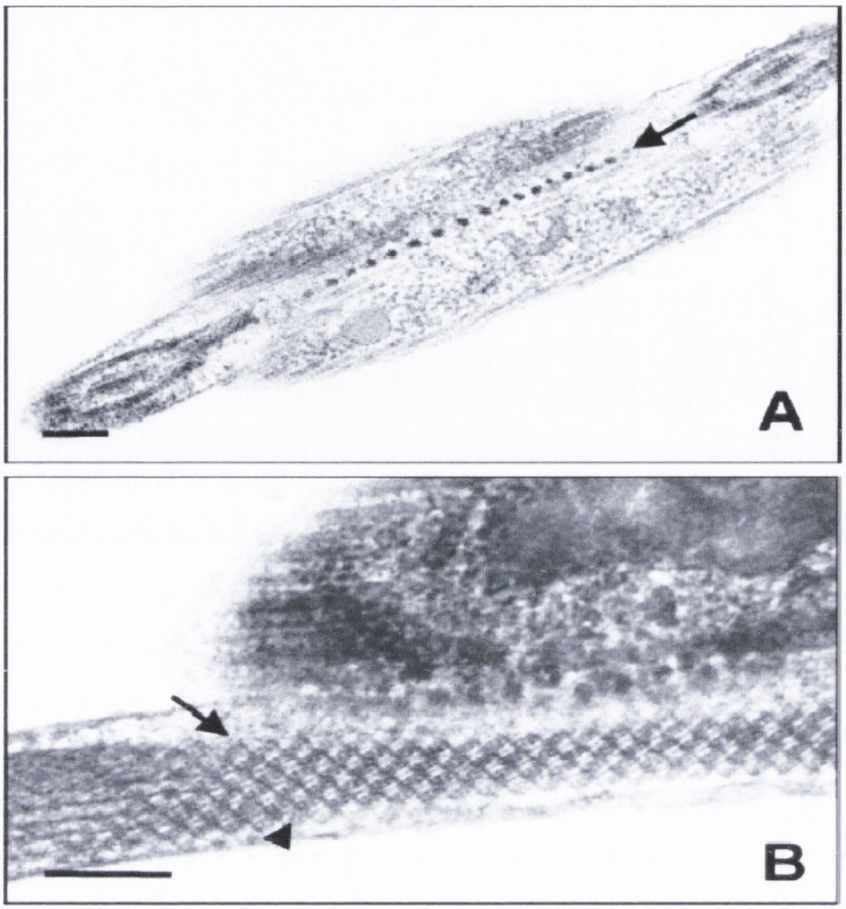

Fig 1.10. Longitudinal views of the flagellum attachment zone (A) and the paraflagellar rod (B). Adapted from (Bastin *et al.*, 2000). The FAZ is seen as a row of punctate structures (A, arrow) intercalated between microtubules of the subpellicular corset. In the PFR, plates of thin (B, arrow) and thick (B, arrowhead) filaments cross each other at a defined angle in the proximal and distal domains.

Fig 1.11. Transverse section of the flagellum of wild-type *T. brucei* (A) and a paralysed *snl*-2 mutant (B) in the region of attachment to the cell body. Adapted from (Bastin *et al.*, 2000). The basic components of the flagellum are indicated in the diagram (C). While a well-developed PFR is present in the wild-type (A), only a rudimentary structure is present in the paralysed mutant (B). Intraflagellar particles, possible related to rafts described in other systems are seen in some cross-sections (arrowheads in A). The axoneme (Ax) is made of the classic 9 + 2 structure with dynein arms (magenta), nexin links (green), radial spokes (red) and the central sheath (yellow). The PFR (blue) can be divided into three domains: proximal (p); intermediate (i); and distal (d), defined by their position relative to the axoneme. Filaments are connecting the proximal domain of the PFR to doublet 4 (light blue) and 7 (dark blue), and to the FAZ region (orange). The FAZ is made of a cytoplasmic filament (brown), intercalated in a gap between two microtubules of the subpellicular corset, and of four specific microtubules associated with the smooth endoplasmic reticulum.

Fig 1.11. Transverse section of the flagellum of wild-type *T. brucei* (A) and a paralysed *snl*-2 mutant (B) in the region of attachment to the cell body. Adapted from (Bastin *et al.*, 2000).

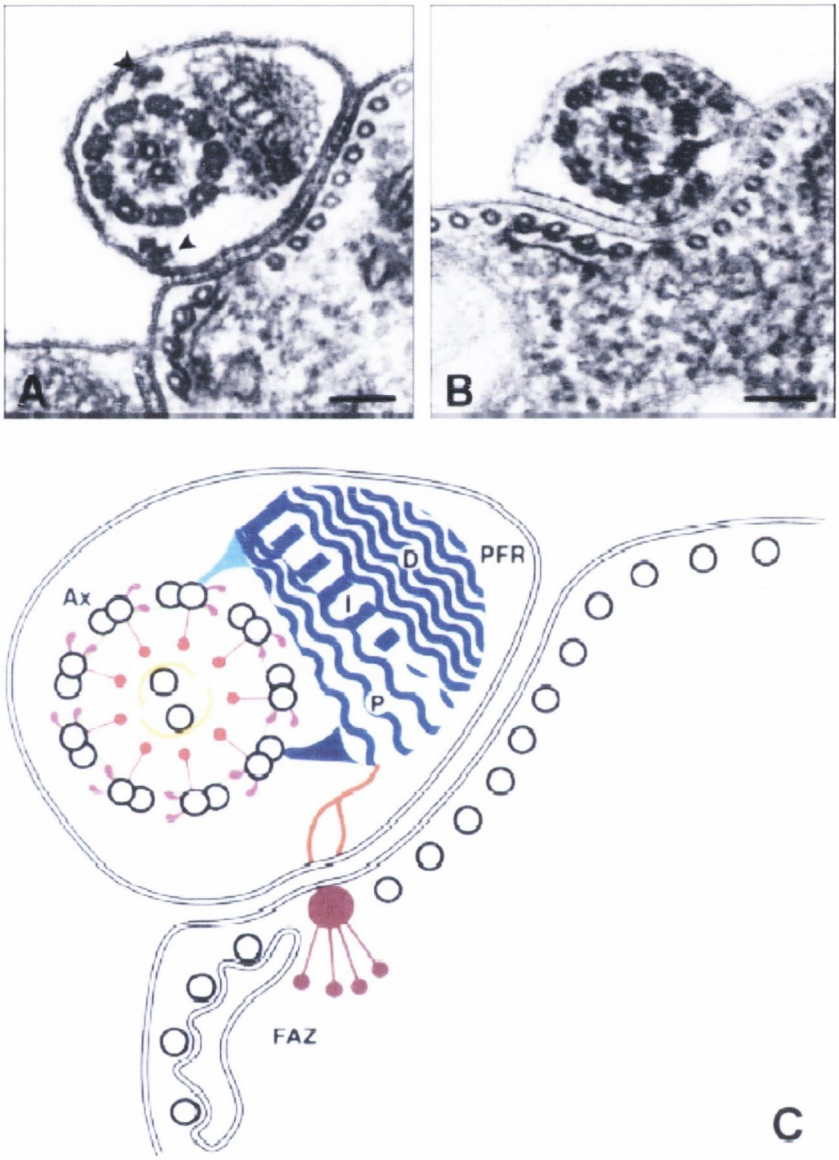

All three proteins are large and only partial sequence is available. In addition to these unknown antigens, calmodulin has been localised to the PFR (Ridgley *et al.*, 2000), as well as some calflagins (flagellar calcium-binding proteins) (Bastin *et al.*, 1999). Molecular ablation of the PFRC in *T. brucei* by an RNA interference strategy (Bastin *et al.*, 1998; Bastin *et al.*, 1999; Bastin *et al.*, 2000) produced a dramatic phenotype: trypanosomes stopped swimming and sedimented to the bottom of the culture flask, showing that the PFR plays a major role in flagellar and cellular motility.

1.7. The flagellar attachment zone (FAZ) of bloodstream form trypanosomes.

The trypanosomal flagellum is attached to the cell body along most of its length. At this site, the flagellum and the cell body membranes are in tight contact and flanked by original structures, which have been defined as the FAZ. The most obvious feature is the presence of a cytoplasmic, electron-dense filament, located in a gap between two particular and constant microtubules of the subpellicular corset (Bastin *et al.*, 2000) (Fig 1.10, A). A longitudinal view of the FAZ displays a row of punctate structures intercalated in the subpellicular corset of microtubules. To the left of this filament, when the cell is viewed towards the anterior end, there is a group of four microtubules always very closely associated to a profile of endoplasmic reticulum (Fig 1.11). On the flagellum side of the FAZ, filamentous structures connect the proximal domain of the paraflagellar rod to the region associated with the FAZ (Fig 1.11). A few proteins have been localised to the FAZ in *T. brucei* and *T. cruzi* (Kohl and Gull, 1998)(Table 1.1). Two monoclonal antibodies were shown to stain the FAZ by immunofluoresence and to recognise a doublet of high molecular weight proteins (Kohl *et al.*, 1999). It is not obvious why trypanosomes anchor their flagellum alongside the cell body. In addition there is no direct evidence that the components of the FAZ are actually involved in flagellar attachment. It has been speculated that the FAZ may play a central role in cell division, possibly for the determination of the axis of cytokinesis (Robinson *et al.*, 1995).

1.8 Agglutination of trypanosomes with VSG specific antibody

Polyclonal antibodies contain a variety of individual antibodies of different specificities and avidities that can bind to the various accessible epitopes on their target antigen. In the presence of an excess of antigen most antigen-antibody complexes are

small and contain only a single antibody molecule with an antigen bound to each of its combining sites, while in the presence of an excess of antibody most complexes consist of a single antigen with antibodies bound to each of its accessible epitopes. Neither of these conditions is favourable for the formation of cross-linked lattices. However, in those cases where there are equal molar concentrations of antigen and antibody, known as the equivalence point, extensive non-covalent but stable cross-linking occurs between the antigen and antibody leading to large aggregates of antigen-antibody complexes. This general principal for the formation of large antigen-antibody complexes also extends to whole cells, which have a large number of different surface antigens leading to agglutination of the cells by surface antigen specific antibodies. Furthermore, the formation of these cellular aggregates is of importance in the effective clearance of these complexes and the invading pathogen from which they arise by the phagocytic cells of the host.

Antibody-mediated agglutination of trypanosomes was first observed in a study of *T. lewisi* and *T. brucei* by Laveran & Mesnil, (1900,1907). The agglutination reaction was used for a variety of experimental purposes ranging from a diagnostic test for trypanosomiasis (Offerman, 1915; Dahmen & David, 1921) to the detection of new variants that arise during antigenic variation (Cunningham and Vickerman, 1962; Gray, 1962; Miller, 1965; Seed *et al.*, 1969 & Gray, 1975). However no investigation of the fate of the agglutinated trypanosomes was undertaken in any of the above-mentioned studies except in the preliminary account by Laveran & Mesnil (1907) who reported that the aggregated cells eventually disaggregated by an uncharacterised mechanism and in the study of Cunningham & Vickerman (1962) who reported that the aggregated cells eventually died. Subsequent to these reports it was observed that trypanosomes agglutinated by IgG antibody can disaggregate following addition of complement to the aggregated cells without any apparent deleterious effects on the cells (Takayanagi *et al.*, 1987 & Takayanagi, 1991). More recently, it was reported that bloodstream forms of *T. brucei* incubated with agglutinating concentrations of acute immune serum eventually disaggregated upon prolonged incubation in an-energy dependent manner and without any adverse effects on the cells (Fig 1.12) (O'Beirne *et al.*, 1998). In addition, it was found that either IgM or IgG anti-VSG antibody was the sole component of the acute immune serum responsible for this observation.

Table 1
Characteristics of cytoskeletal proteins of trypanosomes

Name	Mass [kDa]	Evidence	Characteristics	Reference
p41	41	a	MAP, contains covalently bound fatty acid	[53]
52 K	52	a	MAP	[54]
WCB210	210	b, c	MAP, phosphorylated	[25]
Gb4	28	b, c, d_r	MARP	[55]
p320	320	a, b, c, d_r	MARP, repetitive motif represents a microtubule-binding domain	[56–58]
PFR A	69	b, c, d	PFR, major components	[59]
PFR C	72			[60]
p180	180	b, c, d_r	PFR, minor components	[16]
p200	200			[61]
I_2	>300	b, c, d_r	PFR, minor component	[62]
I_{17}	>300	b, c, d_r	PFR, minor component	[62]
p88	88	b, c	FAZ cytoplasmic filament	[48]
Ag BS7	Multiple	b, c	FAZ cytoplasmic filament, basal body, axoneme	[63]
Ag CD10	>300	b, c	FAZ cytoplasmic filament	[16]
Ag DOT1	200	b, c	FAZ cytoplasmic filament and distal tip of flagellum	[16][L. Kohl unpublished]
GM6	>200	b, c, d_r	FAZ cytoplasmic filament	[64,65]
H49 *T. cruzi*	300	b, c, d_r	FAZ cytoplasmic filament	[64,66]
Ag 2G4 *T. cruzi*	Multiple [700–1200]	b, c	FAZ, set of 4 unique microtubules	[67]

Abbreviations: a, microtubule binding assay; b,immunofluorescence; c, immunoelectron microscopy; d, gene cDNA; d^r, gene cDNA containing repetitive elements.

Table 1.1. Characteristics of cytoskeletal proteins of trypanosomes, adapted from (Kohl and Gull, 1998).

The mechanism responsible for the observed disaggregation did not appear to involve release of the VSG-antibody complex from the cells or cleavage of the cross-linking antibody. However, inhibitors of endosomal/lysosomal homeostasis completely inhibited disaggregation suggesting the involvement of either/both endocytosis or exocytosis in the mechanism responsible for disaggregation. It is clear that even if surface immune complexes are eventually endocytosed, this step cannot occur until any antibody connections that exist between trypanosomes are eliminated. Consequently, it appears most likely that the involvement of the endocytotic/exocytotic cycle in this event involves the export of some component to the outer leaflet of the plasma membrane that is required for disaggregation.

The mechanism of disaggregation in trypanosomes is a regulated process, inhibited by cAMP and its analogues and requiring the presence of a functional protein kinase C or similar kinase but independent of the action of Ca^{2+} (O'Beirne *et al.*, 1998). However, the fate of the VSG within the surface immune complexes remains elusive. The results presented by (O'Beirne *et al.*, 1998) indicate that there is no gross cleavage of the VSG during disaggregation although it was suggested that clustering of the VSG on the surface of the trypanosomes may trigger the controlled trafficking of the GPI—PLC or a protease which would then release a small part of the VSG and the bound IgM or IgG antibody into the surrounding medium and so permit disaggregation. Given that many inhibitors of endosomal/lysosomal homeostasis were also found to be inhibitory for disaggregation it was suggested that the VSG was internalised by a similar mechanism to that of non-agglutinating VSG antibody complexes. The VSG would then be delivered to a degradative compartment within the cell or recycled back to the plasma membrane. These possibilities were investigated and it was found that the VSG was not proteolysed and therefore gross degradation did not occur (O'Beirne *et al.*, 1998). Further studies into the fate of the VSG were undertaken by Brabazon (1999). This worker found that the VSG, internalised from surface immune complexes, was returned to the exterior face of the plasma membrane somewhat faster than the degraded antibody in these complexes was exocytosed to the exterior medium.

1.9 Endocytosis in *T. brucei.*

Endocytosed macromolecules in *T. brucei* have been shown to be internalised exclusively from the flagellar pocket, located towards the posterior end of the cell, into

coated pits and vesicles (Shapiro and Webster, 1989) that bud from the pocket membrane and which appear to fuse and then release their contents into intracellular compartments comparable to the endosomes of higher eukaryotic cells (Langreth and Balber, 1975, Webster, 1989 & Webster, 1989).

The ultrastructure of the flagellar pocket itself has been conserved throughout the family, *Tryanosomatidae*. The plasmalemma of the cell body first invaginates to form the flagellar pocket and then evaginates to cover the flagellum. Once outside the region of the flagellar pocket, the flagellum comes to lie immediately adjacent to the cell body, where its covering membrane becomes secondarily attached to the plasma membrane covering the cell body along a narrow line, known as the flagellar attachment zone, before extending beyond the most anterior part of the cell as a free, unattached flagellum, still encased in its covering plasma membrane. The attachment zone of the flagellum is comprised of a number of bead-like densities that follow a helical course around the cell, parallel to the pellicular microtubules. These junctional complexes, compared to the hemi-desmosomal junctions of epithelial cells, are 25 nm in diameter and do not progress beyond the anterior part of the pocket. The mouth of the flagellar pocket is bordered by a flagellar ring, the function of which is probably to stabilize the position of the flagellar pocket within the pellicular array (Dolan *et al.*, 1986). The flagellar ring may also have a role in keeping the flagellar pocket open, ensuring a constant supply of metabolites for uptake by the trypanosome.

Recent progress on the definition of the endosomal sub-compartments was dependent on the development of antibodies against specific markers (Field *et al.*, 1998, Jeffries, 2001 , Morgan, 2001, Alexander, 2002 & Pal, 2002) and their application in high-resolution and immunoelectron microscopy (Grunfelder *et al.*, 2002 & Engstler, 2004). The clathrin-coated pits of the flagellar pocket are lined on their extracellular face by the GPI-anchored variant surface glycoprotein. Plasma membrane-derived clathrin-coated vesicles (CCVs), which rapidly shed their clathrin lattice but retain the lumenal VSG coat, are on the average 135 nm in diameter and have been termed class I CCVs. Antibodies against the small GTPase RAB5A, a marker for early endosomes in mammalian cells, mainly react with cisternal and vesicular structures close to the lysosome (Engstler *et al.*, 2004). Late endosomes, defined by the presence of RAB7, are also located close to the lysosome, but distinct from the RAB5-reactive area. The posterior half of *T. brucei* contains extended or curved sheet-like structures, at least half of which are decorated with RAB11, an established marker for recycling endosomes. Both early and recycling

Fig 1.12. Morphology of bloodstream forms of *T. brucei* during the cycle of aggregation-disaggregation that occurs during incubation with purified IgM anti-VSG antibodies.

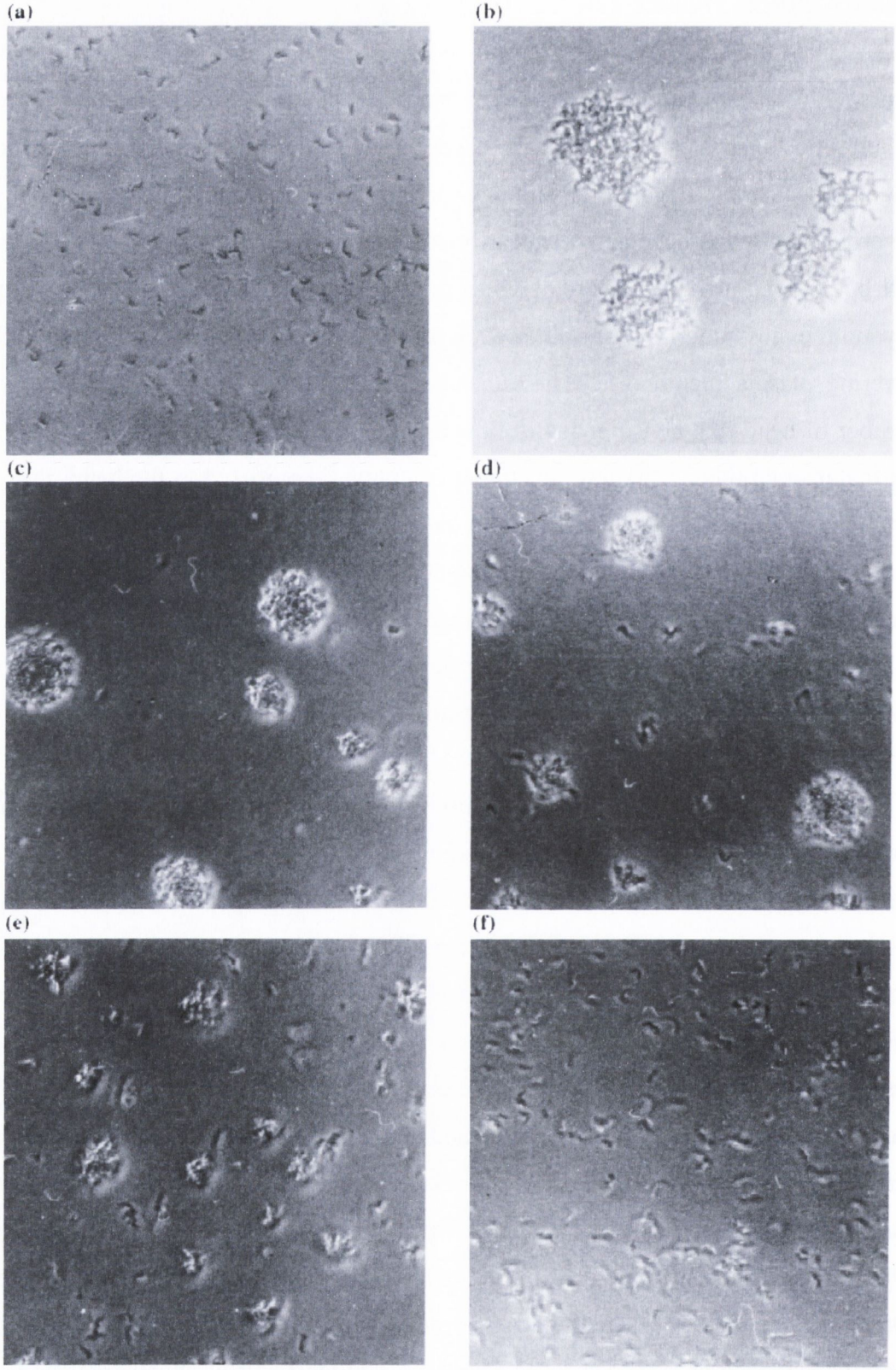

endosomes give rise to a second smaller type of CCV; class II CCVs, average diameter 50-60 nm (Overath and Engstler, 2004), which lack a lumenal VSG coat. Flat disc-like structures that contain high concentrations of both RAB11 and VSG were also observed (Overath and Engstler, 2004). These structures fuse with the flagellar pocket and are designated exocytic carriers (EXCs). It has been suggested that these vesicles arise from recycling endosomes and return endocytosed VSG back to the flagellar pocket (Grunfelder *et al.*, 2003). A schematic drawing of the endosomal structures in the posterior half of the cell is shown in Fig 1.13.

The endocytic pathway of fluid phase cargo is depicted in Fig 1.13. The fluid phase marker fluorescent dextran was used to study this pathway (Engstler *et al.*, 2004). The uptake of this marker is biphasic and consistent with a two-step model comprising a fast, reversible flow between the flagellar pocket and endosomes and a slower transfer from endosomes to the lysosome. The initial rate of internalisation suggests the formation of six to seven class I CCVs per second. The net rate of uptake is only about 10 % of the initial rate implying that 90 % of the pinocytosed dextran is recycled to the flagellar pocket. Pinocytosed dextran initially colocalizes with clathrin-containing structures close to the flagellar pocket and is then observed in RAB5-positive early endosomes. From there it fills the late endosomal compartment and eventually accumulates in the lysosome. Using the fluid phase marker horseradish peroxidase (HRP), it has been observed that all endosomal compartments including cisternal recycling endosomes and the EXCs are positive for this marker (Engstler *et al.*, 2004). This suggests that some recycling of the fluid phase cargo occurs *via* this route. Class II CCVs were positive for HRP and ferritin and from this data it was postulated that the class II CCVs function in collecting fluid phase cargo from early and recycling endosomes and that these vesicles subsequently deliver their content to late endosomes and perhaps directly to the lysosome (see Fig 1.13). Bloodstream forms of *T. brucei* are also capable of endocytosing low-density lipoprotein (Coppens *et al.*, 1987) and transferrin (Webster and Grab, 1988) *via* specific receptors (Grab *et al.*, 1993, Salmon, 1994 & Steverding, 1995) located in the plasma membrane lining of the flagellar pocket. It has been reported that *T. brucei brucei* are non-infective to humans because they are sensitive to the cytolytic activity of normal human serum (Laveran, 1902) (Rifkin, 1978, Rifkin, 1984). Two serum proteins haptoglobin-related protein (HPR) and apolipoprotein L1 (apoL-I) have been proposed as candidates for providing the trypanolytic activity. It has been argued that the characterization of the mechanism of resistance of *T. b. rhodesiense*, as well as the study of

the phenotype of lysis induced by apoL-I, indicates that apoL-I is the sole factor that is responsible for trypanolysis (Pays *et al.*, 2006). Apolipoprotein L-I (apoL-I) is a human-specific serum apolipoprotein bound to high-density lipoprotein (HDL) particles (Duchateau *et al.*, 1997, Page, 2001, Duchateau, 2001). This protein kills the African trypanosome *Trypanosoma brucei brucei*, except subspecies adapted to humans (*T. b. rhodesiense, T. b. gambiense*) (Poelvoorde *et al.*, 2004, Vanhamme, 2004). Trypanosome lysis results from uptake of apoL-I into the lysosome (Vanhamme *et al.*, 2003), and is thought to involve HDL receptor–mediated uptake of the lytic factor (Rifkin, 1991), which would lead to disruption of the lysosomal membrane following lipid peroxidation (Shimamura *et al.*, 2001). Trypanolysis occurs through high-density lipoprotein-particle-mediated endocytosis. Mainly as a result of the pioneering work of Mary Rifkin (Rifkin, 1978), the trypanolytic activity was shown to be associated with high-density lipoprotein (HDL) particles, in particular with the densest HDL subfraction, HDL3 (Gillett and Owen, 1991). Further studies indicated that receptor-mediated endocytosis of these HDL particles by the trypanosome was involved in lysis. In this case, internalization of the lytic particles would involve their delivery to increasingly acidic compartments of the endocytic pathway.

It is probable that bloodstream form trypanosomes do not have an intracellular pool of ferritin (the iron storage protein), although they require iron for several iron containing enzymes, such as the trypanosomal ribonucleotide reductase (Dormeyer *et al.*, 1997). Thus the plasma is an important source of iron for bloodstream form trypanosomes, which is obtained by receptor-mediated endocytosis of host transferrin *via* a specific transferrin receptor (Grab *et al.*, 1992, Salmon, 1994 & Steverding, 1994). The receptor for transferrin has been identified as a heterodimeric protein of very low abundance (approx. 3000 molecules per cell). The receptor is encoded by two homologous expression site-associated genes, ESAG6 and ESAG7 (Steverding *et al.*, 1994, Chaudhri, 1994). Binding of holotransferrin to the receptor takes place in the flagellar pocket. Transferrin bound to its GPI-anchored receptor is presumably translocated into the cell interior by bulk membrane flow. The ligand-receptor complex is delivered into endosomes where the acidic pH triggers the release of iron from transferrin (Maier and Steverding, 1996, Dautry-Varsat, 1983). The apotransferrin dissociates from the receptor and is brought to lysosomes where it is proteolytically degraded (Steverding *et al.*, 1995). The resulting large peptide fractions are released from the trypanosomes while iron remains cell-associated (Steverding *et al.*, 1995). The receptor is probably recycled to the membrane of

the flagellar pocket. It should be noted that the uptake of transferrin in bloodstream forms of *T. brucei* resembles the internalisation of low-density lipoproteins (Goldstein *et al.*, 1975) and asialoglycoproteins (Bridges *et al.*, 1982) by mammalian cells. The rate of transferrin uptake is approximately 4.5 molecules/receptor/hour in trypanosomes (Steverding, 1998 & Steverding, 1995).

1.10 Antibody mediated endocytosis in *T. brucei*

Many workers in the past have found that antibody against surface antigens in trypanosomes caused a redistribution of their surface coat, a process described as patching and capping (Barry, 1979; Webster *et al.*, 1990). In trypanosomes, capping involves movement of the antibody-antigen complexes from a position of random patching over the surface of the cell to the flagellar pocket toward the posterior end of the cell, where internalisation of the complex was reported to occur. For a number of years it was unclear whether a second layer of antibody was required in order to induce endocytosis of the antigen-antibody complex with conflicting reports occurring in the literature. However, two intensive studies into the phenomena of anti-VSG antibody mediated endocytosis in bloodstream forms of *T. brucei* have been reported. Firstly, it was confirmed by (Russo *et al.*, 1993) that a second layer of antibody was not required to stimulate the process of antibody mediated endocytosis in *T. brucei*. These workers also observed internalisation of anti—VSG antibody to endosomal compartments by use of Fluorescein labelled anti—VSG antibody and biotinylated anti-VSG antibody in conjunction with fluorescence microscopy. The second report (O' Beirne, 1994) was a more in depth investigation of the fate of the internalised anti—VSG antibodies. The surface distribution of the antibody was studied using standard epi—fluorescence microscopy. It was found that when purified, fluorescein-labelled anti—VSG antibodies were allowed to bind to live cells at 4°C (where endocytosis is arrested), and the cells, following washing, allowed to warm gradually to room temperature (24°C) while in suspension, extensive redistribution of the antigen-antibody complex occurred within the first 2.5 min. By this time, the labelled antibody is found in a patchy distribution over the surface of the cell with much of the antibody located toward the posterior blunt end of the cell. By 10 min, further concentration of the FITC labelled antibody has occurred with most patches further coalesced into an intensely fluorescent cap in the region of the flagellar pocket with one or more relatively large satellite patches close to the cap. By 30

Fig 1.13. Endocytosis in *T. brucei.* Adapted from (Overath and Engstler, 2004).

A. Schematic drawing of the ultrastructure of *T. brucei.*
B. Enlarged view of structures in the posterior part of a trypanosome.
C. Flow diagram of VSG and fluid phase cargo through endosomal structures. Black arrows indicate trafficking steps common to VSG and fluid phase cargo, while red arrows symbolize steps for fluid phase only.

Ax – axoneme, BB – basal body, CCV-G, clathrin-coated vesicles budding from the Golgi apparatus, CCV I – class I clathrin-coated vesicles, CCV II – class II clathrin-coated vesicles, EE – early endosome, ER – endoplasmic reticulum, EXC – exocytic carrier, FAZ, flagellar attachment zone, FL – flagellum, FP – flagellar pocket, G - Golgi apparatus, K – kinetoplast, L – lysosome, LE - Late endosome, Mt – mitochondrion, N – nucleus, PFR – paraflagellar rod, PMT – pellicular microtubule, RE – recycling endosome, SC – surface coat, VSG – variant surface glycoprotein.

Fig 1.13. Endocytosis in *T. brucei*. Adapted from (Overath and Engstler, 2004).

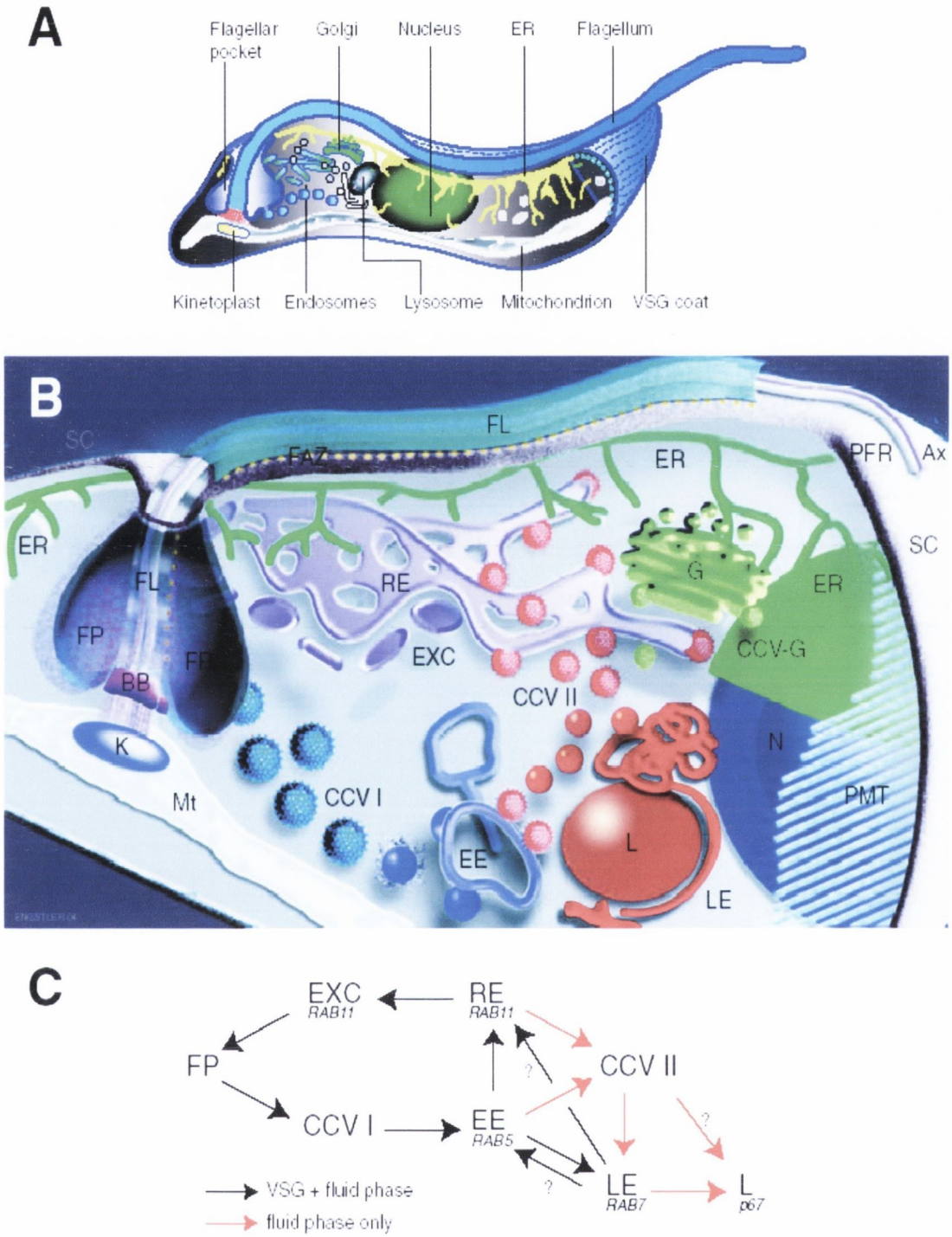

min, the cap breaks up into three or four intensely fluorescent spots, stretching in a roughly linear fashion from the flagellar pocket towards the mid region of the cell. By 45 min, the temperature of the cell suspension was within 1°C of room temperature and part of the intense fluorescence had already been lost from the cells (Fig 1.14). If the entire incubation was carried out at 30°C, the redistribution was apparently complete before a sample could be taken for fixation. Consequently, the spatial redistribution of the antibody attached to these parasites under the normal physiological condition in a mammalian host must occur very rapidly indeed. Further experiments provided evidence that the labelled antibody is extensively degraded within the endosomal system of the trypanosome following endocytosis and that this process could be arrested by a number of protease inhibitors *e.g.* TLCK, PMSF, in addition to compounds which disturb the pH of the endosomal compartments *e.g.* Chloroquine, monensin (O' Beirne, 1994). These experiments were carried out using a continuous spectrofluoremetric assay based upon the pH dependence of fluorescence emission of fluorescein labelled anti-VSG antibody. Cells were incubated with fluorescein labelled anti-VSG antibody at 4°C and subsequently incubated at 30°C where endocytosis of the ligand was assayed by measuring the decrease in fluorescence observed as the ligand entered the endosomal compartments. Following degradation of the antibody, the proteolytic fragments, including those containing covalently-linked Fluorescein, were exported from the cell *via* exocytosis which was assayed by measuring the increase in fluorescence as the fluorescent, proteolytically-cleaved ligand left the low pH of the endosomal compartment and re-appeared in the high pH environment of the extracellular medium. The rise in fluorescence during the export phase to a value higher than the initial position before entry is due to the proteolysis reaction, which creates a different environment for the covalently attached fluorescein ligand. This assay has been validated by several independent measures of endo/exocytosis, and has allowed the rapid and systematic effect of specific inhibitors of endocytosis to be monitored.

The study by O' Beirne (1994) has lead to a better understanding of the process of endocytosis in bloodstream form trypanosomes and has also identified a number of important inhibitors which will be beneficial to any future work in the area of receptor mediated endocytosis in *T. brucei*. Clearly, the process of antibody mediated endocytosis and the consequent degradation of the internalised antibody may play a vital role in aiding the bloodstream form trypanosomes to evade, for a time at least, the humoral immune response of the mammalian host prior to a VSG switching event.

1.11 Aims of the Project

This work is an attempt to resolve the location of the GPI—PLC and its function in bloodstream forms of *T. brucei brucei.* Specifically the objectives are threefold:

a) To discover the true localization of the GPI—PLC in bloodstream forms of *T. brucei.* Surface biotinylation and iodination of trypanosomes as well as immunofluoresence and ELISA were the techniques used to determine this localization.

b) To study the role of the GPI—PLC in the mechanism of aggregation/disaggregation and its role in the endo/exocytic cycle of *T. brucei.* Furthermore, to investigate the mechanism of disaggregation following aggregation of bloodstream forms of *T. brucei.*

c) And finally to investigate further the phenotype of the double deletion mutant for the GPI—PLC.

Fig 1.14. Redistribution and endocytosis of anti-VSG antibody from the cell surface of bloodstream form trypanosomes under energised conditions. Adapted from O'Beirne (1994). Plate (a) shows the surface distribution of FITC labelled anti-VSG antibody following incubation with fixed bloodstream form trypanosomes. Bloodstream form cells were also incubated with Fluorescein labelled anti-VSG antibody at 4°C and washed to remove unbound antibody. The cell suspension was then allowed to warm gradually to room temperature (24°C). By 2.5 min, the labelled antibody was found in a patchy distribution over the surface of the cell with much of the antibody located toward the blunt posterior of the cell. By 10 min, further concentration of the FITC labelled antibody occurred with most patches further coalesced into an intensely fluorescent cap in the region of the flagellar pocket with one or more relatively large satellite patches close to the cap. By 30 min, plate (b), the cap had broken up into three or four in tensely fluorescent spots, stretching in a roughly linear fashion from the flagellar pocket towards the mid-region of the cell. By 45 min, plate (c), the temperature of the cell suspension was within 1°C of room temperature and most of the intense fluorescence had already been lost from the cell.

Fig 1.14. Redistribution and endocytosis of anti-VSG antibody from the cell surface of bloodstream form trypanosomes under energised conditions.

(a). Surface distribution of FITC-labelled anti-VSG IgG on bloodstream form trypanosomes fixed in 3 % paraformaldehyde

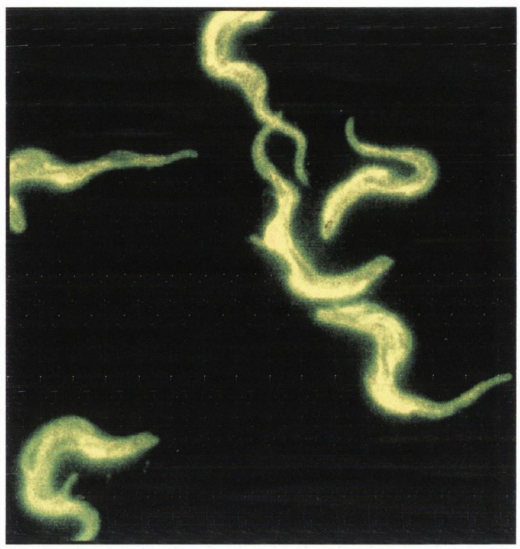

(b). Distribution of VSG on cells after 30 min at room temperature following incubation at 4°C with FITC-labelled anti-VSG IgG

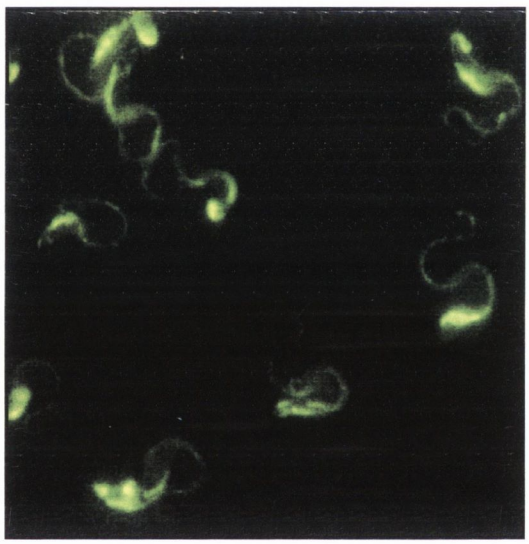

(c). Distribution of VSG on cells after 45 min at room temperature following incubation at 4°C with FITC-labelled anti-VSG IgG

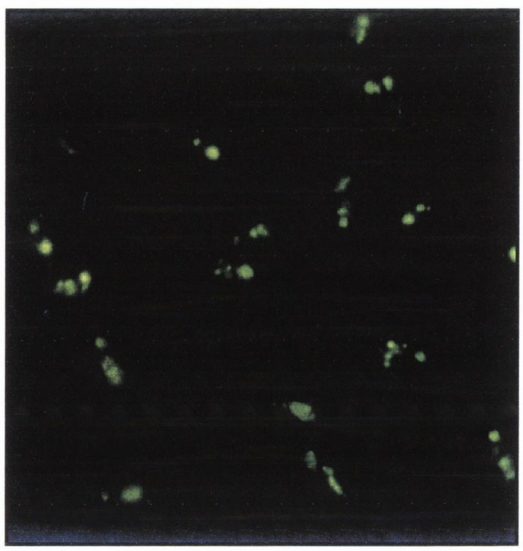

Chapter 2

Materials & Methods

2.1 Equipment

All reagents used were weighed using a Mettler (model KTT) top loading balance or an Oertling analytical balance (model R20) as appropriate. All solutions were made using distilled deionised water unless otherwise stated. Liquid volumes from 1 µl to 5 mls were dispensed using Gilson Pipetteman pipettes. The hydrogen ion concentration of all solutions was measured using an Amagruss glass electrode, which was connected to an EDT RE357 microprocessor pH meter. The hydrogen ion concentration of solutions was adjusted as necessary using HCL (12 M) and NaOH (5 M). The pH meter was calibrated using standard buffer solutions of pH 4, 7 and 10 from Sigma. For absorbance readings, the Cary 50 UV spectrophotometer was used. Centrifugations were carried out using a Mikro 200 bench centrifuge, a Sorvall RC5C refrigerated centrifuge, a Rotanta 460R refrigerated centrifuge and a Sorvall Discovery 100 ultracentrifuge.

Purification of bloodstream forms of *T. brucei*

2.1.1 Source of cells

Trypanosoma brucei brucei (MITat 1.1) was derived from *T. brucei* 427-12/ICI (Holder & Cross, 1981) which was originally isolated by Cunningham and Vickerman (1962) from the blood of a sheep in 1960. The organism was recloned in rats by Voorheis (1974) from which first generation cells were obtained. Organisms used in this study consisted solely of monomorphic long slender bloodstream forms.

GPI-PLC$^-$ mutant bloodstream form trypanosomes and their wild-type parent (MITat 1.2) were a kind gift from Dr. H. Webb and Dr. M. Carrington, University of Cambridge, Cambridge, U.K.

2.1.2 Preparation of stabilates

Heparinized microhaematocrit capillary tubes (Lennox) were three quarters filled with infected blood (approximately 100 µl of blood; 1 x 10^9 cells/ml), which contained glycerol (10%, w/v) and EGTA (100 mM). The infected blood, containing anti-coagulant (EGTA), was cooled to 4°C before mixing with the glycerol cyroprotectant. Both ends of

the capillary tube were flame sealed and the resulting stablilates cooled slowly to –80°C over a period of two hours before storage under liquid nitrogen at –196°C.

2.1.3 Infection of rats

Stabilates were withdrawn from liquid nitrogen immediately prior to use and were allowed to thaw at room temperature. The contents of a single stabilate were flushed with 0.5 ml of TSB buffer, pH 8.0 (see Table 2.1). The host used to propagate the trypanosomes were large male Wistar rats. These were infected by intraperitoneal injection of the stabilate suspension, resulting in a parasitemia of approximately 10^9 cells per ml of blood three days post injection.

2.1.4 Collection of infected rat blood

The infected rats were anaesthetized with sodium pentobarbitone BP (0.4 ml/rat) after approximately 72 h. Blood was withdrawn by aortic puncture using a 20 ml syringe containing 1-2 ml EGTA (100 mM, pH 7.5) attached to a 21-gauge needle. Infected blood was then placed in nitric acid-cleansed, glass pyrex centrifuge tubes which had been washed thoroughly in distilled water followed by iso-osmotic phosphate buffer, (TSB), pH 8.0; (Table 2.1) containing glucose, sucrose and adenosine. Approximately 10-15 mls of blood was obtained from each rat.

2.1.5 Purification of *Trypanosomes* from infected blood

The trypanosomes were isolated from blood according to the method of Lanham (1968) incorporating the modifications of Owen and Voorheis (1976) and Lonsdale-Eccles and Grab (1987). The infected blood was centrifuged at 650 ***g*** for 10 min at four degrees in a Rotanta 460A centrifuge, resulting in a layer of red blood cells at the bottom of the centrifuge tube, above which lay a layer of trypanosomal cells. The layer of serum lying above the trypanosomes was aspirated to waste and replaced with an equal volume of ice-cold TSB buffer, pH 8.0 (Table 2.1). The trypanosomes were resuspended in this buffer solution, care being taken to disturb the red blood cells as little as possible. The resulting suspension was then applied, at 4°C, to a Whatman DEAE-52 column (0.6 cm x 10 cm;

approximately 10 ml bed volume) that had previously been equilibrated with the glucose containing TSB buffer (Table 2.1). Trypanosomes appear in the void volume of the column whilst the red and white blood cells, platelets and non-viable trypanosomes remained bound to the column. Fractions containing the unbound trypanosomes were collected and washed twice by centrifugation/resuspension (600 ***g*** x 10 min, 4°C) before resuspension in buffer. All procedures were carried out at 4°C.

2.1.6 Cell counting

The cell density of each stock suspension was determined by counting samples, which had been diluted 1:200 in iso-osmotic Tes buffer, pH 7.5 (Table 2.1), using a Neubauer haemocytometer with a silvered stage and a Zeiss light microscope.

Immunisation of animals for the production of antibodies

2.1.7 Production of anti-VSG antibodies

New Zealand White rabbits (3.5 kg) were immunised with 6 x 10^4 purified bloodstream forms of *T. brucei* (MITat 1.1) by intravenous injection for the production of anti-VSG antibodies. Blood was withdrawn from an immunised rabbit on day 6 post-immunization for IgM anti-VSG antibodies and day 10 post-immunization for IgG anti-VSG antibodies using heparin as an anticoagulant. Following centrifugation (1,000 ***g***, 10 min) the upper plasma layer was removed and recentrifuged (100,000 ***g***, 1 h). Lipid was removed from the plasma layer by aspiration. Resulting clear serum was divided out into suitable size fractions and stored at –20°C. IgM antibodies were purified as described in Section 2.6.1. IgG antibodies were subsequently purified using a Protein A Sepharose column as described in Section 2.6.3.

2.1.8 Production of anti-GPI-PLC antibodies

New Zealand White rabbits (3.5 kg) were inoculated with the purified recombinant GPI-PLC (~150 μg) in 1 ml of Freunds Complete Adjuvant (Sigma) into both popliteal lymph nodes. Subsequently the rabbits were boosted three times with the

Component	TES Buffer	Trypanosome Separation Buffer (TSB)	Phosphate Buffered saline (PBS)
NaCl	138	44	136
KCl	4	5	3
$MgCl_2$	3		
Na_2HPO_4	1	57	16
KH_2PO_4			3
NaH_2PO_4		3	
Tes	30		
Glucose	10	10	10 *
Sucrose	70		40*
Sodium Azide			15*
Adenosine	0.1	0.1	0.1 *
pH	7.4	8.0	7.5

Table 2.1. Composition of frequently used buffers.

All values, except those for pH, refer to concentration in millimoles per litre.

* These components are only added to the buffer when using cells. The Sodium azide (NaN_3) is added only after fixation of cells to prevent bacterial growth.

antigen (~50 μg per boost) in 1 ml Freunds Incomplete Adjuvant at fortnightly intervals. At week seven, an immune serum sample was withdrawn and following an ELISA, the antibody titre was found to be sufficient for use and the animal was exsanguinated. Following centrifugation (1,000 ***g***, 10 min) the upper plasma layer was removed and recentrifuged (100,000 ***g***, 1 h). Lipid was removed from the plasma layer by aspiration. Resulting clear serum was divided out into suitable size fractions and stored at –20°C. Antibodies were subsequently purified using a Protein A Sepharose column or a GPI-PLC affinity column as described in Section 2.1.11. and Section 2.1.12. respectively.

Purification of antibodies

2.1.9 Purification of anti-VSG IgM antibodies.

Plasma was incubated with polyethylene glycol 6000 (8%, w/v) overnight at 4°C with constant gentle stirring. The solution was centrifuged (1600 ***g***, 30 min, 4°C) and the supernatant removed. The pellet was resuspended in approximately 5 ml of high ionic strength Tris buffer (Tris-HCl, 100 mM, pH 8.0; NaCl, 150 mM) by gentle agitation over a period of 1h. The resuspended pellet was then passed through a 0.22 μm pore filter by positive pressure to remove any aggregates and protein that was not fully in solution.

The IgM antibody fraction was then purified using three successive chromatographic steps. Chromatography by gel filtration on Ultrogel AcA34 (40 cm x 2.5 cm) was the first step (Fig. 2.1). The IgM antibody fraction, peak 1 was applied to a protein A Sepharose column to remove any trace amounts of IgG antibody remaining (Fig. 2.2). The IgM antibody fraction was then applied to a Zn^{2+} affinity column to remove additional contaminating proteins; the predominant protein contaminating the preparation at this stage was tentatively identified as α_2-macroglobulin (Fig. 2.3). Fractions were collected after each purification step and protein content was monitored by measuring absorbance at 280 nm. All purification steps were performed at room temperature as preliminary results indicated that the IgM antibody behaved as a cryoglobulin. The purified IgM antibody was concentrated when necessary by ultracentrifugation in an Amicon ultracentrifugation device (2 ml capacity) that contained a membrane with a 10,000 molecular weight cut off. Antibody solutions were then divided into suitable size fractions and stored at –20°C until required.

Figure 2.1. Separation of IgM antibody from plasma treated with polyethylene glycol 6000 on Ultrogel AcA34.

The polyethylene glycol 6000 precipitate of protein was resuspended in approximately 5 ml of high ionic Tris buffer (Tris-HCl, 0.1 M, pH 8.0; NaCl, 0.15 M) and then applied to an Ultrogel ACA34 column (40 cm x 2.5 cm) equilibrated in the same Tris buffer at room temperature. The protein was eluted at a flow rate of 30 ml/h and collected in 5 ml fractions. The eluant was monitored for protein at 280 nm.

Figure 2.2. Chromatography of IgM antibody on protein A Sepharose.

The pooled IgM antibody containing fractions from chromatography on Ultrogel were applied to a protein A Sepharose column (2 ml bed volume) equilibrated with high ionic strength Tris buffer (Tris-HCl, 0.1 M, pH 8.0; NaCl, 0.15M). The column was washed with the same Tris buffer and eluant monitored for protein at 280 nm. The IgM antibody containing samples (flow through) were collected in 1 ml fractions. Following extensive washing of the column with Tris buffer until no further protein eluted any bound IgG antibody was specifically eluted with glycine buffer (glycine.HCl, 0.1 M, pH 3.0). The eluant was immediately neutralized with Tris base.

Figure 2.3. Chromatography of IgM antibody on a Zn^{2+} affinity column.

The pooled IgM antibody fractions from chromatography on a protein A Sepharose column was applied to a zinc affinity column (2 ml bed volume) equilibrated with high ionic strength Tris buffer (Tris-HCl, 0.1 M, pH 8.0; NaCl, 0.15M). The column was washed with Tris buffer until no further protein was detected in the eluant and then the following buffers were applied as indicated: (1) phosphate buffer (sodium phosphate, 0.1 M, pH 6.5); (2) phosphate buffer containing NaCl (0.8M); (3) acetate buffer (sodium acetate, 0.1M, pH 4.5; NaCl, 0.15 M); (4) EDTA solution (EDTA, 0.05 M, pH 7.5; NaCl, 0.5 M). The eluant was collected in 2 ml fractions and monitored for protein at 280 nm.

Fig 2.1

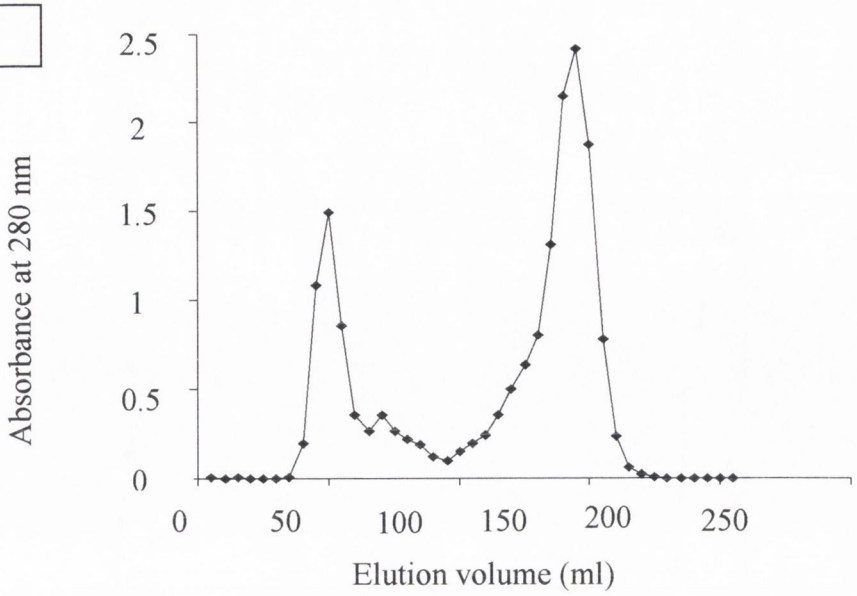

Fig 2.2

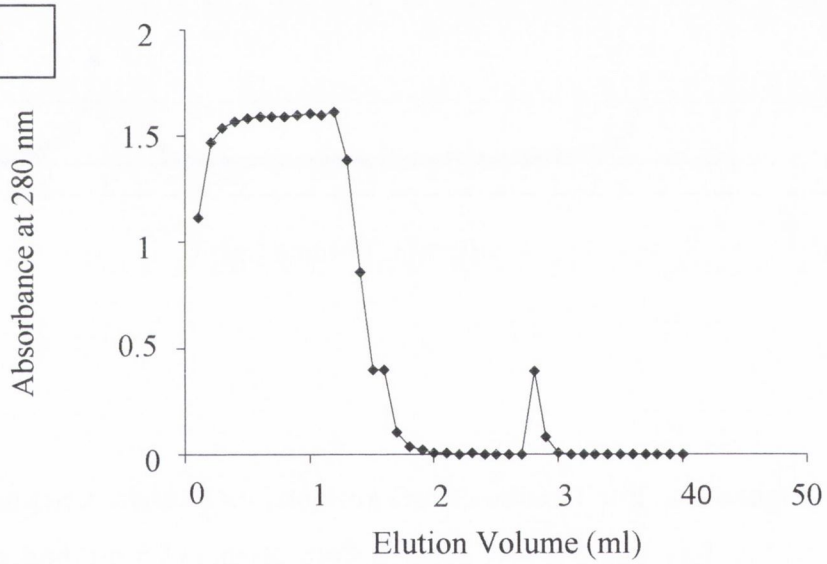

Fig 2.3

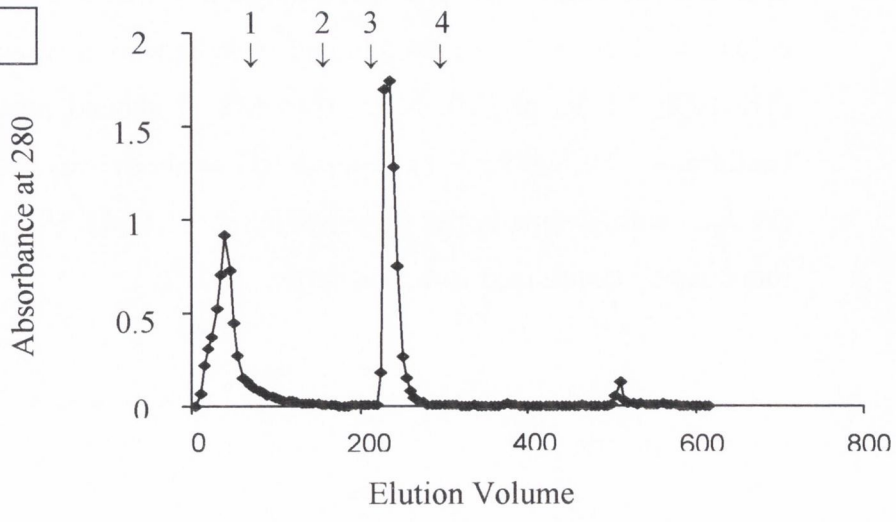

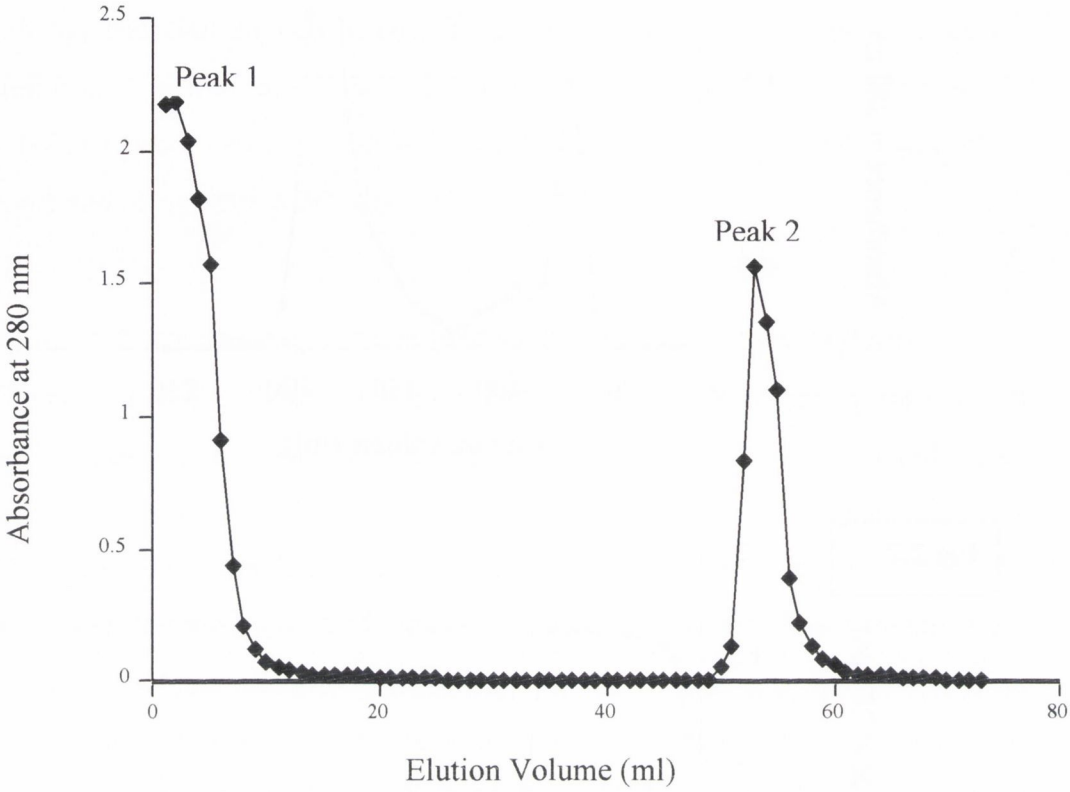

Figure 2.4. Purification of IgG antibody on Protein A Sepharose.

IgG antibody was purified from plasma (1.5 ml diluted to 5 ml with equilibration buffer) by passage through a Protein A sepharose CL-4B column (2.2 cm x 1 cm) equilibrated with high ionic strength Tris buffer (Tris-HCl, 0.1 M, pH 8.0; NaCl, 0.15 M). Unbound protein eluted with equilibration buffer (Peak 1). Bound IgG antibody was specifically eluted (Peak 2) with glycine buffer (glycine-HCl, 0.1 M, pH 3.0). The eluant was immediately neutralized with Tris buffer.

2.1.10 Preparation of Zn^{2+} affinity column.

A Zn^{2+} affinity column was prepared as described by Porath *et al.* (1975) and Kurecki *et al.* (1979). Briefly, a 2 ml column was packed with iminodiacetic acid agarose. The column was washed with at least 10 column volumes of EDTA (.05 M, pH 7.5) containing NaCl (0.5 M) followed by the same volume of distilled deionized water. The column was then converted to a Zn^{2+} chelate by equilibrating with $(CH_3COO)_2Zn.2H_20$ (22 mM). The column was washed with acetate buffer (sodium acetate, 0.1 M, pH 4.5; NaCl, 0.15 M) before equilibrating with starting buffer (Na_2HPO_4, 0.1M, pH 6.5; NaCl, 0.15 M). The column was stored at 4°C in starting buffer containing sodium azide (0.02%, w/v).

2.1.11 Purification of anti-VSG IgG antibody

IgG antibodies were purified from plasma by passage through a Protein A Sepharose CL-4B column equilibrated with Tris buffer (Tris-HCl, 0.1 M, pH 8.0; NaCl, 0.15 M). The column was washed with Tris buffer and any non-bound protein eluted was collected in 1 ml fractions and measured for protein by absorbance at 280 nm. The column was extensively washed until no further protein was eluted. The bound IgG was then specifically eluted (Fig 2.4) with glycine buffer (glycine-HCl, 0.1 M, pH 3.0). The eluant was immediately neutralised with Tris base. Fractions (1 ml) were collected. Protein content was monitored by measuring absorbance at 280 nm. The purified IgG antibody was concentrated when necessary by ultracentrifugation in a vivaspin (centrifugation device) (6 ml capacity) that contained a membrane with a 5,000 molecular weight cut off (Section 2.1.63). Antibody solutions were then divided into suitable size fractions and stored at –20°C until required.

2.1.12 Affinity purification of anti-GPI-PLC antibodies

Epoxy-activated Sepharose 6B beads (0.5 g; swells to 1.5 ml) were swollen in distilled deionized H_2O for 15 min. The swollen gel was transferred to a sintered glass funnel and washed with 50 mls of dH_2O (100 ml/g beads). The gel was then washed with 20 ml coupling buffer ($NaHCO_3$, 0.25 M, pH 10; NaCl, 0.5 M) and quickly transferred to a solution of purified maltose binding protein-GPI-PLC fusion protein in coupling buffer (1

mg/ml), giving a final 1:1 ratio of gel: protein solution. The suspension was rotated end over end for 16 h at room temperature. Excess ligand was washed away using coupling solution followed by distilled water and solutions of low and high pH (0.1 M acetate buffer, pH 4.0, NaCl, 0.5 M and 0.1 M bicarbonate buffer, pH 8.0, NaCl, 0.5 M). Remaining excess groups were subsequently blocked overnight at room temperature using ethanolamine (1 M). The affinity column was washed with Tris, pH 8.0 and stored in this buffer containing sodium azide, (15 mM) at 4°C.

Anti-GPI-PLC antibody was purified from serum by passage through the GPI-PLC affinity column equilibrated with Tris buffer (Tris-HCl, 0.1 M, pH 8.0; NaCl, 0.15 M). The column was washed with Tris buffer and any non-bound protein eluted was collected in 1 ml fractions measured for protein by absorbance at 280 nm. Following extensive washing of the column with Tris buffer until no further protein eluted, the bound IgG antibody was specifically eluted with glycine buffer (glycine-HCl, 0.1 M, pH 2.5). The eluant was immediately neutralized with Tris base. The purified anti-GPI-PLC IgG antibody was concentrated when necessary by using vivaspin centrifugal concentrators with a MWCO of 5000. (Sartorius). Concentrated antibody was divided into suitable portions and stored at -20°C.

SDS-PAGE and Western Blot analysis

2.1.13 SDS-Polyacrylamide Gel Electrophoresis (SDS-PAGE)

SDS-PAGE was performed using a modification of the method of Laemmli (1970). Gel components are given in Table 2.2. Ammonium persulphate solutions were prepared immediately prior to use. Samples for gel electrophoresis were prepared in an equal volume of sample buffer (1.5 M Tris buffer, pH 6.8, 110 µl; glycerol, 1 ml; 0.2% bromophenol blue in ethanol, 60 µl; 20% (w/v) SDS, 1 ml; made up to a final volume of 5 ml with deionised water) containing DTT (30 mg/ml). All samples were boiled for 5 min prior to loading. Running buffer contained glycine (28.8 g), Tris base (6 g), and SDS (1 g) in a final volume of 1 L. Gels were run at a constant current of 19 mA and were subsequently stained in a solution of methanol: acetic acid: water (10:7:83 by volume) containing 0.2% Coomassie Brilliant Blue R-250. Destaining was carried out in methanol: acetic acid: water (10:7:83 by volume) with several changes.

Gel Components.	**10% Separating Gel**	**15% Separating Gel**	**5% Stacking Gel.**
40% acrylamide/ 1% bisacrylamide stock solution.	5 ml	7.5 ml	500 µl
1.5M Tris pH 8.8	5ml	5 ml	-
0.5M Tris pH 6.8	-	-	1.25 ml
10% SDS solution	200 µl	200 µl	50 µl
Distilled/deionised water.	9.75 ml	7.25 ml	3.165 ml
10% Ammonium persulfate solution.	50 µl	50 µl	25 µl
TEMED	10 µl	10 µl	10 µl

Table 2.2. Components of SDS-PAGE gels

2.1.14 Preparation of SDS-PAGE gels for autoradiography.

After staining with Coomassie blue and destaining as described above, gels containing radioactive samples were dried using a slab gel dryer (Savant) connected to a vacuum pump for 1 h 30 min at 80 °C. Dried gels were placed in film cassettes with a Kodak X-Omat LS film (Sigma) on top, and left at –80 °C for varying periods of time (from overnight to thirty days) depending on the amount of labelled protein present in the sample loaded onto the gel. Film was developed using an X-ray film processor (Fuji).

2.1.15 Semi-Dry Western Blotting of SDS-PAGE gels

Transfer of protein to polyvinylidene difluoride (PVDF) or nitrocellulose was carried out by the method of Matsudairi (1987). The electrophoresed gel, PVDF/nitrocellulose sheets and sections of chromatography paper were soaked in blotting buffer (Caps, 10 mM; pH 11, methanol, 10% v/v containing 1.85 ml of 20% SDS per litre) for 10 min approx. The gel was then overlaid onto the PVDF/nitrocellulose sheet ensuring no air bubbles were present. Soaked chromatography paper was placed on both sides of the gel and PVDF/nitrocellulose forming a sandwich arrangement with 6 sheets of chromatography paper on either side. This assembly was then placed in a Hoefer semi-dry blotter and proteins transferred at 100 mA for 1hr. Following transfer, the markers on the PVDF were cut out and subsequently stained with Coomassie Brilliant Blue R-250 in a solution of methanol: acetic acid: water (40:10:50 by volume) and the gel Coomassie Blue stained to ascertain the efficiency of transfer.

2.1.16 Immunoblotting and the enhanced chemiluminesence protocol

The PVDF/nitrocellulose membrane was blocked in 5%(w/v) marvel and 0.05%(w/v) Tween (TBST, 150 mM NaCl, 5mM Tris, pH 7.4, containing 0.05% Tween) overnight at 4°C or at room temperature for 1 h, with gentle agitation. The membrane was washed (4 x 5 min) in TBST and incubated with primary antibody (diluted in 1%(w/v) marvel in TBST) overnight at 4°C with gentle agitation. The PVDF/nitrocellulose membrane was washed (4 x 5 min) and incubated with a horseradish peroxidase conjugated secondary antibody in 1%(w/v) marvel in TBST at room temperature for 1 h with gentle agitation. The PVDF membrane was washed again (4 x 5 min).

Enhanced chemiluminence was carried out as follows: luminol (25 mg) was dissolved in 100 ml Tris (0.1 M, pH 8.5). 4-Iodophenol (9 mg/ml in DMSO) was then added dropwise to this solution followed by 31 µl of hydrogen peroxide (30% w/v). The washed PVDF membrane was incubated in this substrate solution for 1 min with gentle agitation. Excess liquid was removed and the PVDF membrane was placed protein side up in an X-ray cassette and covered with cling film to separate the wet PVDF membrane from the X-ray film. The result was recorded on a sheet of Kodak X-omat LS film, placed for various amounts of time (from 1 min - O/N) over the PVDF membrane in the dark, in the X-ray development cassette. The film was then processed in an X-ray developer.

2.1.17 Preparation of solubilized cells for SDS-PAGE.

Procyclic and bloodstream form trypanosomes (2.5×10^8), following washing with TES buffer, pH 7.4, were resuspended in a final volume of 50 µl. Sample buffer (0.95 ml) was added and the sample was boiled for 5 min. 5×10^6 cells (20 µl) was loaded per well and SDS-PAGE carried out as described in Section 2.1.13.

2.1.18 Preparation of water lysed cells for SDS-PAGE

Trypanosomes (5×10^8), following washing with TES buffer, pH 7.4, were resuspended in 100 µl TES, containing protease inhibitors (Table 2.3) at 0°C. Subsequently 900 µl of deionised water containing protease inhibitors (Table 2.3) was added at 37°C and the cells were incubated at 37°C for 10min. Following this incubation, 2×10^7 cells (40 µl) were added directly to an equal volume of SDS-PAGE sample buffer (1.5 M Tris buffer, pH 6.8, 110 µl; glycerol, 1 ml; 0.2 % bromophenol blue in ethanol, 60 µl; 20 % w/v SDS, 1 ml; made up to a final volume of 5 ml with water). 2.5×10^6 cell equivalents (20 µl) were loaded per lane and SDS-PAGE was carried out as described in Section 2.1.13.

2.1.19 Preparation of de-energized cells for SDS PAGE

Cells (5×10^7/ml) were incubated in iso-osmotic Tes buffer pH 7.5 at 37°C in a final volume of 10 ml with constant gentle stirring. Following a 15 min energization

incubation, the cells were cold quenched by adding ice-cold iso-osmotic Tes buffer (4 x volume of cell suspension) and centrifuged (9,000 ***g*** x 10 seconds on one side of centrifugation tube followed by 5,000 ***g*** x 10 seconds on the other side of the centrifugation tube at 4°C). The pellets were resuspended in ice-cold iso-osmotic phosphate buffer (Na_2HPO_4, 20 mM; sucrose, 360 mM; pH 7.5) containing protease inhibitors (Table 2.3) to give a final concentration of 5 x 10^8 cells. The cells (5 x 10^8 cells) were then resuspended in phosphate buffer (Na_2HPO_4, 20 mM; sucrose, 360 mM; protease inhibitors, pH 8.0) containing 2-deoxy-D-glucose (10 mM) to give a final cell concentration of 5 x 10^7/ml. The cells were incubated at 37°C for 45min. Following this procedure the cells were cold quenched in ice-cold phosphate buffer (Na_2HPO_4, 20 mM; sucrose, 360 mM; pH 7.5) and centrifuged as above. The cells were then resuspended in ice-cold phosphate buffer and an equal volume of sample buffer to give a final concentration of 5 x 10^8 cell equivalents. 5 x 10^6 cell equivalents (20 µl) were loaded per well and SDS-PAGE carried out as described in Section 2.1.13. For confocal microscopy, cells were resuspended in ice-cold phosphate buffer and an equal volume of paraformaldehyde fixative (3 % final). Cells were fixed for 10 min on ice and subsequently prepared for confocal microscopy (Section 2.1.53).

Immunoprecipitations and Cell Surface Labelling

2.1.20 Cell surface iodination of trypanosomes

Enzymatic surface radio-iodination was carried out by incubating trypanosomes (10^8 cells) in 0.5 ml of phosphate buffer (8 mM Na_2HPO_4, 1.5 mM KH_2PO_4, 137 mM NaCl, 2.7 mM KCl, 5 mM glucose; pH 7.5), containing lactoperoxidase (660 milliunits), glucose oxidase (165 milliunits), and carrier-free $Na^{125}I$ (1 mCi) for 10 min at 25°C. The iodination reaction was terminated by the addition of ice-cold phosphate buffer (0.5 ml) containing cysteine (1 mM), PMSF (0.5 mM), leupeptin (50 µg/ml), and EDTA (1mM), followed by washing the cells three times by centrifugation (9,000 ***g*** 30 s) and resuspension in this same medium.

Table 2.3. Protease Inhibitors used during Purification of VSG and MBP-PLC

Protease Inhibitor	**For 50 mls**	**Final Concentration**
PMSF	3 mg	0.3 mM
TLCK	2 mg	0.1 mM
Leupeptin	1 mg	10 μg/ml
Pepstatin A	4 μl of 25 mg/ml soln.	2 μg/ml

Table 2.3a. Inhibitory actions of the Protease Inhibitors

Protease Inhibitor	**Action**
PMSF	Serine protease Inhibitor; inhibits trypsin and chymotrypsin.
TLCK	Serine Protease Inhibitor; inhibits trypsin, chymotrypsin and papain.
Leupeptin	Cysteine Protease Inhibitor; inhibits plasmin and cathespin B.
Pepstatin A	Aspartic Protease Inhibitor; inhibits pepsin, cathespin D and rennin.

2.1.21 Cell surface biotinylation of trypanosomes

All solutions were maintained on ice at 4°C throughout the labelling and washing of cells. Trypanosomes were purified from infected blood as described above (section 2.1.5). Purified trypanosomes were subsequently washed in ice-cold TSB (x2) and the pellet was finally resuspended at 5 x 10^7 cells/ml. The suspension of trypanosomes was then transferred to a clean glass conical flask and equilibrated on ice for 10 min. Sulfo-NHS-LC-Biotin was weighed and added immediately to PBS (3 mg/ml, final concentration). Portions (100 µl) of this solution were added to 1ml of cells (5 x 10^7 cells/ml) and incubated on ice at 4°C for 20 min. The biotinylation reaction was quenched by addition of excess ice-cold TSB (10X) containing 5mM glycine. The biotinylated trypanosomes were washed twice by centrifugation (2500 rpm, 4 °C, 5 min) and resuspension.

2.1.22 Lysis of surface labelled trypanosomes.

Biotinylated/iodinated cell pellets were finally resuspended in Tris buffer (50 mM, pH 7.5), NaCl (150 mM), 0.1% NP-40 and 0.5% Chaps containing leupeptin (30 µg/ml), PMSF (0.3 mM) and TLCK (0.1 mM) at a cell equivalent concentration of 1-2 x 10^9 cell equivalents/ml. Samples were incubated at 4 °C for 30 min with occasional mixing, then centrifuged at 15,000 ***g***, 4 °C for 15 min. Supernatants were retained and stored at –80 °C (Polar 530 V freezer) for subsequent analysis.

2.1.23 Immunoprecipitation of surface labeled proteins from trypanosomes.

Immunoprecipitation of proteins in *Trypanosomes* was performed using a modification of the general method of Anderson and Blobel (1983). Protein A-sepharose slurry (for rabbit anti-IgG) or protein G-sepharose (for rat and sheep anti-IgGs) was prepared by making a 5% (w/v) suspension of the sepharose in PBS with added sodium azide (0.02%). After swelling overnight the beads were adjusted to give a final 1:1 by volume gel : buffer ratio. The relevant antibodies, 10 – 200 µl (determined by titration) were coupled to 30 µl of a 50% (w/v) protein A/G slurry by incubating overnight at 4°C with gentle mixing. Samples of the lysed cells described above (Section 2.1.22.) were then added to the protein A/G-IgG mixtures and incubated for a further 2 hr at 4°C with gentle

agitation before centrifugation at 9000 ***g*** for 30 s to sediment the resin bound immune complexes.

2.1.24 Washing and elution of resin bound protein.

Sedimented resin was washed by centrifugation / resuspension twice for 5 min each with Tris (50 mM), NaCl (100mM), Chaps (0.2%), pH 7.5. Following this procedure the immune complexes were washed once with Tris (50 mM), NaCl (500 mM), Tx-100 (0.1%), pH 7.5, then with Tris (50mM), Tx-100 (0.1%) (x3). The resin was then centrifuged for 2 min and repeated if necessary to pellet the resin and remove as much excess buffer as possible. The beads were then finally resuspended in 40µl of sample buffer and boiled for 5 minutes. SDS-PAGE followed by western blot analysis was performed on the complexes solubilized from the resin beads.

2.1.25 Fluorescein isothiocyanate labelling of protein.

Prior to the labelling reaction the protein to be labelled was either gel filtered on Sephadex G-25 or concentrated a number of times by ultrafiltration (5,000 molecular weight cut off filter, see Section 2.24.) to remove any Tris/glycine. Protein (final concentration 0.5 mg-1 mg/ml) was diluted with carbonate buffer (sodium carbonate 0.25 M, pH 9.3) and transferred to a small vessel with subsequent gentle stirring in the dark. The fluor (5 mg) to be used in the procedure was dissolved in DMF and diluted to 1 ml with carbonate buffer. The required volume of diluted fluor (10 – 300 molar excess of fluor to protein) was then added dropwise to the antibody solution over a few minutes (maximum final volume <1.5 ml). Following a 2.5 h incubation at room temperature in the dark with constant gentle stirring, the unreacted fluor was separated from the fluorescent labelled protein conjugate by passage through a column of Sephadex G-25 (0.4 cm x 42 cm; medium grade) which had been previously equilibrated with iso-osmotic TES buffer, pH 7.4. Free fluor eluted in approximately twice the inclusion volume of the column, suggesting that the free fluor was retarded by weak binding to the resin, whereas the conjugated protein eluted in the exclusion volume (Fig 2.5).

Fig 2.5. Separation of FITC labeled protein from free fluor by gel filtration on Sephadex G-25.

Anti-VSG antibody (0.5 mg/ml; 2.75 μM) was diluted with carbonate buffer (sodium carbonate, 0.5 M, pH 9.3) and transferred to a small dark vessel with subsequent gentle stirring. FITC (5 mg) was dissolved in 0.1 ml of DMF and diluted to 1 ml with carbonate buffer. Diluted fluor (22 μl of 275 μM final fluor concentration; 100 fold molar excess of fluor to protein) was then added dropwise to the antibody solution over a period of a few minutes. Following a 2.5 h incubation at room temperature with constant gentle stirring in the dark, the unreacted fluor was separated from the fluorescent labeled protein conjugate by passage through a Sephadex G-25 column (0.4 cm x 42 cm; bed volume 21 ml) which had been previously equilibrated in iso-osmotic TES buffer, pH 7.4. The Fluorescence emission of each fraction was measured with the excitation wavelength at 476 nm and the emission wavelength at 515 nm. Both excitation and emission slit widths were 5 nm. Free fluor eluted in approximately twice the inclusion volume of the column (Peak 2) whereas the conjugated protein eluted in the exclusion volume (Peak 1).

Fig 2.5. Separation of FITC labeled protein from free fluor by gel filtration on Sephadex G-25.

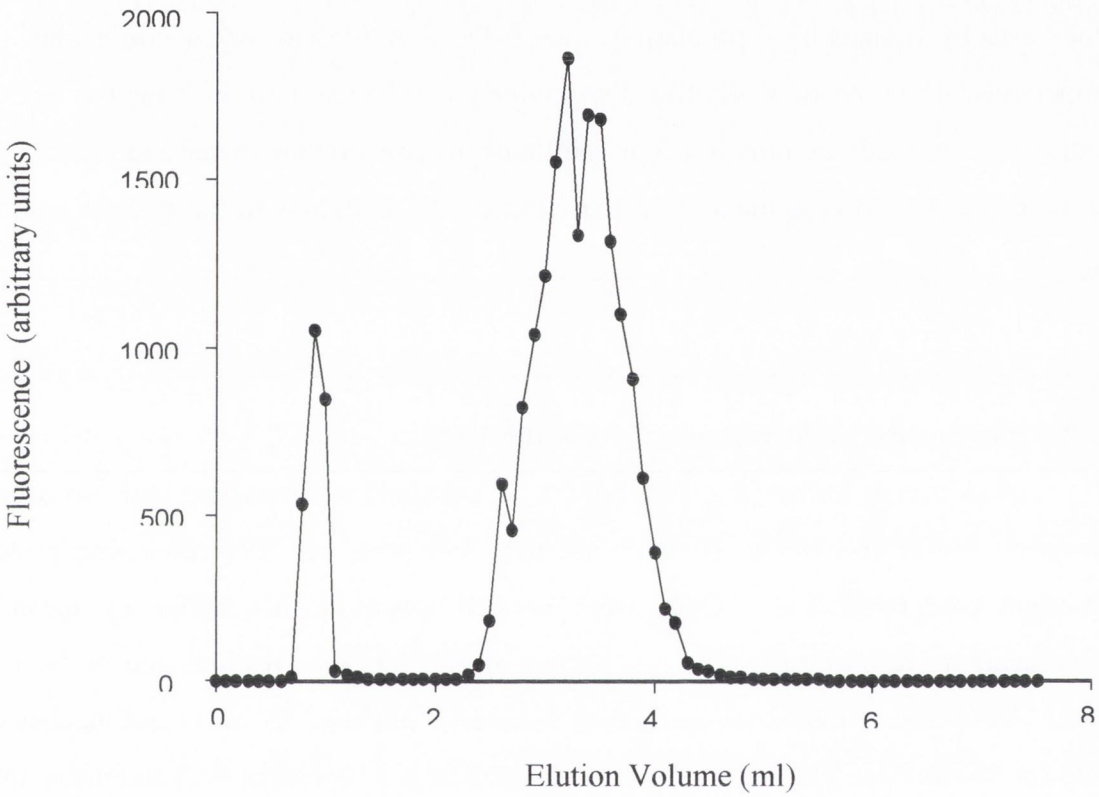

2.1.26 Fluorescent spectrophotometry

Changes in fluorescence of labelled antibody following incubation with trypanosomes was monitored continuously in a Perkin Elmer fluorescence spectrometer (model LS-50B) coupled to a Digital Dec 386 or Gateway 2000 P5-120 computer. The slit width on each monochromator was 5 nm. Matching four - sided quartz or four sided polymethylacrylate cuvettes, with a 3 ml capacity, were used throughout the study. Constant stirring of the incubation medium was achieved by means of a magnetic stirrer at the base of the cuvette holder. Constant temperature was maintained throughout the experiment by connecting a circulating water bath set at 32°C to the cuvette holder. The temperature of the incubation buffer was routinely checked and always found to be 30°C. Additions were made by rapidly lifting the lid of the spectrophotometer and pipetting the solution into the buffered medium in the cuvette. All additions to the cuvette took less than 10s.

2.1.27 Purification of the released form of the VSG.

Bloodstream forms of *T. brucei* (1 x 10^9cells/ml) were washed with iso-osmotic phosphate buffer (Na_2HPO_4, 20 mM; sucrose, 360 mM; pH 8.0) containing protease inhibitors (see table 2.3). Cells were washed twice in this buffer by means of centrifugation / resuspension (650 ***g*** x 10 min, at 4°C) and then resuspended in the above buffer plus protease inhibitors containing 2-deoxy-D-glucose (25 mM) and incubated at 37°C for 35 minutes. The cells were centrifuged (650 ***g*** x 10 min, at 4°C) and the resulting supernatant applied to a DEAE cellulose column (5.5 ml bed volume/10^{10} cells) equilibrated with phosphate buffer (Na_2HPO_4, 20 mM; sucrose, 360 mM; pH 8.0). Fractions (1 ml) were collected and protein concentration was determined by measuring the absorbance of each fraction at 280nm (Fig 2.6a). The first peak of absorbance corresponded to the VSG as assessed by SDS-PAGE (Fig 2.6b). Protein, which remained bound to the DEAE cellulose resin, was eluted by applying 1 M NaCl in phosphate buffer. Fractions containing the VSG were pooled and concentrated by using vivaspin centrifugal concentrators with a MWCO of 5000 (Sartorius). Samples of the VSG were divided into suitable portions and stored at -20°C until required. The time course for release of trypanosomal protein by this method is shown in Fig 2.7.

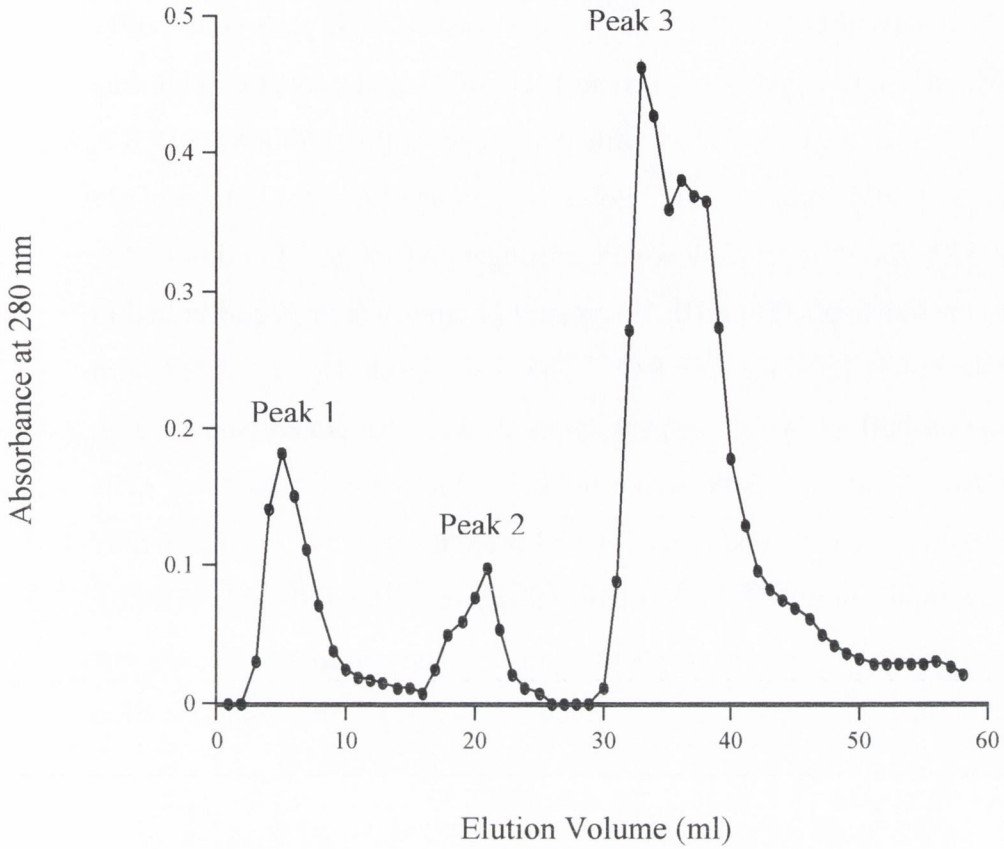

Figure 2.6a. Purification of the released form of the VSG by ion exchange chromatography.

Trypanosomes (1 x 10^{10} cells) were washed with phosphate buffer (20 mM, pH 8.0) containing sucrose (360 mM) and protease inhibitors (Table 2.3) and then incubated with phosphate buffer (20 mM, pH 8.0, sucrose, 360 mM, protease inhibitors) containing 2-deoxy-D-glucose (25 mM) at 37°C for 35 min. Following centrifugation (650 ***g***, 10 min, 4°C) the supernatant was applied to a DEAE column (2 cm x 0.6 cm) equilibrated in phosphate buffer (20 mM, pH 8.0). The VSG (peak 1) was eluted with equilibration buffer. A further peak (peak 2) was also eluted isocratically, and probably corresponds to hypoxanthine, which is released from cells under energy-deprived conditions. Bound protein (peak 3) was specifically eluted by application of 1 M NaCl in phosphate buffer (20 mM, pH 8.0).

Figure 2.6b. Purification of the released form of the VSG by ion exchange chromatography.

Trypanosomes (1 x 10^{10} cells) were washed with phosphate buffer (20 mM, pH 8.0) containing sucrose (360 mM) and protease inhibitors (Table 2.2) and then incubated with phosphate buffer (20 mM, pH 8.0, sucrose, 360 mM, protease inhibitors) containing 2-deoxy-D-glucose (25 mM) at 37°C for 35 min. Following centrifugation (650 ***g***, 10 min, 4°C) the supernatant was applied to a DEAE column (2 cm x 0.6 cm) equilibrated in phosphate buffer (20 mM, pH 8.0). The VSG (peak 1) was eluted with equilibration buffer. A further peak (peak 2) was also eluted isocratically, and probably corresponds to hypoxanthine, which is released from cells under energy-deprived conditions. Bound protein (peak 3) was specifically eluted by application of 1 M NaCl in phosphate buffer (20 mM, pH 8.0). Discontinuous SDS gel electrophoresis of fractions from each peak was performed on a 10 % resolving gel, which was stained with Coomassie Blue R-250.

Lane 1:High Molecular weight markers (Sigma)
Lane 2:Low Molecular weight markers (Sigma)
Lane 3:First fraction from peak 1 (Fig 2.7b)
Lane 4:Second fraction from peak 1 (Fig 2.7b)
Lane 5:Third fraction from peak 1 (Fig 2.7b)
Lane 6:Fourth fraction from peak 1 (Fig 2.7b)
Lane 7:First fraction from peak 2 (Fig 2.7b)
Lane 8:Second fraction from peak 2 (Fig 2.7b)
Lane 9:Third fraction from peak 2 (Fig 2.7b)
Lane 10:Fourth fraction from peak 2 (Fig 2.7b)
Lane 11:First fraction from peak 3 (Fig 2.7b)
Lane 12:Second fraction from peak 3 (Fig 2.7b)

Figure 2.6b. Purification of the released form of the VSG by ion exchange chromatography.

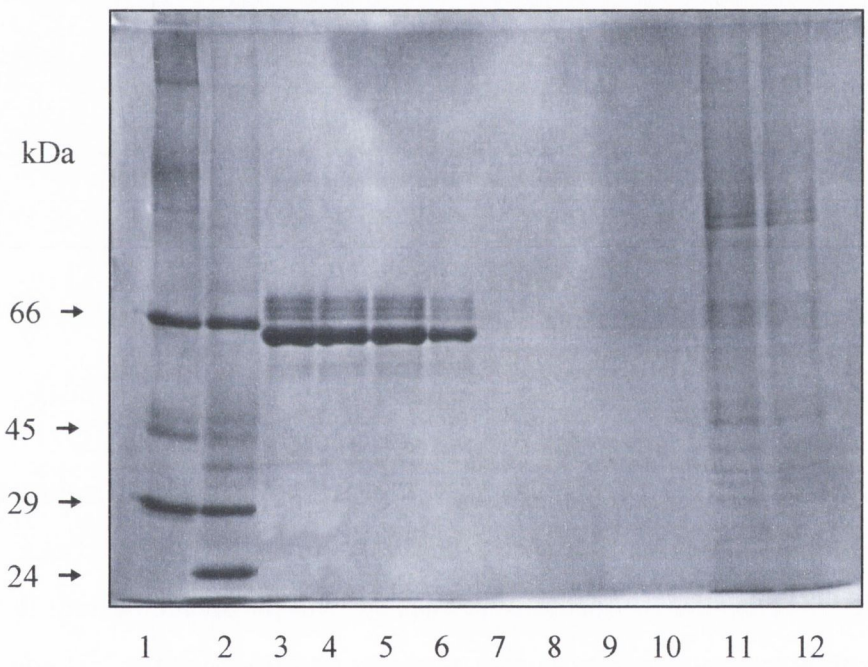

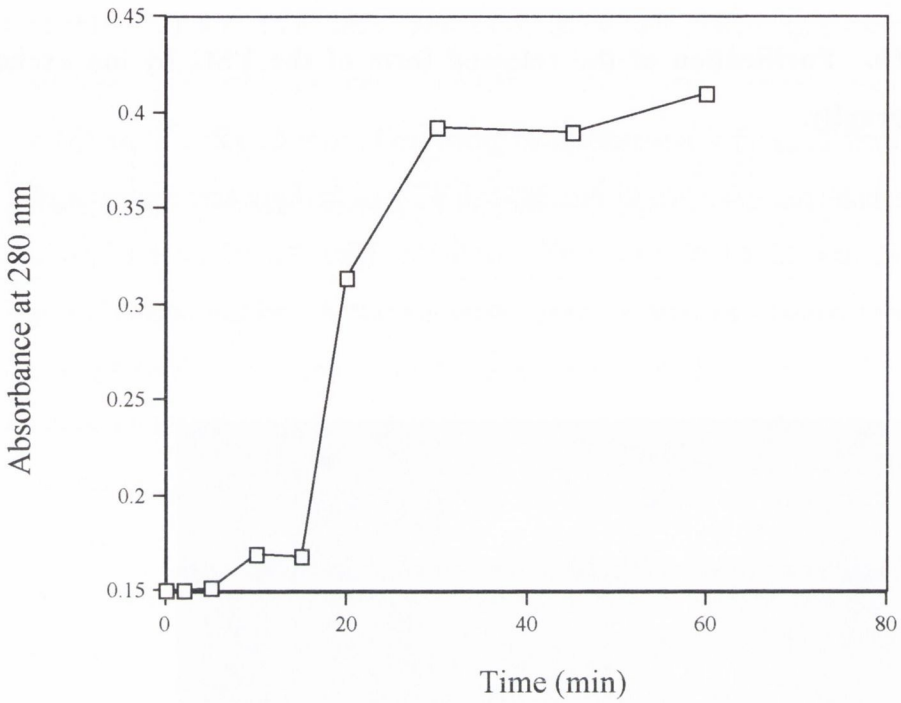

Figure 2.7. Time Course of the release of protein from bloodstream form trypanosomes following incubation with 2-deoxy-D-glucose.

MITat 1.1 cells (1 x 10^{10} cells) were washed with phosphate buffer (20 mM, pH 8.0) containing sucrose (360 mM) and protease inhibitors (Table 2.3) and then incubated (3.5 x 10^{9} cells/ml) with phosphate Buffer (20 mM, pH 8.0, sucrose, 360 mM, protease inhibitors) containing 2-deoxy-D-glucose (25 mM) at 37°C for 60 min. At various times during the incubation, samples were withdrawn (250 µl, corresponding to 8.75 x 10^{10} cells) centrifuged and the resultant supernatant assayed for protein by measuring the absorbance at 280 nm.

2.1.28 The Isolation of the Plasma Membrane from *Trypanosoma Brucei*

Isolation of the plasma membrane from trypanosomes was carried out by the method of Voorheis (1978). A fresh preparation of 3 x 10^{10} bloodstream forms of *T. brucei* was centrifuged (650 ***g***, 10 min, 4°C) and the pellet resuspended in Tes buffer (10 ml) containing 20 mM Tes, pH 7.5; 150 mM KCL, 1 mM EDTA, 1 mM –2-mercapoethanol and 0.1 mM PMSF. Distilled deionised water (3 x 10 ml) containing 0.1 mM PMSF was added with vigorous swirling in successions of 10 ml portions. The progress of cell swelling was followed by examining samples of the suspension after each addition of water with phase-contrast microscopy. The swollen cells were ruptured by the use of a Stansted cell disrupter (Stansted Fluid Power Ltd) at a constant back pressure of 25 psi (Fig 2.8).

Immediately after rupturing of the cells the ionic strength of the homogenate was raised by the addition of 2 ml of 3 M KCl for each 40 ml homogenate. The homogenate was centrifuged (25,000 ***g*** x 10 s) and the pellet resuspended in Tes buffer (10 ml) without EDTA and containing $MgCl_2$ (5 mM) and warmed to 20°C. DNAase (240 units) was added and the suspension was incubated at 20°C for 5 minutes. The reaction was terminated by adding ice-cold Tes buffer (50 ml), mixing and centrifuging (Sorvall SC Centrifuge brought to 25,000 ***g*** and then allowed to decelerate with the break on after 10 s). The pellet was resuspended in 40 % (w/v) sucrose in Tes buffer (4 ml for each 10^{10} cells starting material).

The suspension (4 ml/gradient) was layered on top of a linear 40 – 60 % (w/v) sucrose gradient (25 ml) with a 60 % (w/v) sucrose bottom cushion (2 ml) and was centrifuged (70,000 ***g***, 3 hr, 4°C). The gradient and the cushion were prepared in Tes buffer.

Two constant and prominent bands as well as several more variable smaller bands resulted from the centrifugation procedure. Plasma - membrane sheets comprised the largest and most prominent dense band. The band of plasma membranes was removed with a Pasteur pipette after aspiration of the overlying gradient. These were diluted to 50 ml with Tes buffer and centrifuged (25,000 ***g*** x 2 min). The pellet was resuspended in Tes buffer (5 ml/10^{10} cells starting material) and aliquots were stored frozen at – 80°C.

Figure 2.8. Calibration of the Stansted Cell Disrupter for use in the isolation of Plasma Membrane from *Trypanosoma Brucei*.

MITat 1.1 trypanosomes (6 x 109 cells) in Tes buffer (20 mM Tes, pH 7.5; 150 mM KCL, 1 mM EDTA, 1 mM –2-mercapoethanol and 0.1 mM PMSF) were swollen by the addition of distilled deionized water containing PMSF (0.1 M). These cells were then passed through the Stansted Cell Disrupter at different psi settings and live cells were counted using phase-contrast microscopy. The percentage cell breakage was calculated according to the following equation:

$$\frac{(\text{Number of live cells at } psi_0 - \text{Number of live cells at } psi_X) \times 100}{\text{Number of live cells at } psi_0}$$

Figure 2.8. Calibration of the Stansted Cell Disrupter for use in the isolation of Plasma Membrane from *Trypanosoma Brucei*.

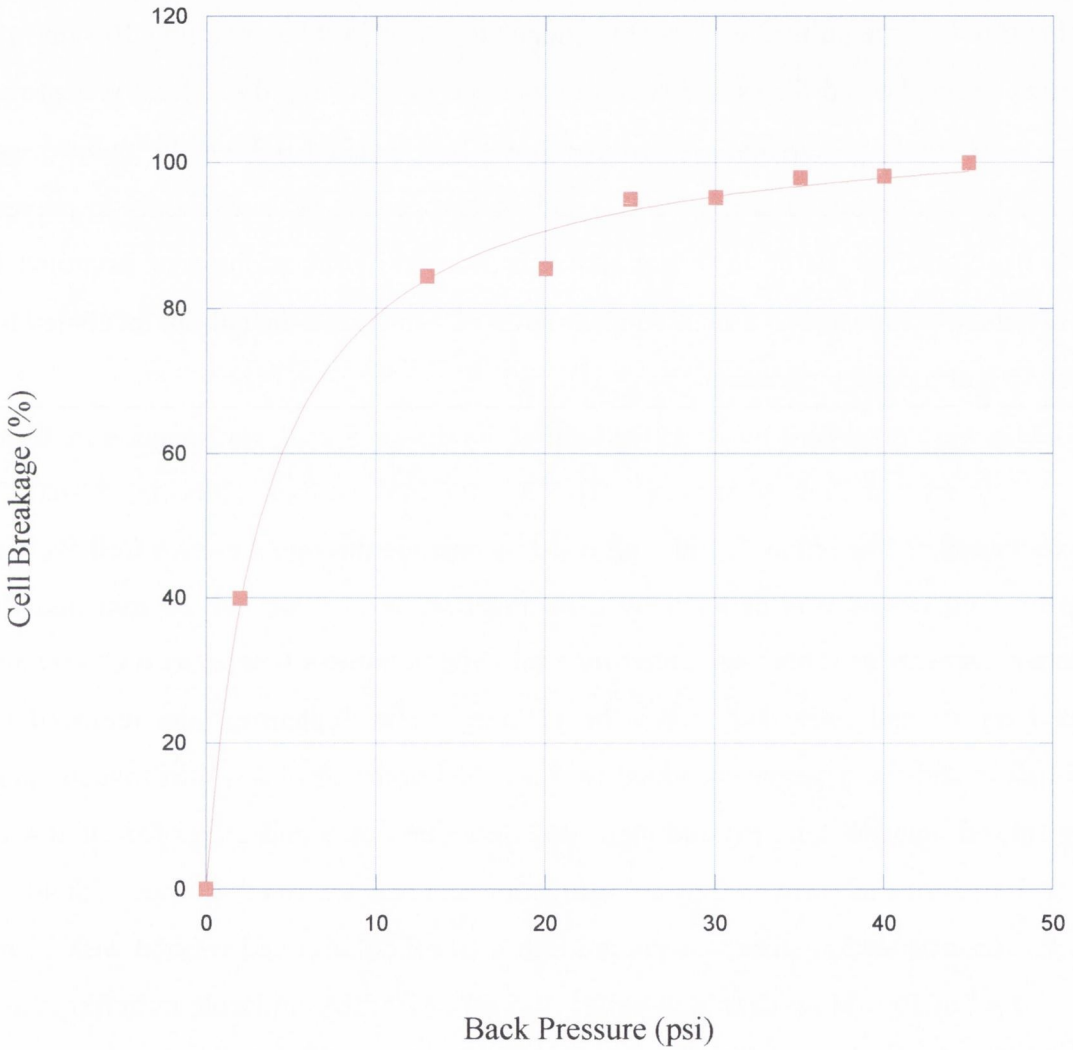

2.1.29 Expression of GPI-PLC in *E. coli* BL21 (DE3)

The *T. brucei* GPI-PLC expression plasmid (p1313) was constructed by inserting the open reading frame of GPI-PLC as a NcoI-XhoI fragment into pET21d (Novagen) by Mark Carringtons lab (Carnall *et al*, 1997). Subsequently these expression plasmids were transformed into *E. coli* BL21 (DE3) and stored as glycerol stocks at –70°C.

Cultures for expression were always started from a single colony from a freshly streaked plate. The single colony was used to inoculate a 10 ml culture in 2xYT (16 gl^{-1} tryptone, 10 gl^{-1} yeast extract, 5 gl^{-1} sodium chloride) containing 100 $\mu g\ ml^{-1}$ ampicillin. This was grown at 37°C, with vigorous shaking. When the A600 had reached approximately 0.5, the culture was used to inoculate 1 l of 2xYT containing 100 $\mu g\ ml^{-1}$ ampicillin, the media and flasks had been pre-warmed to 37°C and the culture was grown at 37°C, with vigorous shaking. When the A600 had reached 0.7-0.8 the culture was transferred to room temperature (18-20°C) and shaken gently, but sufficiently to prevent the cells from settling. After 1h, expression was induced by the addition of isopropyl-1-thio-β-D-galactopyranoside to a final concentration of 1 mM, and the culture incubated for a further 16 h at room temperature.

Cells were recovered by centrifugation at 4000*g* for 5 min, resuspended in 40 ml buffer A (50 mM sodium phosphate, pH 7.8, 300 mM sodium chloride, 5 mM 2-mercaptoethanol, 0.5% Triton X-100) and lysed by passage through a French Cell Press at 1000 psi. Cell debris was pelleted by centrifugation at 12,000***g*** for 20 min and the supernatant recovered. This was added to 4 ml (bed volume) of Sepharose CL-4B and incubated on an end over end mixer for 10 min. The Sepharose was removed by centrifugation and the supernatant added to 4 ml (bed volume) nickel nitriltriacetic acid agarose (nickel agarose, Qiagen) and incubated on an end over end mixer for 1h at 4°C. The nickel agarose was recovered by centrifugation and batch washed 4 times with 40 ml buffer A. Resuspended agarose was poured into a 10 ml column and washed with 15 ml buffer A, 5 ml of 10 mM imidazole in buffer A, 5 ml of 20 mM imidazole in buffer A and 5 ml of 100 mM imidazole in buffer A, prior to elution of GPI-PLC in 7 ml 100 mM imidazole in buffer A. The eluate was then passed through a Sephadex G-75 column (42 cm x 0.4 cm, bed volume 21 ml), pre-equilibrated with buffer B (25 mM Tris-HCl, pH 8.0, 0.5% Triton X-100, 5 mM 2-mercaptoethanol). Fractions (5 ml) were collected and those samples containing the GPI-PLC were applied to a 10 ml column of DEAE

cellulose equilibrated with buffer B and the flow through collected. Samples were analysed by SDS-PAGE (Fig 2.9) and stored at – 80°C.

Cloning

2.1.30 Polymerase Chain Reaction.

Primers were designed with standard criteria using cDNA sequence data for the GPI-PLC as shown in table 2.4. Restriction enzyme sites were incorporated into the ends of each primer. PCR reaction mixtures were made up in 50 µl total reaction volumes in thin wall PCR tubes (Molecular bioproducts) with components as shown in table 2.5. The cDNA clone for each fragment was used as template DNA. After all additions had been made samples were centrifuged briefly then placed in a PCR *Sprint* machine (MSC). Amplification of DNA was achieved using the conditions in table 2.6.

2.1.31 Spin column purification of PCR products

PCR products were purified using *High Pure PCR Product Purification Kit* (Roche) spin columns.

2.1.32 Agarose Gel Electrophoresis of DNA.

Agarose powder (1% w/v) was mixed with TAE electrophoresis buffer (Tris base, 40 mM; pH 8.0; Glacial Acetic Acid, 20 mM; EDTA (2 mM), and heated in a microwave until completely dissolved. The solution was allowed to cool to ~ 60 °C and poured into a casting tray containing a sample comb to give a well depth of ~ 5/6 mm). The gel was allowed to solidify at room temperature. The comb was removed and the gel placed horizontally into an electrophoresis chamber (Medical Supply Company). TAE was added until just covering the gel. Samples for gel analysis were prepared in loading buffer (20% Ficoll 400, 0.1 M EDTA pH 8, 1% SDS, 0.025% bromophenol blue). After loading, the gel was run at 70 V for ~ 1h 30 min. The electrophoresed gel was placed in a solution of ethidium bromide (0.5 µg/ml) in TAE and left to soak for 60 min to stain the DNA. Stained samples were visualised using a UV transilluminator.

Fig 2.9. SDS-gel electrophoresis of whole cells, soluble and insoluble fractions and purified GPI-PLC protein.

Cultures (500 ml) were grown at 37oC until A600 of ~0.8 was reached. The culture was transferred to 18oC and after 1 hour IPTG (1mM final concentration) was added and the cultures were incubated overnight at 18oC. Cells were harvested and resuspended in 0.01 –0.02 volumes of buffer, prior to lysis by French Press. 4 x 107 cell equivalents from each fraction are shown in each lane. Protein was purified from the soluble fraction by nickel agarose affinity chromatography and then DEAE-cellulose chromatography, 10 μl of each purified fraction was loaded in each lane.

Lane 1: Low molecular weight markers (Sigma)
Lane 2:Pre-induced sample
Lane 3:Post-induced sample
Lane 4:Cell lysate - supernatant
Lane 5:Cell lysate – pellet
Lane 6:Supernatant from sepharose CL-4B step
Lane 7:Supernatant from nickel agarose end-over-end mix
Lane 8:10 mM Imidazole eluant
Lane 9:100 mM Imidazole eluant
Lane 10: DEAE-cellulose flow through fraction 1
Lane 11: DEAE-cellulose flow through fraction 2

Fig 2.9. SDS-gel electrophoresis of whole cells, soluble and insoluble fractions and purified GPI-PLC protein.

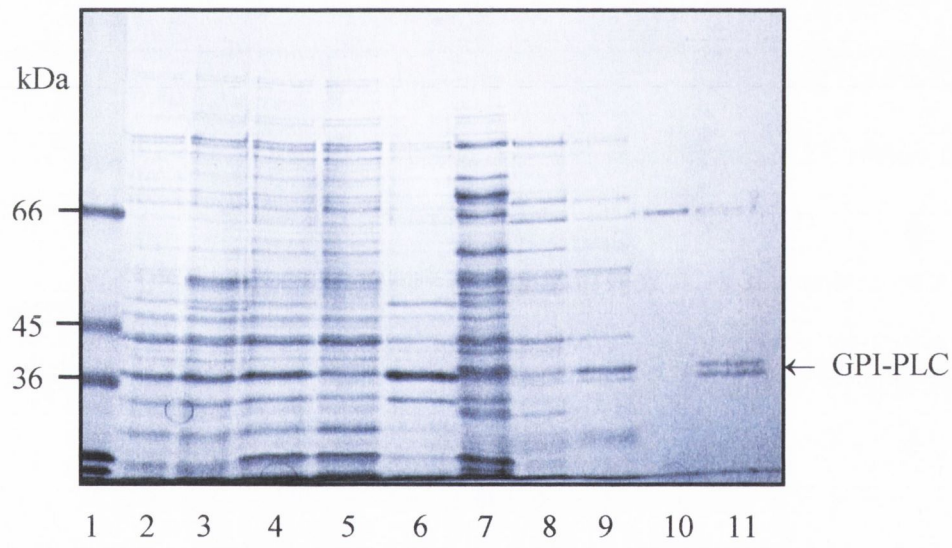

GPI-PLC-complete forward primer- BamH1	5'- AGG GAT CCT TTG GTG GTG TAA AGT GGT CAC CGC AG- 3'
GPI-PLC-complete reverse primer- XHO1	5'- AGC AAC TCG AGT TAT GAC CTT GCG GTT TGG TTG GT- 3'

Table 2.4. Primers used in PCR

Component	**Amount**
10x PCR buffer	5 µl
dNTPs	10 mM (3µl)
Primers	13.5 pmol (reverse) 9.5 pmol (forward)
Template DNA	750 pg (1.35 µl)
dH_2O	39 µl
Expand high fidelity PCR enzyme.	1.75 U

Table 2.5. Components of PCR reaction mix

Conditions	
Step 1	5 min 96 °C
Step 2	30 sec 93 °C
Step 3	30 sec 55 °C
Step 4	1 min 68 °C
Step 5	6 min 68 °C

Table 2.6. PCR conditions. Steps 2- 4 were repeated 30 times. After step 5 the holding temperature was 4 °C

2.1.33 Restriction enzyme digestion of vector and purified PCR product

DNA samples were singly or doubly digested in sterile eppendorfs minifuge tubes using 1 µl of each restriction enzyme (20 units/µl, kept at – 20°C at all times) in appropriate buffer (1/10 dilution of 10 X stock as supplied with the enzyme) for 3 hours or overnight at 37 °C in a heated water bath to ensure complete digestion (see Table 2.7. for typical reaction mixture). Vector and DNA samples were subsequently purified using spin columns as described above to remove restriction enzymes, small cleaved DNA fragment and buffer components that interfere with the ligation process.

2.1.34 Expression cloning.

The pMAL system was used to express protein of interest (Fig. 2.10). In this system, the cloned gene is inserted into a pMAL vector down-stream from the *malE* gene, which encodes maltose-binding protein (MBP). This results in the expression of an MBP-fusion protein. The technique uses the strong Ptac promoter and the translation initiation signals of MBP to express large amounts of the fusion protein. The system uses the pMAL vectors, which are designed so that insertion interrupts a *lacZ*α gene allowing a blue-to-white screen for inserts on X-gal. The vectors include a sequence coding for the recognition site of a specific protease. This allows the protein of interest to be cleaved from MBP after purification. IPTG is used to induce expression of protein by this system.

2.1.35 Gel purification of DNA

Vector DNA was gel purified to remove unwanted cut DNA. Samples were run on 1% agarose gels as described above (2.1.32.) and bands excised using a sterile scalpel. DNA was then extracted from gel slices using spin columns as described above. DNA was then quantified by reference to known quantities of DNA markers.

2.1.36 Ligation of digested DNA fragments into digested vector

Ligation reactions were performed at 16 °C, overnight, in a thermal cycler using T4 DNA ligase (400 units/ µl) in T4 ligase buffer, an appropriate dilution depending on the final reaction volume (see Table 2.8 for typical ligation reaction mixture). Molar

Figure 2.10. The pMal Expression System (from New England BioLabs).

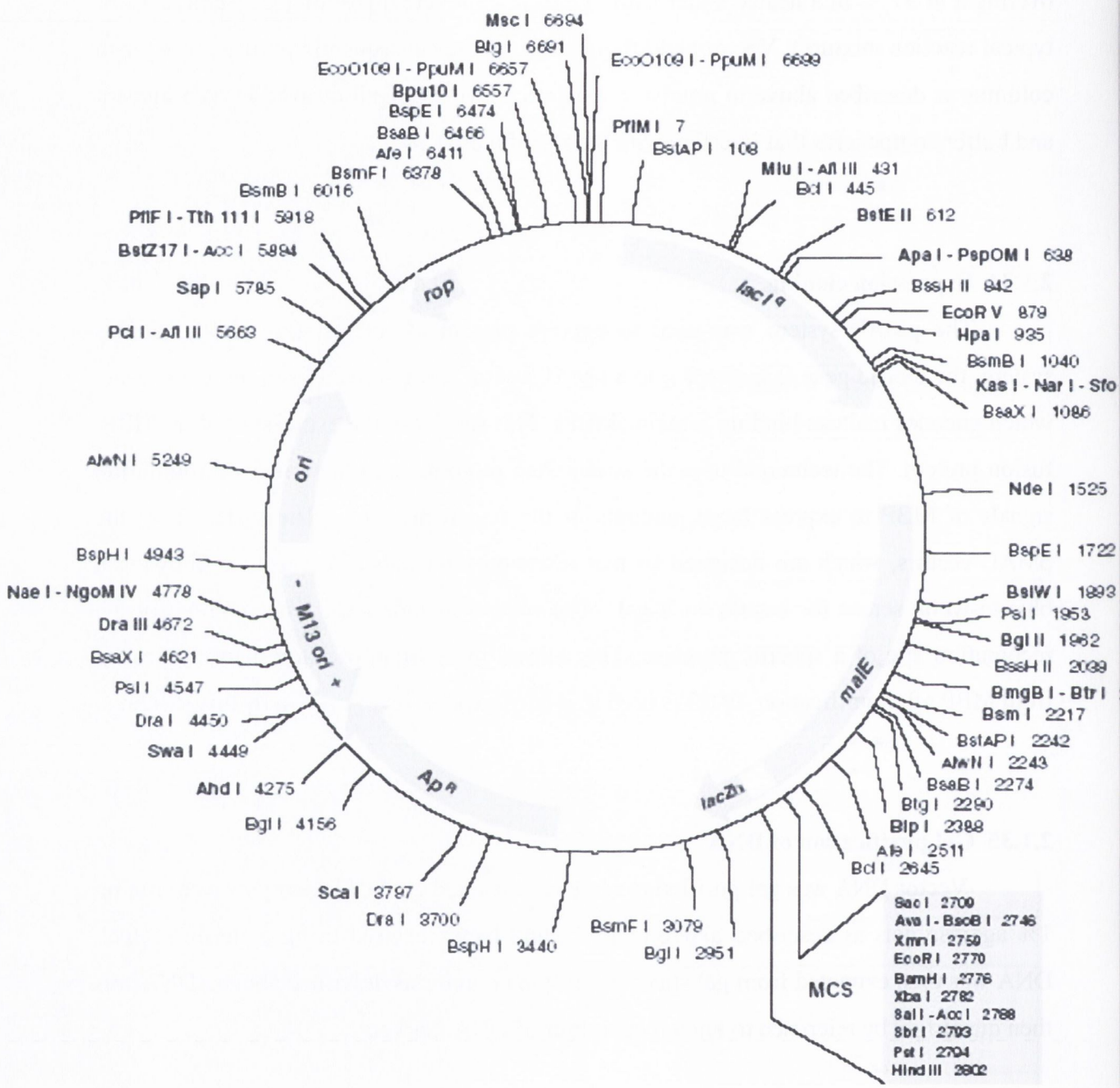

ratios of 5:1 and 3:1 of insert to vector were used to ensure sufficient molar excess of viral DNA to cut vector. Solutions containing the ligation products were stored at -80°C until use.

2.1.37 Transformation of *E. Coli.*

A single bacterial colony from a fresh plate was used to inoculate SOB media (see Table 2.9). 2.5 ml of SOB was used for each transformation. This was incubated at 37°C until the A600 reached 0.5. The culture was then placed on ice for 10 minutes. Cells were recovered by centrifugation at 3000 rpm x 10 min in a benchtop centrifuge. The cell pellet was resuspended in 1/3 the original culture volume of TFB (Table 2.9) and stored on ice for a further 15 minutes. Cells were again centrifuged (3000 rpm x 10 min) and the pellet resuspended in TFB (0.2 ml for each 2.5 ml of starting culture). DND (Table 2.9) was then added (7 µl per 200 µl of cells) and the sample stored on ice for 10 minutes. Following this, another 7 µl of DND was added per 200 µl of cells and subsequently stored on ice for a further 10 minutes. The DNA (not more than 20 ng / 10 µl) for transformation was placed in sterile minifuge tubes and kept on ice. Bacterial cells (210 µl) were added to the DNA, mixed by gentle agitation and left on ice for 30 minutes. Following the incubation time, cells were heat shocked for 120 seconds at 42°C and then returned to ice. Cells (100 µl) were taken and aseptically spread on sterile LB agar plates containing ampicillin (100 µg/ml). Plates were incubated overnight at 37 °C in a bacterial incubator.

2.1.38 Selection of transformed colonies.

In order to select for bacterial colonies that contained the vector with the inserted DNA present, random colonies were selected from those that had grown on LB Amp^+ plates, and transferred to 5 ml LB broth containing ampicillin (100 µg/ml). Broth was incubated at 37 °C overnight at 250 rpm in a rotary shaker. DNA was isolated from cell cultures (see below) and digested at the restriction enzyme sites at which the insert was ligated. Digested DNA was loaded onto 1 % agarose gels to check for the presence of the insert.

Component of Reaction	**Amount**
DNA	Variable
Restriction enzyme	1 µl each enzyme
10x Buffer	5 µl
Sterile de-ionised water (SDW)	Up to 50 µl

TABLE 2.7. Typical digestion reactions.

Component of Reaction	**Amount**
DNA	Variable
T4 DNA Ligase	1 µl
10x Buffer	2 µl
SDW	Up to 20 µl

TABLE 2.8. Typical ligation reaction.

SOB	**TFB (filter sterilize)**	**DND (adjust to 10 ml)**
20 g/L bactotryptone	10 mM MES-KOH pH 6.2	1.53 g DTT
5 g/L bacto-yeast extract	100 mM potassium chloride	9 ml DMSO
10 mM sodium chloride	45 mM manganese (II) chloride	100 µl 1 M potassium acetate pH 7.5
2.5 mM potassium chloride (after autoclaving add 1/100 vol)	3 mM hexamine cobalt (III) chloride	
1 M magnesium sulphate	10 mM calcium chloride	
1 M magnesium chloride		

Table 2.9. Buffers used for transformation of bacterial cells.

2.1.39 Generation of glycerol stocks.

700 µl of selected transformant cells in LB broth were mixed with a final concentration of 30% glycerol in a sterile cryotube (Greiner bio-one) and stored at -80° C.

2.1.40 Purification of plasmid DNA.

DNA from bacterial colonies was isolated using Wizard® *Plus* SV Minipreps DNA Purification System (Promega, Madison WI, USA). Briefly, bacterial cultures were grown in 5 ml LB medium. Bacteria were pelleted and resuspended in 250 µl Cell Resuspension Solution. Cells were incubated for 5 minutes with the addition of 250 µl Cell Lysis Solution before addition of 350 µl neutralization solution. The mixture was centrifuged at 13,000 ***g*** for 10 minutes at room temperature. The cleared lysate was transferred to a spin column inserted into a 2 ml collection tube. The supernatant was centrifuged for 1 minute at room temperature and then washed with 750 µl and then 250 µl Column wash solution. The DNA was eluted by addition of 100 µl Nuclease Free H_20. The insert was then sequenced to verify that selected clones contained the desired mutation.

2.1.41 UV quantitation of DNA

DNA samples in SDW were quantified at 260nm in a spectrophotometer using the formula:

$$\textbf{[DNA] µg/µl} = \mathbf{A_{260}} \textbf{ . Dilution Factor/20}$$

Purity of DNA was assessed by analysis at 280 nm and 260 nm and using the 260 nm / 280 nm ratio as an index of contamination. Quantities were verified by comparison of DNA bands to known DNA ladder amounts.

2.1.42 Expression of recombinant MalE-TbGPI-PLC in bacteria.

Cultures for expression were always started from a single colony from a freshly streaked plate. The single colony was used to inoculate a 10 ml culture in LB containing 100 µg / ml ampicillin. This was grown at 37°C, with vigorous shaking. When the A600

had reached approximately 0.5, the culture was used to inoculate 1 l of LB containing 100 μg/ml ampicillin, the media and flasks had been pre-warmed to 37°C and the culture was grown at 37°C, with vigorous shaking. When the A600 had reached 0.4-0.5 the culture was transferred to room temperature (18-20°C) and shaken gently, but sufficiently to prevent the cells from settling. After 1h, expression was induced by the addition of isopropyl-1-thio-β-D-galactopyranoside (IPTG) to a final concentration of 50 μM, and the culture incubated for a further 16 h at 18°C. Cells were recovered by centrifugation at 4,000 ***g*** for 20 min, resuspended in Column Buffer (20 mM Tris, pH 7.4; 200 mM NaCl, 10 mM β-Mercaptoethanol, 1 mM EDTA) containing Lysozyme (10 mg/ml) and protease inhibitors (see Table 2.3) and lysed by passage through a French Cell Press at 1000 psi. Cell debris was pelleted by centrifugation at 9000 ***g*** for 30 min and the supernatant recovered.

2.1.43 Purification of the MalE-TbGPI-PLC on Amylose Resin.

The supernatant following French Press lysis was diluted one in five with Column Buffer (20 mM Tris, pH 7.4; 200 mM NaCl, 10 mM β-Mercaptoethanol, 1 mM EDTA) containing protease inhibitors (Table 2.3) and then applied to a column of amylose resin (10 cm x 0.5 cm) pre-equilibrated in Column Buffer. The amylose was then washed overnight in Column Buffer. The bound protein was eluted at a flow rate of 1 ml / min at 4°C with the same buffer containing maltose (10 mM). Fractions (1 ml) were collected and protein was detected by UV absorbance at 280 nm. All fractions containing protein were pooled and concentrated using vivaspin concentrators if necessary. The amylose column was regenerated with the following sequence of washes: Water, 3 column volumes, 0.1 % SDS, 3 column volumes, Water, 1 column volume and column Buffer, 3 column volumes. The amylose column can be reused up to 5 times using this method of regeneration.

2.1.44 Gel filtration of MalE-TbGPI-PLC on Sephacryl S-200 column.

Preswollen Sephacryl S-200 (Pharmacia; High resolution) was suspended in Column Buffer (20 mM Tris, pH 7.4; 200 mM NaCl, 10 mM β-Mercaptoethanol, 1mM EDTA) and the fines were removed by decanting and resuspending. The column was

prepared by pouring a thick slurry of gel particles suspended in buffer solution into a vertical glass column (1.1 cm internal diameter, 1m height) partly filled with buffer, and packed by allowing buffer to percolate through the growing gel bed. The addition of gel was continued until a bed height of 95 cm was obtained and then a solvent reservoir was connected to the top of the column and the flow of buffer maintained at a rate of 0.5 ml / 8 min. All experiments were performed at 4 °C with the column equilibrated in column buffer and a flow rate of 0.125 ml/min was maintained with the application of various amounts of hydrostatic pressure to the top of the column by adjustment of the position of the solvent reservoir.

Eluted fractions containing MBP-PLC from the amylose column were combined and concentrated to give a final volume of 1 ml. The whole sample was applied to the Sepahacryl S – 200 column (internal diameter 1.1 cm, height 90 cm) pre-equilibrated with Column Buffer containing 0.1% N-octylglucoside and protease inhibitors [0.1 mM TLCK, 0.3 mM PMSF and 0.1 %(w/v) leupeptin] by allowing the column to almost run dry before application of the sample. The protein was eluted in the same buffer and fractions (1 ml) were collected at a rate of 0.125 ml/min. All fractions were analysed by gel electrophoresis on a 15% SDS-PAGE gel.

The column was calibrated with blue dextran (2,000 kDa), bovine serum albumin (66 kDa), ovalbumin (45 kDa), carbonic anhydrase (29 kDa), and cytochrome C (12.4 kDa). An elution profile of these molecular weight markers on Sephracryl S-200 is shown in Fig 6.7. When not in use the column was stored at 4 °C in equilibration buffer containing sodium azide (0.02 % w/v).

2.1.45 Preparation of the Tobacco Etch Virus (TEV) protease

A single colony from a freshly streaked plate containing *E. coli* that carried the gene for the TEV protease was used to inoculate a 10 ml culture in LB containing 30 μg/ml kanamycin and 34 μg/ml chloramphenicol. The culture was grown at 37°C overnight, with vigorous shaking. The following day the overnight culture was diluted into 500 ml of LB containing the same antibiotics and incubated at 37°C. When the A600 had reached approximately 0.5, the culture was transferred to 30°C and shaken gently. Expression of protein was induced by the addition of isopropyl-1-thio-β-D-galactopyranoside (IPTG) to a final concentration of 1 mM, and the culture incubated for a

further 4 h at 30°C. Cells were recovered by centrifugation at 4000 ***g*** for 20 min, and the pellet was resuspended in 50 ml of PBS (pH 7.5) supplemented with 0.6 M NaCl, 2 % w/v Triton X-100, 40 mM Imidazole and protease inhibitors (Table 2.3). The whole suspension was centrifuged (20000 ***g***, 30 min at 4°C) and the resulting supernatant was incubated with Ni-NTA resin (1 ml) for 90 minutes at 4°C on an end-over-end mixer. The mixture was centrifuged (800 rpm, 2 min, 4°C) and washed twice in PBS (pH 7.5) containing 0.1 % w/v Triton X-100, 300 mM NaCl and 20 mM Imidazole. Protein was eluted with 50 mM Tris-HCl, pH 8.0 containing 0.1 % w/v Triton X-100 and 125 mM Imidazole. Eluted protein was dialyzed against 50 mM Tris-HCl, 2 mM DTT, 1 mM EDTA and 50 % glycerol for 2 hours at 4°C. The dialyzed protein was divided into suitable portions and stored at –80°C until use.

2.1.46 Incubation of TEV protease with purified MBP-PLC

MalE-TbGPI-PLC was purified from BL21 crude extract as described in section 2.14. Following this a sample (1 ml) was removed and incubated with 10 µl of purified TEV protease (see section 2.15) at either 4°C, room temperature or 30°C. Samples (20 µl) were taken at various time points in order to assay the activity of the protease and resuspended in equal volumes of 2x sample buffer. The samples were subjected to SDS-PAGE on a 15 % (w/v) acrylamide gel.

2.1.47 Removal of maltose by hydroxylapatite chromatography and domain separation by rebinding MBP to amylose

Protein eluted from the Sephacryl S-200 column was used directly or cleaved using Tobacco etch virus (TEV) in order to purify the GPI-PLC from the cleaved MalE-TbGPI-PLC fusion protein. Following cleavage of the fusion protein with the TEV protease the most efficient means of domain separation is the rebinding of MBP to amylose. In order for this to be successful the maltose had to be removed from the sample to allow it to rebind to the amylose.

Hydroxylapatite (1 g) was swollen in 20 mM sodium phosphate, 200 mM NaCl, pH 7.2. This was poured into a column (1 cm x 10 cm) and washed with ten column volumes of the same buffer. The fusion protein from the Sephacryl S-200 elution was loaded onto

the column, which was subsequently washed with 80 ml of phosphate buffer, pH 7.2. The protein was eluted with 0.5 M sodium phosphate, pH 7.2. Fractions (1 ml) were collected and protein was detected by measuring the UV absorbance at 280 nm.

Fractions containing protein were added to an amylose column pre-equilibrated in column buffer (20 mM Tris, pH 7.4; 200 mM NaCl, 10 mM β-Mercaptoethanol, 1 mM EDTA). The flow through was collected in 1 ml samples and assayed for protein by means of SDS-PAGE on a 15 % w/v acrylamide gel.

2.1.48 Release of the VSG from GPI-PLC$^-$ mutant bloodstream form trypanosomes and plasma membranes prepared from GPI-PLC$^-$ mutant bloodstream form trypanosomes using purified MBP-PLC

GPI-PLC – mutant trypanosomes at a concentration of 5 x 10^8 cells/ml, following washing with TES buffer (Table 2.1; 30 mM Tris-chloride replacing 30 mM Tes), pH 7.4, were incubated in the presence or absence of the MBP-PLC fusion protein (20 μg) or the purified PLC derived from the TEV-cleaved MBP-PLC (20 μg), +/- tritonX-100 (0.2% w/v) at 37°C. Plasma membranes were prepared from GPI-PLC$^-$ mutant trypanosomes (see Section 2.1.28) and following washing with TES buffer (see Table 2.1; 30 mM Tris-chloride replacing 30 mM Tes), pH 7.4, plasma membranes at a concentration equivalent to 5 x 10^8 cells/ml (measured by light scattering at 600 nm, see Fig 2.11) were incubated in the presence or absence of the MBP-PLC fusion (20 μg) +/- Tx-100 (0.2%) or the Tev cleaved MBP-PLC (20 μg), +/- tritonX-100 (0.2% w/v) at 37°C for 15 mins.

Immunofluoresence Techniques.

2.1.49 Preparation of fixative.

Paraformaldehyde (3-6% w/v) was prepared freshly on the day of the experiment or frozen in portions at -20°C. The required weight of paraformaldehyde was added to 5 volumes of distilled, deionised water. The insoluble paraformaldehyde was then titrated with NaOH (5 M) and stirred vigorously until the paraformaldehyde was fully dissolved. 10 volumes of PBS were then added to the fixative. HCl (12 M) was added to the fixative

Figure 2.11. Folin-Lowry Standard Curve using *Trypanosoma brucei* as the protein Standard and Light Scattering of the cells at 640 nm.

(a). A stock solution of trypanosomes (1 x 10^9 cells /ml) and the samples to be assessed for protein content, were prepared in TES buffer, pH 7.4. The samples and the indicated concentrations of trypanosomes, in a final volume of 200 µl, were mixed with 1 ml of Reagent C (50 ml of Reagent A [Na_2CO_3, 2 % w/v in 0.1 M NaOH] plus 1 part Reagent B, which contains equal volumes of Reagent B1 [$CuSO_4.5H_20$, 1% w/v] and Reagent B2 [Sodium Potassium Tartrate, 2 % w/v] and allowed to stand at room temperature for 10 minutes. Reagent E (100 µl of a 1:1 solution of Folins Reagent :water) was added to each standard and sample, which were then incubated for a further 30 minutes at room temperature. The absorbance of both standards and samples was read at 650 nm (■) and was measured using a Reagent Blank (prepared as above using only 200 µl TES buffer, pH 7.4). Data are the mean +/- the standard deviation of triplicate measurements and where no error bars are shown the error is smaller than the symbol used.

(b). A stock solution of trypanosomes (1 x 10^9 cells /ml) and the samples to be assessed for protein content, were prepared in TES buffer, pH 7.4. The samples and the indicated concentrations of trypanosomes were assessed for light scattering by measuring their absorbance at 640 nm (◆).

Figure 2.11. Folin-Lowry Standard Curve using *Trypanosoma brucei* as the protein Standard and Light Scattering of the cells at 640 nm.

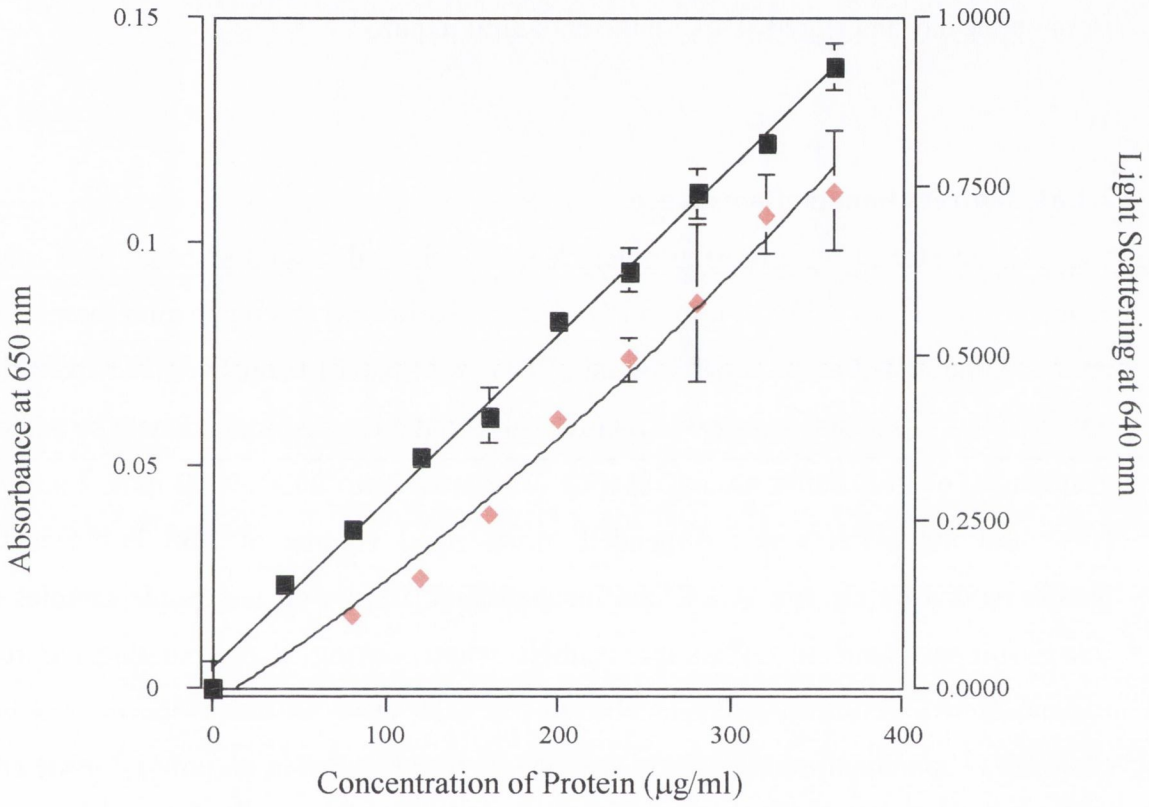

until the pH of the solution reached 7.5. Sufficient distilled deionised water was added to bring the solution to the required concentration. The fixative was filtered through a 0.2 μm pore filter before use.

2.1.50 Preparation of antiquench solution.

The anti-oxidant *p*-phenyldiamine (2 mg/ml) was dissolved in PBS buffer containing sodium azide (15 mM) and glycerol (50% w/v). This solution was always made fresh on the day and stored at 4°C in the dark until required.

2.1.51 Indirect Immunofluoresence.

Bloodstream form trypanosomes (5 x 10^7 cells /ml) were incubated with constant gentle stirring at 37°C for 20 min in PBS buffer. Following this incubation samples were removed and added to an equal volume of 6% (w/v) paraformaldehyde and fixed for 10 min at 37°C. A second sample was removed and cold quenched immediately by adding an excess (5x) of PBS buffer already at 0°C. This was centrifuged (9000 rpm, 2 min, 4°C) (w/v) and the pellet was resuspended in an equal volume of PBS buffer and 6% paraformaldehyde already at 4°C and incubated for 10 min on ice (Some samples were fixed with methanol at –20°C; for example when looking at the paraflagellar rod of trypanosomes). Following this incubation the cells were washed twice in PBS buffer (Table 2.1) containing sodium azide (15 mM) before incubation on poly-L-Lysine coated coverslips (100 μl/coverslip).

Procyclic trypanosomes (1 x 10^7 cells/ml) were fixed by addition to an equal volume of paraformaldehyde (6 % w/v). Following 1hr incubation at room temperature the cells were washed twice in PBS buffer (Table 2.1) containing sodium azide (15 mM) before incubation on poly-L-Lysine coated coverslips (100 μl/coverslip).

Following fixation bloodstream and procyclic form trypanosomes were allowed to settle on poly-L-lysine coverslips for 15 minutes, the cells on the coverslips were then incubated with blocking buffer (PBS containing 5 % BSA and methylamine, 0.1 M) for 1h at room temperature, to inactivate any remaining formaldehyde and block non-specific binding. The cells on the coverslips were incubated with primary antibody diluted in PBS containing 5% (w/v) BSA overnight at room temperature. Following washing with PBS

(x3) the cells on the coverslips were incubated with the secondary antibody conjugated to a fluor diluted with PBS (x3) for 3 h at room temperature. The cells on the coverslips were then washed with PBS containing Hoechst (0.1 μg/ml final) and finally mounted onto glass slides using 5 μl of anti-quench solution.

2.1.52 Incubation of cells with a non-aggregating concentration of anti-VSG IgM.

Bloodstream form trypanosomes (5 x 10^7 cells /ml) were incubated with constant gentle stirring at 30°C for 20 min in isosmotic TES buffer. The cells were then immediately diluted (5x) in ice-cold isosmotic TES buffer and washed (x1) by centrifugation (6,000 ***g***, 2 min, 4°C). The pellet was resuspended in the same buffer to give a final concentration of 5 x 10^7 cells/ml. A non-aggregating concentration of anti-VSG IgM was then added to these cells at 0°C. Following a 30 min incubation on ice the cells were washed (x1) by centrifugation at 0°C. The pellet was resuspended in isosmotic TES buffer already at 30°C and samples were withdrawn for fixing at 0°C with an equal volume of 6% paraformaldehyde at the following time points:0, 1, 2, 3, 5, 10, 20, 30 and 60 mins.

2.1.53 Confocal Microscopy.

In order to preserve the three-dimensional structure of the trypanosomes, a varnish spacer was constructed on each poly-L-lysine coverslip by brushing along each side of the slip with clear nail varnish and then allowed to dry prior to addition of cells. The coverslips with the anti-quench solution were gently placed on clean slides and were affixed to the glass slide by applying a thin film of nail varnish to the edges of the coverslip. This procedure also prevented the samples from drying out. The slides were examined by phase contrast and confocal microscopy with an Olympus Fluoview FV1000 Imaging system. The excitation light for imaging was provided by the 457-514 nm lines of a multi-line Argon laser, the 543 nm line of a Green Helium-Neon laser and the 633 nm line of a Red Helium-Neon laser. Images were collected and processed with the Olympus Fluoview software (Version 1.3c).

2.1.54 Immunoassay of GPI-PLC by direct ELISA.

Samples were solubilized with 0.1 M NaOH and incubated for 30 min at room temperature in this solution. Samples were then spun on bench centrifuge for 10 min and supernatant removed and used for the coating of the plate. Samples were diluted with coating buffer (Glycine 100 mM, pH 9.4) and 100 µl of each sample added, in quintriplicate, to high binding polystyrene microtitre immunoassay plates (Immulon 2). The plates were incubated at 37°C for 1.5 h in a humidified chamber. Following washing of the wells (x4) with Tris-Tween (100 mM; pH 7.4; containing Tween-20, 0.05%, w/v) the plates were blocked with 200 µl of blocking buffer (Tris-Tween containing BSA, 0.5%, w/v) and incubated at 37°C for 30 min. The plates were again washed (x4) with Tris-Tween and incubated with rabbit anti-GPI-PLC antibody (100 µl of 1/1000 dilution in blocking buffer; stock concentration 1.5 mg/ml) for 1 h at 37°C. After washing (x4) with Tris-Tween, binding of the primary antibody was detected by incubating the plates with an anti-rabbit IgG alkaline phosphatase conjugate (100 µl of a 1/30,000 dilution in blocking buffer) for 1 h at 37°C. Subsequent to a final washing (x4) with Tris-Tween, the plates were developed with 100 µl/well of an alkaline phosphatase substrate solution (diethanolamine, 10% (v/v); $MgCl_2$, 1 mg/ml; pH 9.8; containing *p*-nitrophenyl phosphate, 1 mg/ml). The reaction was stopped by addition of 100 µl of NaOH (1.5 M). Absorbance readings were taken at 405 nm in a microtitre plate reader.

2.1.55 Immunoassay of GPI-PLC by sandwich ELISA.

High binding polystyrene microtitre immunoassay plates (Immulon 2) were incubated with sheep anti-GPI-PLC antibody (100 µl of 1/500 dilution in 100 mM Glycine, pH 9.4 per well) at 37°C for 1.5 h in a humidified chamber. Following washing of the wells (x4) with Tris-Tween (100 mM; pH 7.4; containing Tween-20, 0.05%, w/v) the plates were blocked with 200 µl of blocking buffer (Tris-Tween containing BSA, 0.5%, w/v) and incubated at 37°C for 30min. The plates were again washed (x4) with Tris-Tween. The samples containing the GPI-PLC were solubilized with 0.1 M NaOH and incubated for 30min at room temperature. The samples were then diluted with blocking buffer and 100µl was added to each well, and incubated for 1h at 37°C. After washing (x4) with Tris-Tween, the plates were incubated with rabbit anti-GPI-PLC antibody (100 µl/well of a 1/1000 dilution in blocking buffer) for 1 h at 37°C. Following washing (x4)

with Tris-Tween, binding of the second antibody was detected by incubating the plates with an alkaline phosphatase conjugate (100 µl of a 1/30,000 dilution in blocking buffer) for 1 h at 37°C. Subsequent to a final washing (x4) with Tris-Tween, the plates were developed with 100µl/well of an alkaline phosphatase substrate solution (diethanolamine, 10% (v/v); $MgCl_2$, 1 mg/ml; pH 9.8; containing *p*-nitrophenyl phosphate, 1mg/ml). The reaction was stopped by addition of 100 µl of NaOH (1.5 M). Absorbance readings were taken at 405 nm in a microtitre plate reader.

2.1.56 Immunoassay of GPI-PLC by Direct ELISA followed by Cycling assay.

Samples were solubilized with 0.1 M NaOH and incubated for 30 min at room temperature in this solution. Samples were then spun on bench centrifuge for 10 min and supernatant removed and used for the coating of the plate. Samples were diluted with coating buffer (Glycine 100 mM, pH 9.4) and 100 µl of each sample added, in quintriplicate, to high binding polystyrene microtitre immunoassay plates (Immulon 2). The plates were incubated at 37°C for 1.5h in a humidified chamber. Following washing of the wells (x4) with Tris-Tween (100 mM; pH 7.4; containing Tween-20, 0.05%, w/v) the plates were blocked with 200 µl of blocking buffer (Tris-Tween containing BSA, 0.5%, w/v) and incubated at 37°C for 30 min. The plates were again washed (x4) with Tris-Tween and incubated with rabbit anti-GPI-PLC antibody (100 µl of 1/1000 dilution in blocking buffer; stock concentration 1.5 mg/ml) for 1h at 37°C. After washing (x4) with Tris-Tween, binding of the primary antibody was detected by incubating the plates with an anti-rabbit IgG alkaline phosphatase conjugate (100 µl of a 1/30,000 dilution in blocking buffer) for 1 h at 37°C. Subsequent to a final washing (x8) with Tris-Tween, the plates were developed with 100 µl/well of a substrate solution (50 mM diethanolamine, 1 mM $MgCl_2$; pH 9.5; 0.7 M ethanol; containing 0.1 mM NADPH). This was left for 20 min at room temperature. Following this, the plates were further developed using the cycling assay (Fig 2.12). 200 µl/well of amplifier buffer (Na2HPO4, 20 mM, pH 7.2; Triton X-100 (0.05% v/v); 1 mM INT-violet containing 600 U alcohol dehydrogenase from yeast and 15 U pig heart diaphorase per 12ml of amplifier buffer) was added. The reaction was stopped by addition of 50 µl of sulphuric acid (0.2 M). Absorbance readings were taken at 495 nm in a microtitre plate reader.

Fig 2.12. Principle of enzyme amplification for the detection of alkaline phosphatase label by the production of Formazan.

A critical feature of the enzyme amplification system is that the activator is not consumed as a result of the activity of the secondary system. However, a key factor in the development of the system was the realization that the activator could be consumed as long as it was reformed. This led to the development of cyclic amplifiers. In these the labelling enzyme produces a substance, such as a cofactor, which is recycled by a cycling system, the operation of which produces the substance to be detected. As shown in the diagram, the alkaline phosphatase may be quantitated by its activity in dephosphorylating NADPH to produce NADH. The NADH formed completes a cycle in a second step catalysed by alcohol dehydrogenase and diaphorase, in the presence of ethanol and INT-violet, giving rise to an intensely coloured purple formazan. Thus the NADH produced by the action of the immunochemical labelling enzyme, alkaline phosphatase, is converted to NAD by the action of the alcohol dehydrogenase, and when reformed by the action of diaphorase INT-violet is reduced to form the highly coloured formazan. One molecule of formazan is produced in each 'turn' of the cycle and the speed at which the cycling reactions operate depends on the concentration of the two enzymes and of the NADH.

Fig 2.12. Principle of enzyme amplification for the detection of alkaline phosphatase label by the production of Formazan.

Principle of cycling assay

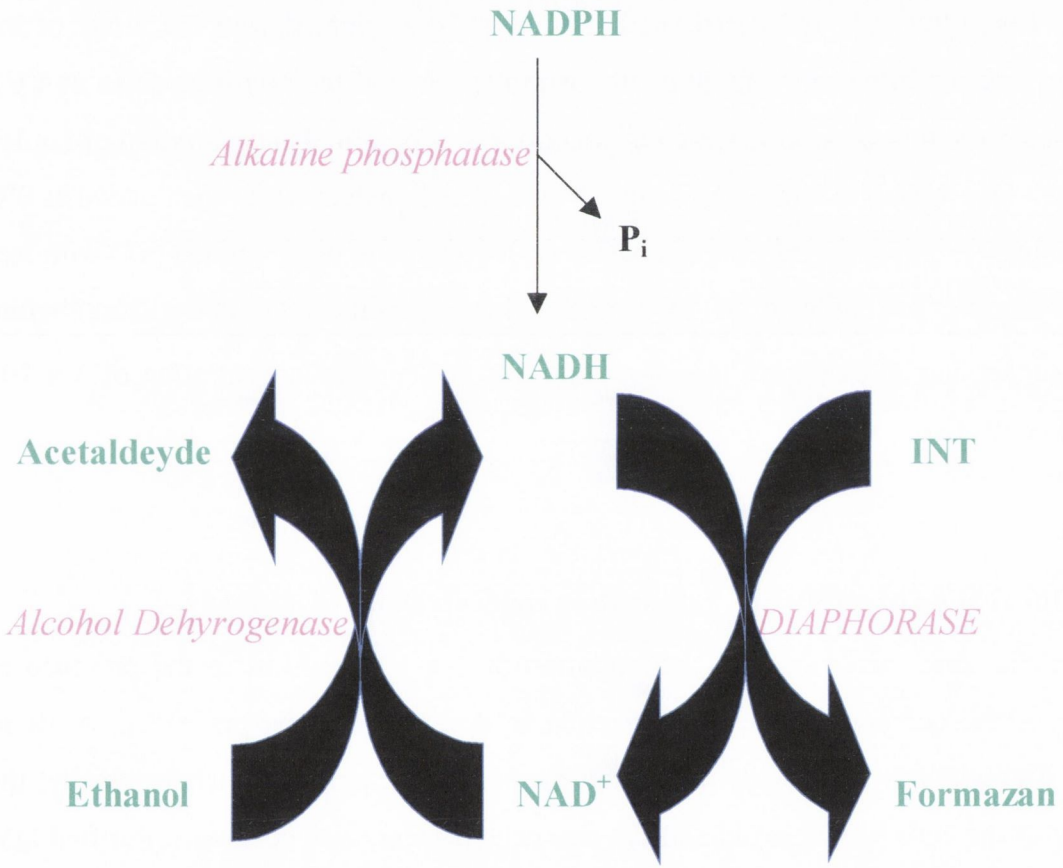

2.1.57 Measurement of oxygen consumption by *T. brucei.*

Glucose supported respiration was measured with a Rank oxygen electrode using the following incubation conditions: final density of cells, 2 x 10^7/ml; final volume in the electrode chamber, 4 ml; temperature 37°C.

2.1.58 Incubation of cells with FITC labeled antibody.

Cells (5 x 10^7/ml) were incubated in iso-osmotic Tes buffer pH 7.5 at 37°C in a final volume of 10 ml. Following a 15 min period of incubation under these conditions to ensure a normal level of cellular ATP, the cells were cold quenched in ice-cold iso-osmotic Tes buffer (x4) and centrifuged (10,000 ***g***, 10 s oriented with the hinge of the minifuge tube up followed by 3,000 ***g***, 10 s with the hinge of the minifuge down at 4°C). The pellets were resuspended in ice-cold Tes buffer to give a final concentration of 2 x 10^8 cells/ml. Fluorescein labeled IgM or IgG antibody or transferrin was then added at 0°C with mixing. Following a 30 min incubation at 0°C the cells were washed (x2) with ice-cold iso-osmotic Tes buffer (1 ml) by centrifugation/resuspension (12,000 ***g***, 20 s) before final resuspension and addition to iso-osmotic Tes buffer at a concentration of 3 x 10^7 cells/ml at 30° C.

2.1.59 Incubation of cells with agglutinating concentrations of antibody.

Cells were incubated at a concentration of 2 x 10^7 cells/ml in the presence or absence of the compound under investigation in a stirred chamber at 30°C. A 10 µl sample was withdrawn from the incubation medium and examined microscopically; the viability of the cells was checked and the free cells present were counted. Purified IgM antibody was added to the incubation medium at the concentrations indicated in the legends at a time designated (t_0) and at subsequent specified times (t_X) samples (10 µl) were removed from the incubation medium and the number of free, unaggregated cells was counted by microscopy. The percentage aggregation was calculated according to the following equation:

$$\frac{(\text{Number of free cells at } t_0 - \text{number of free cells at } t_X) \times 100}{\text{Number of free cells at } t_0}$$

2.1.60 Removal of Sodium Dodecyl Sulfate from Protein Samples Prior to Matrix-assisted Laser Desorption/ionization Mass Spectrometry (MALDI/MS)

This procedure is a modification of the extraction method by Wessel and Flugge (1984). Methanol (800 µl) was mixed with the protein sample (200 µl). The sample was centrifuged (10 seconds; 9,000 ***g***). Chloroform (200 µl) was added and the sample was vortexed and centrifuged (10 seconds; 9,000 ***g***). Deionised water (600 µl) was added and the sample was centrifuged (1 min, 9,000 ***g***). The precipitated proteins were localised at the interphase. The upper supernatant (S1) was carefully removed and stored. An additional volume of methanol (600 µl) was added to the lower chloroform phase. The sample was mixed and centrifuged (2 min; 9,000 **g**) in order to pellet the protein. The supernatant (S2) was removed and stored. The pellet was dried under air stream in a speedy vac. The organic phases were then evaporated under a stream of air in a speedy vac.

2.1.61 MALDI-TOFMS

The sample matrix used was sinapinic acid (3,5-dimethoxy-4-hydroxy cinnamic acid), 10 mg, dissolved in acetonitrile (300 µl) and 0.1 % (w/v) trifluoroacetic acid (700 µl) in deionized water (300 µl and 700 µl respectively). Protein pellets from chloroform/methanol extraction (section 2.x) were dissolved in 20 µl of 20 mM N-octylglucoside. The samples were prepared with the seed layer method (Westman, *et al*). Briefly, a matrix seed layer was created by depositing a droplet (1 µl) of a 10 mg/ml solution of matrix onto a well on the stainless steel probe. A droplet (1 µl) of the protein solution was added to the matrix seed layer. The samples were left to dry at ambient conditions.

All MALDI spectra were acquired using a Voyager-DE PRO MALDI-TOF mass spectrometer equipped with a nitrogen laser.

2.1.62 Protein Determination

Protein concentrations were determined by the method of Markwell *et al.* (1978) using bovine serum albumin as a protein standard (Fig 2.13). For less critical protein

determinations the absorbance at 280 nm was used where the absorbance could be used to work out concentration of protein based on the following equation (Perkins, 1986):

$$\varepsilon = 5550\ (W) + 1340\ (Y) + 150\ (C)$$

where ε represents the extinction coefficient

W corresponds to the number of tryptophan residues / mole of protein

Y corresponds to the number of tyrosine residues / mole of protein

C corresponds to the number of cysteine residues / mole of protein.

2.1.63 Concentration of Protein

Protein was concentrated by ultra filtration using Vivaspin centrifugal concentrators (Sartorius). Generally vivaspins with 5,000 molecular weight cut off, low adsorption, hydrophillic membranes were used which held a maximum sample volume of 6 ml. The sample was centrifuged (4,000 ***g*** x 30 min) and the retentate containing the concentrated protein separated from filtrate, prior to resuspension in an appropriate buffer or other manipulation.

2.1.64 Ultraviolet and visible spectrophotometry

Routine measurements (*e.g.* absorbance at 280 nm) were made using a Pye Unicam single beam spectrophotometer. Samples of fluorescent labelled protein was scanned between the wavelengths 240-800 nm using a Hewlet-Packard 8452A Diode array spectrophotometer coupled with a Hewlet-Packard Vectra ES/12 computer. Samples were measured in a 1 ml quartz cuvette.

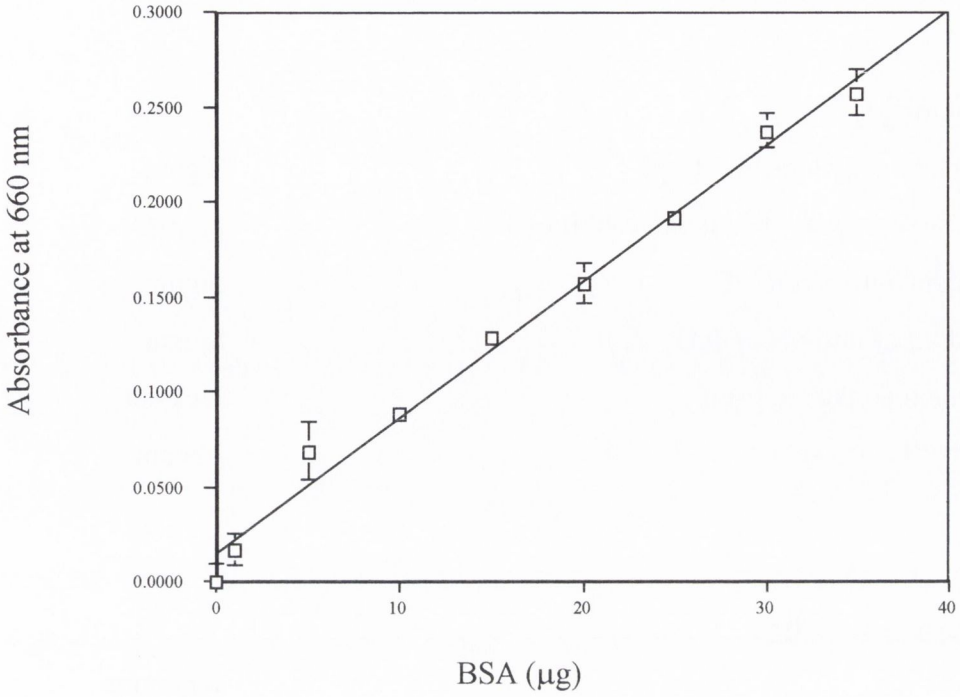

Fig 2.13. Markwell Standard Curve using BSA as a protein standard.

A stock solution of BSA (1mg/ml) and the samples to be assessed for protein content, were prepared in Tris buffer, pH7.5 (10mM). The samples and the indicated concentrations of BSA, in a final volume of 250µl, were mixed with 750µl of Markwell Reagent C (100 parts Reagent A [Na_2CO_3, 2% (w/v); NaOH, 0.4% (w/v); sodium tartrate, 0.16% (w/v); SDS,1% (w/v)] plus 1 part Reagent B [$CuSO_4.5H_2O$, 4% (w/v)]) and incubated for 20min at room temperature. Reagent D (75µl of a 1:1 solution of Folins Reagent: water) was added to each standard and sample, which were then incubated for a further 45min at room temperature in the dark. The absorbance of both BSA standards and samples was read at 660nm and was measured against a reagent blank [prepared as above using only 250µl Tris buffer, pH7.5 (10mM)]. Data are the mean +/- the standard deviation of triplicate measurements and where no error bars are shown the error is smaller the symbol used. Data for the standard BSA curve was plotted using Cricket Graph and the equation for the line ($y = 0.014x + 0.030$) was used to estimate protein concentration from the absorbance values obtained for the samples.

2.2. Materials.

2.2.1 Immunochemicals

Peroxidase conjugated goat anti-rabbit IgG	Sigma
Alkaline phosphatase conjugated goat anti rabbit IgG	Sigma
FITC conjugated goat anti-rabbit IgG	Sigma
FITC conjugated donkey anti-sheep IgG	Sigma
Texas Red conjugated donkey anti-rat	Jackson
Anti-alpha tubulin (YOL1/34)	Abcam

2.2.2 Chromatographic media

DEAE 52	Whatman
Sephadex G-25	Sigma
Protein A Sepharose CL-4B	Sigma
Ultrogel AcA34	LKB
CNBr activated Sepharose CL-4B	Sigma
Epoxy-activated Sepharose 6B	Sigma
Sephacryl S-200	Pharmacia
Hydroxylapatite	Bio-Rad
PBE 94 Polybuffer^{TM} Exchanger	Amersham
Amylose Resin	NEB

2.2.3 Protease inhibitors

Leupeptin	Sigma
Phenylmethylsulphonyl fluoride (PMSF)	Sigma
Tosyl lysine chloromethylketone (TLCK)	Merck
Pepstatin	Sigma

2.2.4 Molecular weight markers

Low molecular weight markers for SDS-PAGE:	Sigma
Albumin (bovine serum)	66 kDa
Ovalbumin (chicken egg)	45 kDa
Glyceraldehyde-3-phosphate Dehydrogenase	36 kDa
Carbonic anhydrase (bovine erythrocyte)	29 kDa
Trypsinogen (bovine pancreas)	24 kDa
Trypsin Inhibitor, soyabean	20.1 kDa
Lactalbumin (Bovine milk)	14.2 kDa

Molecular weight markers for gel filtration:	Sigma
Blue Dextran	2,000 kDa
Bovine Serum Albumin	66 kDa
Ovalbumin (egg)	45 kDa
Cytochrome C	12.4 kDa

2.2.5 Solvents

Dimethylsulphoxide	BDH
Dimethylforamide	BDH
Methanol	BDH
Ethanol	BDH

2.2.6 Detergents

Tween-20	Sigma
Triton X-100	Sigma

2.2.7 Acids/Bases

Acetic Acid	BDH
Hydrochloric Acid	BDH
Nitric Acid	BDH

Sulphuric Acid	BDH
Sodium Hydroxide	Sigma

2.2.8 Molecular Biology

dNTPs	MSC
25mM $MgCl_2$	Sigma
PCR primers	MWG Biotech
10X PCR buffer	Sigma
Taq polymerase	Sigma
Restriction enzymes	Roche/Sigma
10X restriction enzyme buffer	Roche/Sigma
T4 DNA ligase	NEB
10X ligase buffer	NEB

2.2.9 Miscellaneous

Acrylamide	Lennox
Adenosine	Sigma
Albumin, Bovine	Sigma
Ammonium persulphate	Sigma
Bisacrylamide	Lennox
Chloroquine	Sigma
Coverslides for microscopy	Lennox
2-Deoxy-D-Glucose	Sigma
EGTA	Sigma
Extravidin (alkaline phosphatase conjugate)	Sigma
Filter Paper	Lennox
Fluorescein isothiocyanate	Sigma
Glucose	Duchefa
Glycerol	Sigma
Heparinised microhaematocrit tubes	Lennox
Hydrogen Peroxide	Sigma
Iodine –125	Amersham

4-Iodophenol	Aldrich
Luminol	Sigma
Marvel (low fat milk)	Purchased from local food stores
Peroxidase conjugated Protein A	Merck
Peroxidase conjugated Protein G	Merck
Peroxidase conjugated Streptavidin	Merck
Polyethlyene glycol 6000	Lennox
Poly-L-Lysine solution	Sigma
Sodium Dodecyl Sulphate	Duchefa
Slides for microscopy	Lennox
Sulfo-NHS-LC-Biotin	Pierce
TEMED	Sigma

2.3 Addresses of suppliers

Lennox Laboratory Supplies, J.F.K Drive, Naas Road, Dublin 12.	**Sigma-Aldrich Ireland Ltd.** Dublin, Ireland
Merck Biosciences, Ltd. Boulevard Industrial Park Padge Road Beeston Nottingham NG9 2JR United Kingdom	**Perbio Science UK Ltd.** Unit 9, Atley Way North Nelson Industrial Estate Cramlington, Northumberland NE231WA United Kingdom
Roche Diagnostics Ltd. Bell Lane, Lewes East Sussex BN7 1LG, United Kingdom	**New England Biolabs (UK) Ltd.** 73 Knowl Piece, Wilbury Way Hitchin, Herts. SG4 0TY United Kingdom
Mwg-Biotech AG Anzingerstr. 7a 85560 Ebersberg Germany	**Medical Supply Co. Ltd.** Damastown Mulhuddart Dublin 15 Ireland
Amersham plc Amersham Place Little Chalfont Buckinghamshire HP7 9NA United Kingdom	**Pharmacia LKB Biotechnology** S-75182 Uppsala Sweden
Stratech Scientific Ltd. Unit 4 Northfield Business Park Northfield Road Soham Cambridgshire CB7 5UE England	**Abcam plc** 332 Cambridge Science Park Milton Road Cambridge CB4 0FW UK

Chapter 3

Localisation of the GPI-PLC in bloodstream forms of T. brucei using confocal microscopy

3.1. Introduction

There has been considerable controversy over the location of the GPI-PLC in bloodstream form trypanosomes. Three conflicting findings were published in the 1980s. Firstly, in 1984 it was reported that the GPI-PLC was located in the plasma membrane (Turner, 1984). Secondly, in 1987 it was reported that the GPI-PLC was present in, or enclosed by, membranes of the flagellum and flagellar pocket, as well as in the Golgi fraction of bloodstream form trypanosomes (Grab *et al.*, 1987). Subsequently, in 1989 it was reported that the GPI-PLC was not associated with the inner or outer face of the plasma membrane, including the specialized region forming the flagellar pocket but was in fact, associated with the cytoplasmic face of intracellular vesicles located in the region of the cytoplasm between the golgi and the flagellar pocket (Bulow *et al.*, 1989). Then, in 2003 the presence of a portion of the cellular pool of GPI-PLC was reported to be located on the surface of non-dividing short stumpy trypanosomes (Gruszynski *et al.*, 2003) but absent from the surface of dividing long thin trypanosomes. This finding is consistent with the direct release of the VSG from the cell surface by activated, extracellular GPI-PLC during differentiation of bloodstream forms to procyclic forms (Ziegelbauer *et al.*, 1993) but does not account for the rapid and complete release of the VSG during hypotonic lysis of long-thin bloodstream forms (Cardoso De Almeida *et al.*, 1999). To explain the release of the VSG during hypotonic lysis, it was argued that the GPI-PLC was located on the inner face of the plasma membrane in intact cells and then translocated to the outer face by diffusion around the fractured, open end of the plasma membrane following cell lysis (Cardoso De Almeida *et al.*, 1999). However this explanation fails to account for release of the VSG from intact bloodstream forms during treatment with Ca^{2+} and the calcium ionophore, A23187 (Bowles and Voorheis, 1982, Voorheis, 1982). The most recent report has concluded that the GPI-PLC is predominantly a glycosomal protein and under alkaline conditions the enzyme is translocated to the endoplasmic reticulum. It was also concluded in this last report that the translocation of GPI-PLC from glycosomes to the endoplasmic reticulum was important for the *in vivo* cleavage of GPIs (Subramanya and Mensa-Wilmot, 2006). The mfVSG covers the entire plasma membrane of the cell (Vickerman, 1969) and is the major substrate for the GPI-PLC in bloodstream form trypanosomes. If the GPI-PLC becomes active, how can it then bind its major substrate if the enzyme is localized in intracellular vesicles, in the golgi apparatus, on the inner face of the plasma membrane or in glycosomes, if the substrate is in the plasma membrane?

In summary, there has been a great deal of work done on the cellular distribution of the GPI-PLC and many different and conflicting locations have been reported:

A. The plasma membrane (Turner, 1984)
B. The flagellar pocket and golgi apparatus (Grab *et al.*, 1987)
C. The cytoplasmic face of intracellular vesicles located between the golgi and the flagellar pocket (Bulow *et al.*, 1989)
D. The surface of stumpy form trypanosomes but not long slender bloodstream form trypanosomes (Gruszynski *et al.*, 2003)
E. Predominantly a glycosomal localization (Subramanya and Mensa-Wilmot, 2006)

This chapter attempts to clarify our view of the localization of the GPI-PLC in bloodstream form trypanosomes by reference to results of new experiments designed to address this question. The localization of the GPI-PLC in bloodstream forms of *T. brucei* was studied by using Cy3-labelled IgG anti-GPI-PLC together with confocal laser-scanning fluorescence microscopy. The localization of the VSG and tubulin, which are known to be attached to the outer leaflet of the plasma membrane and to a protein within the inner leaflet of the plasma membrane respectively, were used as controls in all experiments. In addition, a further control employed Cy3-labelled anti-ISG-70, which is located on the outer leaflet of the plasma membrane but shielded by the VSG. In addition, the distribution of the GPI-PLC was investigated with respect to the plasma membrane of bloodstream form trypanosomes by using a Cy3-conjugated membrane dye and also with respect to the inner leaflet of the plasma membrane by comparing the localization of GPI-PLC with that of pellicular tubulin, which is located immediately adjacent to the inner (cytoplasmic) surface of the plasma membrane covering the cell body. Furthermore, both the para-flagellar rod and the flagellar attachment zone of bloodstream form trypanosomes were studied by immunofluoresence in conjunction with studies of the GPI-PLC to provide further markers for the structures close to the location of the GPI-PLC.

3.2. *Results*

3.2.1 Detection of the GPI-PLC in bloodstream form trypanosomes and in plasma membranes prepared from them.

Antibodies against the GPI-PLC were produced in New Zealand White rabbits (3.5 kg) by inoculation of the popliteal lymph nodes with purified recombinant GPI-PLC (~150 μg) followed by a subcutaneous boost after both weeks two and four. At week seven, an immune serum sample was withdrawn and following an ELISA, the antibody titre was found to be sufficient for use and the animal was exsanguinated. Following centrifugation (1,000 ***g***, 10 min) the upper plasma layer was removed and recentrifuged (100,000 ***g***, 1 h). Lipid was removed from the plasma layer by aspiration. Resulting clear serum was divided into suitable size fractions and stored at –20°C. Antibodies were subsequently purified using a Protein A Sepharose column (Section 2.1.11. & Fig 2.4).

This purified IgG anti-GPI-PLC antibody was used throughout the project for detection of the GPI-PLC in bloodstream from trypanosomes by the methods of ELISA, Western blotting, immunofluoresence and immunoprecipitation. To validate the specificity of the IgG anti-GPI-PLC, this antibody was used to detect the presence of the GPI-PLC in wild-type bloodstream from trypanosomes, as well as its absence from procyclic trypanosomes and from GPI-PLC $^{-}$ mutant bloodstream form trypanosomes. The antibody was found to be specific for the GPI-PLC. It detected a single protein band at approximately 39 kDa which was absent in GPI-PLC $^{-}$ mutant trypanosomes (Fig 3.1 A, lane 1). This demonstrates that the GPI-PLC $^{-}$ mutant trypanosomes that were used as a negative control in all experiments did not express the protein, since the antibody was unable to detect any protein in these cells at the molecular weight of the GPI-PLC. Immunofluorescent studies of GPI-PLC $^{-}$ mutant trypanosomes and procyclic trypanosomes revealed no fluorescence when probed with IgG anti-GPI-PLC antibody (Plate 3.1, Panel A & Panel B). In addition, the anti-GPI-PLC IgG was used to immunoprecipitate the GPI-PLC from a mixture of TEV cleaved MBP-TbGPI-PLC fusion protein, which contained uncleaved MBP-TbGPI-PLC, MBP and GPI-PLC. SDS-PAGE was performed on the immunoprecipitated sample and the band corresponding to the GPI-PLC (~ 39 kDa) on a Coomassie stained gel was cut out and analysed by mass spectrometry. This analysis revealed that the protein immunoprecipitated by the anti-GPI-PLC IgG was indeed the GPI-PLC (Fig 3.2). These results confirm that the anti-GPI-PLC antibody truly identifies the GPI-PLC.

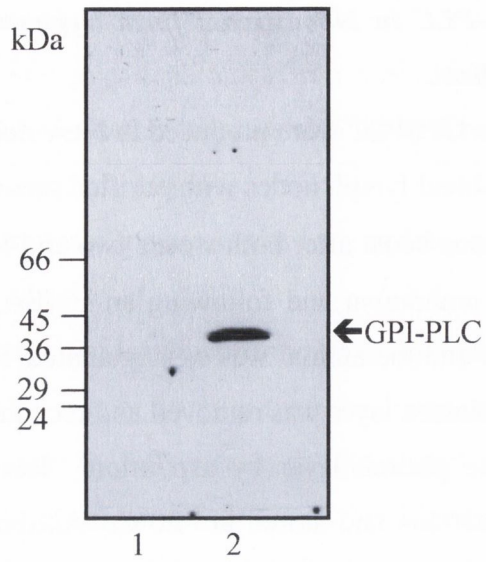

Fig 3.1. SDS-PAGE showing the detection of the GPI-PLC in bloodstream form trypanosomes.

Bloodstream form trypanosomes and GPI-PLC $^{-}$ mutant trypanosomes were separated by SDS-PAGE on 15 % (w/v) gels. These gels were then electrotransferred to PVDF membrane and subsequently probed with IgG anti-GPI-PLC antibody (1/1000 dilution) and developed by chemiluminesence.

Lane 1: GPI-PLC $^{-}$ mutant trypanosomes (2 x 10^7 cell equivalents)

Lane 2: Wild-type bloodstream form trypanosomes (2 x 10^7 cell equivalents)

Protein	**Colour**
1. GPI-PLC	Magenta
2. VSG	Red
3. ISG-70	Yellow
4. Tubulin	Cyan
5. Paraflagellar rod	Green
6. Membrane marker	Green
7. Flagellar attachment zone	Orange (Plate 3.15) Cyan (Plate 3.14)

Table 3.1. Colour assigned to proteins studied by confocal microscopy in this chapter.

This table lists the proteins of *T. brucei* that have been studied by confocal microscopy in this chapter. Each protein is represented by a different colour, as shown in this table, when detected by laser scanning confocal fluorescence microscopy and then displayed in the Plates that accompany this chapter.

Plate 3.1. Confocal images showing GPI-PLC $^{-}$ mutant trypanosomes and procyclic trypanosomes incubated with anti-GPI-PLC antibody.

GPI-PLC $^{-}$ mutant trypanosomes were fixed (5 x 10^7 cells) and procyclic trypanosomes (5 x 10^7 cells) were fixed as described in Section 2.1.51, blocked with BSA (5% w/v) for 1 hr at room temperature and following washing incubated with anti-GPI-PLC antibody (1/1000 dilution) overnight at room temperature. The cells were washed and binding of primary antibodies to the cell was detected by incubating the cells with a Cy3 conjugated anti-rabbit IgG antibody (1/1000 dilution) for the anti-GPI-PLC antibody detection. This was incubated for 1 hr at room temperature. The cells were washed and mounted onto slides as described in section 2.1.51. An Olympus FV-1000 Confocal microscope was used to collect images.

Panel A shows a GPI-PLC $^{-}$ mutant trypanosome incubated with anti-GPI-PLC antibody.

Panel B shows a procyclic trypanosome incubated with anti-GPI-PLC antibody.

Image 1 of each panel displays a phase-contrast image of the cell.

Image 2 displays the location of the nucleus and kinetoplast (blue)

Image 3 displays the GPI-PLC in GPI-PLC $^{-}$ mutant trypanosomes and procyclic trypanosomes

Plate 3.1. Confocal images showing GPI-PLC $^{-}$ mutant trypanosomes (Panel A) and procyclic trypanosomes (Panel B) incubated with anti-GPI-PLC antibody.

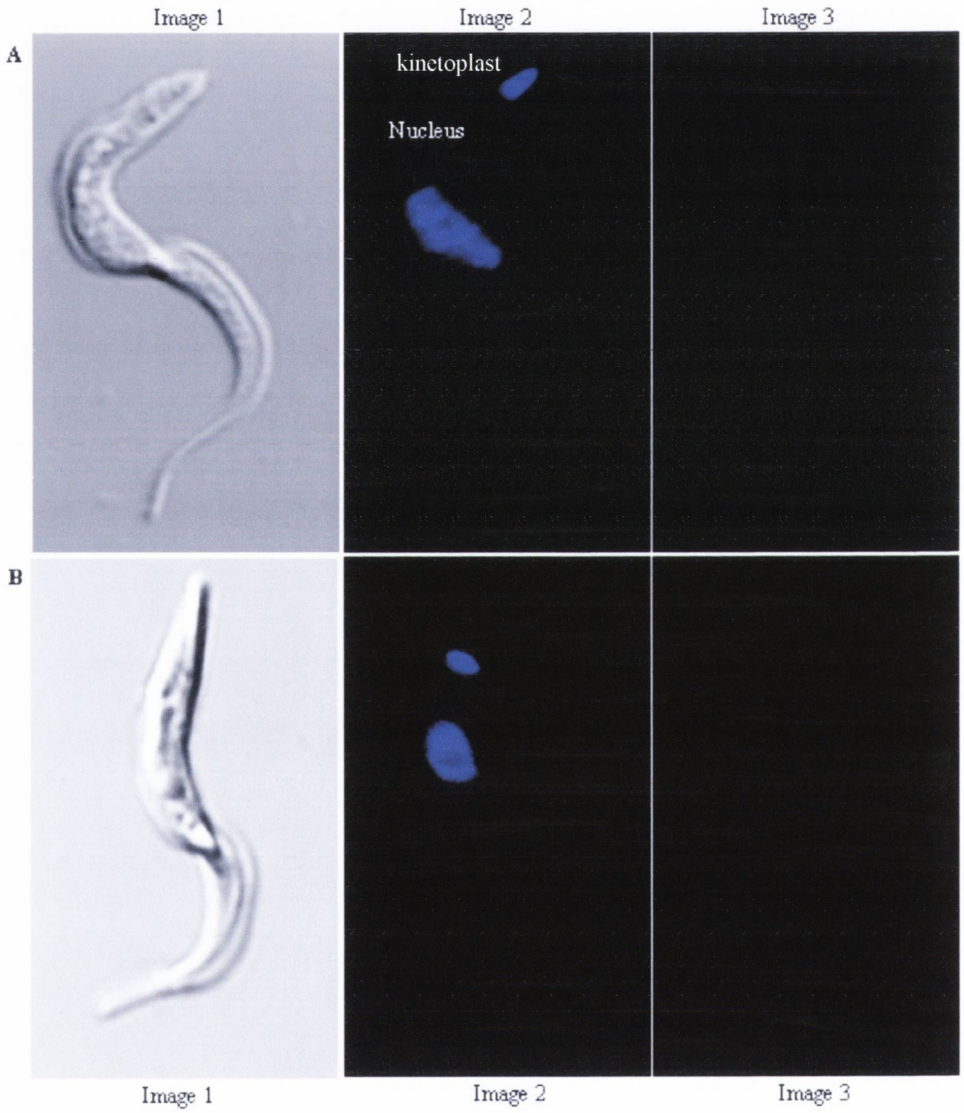

MFGGVKWSPQSWMSDTRSSIEKKCIGQVYMVGAHNAGTHGIQMFSPFGLDAPEKLRSLPP
WSPQSWMSDTR SLPP

YVTFLLRFLTVGVSSRWGRCQNLSIRQLLDHGVRYLDLRMNISPDQENKIYTTHFHISVP
YVTFLLRFLTVGVSSR IYTTHFHISVP

LQEVLKDVKDFLTTPASANEFVILDFLHFYGFNESHTMKRFVEELQALEEFYIPTTVSLT
LQEVLKDVK

TPLCNLWQSTRRIFLVVRPYVEYPYARLRSVALKSIWVNQMELNDLLDRLEELMTRDLED
SIWVNQMELNDLLDRLEELMTRDLED

VSIGGVPSKMYVTQAIGTPRNNDFAVAACCGACPGSHPDLYSAAKHKNPHLLKWFYDLNV
MYVTQAIGTPR

NGVMRGERVTIRRGNNTHGNILLLDFVQEGTCTVKGVDKPMNAVALCVHLNTNQTAR

Fig 3.2. Amino acid sequence of the genomic GPI-PLC shown in black and the actual peptides produced from the tryptic digestion as detected by mass spectrometry are shown in red underneath.

3.2.2. Cellular distribution of GPI-PLC, VSG and tubulin in bloodstream form trypanosomes.

Confocal laser scanning microscopy in conjunction with immunofluorescence was used to determine the distribution of the GPI-PLC in bloodstream form trypanosomes. Bloodstream form trypanosomes were fixed as described in Section 2.1.51, and incubated with anti-GPI-PLC antibody, anti-VSG antibody, anti-ISG-70 antibody or anti-α-tubulin antibody. Binding to the cells was detected with a Cy3-labelled anti-rabbit IgG antibody in the case of GPI-PLC, VSG and ISG-70 and an Alexa 488 labelled anti-IgG antibody in the case of tubulin localization.

The control for labelling and detecting the position of the outer surface of the trypanosomes was to label the cells with anti-VSG antibody. The VSG is the predominant protein in the surface coat of bloodstream form trypanosomes and it forms the most distal, exterior part of these cells. Therefore, anti-VSG antibody will label the outside of the cell easily. The VSG was found evenly distributed over the entire surface of the trypanosome (for low power views see plates 3.2 - 3.5, image 2, and for high power views see plates 3.6 – 3.9, panel B) confirming many previous reports from a wide variety of laboratories (Vickerman, 1969, Cross, 1975). The VSG was visible under all conditions of fixation, at $0^{o}C$ or $37^{o}C$ and in both the presence and absence of triton X-100 and had the same even distribution over the entire cell body under all of these conditions.

The control for labelling the inner surface of bloodstream form trypanosomes was to label the cells with anti-α-tubulin antibody. Tubulin is one of the basic subunits of microtubules within the trypanosomal cytoskeleton, which is organized as a regular array attached to the cytoplasmic face of the plasma membrane and therefore, labelling the trypanosomes with Alexa 488 anti-α-tubulin will identify the position of the inner-most surface of the plasma membrane, which is located immediately exterior to the position of the pellicular tubulin. Tubulin was detected by Alexa 488 anti-tubulin only when the trypanosomes were incubated with 0.1 % triton X-100 following fixation at either $0^{o}C$ or $37^{o}C$ (for low power views see plates 3.2 – 3.5, image 4 and for high power views compare plates 3.6 – 3.9, panel D). The distribution of tubulin was found to produce a uniform fluorescence from FITC-labelled anti-tubulin along the inner surface of the cell.

ISG-70 is an externally disposed integral membrane glycoprotein present only in bloodstream forms of *T. brucei* and is found distributed over the entire surface of the plasma membrane covering the cell body and flagellum. It has been reported that the

VSG from a number of different variants masks the presence of ISG-70 in live but not in fixed cells (Jackson *et al.*, 1993). Labelling the trypanosomes with Cy3-anti-ISG-70 antibody will identify the area of the outer plasma membrane shielded by the VSG. The ISG-70 was found distributed over the entire surface of the trypanosome (for low power views see plates 3.2 - 3.5, image 3 and for high power views see plates 3.6 – 3.9, panel C) in an irregular, patchy pattern. The ISG-70 was visible under all conditions of fixation, at $0^{o}C$ or $37^{o}C$ and in both the presence and absence of triton X-100 and had the same patchy distribution over the entire cell body under all conditions. This patchy distribution differs from the original description of a more uniform distribution (Jackson *et al.*, 1993) and is attributed to the greater resolution obtained by laser scanning confocal fluorescence microscopy in the present study compared to the earlier epifluoresence study. The increased resolution results from the elimination of stray light from positions in the sample outside the depth of sections being recorded as a consequence of the confocal pinhole arrangement.

The GPI-PLC was detected by Cy3-labelled anti-GPI-PLC in cells that had been fixed at $0^{o}C$, while fixation at $37^{o}C$ resulted in loss of almost all of the fluoresence (for low power views see plates 3.2 - 3.5, image 1 and for high power views see plates 3.6 – 3.9, panel A). However, detection of the GPI-PLC was insensitive to the presence or absence of detergent and could be clearly seen when cells were fixed at $0^{o}C$ whether or not triton X-100 was used. The GPI-PLC was found aligned along the outside of the cell body and the fluorescence produced a patchy string-like appearance. No fluorescence was detected on the main portion of the surface of the cell body. The fluorescence of the GPI-PLC begins at a point between the nucleus and the kinetoplast (see Plate 3.6 & 3.7, image 3 & 4) and extends beyond the anterior limit of the cell body. The location of the GPI-PLC signal suggests a flagellar membrane localization (Plate 3.6 & 3.7, image 3 & 4).

In addition to examining the cellular distribution of GPI-PLC in long slender bloodstream form trypanosomes, its localization in stumpy form trypanosomes was also investigated. In natural infections in the mammalian host, parasitaemias are generally pleomorphic and consist of rapidly dividing slender forms that predominate in the ascending parasitaemia, but which are gradually replaced by a shorter and broader form of the cell, termed stumpy, as the parasitaemic wave decreases (Vickerman, 1965, Balber, 1972, Vickerman, 1985). The stumpy forms are preadapted at a metabolic level to life in the fly vector (Vickerman, 1965, Hecker, 1973). It has been reported that the

Plate 3.2. Low power confocal images of the cellular distribution of GPI-PLC (Image 1), VSG (Image 2) and ISG-70 (Image 3) on bloodstream form trypanosomes fixed at 0°C in the absence of triton X-100.

Bloodstream form trypanosomes (5 x 10^7 cells/ml) were fixed as described in Section 2.1.51, blocked with BSA (5% w/v) for 1 hr at room temperature and following washing incubated with either anti-GPI-PLC antibody (1/1000 dilution), anti-VSG antibody (1/1000 dilution), anti-α-tubulin (1/350 dilution of mouse monoclonal antibody, Clone DM1A) or anti-ISG70 antibody (1/1000 dilution) overnight at room temperature. The cells were washed and binding of primary antibodies to the cells was detected by incubating the cells with a Cy3 conjugated anti-rabbit IgG antibody (1/500 dilution) for the anti-VSG, anti-GPI-PLC and anti-ISG70 antibody detection. The anti-α-tubulin was detected with Alexa 488 anti-mouse IgG (1/2000 dilution). These were all incubated for 1 hr at room temperature. The cells were washed and mounted onto slides as described in section 2.1.53. Plate 3.2 displays three images.

Image 1 displays a low power view of the localization of the GPI-PLC on bloodstream form trypanosomes fixed at 0°C in the absence of triton X-100.

Image 2 displays a low power view of the localization of the VSG on bloodstream form trypanosomes fixed at 0°C in the absence of triton X-100.

Image 3 displays a low power view of the localization of ISG-70 on bloodstream form trypanosomes fixed at 0°C in the absence of triton X-100.

An Olympus FV-1000 Confocal microscope was used to collect images. The laser power was at 1 % and the Kalman filter was used during data collection.

Plate 3.2. Low power confocal images of the cellular distribution of the GPI-PLC (Image 1), the VSG (Image 2), ISG-70 (Image 3) and tubulin (image 4) on bloodstream form trypanosomes fixed at 0°C in the absence of triton X-100.

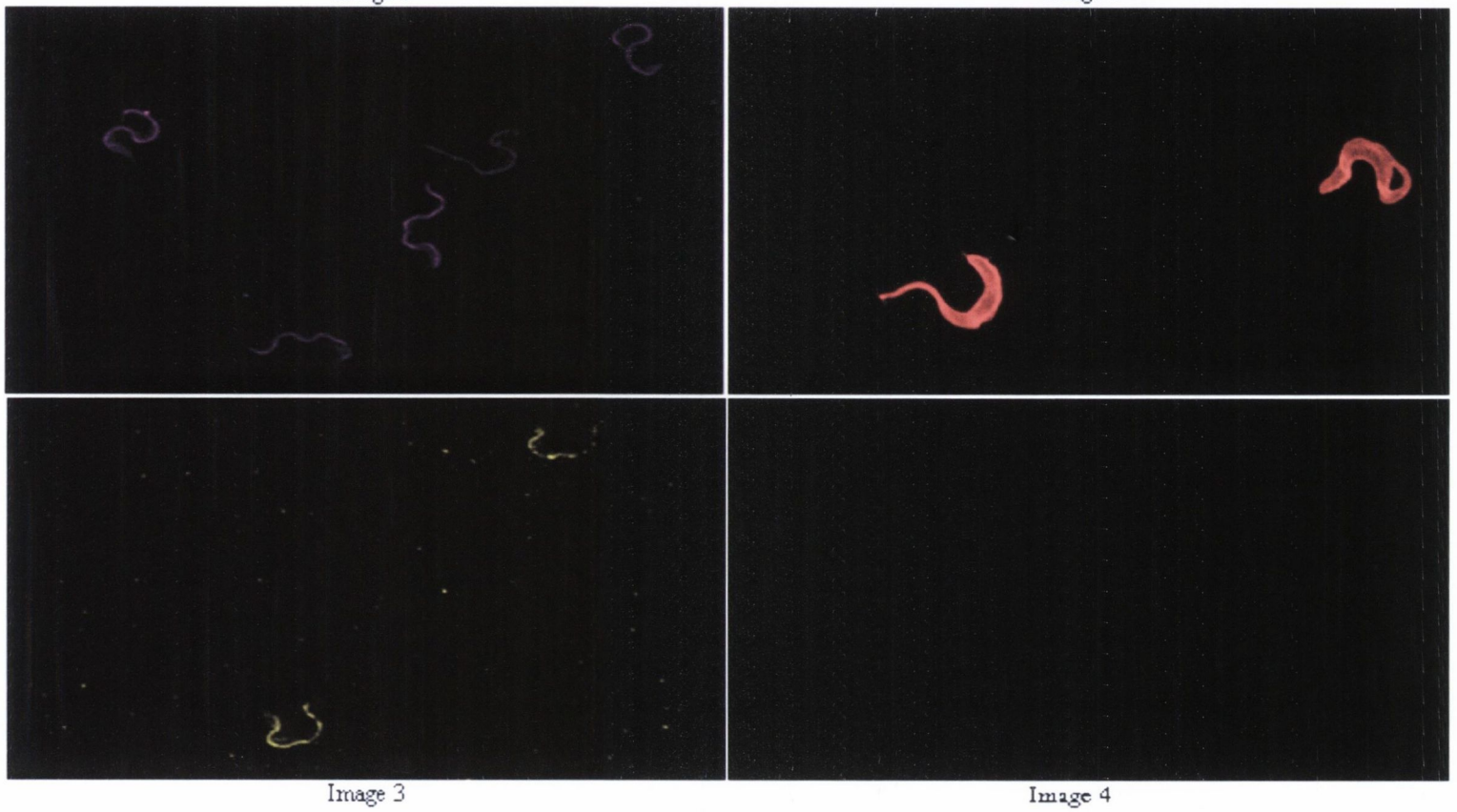

Plate 3.3. Low power confocal images of the cellular distribution of GPI-PLC (Image 1), VSG (Image 2), ISG-70 (Image 3) and tubulin (Image 4) on bloodstream form trypanosomes fixed at 0°C in the presence of triton X-100.

Bloodstream form trypanosomes (5 x 10^7 cells/ml) were fixed as described in Section 2.1.51, blocked with BSA (5% w/v) for 1 hr at room temperature and following washing incubated with either anti-GPI-PLC antibody (1/1000 dilution), anti-VSG antibody (1/1000 dilution), anti-α-tubulin (1/350 dilution of mouse monoclonal antibody, Clone DM1A) or anti-ISG70 antibody (1/1000 dilution) overnight at room temperature. The cells were washed and binding of primary antibodies to the cells was detected by incubating the cells with a Cy3 conjugated anti-rabbit IgG antibody (1/500 dilution) for the anti-VSG, anti-GPI-PLC and anti-ISG70 antibody detection. The anti-α-tubulin was detected with Alexa 488 anti-mouse IgG (1/2000 dilution). These were all incubated for 1 hr at room temperature. The cells were washed and mounted onto slides as described in section 2.1.53. Plate 3.3 displays four images.

Image 1 displays a low power view of the localization of the GPI-PLC on bloodstream form trypanosomes fixed at 0°C in the presence of triton X-100.

Image 2 displays a low power view of the localization of the VSG on bloodstream form trypanosomes fixed at 0°C in the presence of triton X-100.

Image 3 displays a low power view of the localization of ISG-70 on bloodstream form trypanosomes fixed at 0°C in the presence of triton X-100.

Image 4 displays a low power view of the localization of tubulin on bloodstream form trypanosomes fixed at 0°C in the presence of triton X-100.

An Olympus FV-1000 Confocal microscope was used to collect images. The laser power was at 1 % and the Kalman filter was used during data collection.

Plate 3.3. Low power confocal images of the cellular distribution of the GPI-PLC (Image 1), the VSG (Image 2), ISG-70 (Image 3) and tubulin (Image 4) on bloodstream form trypanosomes fixed at 0°C in the presence of triton X-100.

Image 1

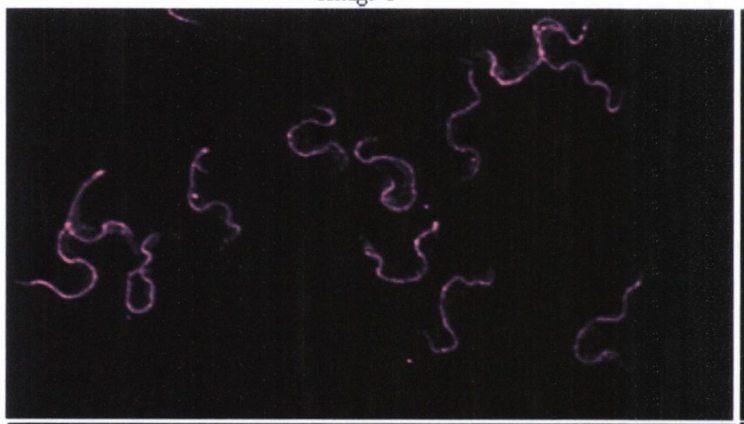

Image 2

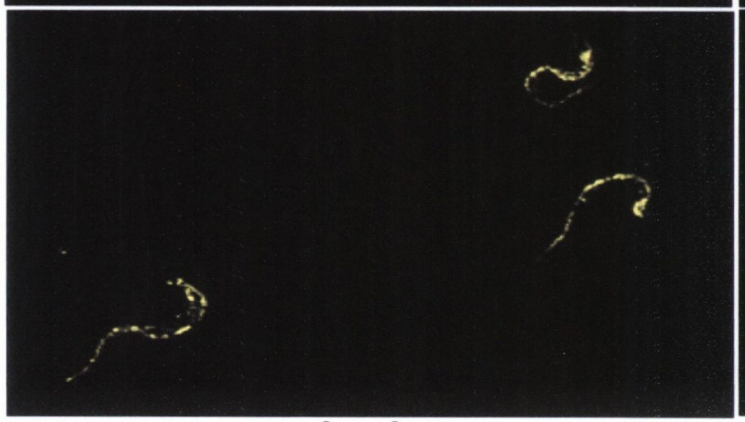

Image 3

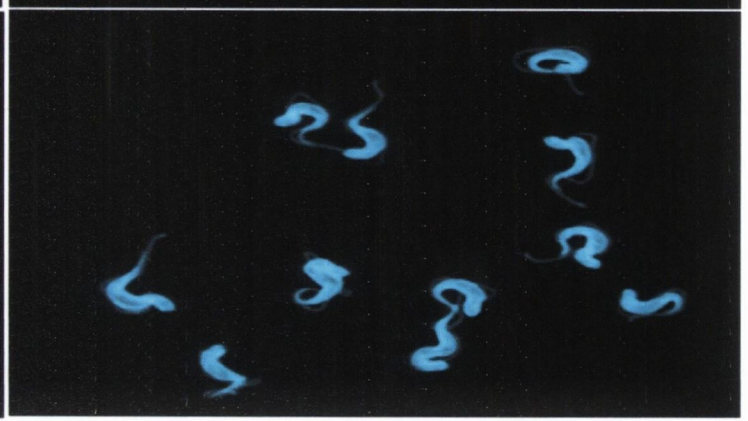

Image 4

Plate 3.4. Low power confocal images of the cellular distribution of GPI-PLC (Image 1), VSG (Image 2) and ISG-70 (Image 3) on bloodstream form trypanosomes fixed at 37°C in the absence of triton X-100.

Bloodstream form trypanosomes (5 x 10^7 cells/ml) were fixed as described in Section 2.1.51, blocked with BSA (5% w/v) for 1 hr at room temperature and following washing incubated with either anti-GPI-PLC antibody (1/1000 dilution), anti-VSG antibody (1/1000 dilution), anti-α-tubulin (1/350 dilution of mouse monoclonal antibody, Clone DM1A) or anti-ISG70 antibody (1/1000 dilution) overnight at room temperature. The cells were washed and binding of primary antibodies to the cells was detected by incubating the cells with a Cy3 conjugated anti-rabbit IgG antibody (1/500 dilution) for the anti-VSG, anti-GPI-PLC and anti-ISG70 antibody detection. The anti-α-tubulin was detected with Alexa 488 anti-mouse IgG (1/2000 dilution). These were all incubated for 1 hr at room temperature. The cells were washed and mounted onto slides as described in section 2.1.53. Plate 3.4 displays three images.

Image 1 displays a low power view of the localization of the GPI-PLC on bloodstream form trypanosomes fixed at 37°C in the absence of triton X-100.

Image 2 displays a low power view of the localization of the VSG on bloodstream form trypanosomes fixed at 37°C in the absence of triton X-100.

Image 3 displays a low power view of the localization of ISG-70 on bloodstream form trypanosomes fixed at 37°C in the absence of triton X-100.

An Olympus FV-1000 Confocal microscope was used to collect images. The laser power was at 1 % and the Kalman filter was used during data collection.

Plate 3.4. Low power confocal images of the cellular distribution of the GPI-PLC (Image 1), the VSG (Image 2), ISG-70 (Image 3) and tubulin (image 4) on bloodstream form trypanosomes fixed at 37°C in the absence of triton X-100.

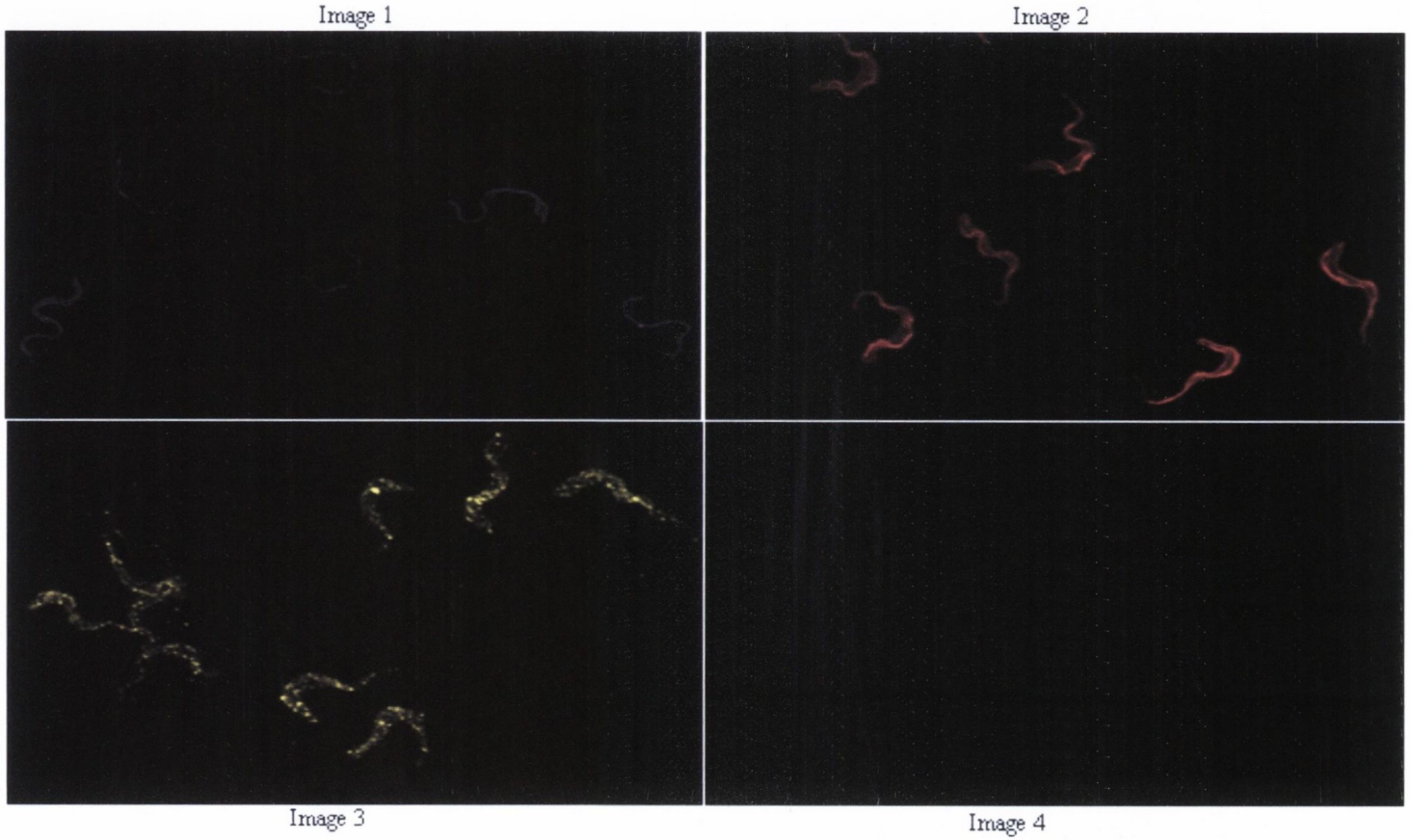

Plate 3.5. Low power confocal images of the cellular distribution of GPI-PLC (Image 1), VSG (Image 2), ISG-70 (Image 3) and tubulin (Image 4) on bloodstream form trypanosomes fixed at 37°C in the presence of triton X-100.

Bloodstream form trypanosomes (5 x 10^7 cells/ml) were fixed as described in Section 2.1.51, blocked with BSA (5% w/v) for 1 hr at room temperature and following washing incubated with either anti-GPI-PLC antibody (1/1000 dilution), anti-VSG antibody (1/1000 dilution), anti-α-tubulin (1/350 dilution of mouse monoclonal antibody, Clone DM1A) or anti-ISG70 antibody (1/1000 dilution) overnight at room temperature. The cells were washed and binding of primary antibodies to the cells was detected by incubating the cells with a Cy3 conjugated anti-rabbit IgG antibody (1/500 dilution) for the anti-VSG, anti-GPI-PLC and anti-ISG70 antibody detection. The anti-α-tubulin was detected with Alexa 488 anti-mouse IgG (1/2000 dilution). These were all incubated for 1 hr at room temperature. The cells were washed and mounted onto slides as described in section 2.1.53. Plate 3.5 displays four images.

Image 1 displays a low power view of the localization of the GPI-PLC on bloodstream form trypanosomes fixed at 37°C in the presence of triton X-100.

Image 2 displays a low power view of the localization of the VSG on bloodstream form trypanosomes fixed at 37°C in the presence of triton X-100.

Image 3 displays a low power view of the localization of ISG-70 on bloodstream form trypanosomes fixed at 37°C in the presence of triton X-100.

Image 4 displays a low power view of the localization of tubulin on bloodstream form trypanosomes fixed at 37°C in the presence of triton X-100.

An Olympus FV-1000 Confocal microscope was used to collect images. The laser power was at 1 % and the Kalman filter was used during data collection.

Plate 3.5. Low power confocal images of the cellular distribution of the GPI-PLC (Image 1), the VSG (Image 2), ISG-70 (Image 3) and tubulin (Image 4) on bloodstream form trypanosomes fixed at 37°C in the presence of triton X-100.

Image 1

Image 2

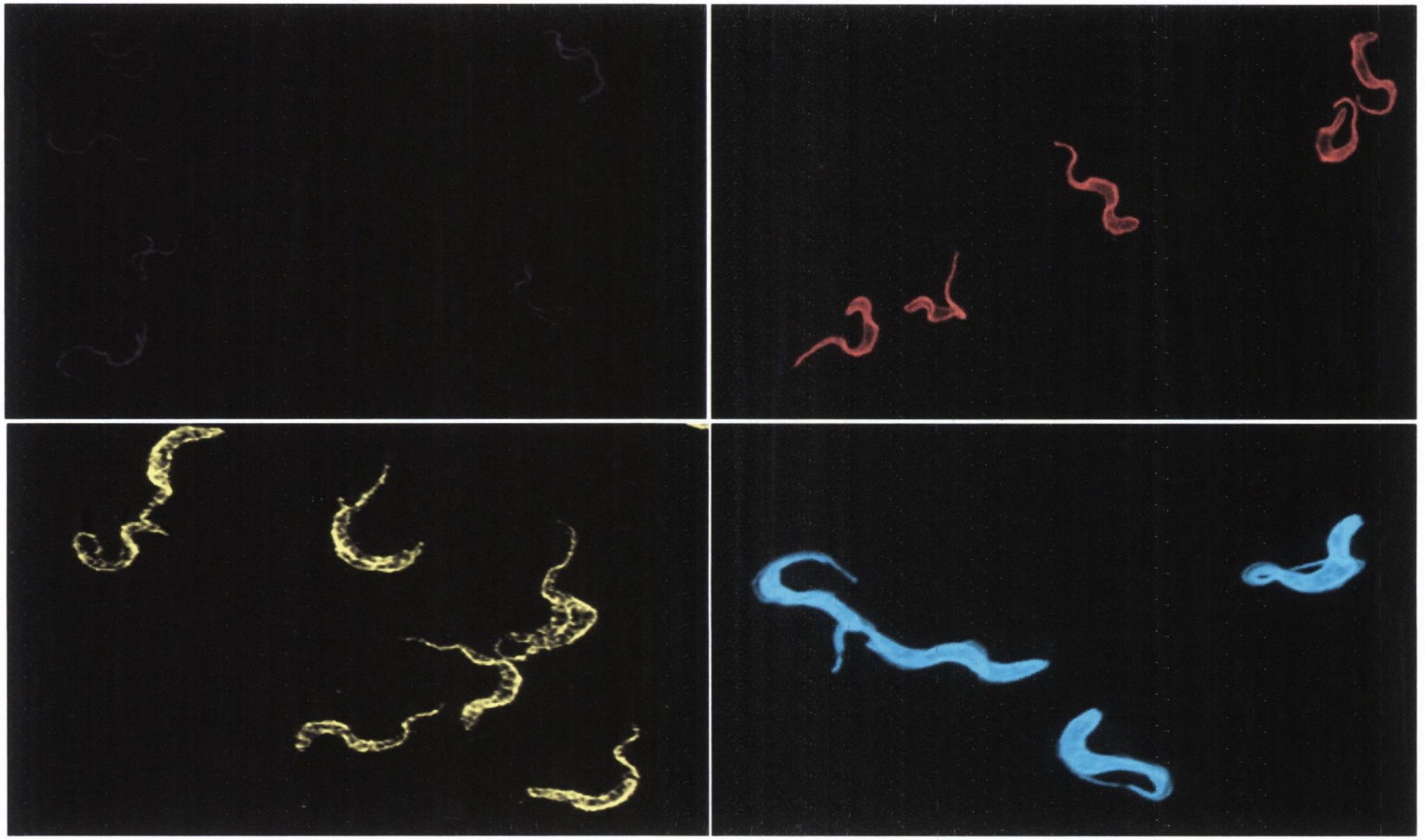

Image 3

Image 4

Plate 3.6. Confocal images of the cellular distribution of GPI-PLC (Panel A), VSG (Panel B), ISG-70 (Panel C) and tubulin (Panel D) on bloodstream form trypanosomes fixed at 0°C in the absence of triton X-100.

Bloodstream form trypanosomes (5 x 10^7 cells/ml) were fixed as described in Section 2.1.51, blocked with BSA (5% w/v) for 1 hr at room temperature and following washing incubated with either anti-GPI-PLC antibody (1/1000 dilution), anti-VSG antibody (1/1000 dilution), anti-α-tubulin (1/350 dilution of mouse monoclonal antibody, Clone DM1A) or anti-ISG70 antibody (1/1000 dilution) overnight at room temperature. The cells were washed and binding of primary antibodies to the cells was detected by incubating the cells with a Cy3 conjugated anti-rabbit IgG antibody (1/500 dilution) for the anti-VSG, anti-GPI-PLC and anti-ISG70 antibody detection. The anti-α-tubulin was detected with Alexa 488 anti-mouse IgG (1/2000 dilution). These were all incubated for 1 hr at room temperature. The cells were washed and mounted onto slides as described in section 2.1.53. **Panel A** shows the localization of the GPI-PLC on bloodstream form cells fixed at 0°C in the absence of triton X-100. **Panel B** shows the localization of the VSG on bloodstream form trypanosomes fixed at 0°C in the absence of triton X-100. **Panel C** shows the localization of ISG70 on bloodstream form trypanosomes fixed at 0°C in the absence of triton X-100 and **Panel D** shows the localization of tubulin on bloodstream form trypanosomes fixed at 0°C in the absence of triton X-100. An Olympus FV-1000 Confocal microscope was used to collect images. The laser power was at 1 % and the Kalman filter was used during data collection. Each panel of plate 3.6 displays four images.

Image 1 of each panel displays a phase-contrast image of the cell.

Image 2 displays the location of the nucleus and kinetoplast (blue)

Image 3 displays the protein of interest

Image 4 displays a merge of images 1, 2 & 3.

Plate 3.6, panel A. Confocal images of the cellular distribution of the GPI-PLC on bloodstream form trypanosomes fixed at 0°C in the absence of tritonX-100. Image 1-Phase image of cell, image 2-nucleus & kinetoplast, image 3-GPI-PLC, image 4- merge of 1, 2 &3.

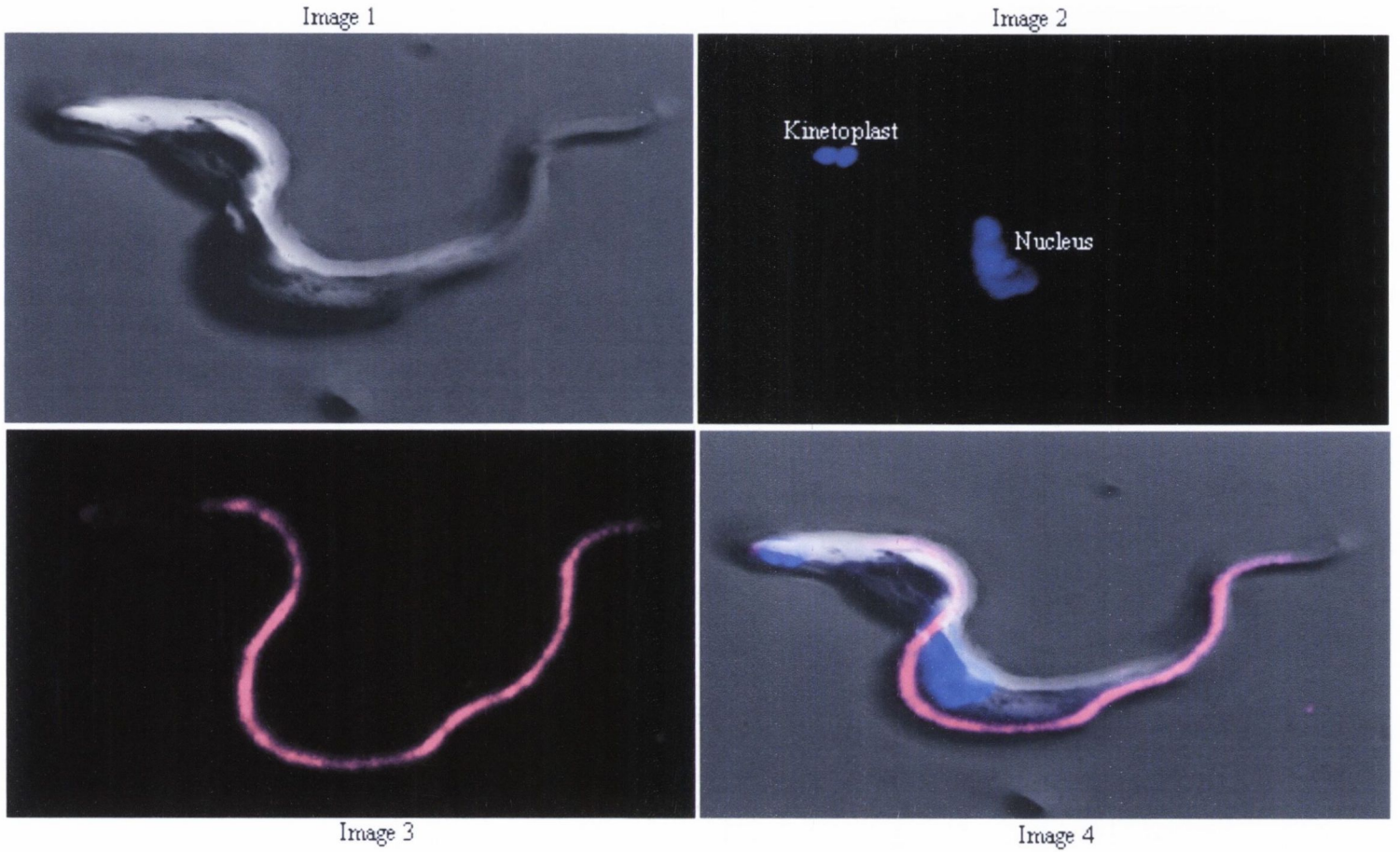

Plate 3.6, panel B. Confocal images of the cellular distribution of the VSG on bloodstream form trypanosomes fixed at 0°C in the absence of tritonX-100. Image 1-Phase image of cell, image 2-nucleus & kinetoplast, image 3- VSG, image 4-merge of 1, 2 & 3.

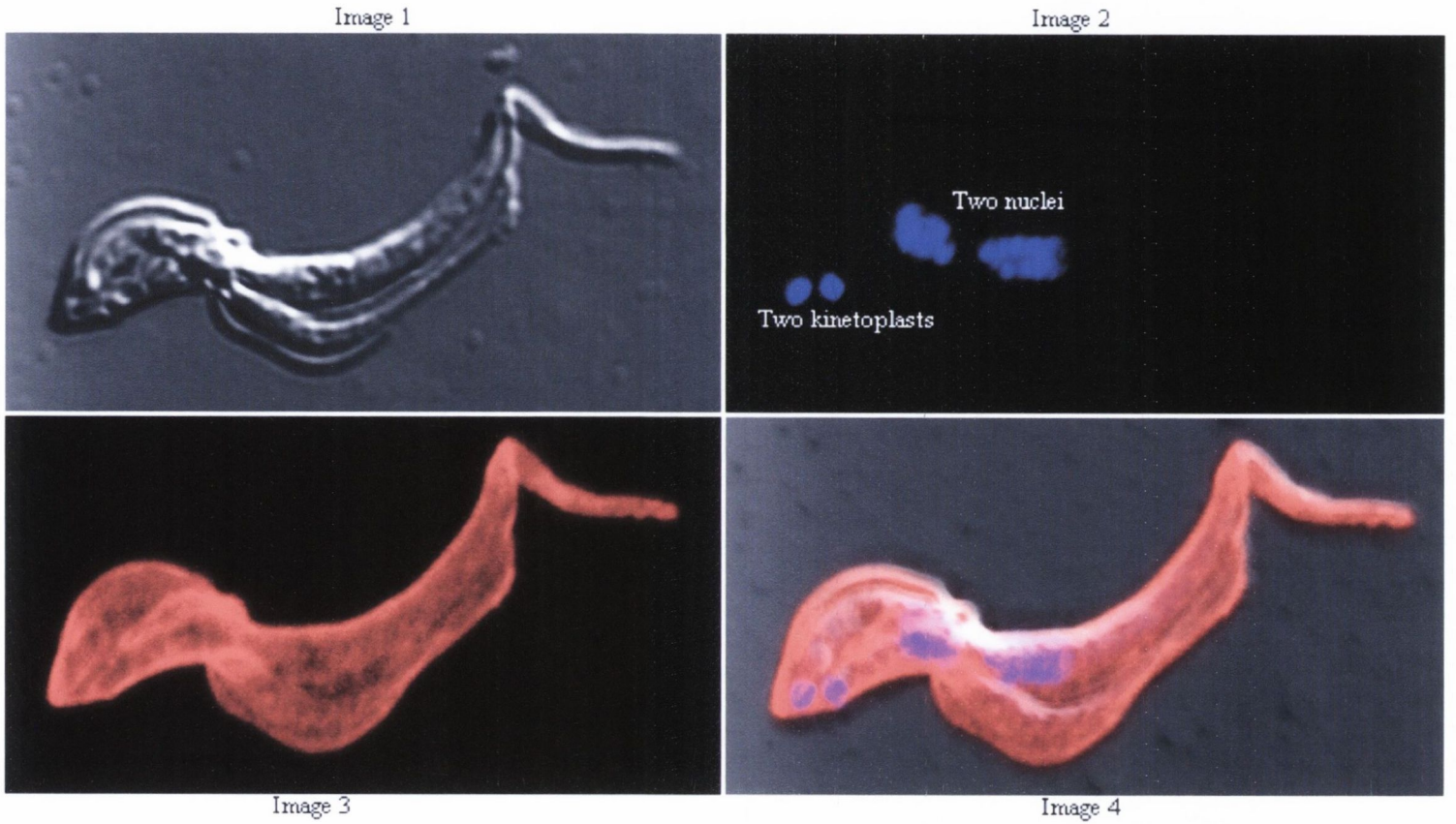

Plate 3.6, panel C. Confocal images of the cellular distribution of the ISG-70 on bloodstream form trypanosomes fixed at 0°C in the absence of tritonX-100. Image 1-Phase image of cell, image 2-nucleus & kinetoplast, image 3- ISG-70, image 4-merge of 1, 2 &3.

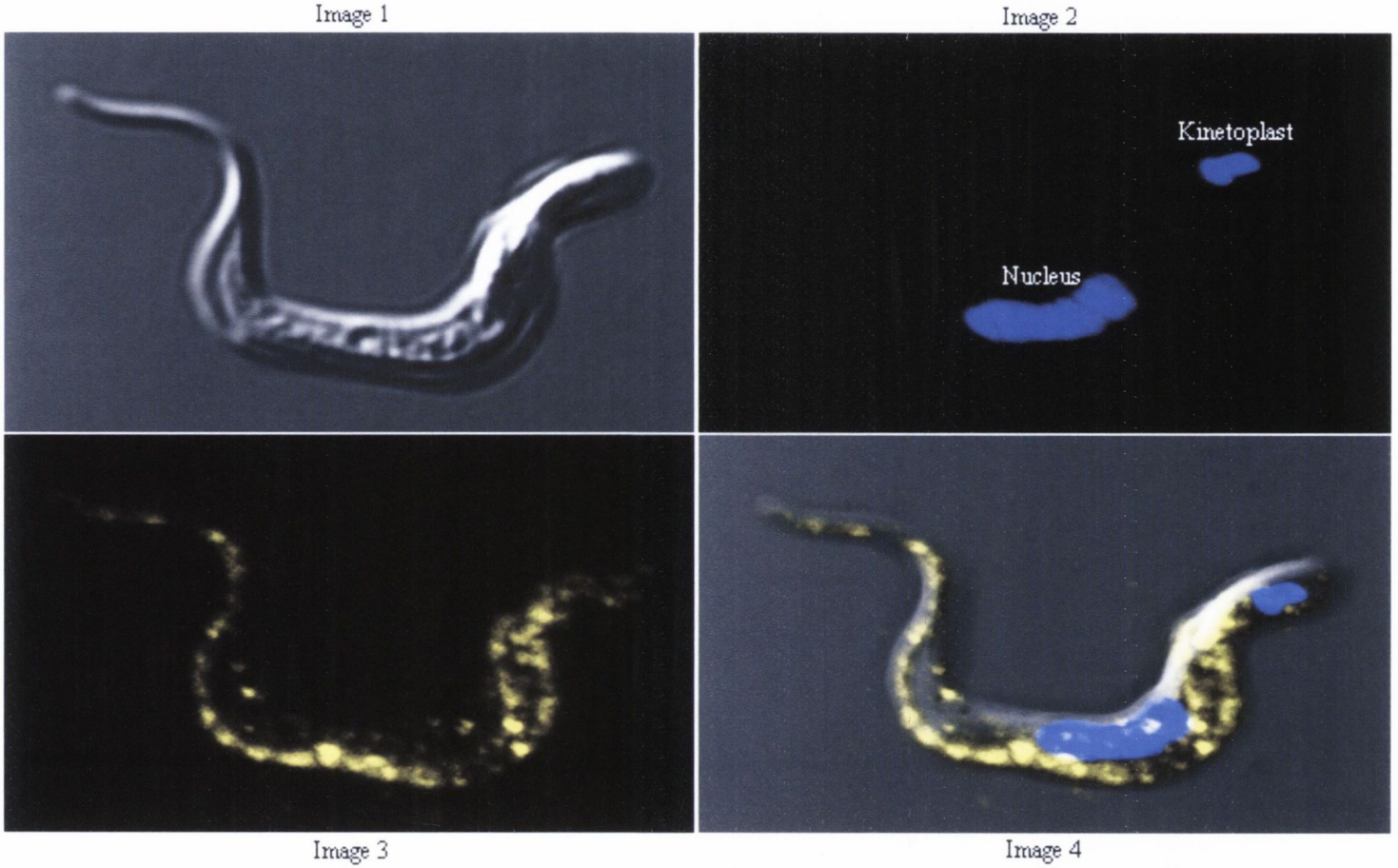

Plate 3.6, panel D. Confocal images of the cellular distribution of tubulin on bloodstream form trypanosomes fixed at 0°C in the absence of triton X-100. Image 1-Phase image of cell, image 2-nucleus & kinetoplast, image 3-tubulin & image 4- merge of 1,2 & 3.

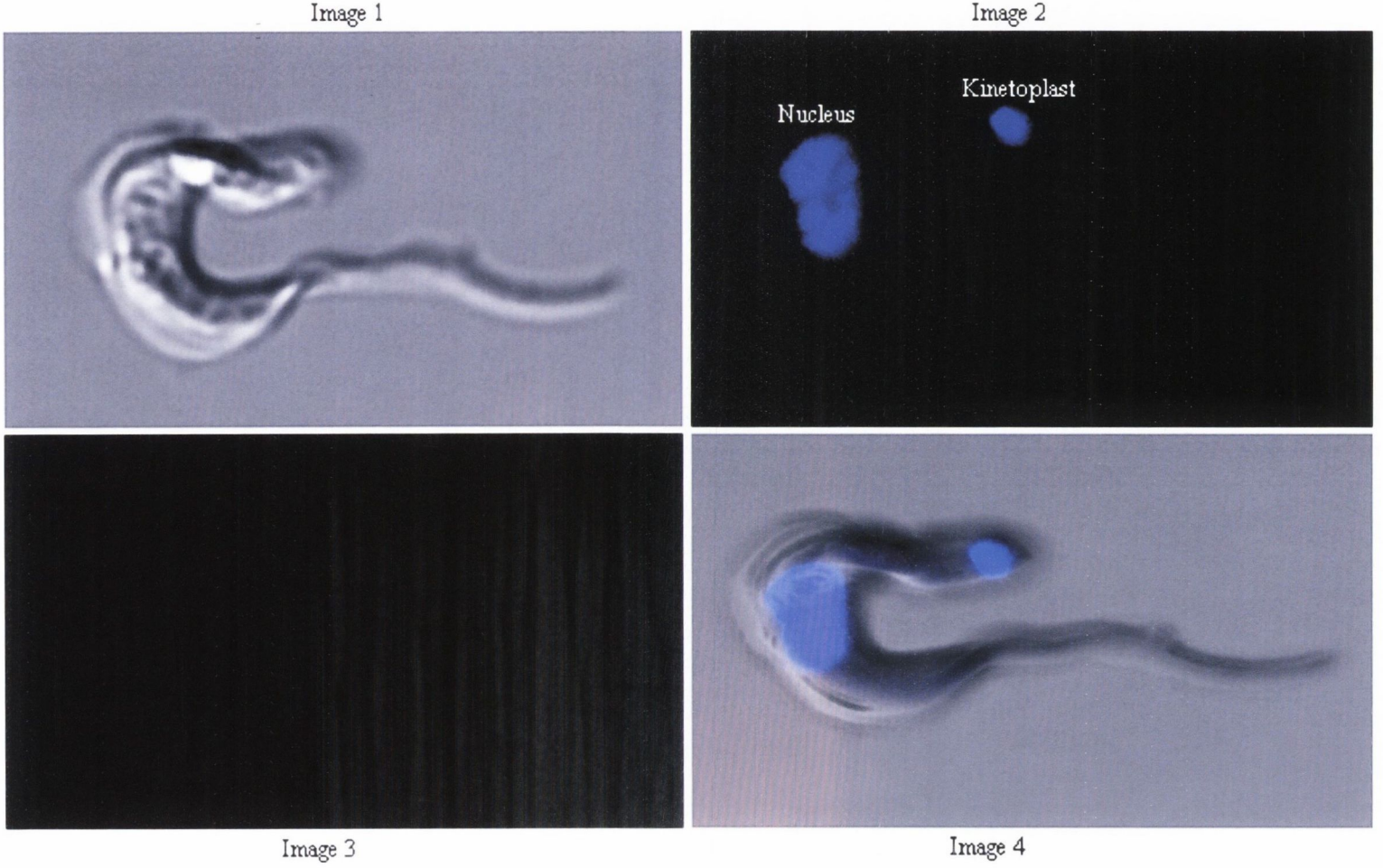

Plate 3.7. Confocal images of the cellular distribution of GPI-PLC (Panel A), VSG (Panel B), ISG70 (Panel C) and tubulin (Panel D) on bloodstream form trypanosomes fixed at 0°C in the presence of Triton X-100.

Bloodstream form trypanosomes (5 x 10^7 cells/ml) were fixed as described in Section 2.1.51, blocked with BSA (5% w/v) for 1 hr at room temperature and following washing incubated with either anti-GPI-PLC antibody (1/1000 dilution), anti-VSG antibody (1/1000 dilution), anti-α-tubulin (1/350 dilution of mouse monoclonal antibody, Clone DM1A) or anti-ISG70 antibody (1/1000 dilution) overnight at room temperature. The cells were washed and binding of primary antibodies to the cells was detected by incubating the cells with Cy3 conjugated anti-rabbit IgG antibody (1/500 dilution) for the anti-VSG, anti-GPI-PLC and anti-ISG70 antibody detection. The anti-α-tubulin was detected with Alexa 488 anti-mouse IgG (1/2000 dilution). These were all incubated for 1 hr at room temperature. The cells were washed and mounted onto slides as described in section 2.1.53. **Panel A** shows the localization of the GPI-PLC on bloodstream form cells fixed at 0°C (+ 0.1 % Tx-100). **Panel B** shows the localization of the VSG on bloodstream form trypanosomes fixed at 0°C (+ 0.1 % Tx-100). **Panel C** the localization of ISG70 on bloodstream form trypanosomes fixed at 0°C (+ 0.1 % Tx-100) and **Panel D** the localization of tubulin on bloodstream form trypanosomes fixed at 0°C (+ 0.1% Tx-100). An Olympus FV-1000 confocal microscope was used to collect images. The laser power was at 1 % and the Kalman filter was used during data collection. Each panel of plate 3.7 displays four images.

Image 1 of each panel displays a phase-contrast image of the cell.

Image 2 displays the location of the nucleus and kinetoplast (blue).

Image 3 displays the protein of interest.

Image 4 displays a merge of images 1,2 & 3.

Plate 3.7, panel A. Confocal images of the cellular distribution of the GPI-PLC on bloodstream form trypanosomes fixed at 0°C in the presence of tritonX-100. Image 1-Phase image of cell, image 2- nucleus & kinetoplast, image 3-GPI-PLC, image 4- merge of 1, 2 & 3.

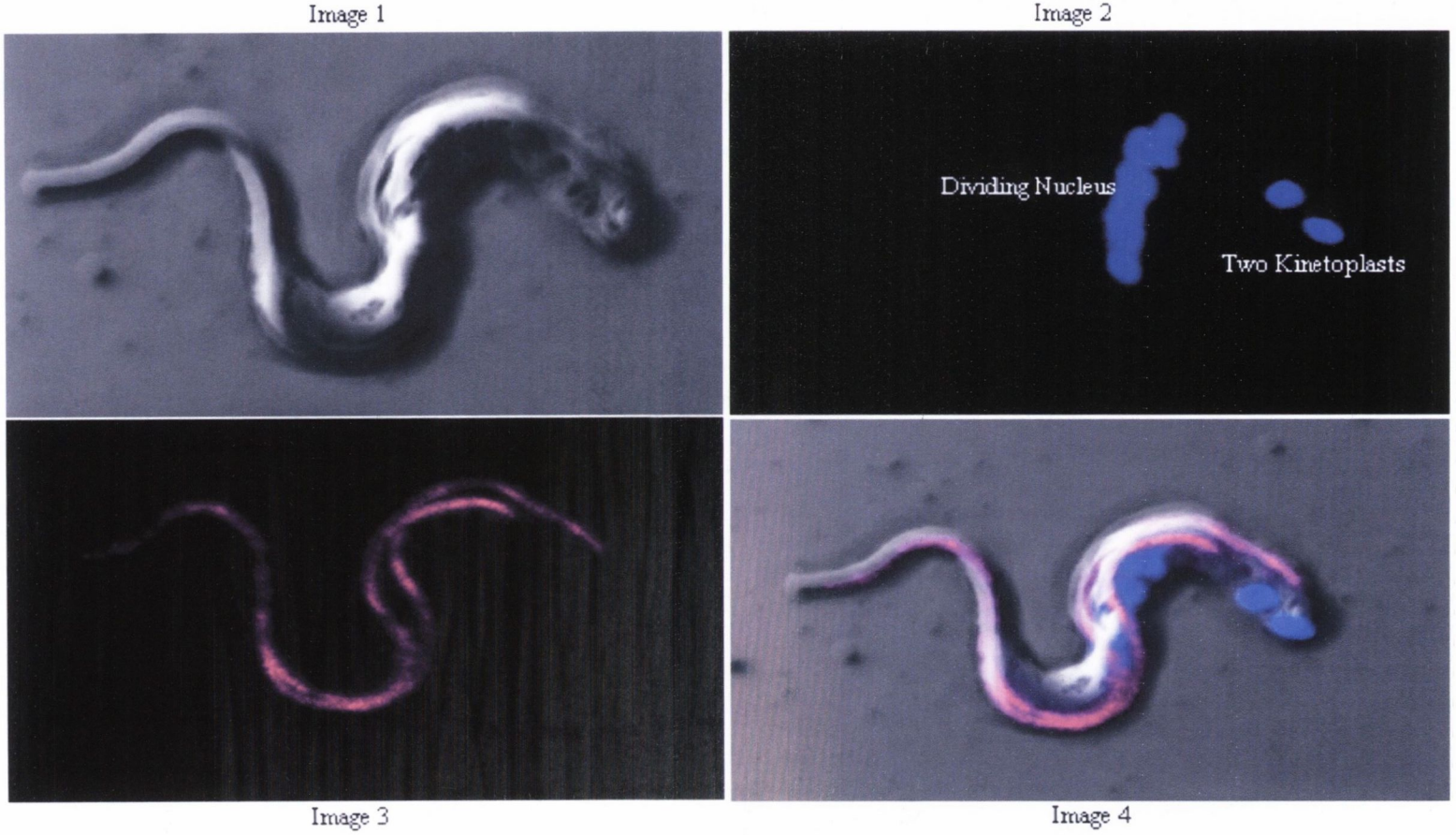

Plate 3.7, panel B. Confocal images of the cellular distribution of the VSG on bloodstream form trypanosomes fixed at 0°C in the presence of tritonX-100. Image 1-Phase image of cell, image 2-nucleus & kinetoplast, image 3-VSG, image 4- merge of 1, 2 & 3.

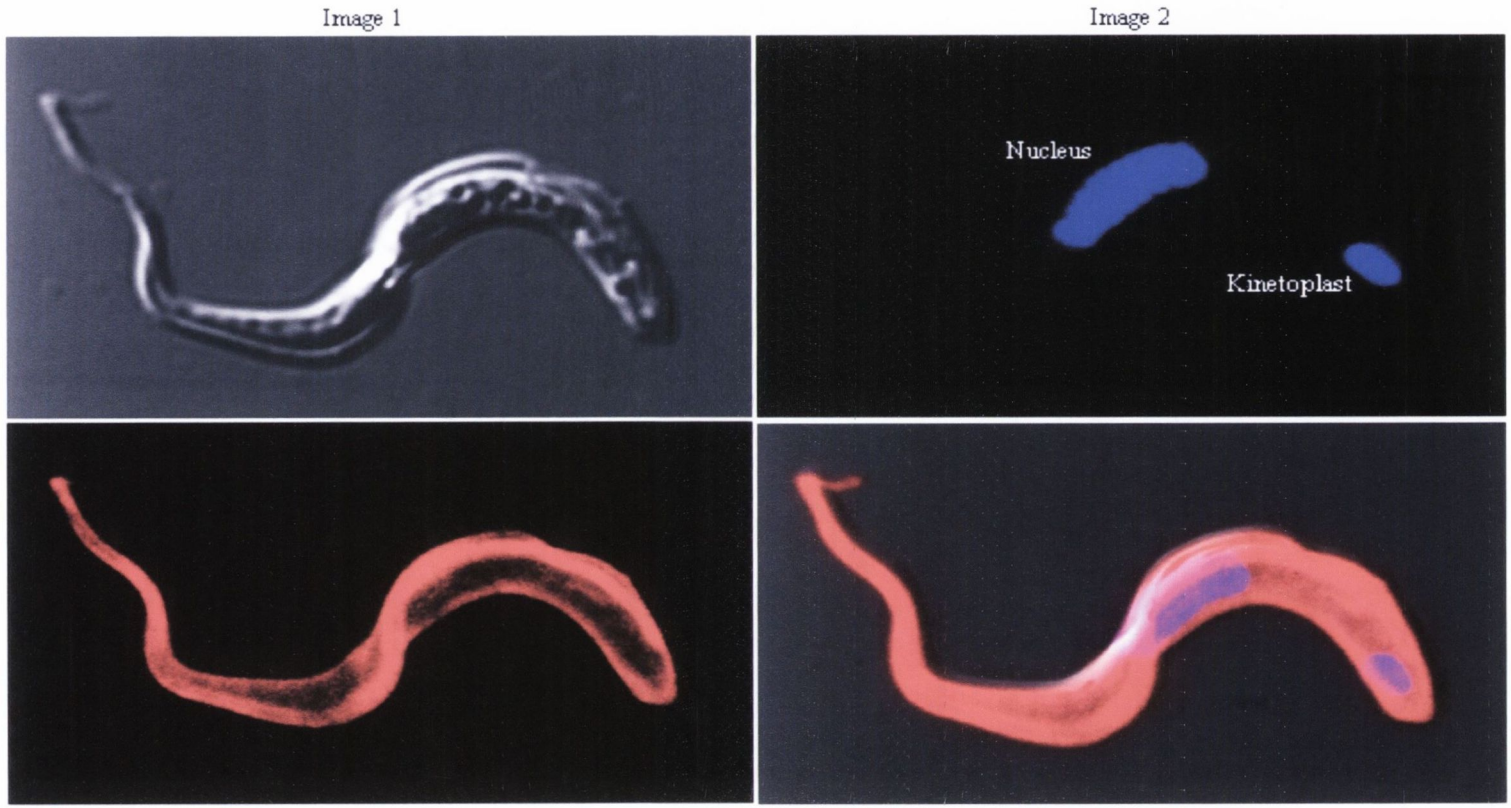

Plate 3.7, panel C. Confocal images of the cellular distribution of the ISG-70 on bloodstream form trypanosomes fixed at 0°C in the presence of tritonX-100. Image 1-Phase image of cell, image 2-nucleus & kinetoplast, image 3-ISG-70, image 4- merge of 1, 2 & 3.

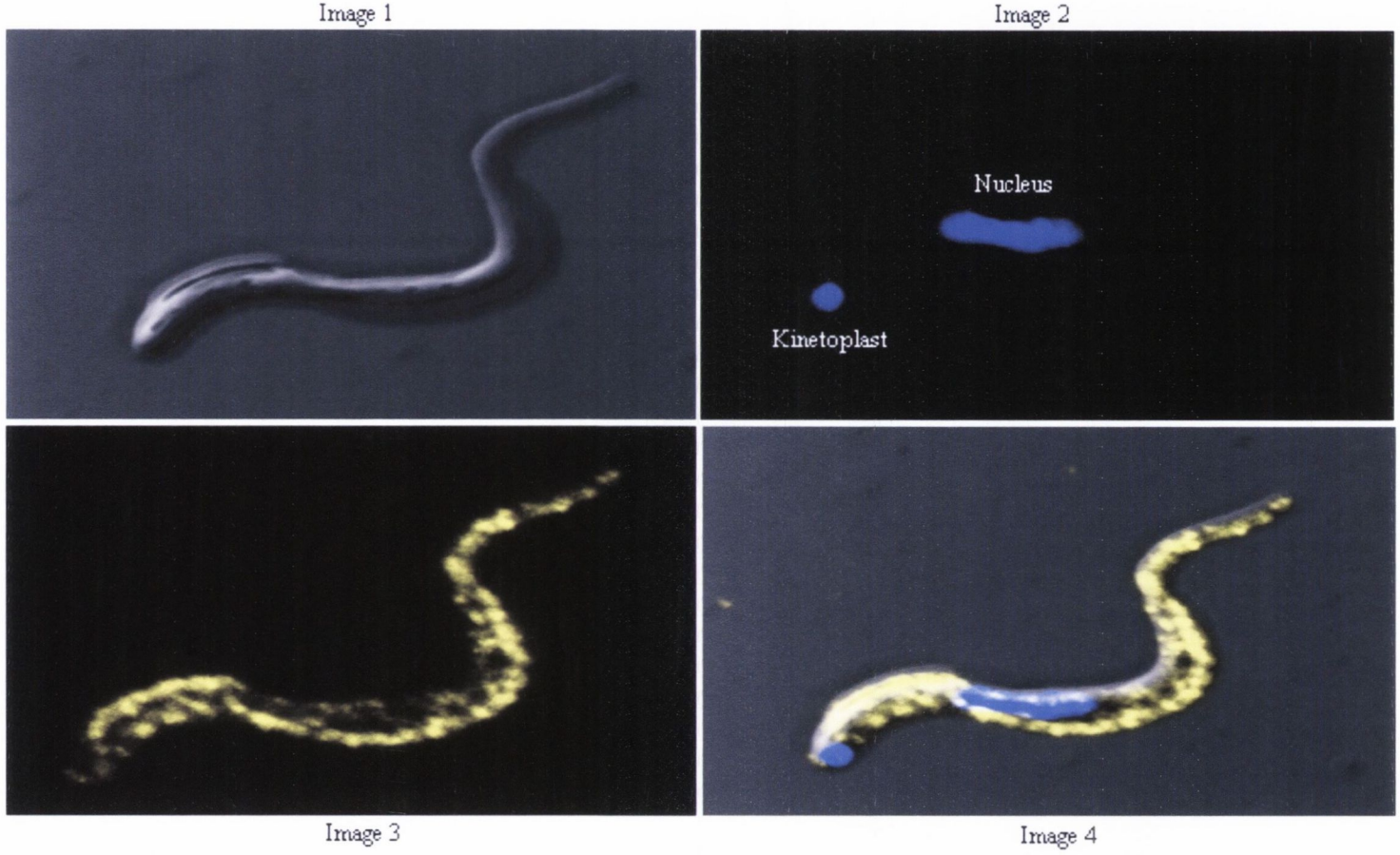

Plate 3.7, panel D. Confocal images of the cellular distribution of tubulin on bloodstream form trypanosomes fixed at 0°C in the presence of tritonX-100. Image 1-Phase image of cell, image 2- nucleus & kinetoplast, image 3- tubulin, image 4-merge of 1, 2 & 3.

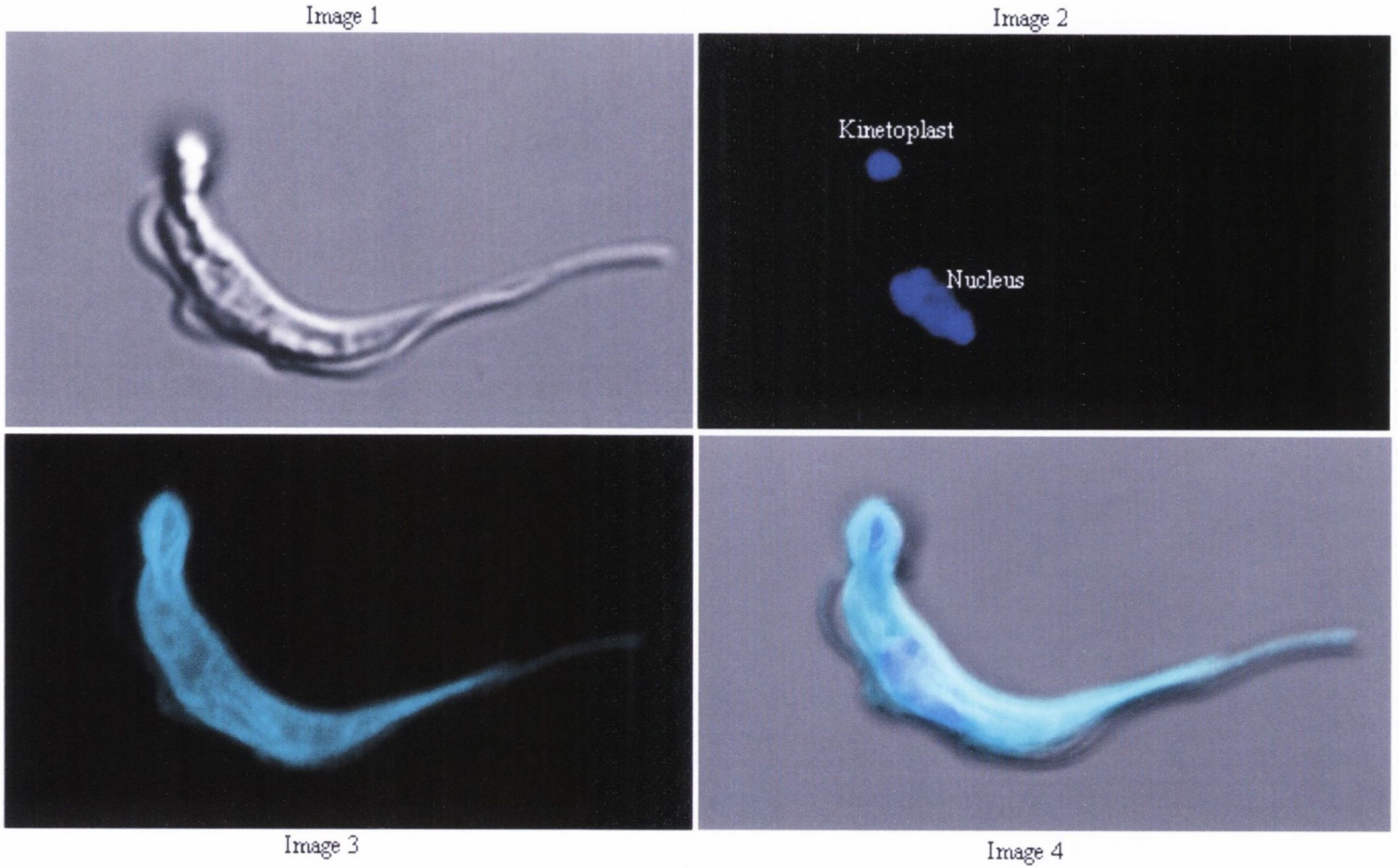

Plate 3.8. Confocal images of the cellular distribution of GPI-PLC (Panel A), VSG (Panel B), ISG70 (Panel C) and tubulin (Panel D) on bloodstream form trypanosomes fixed at 37°C in the absence of Triton X-100.

Bloodstream form trypanosomes (5 x 10^7 cells/ml) were fixed as described in Section 2.1.51, blocked with BSA (5% w/v) for 1 hr at room temperature and following washing incubated with either anti-GPI-PLC antibody (1/1000 dilution), anti-VSG antibody (1/1000 dilution), anti-α-tubulin (1/350 dilution of mouse monoclonal antibody, Clone DM1A) or anti-ISG70 antibody (1/1000 dilution) overnight at room temperature. The cells were washed and binding of primary antibodies to the cells was detected by incubating the cells with a Cy3 conjugated anti-rabbit IgG antibody (1/500 dilution) for the anti-VSG, anti-GPI-PLC and anti-ISG70 antibody detection. The anti-α-tubulin was detected with Alexa 488 anti-mouse IgG (1/2000 dilution). These were all incubated for 1 hr at room temperature. The cells were washed and mounted onto slides as described in section 2.1.53. **Panel A** shows the localization of the GPI-PLC on bloodstream form cells fixed at 37°C in the absence of triton X-100. **Panel B** shows the localisation of the VSG on bloodstream form trypanosomes fixed at 37°C in the absence of triton X-100. **Panel C** shows the localization of ISG70 on bloodstream form trypanosomes fixed at 37°C in the absence of triton X-100 and **Panel D** shows the localization of tubulin on bloodstream form trypanosomes fixed at 37°C in the absence of triton X-100. An Olympus FV-1000 confocal microscope was used to collect images. The laser power was at 1 % and the Kalman filter was used during data collection. Each panel of plate 3.8 displays four images.

Image 1 of each panel displays a phase-contrast image of the cell.

Image 2 displays the location of the nucleus and kinetoplast (blue).

Image 3 displays the protein of interest.

Image 4 displays a merge of images 1,2 & 3.

Plate 3.8, panel A. Confocal images of the cellular distribution of the GPI-PLC on bloodstream form trypanosomes fixed at 37°C in the absence of tritonX-100. Image 1 – Phase image of cell, image 2 – kinetoplast & nucleus, image 3 – GPI-PLC, image 4 – merge of 1, 2 & 3.

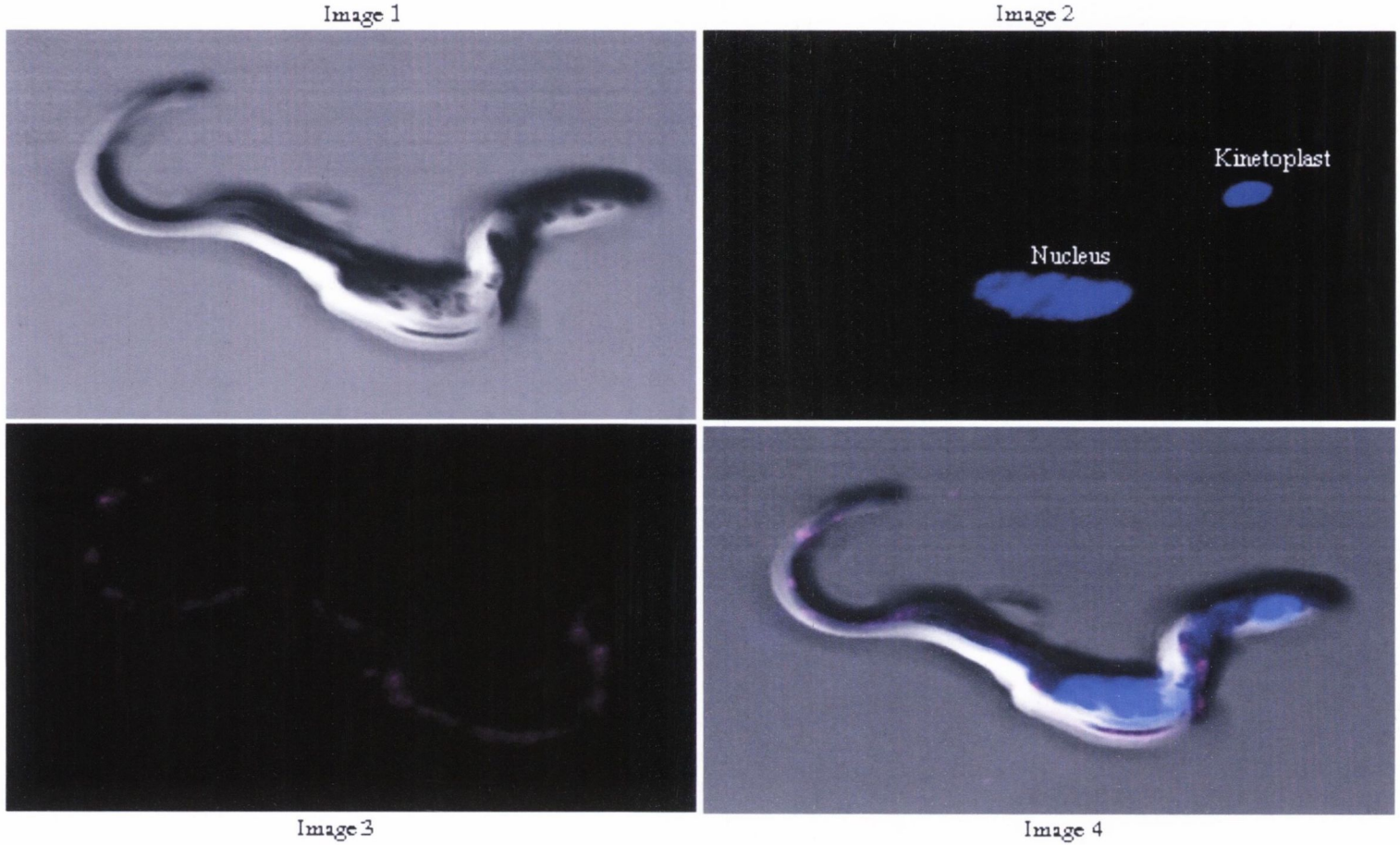

Plate 3.8, panel B. Confocal images of the cellular distribution of the VSG on bloodstream form trypanosomes fixed at 37°C in the absence of tritonX-100. Image 1 - Phase image of cell, image 2 – nucleus & kinetoplast, image 3 – VSG, image 4 – merge of 1, 2 & 3.

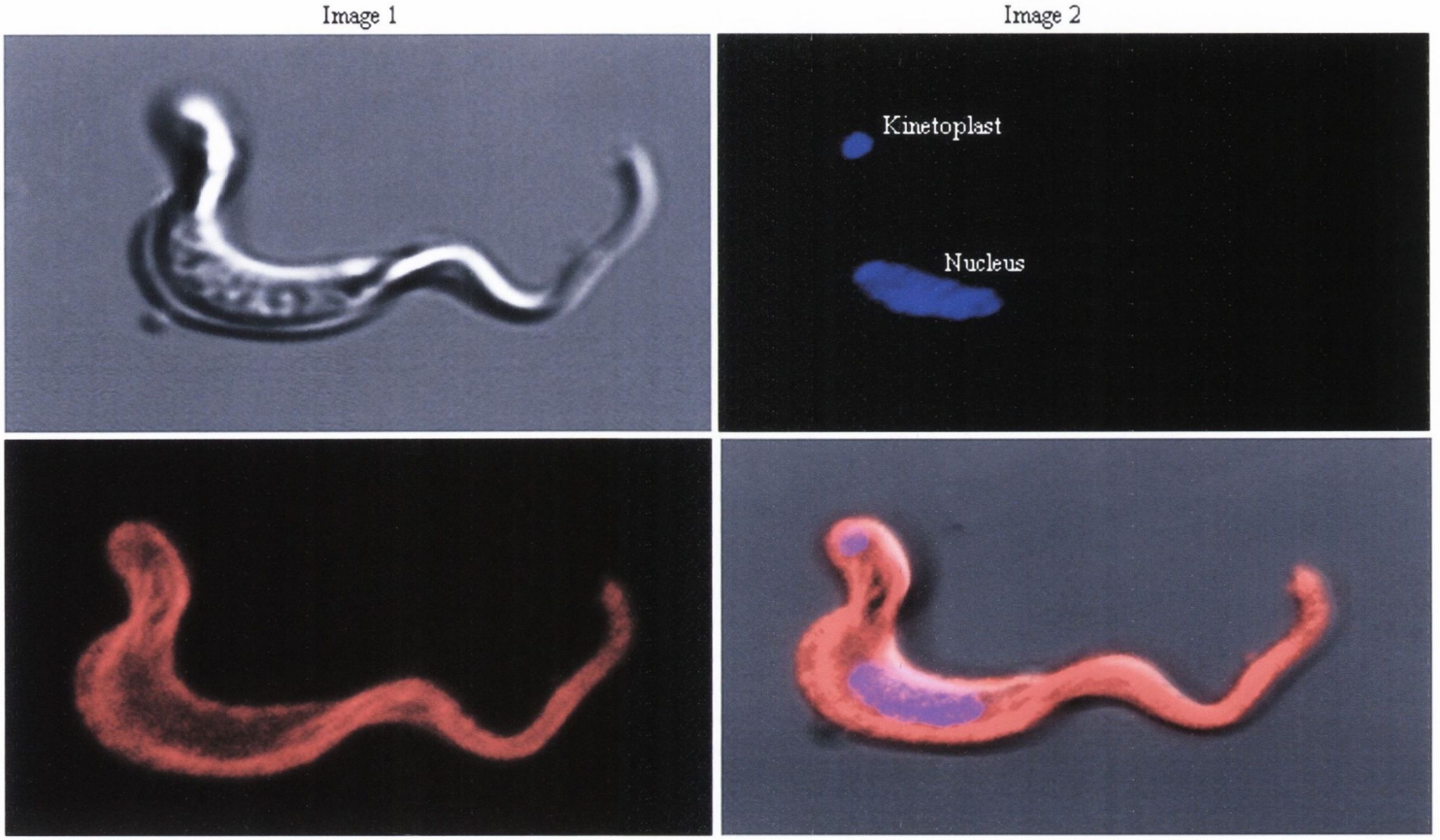

Plate 3.8, panel C. Confocal images of the cellular distribution of the ISG-70 on bloodstream form trypanosomes fixed at 37°C in the absence of tritonX-100. Image 1 - Phase image of cell, image 2 - nucleus & kinetoplast, image 3 - ISG-70, image 4 - merge of 1, 2 & 3.

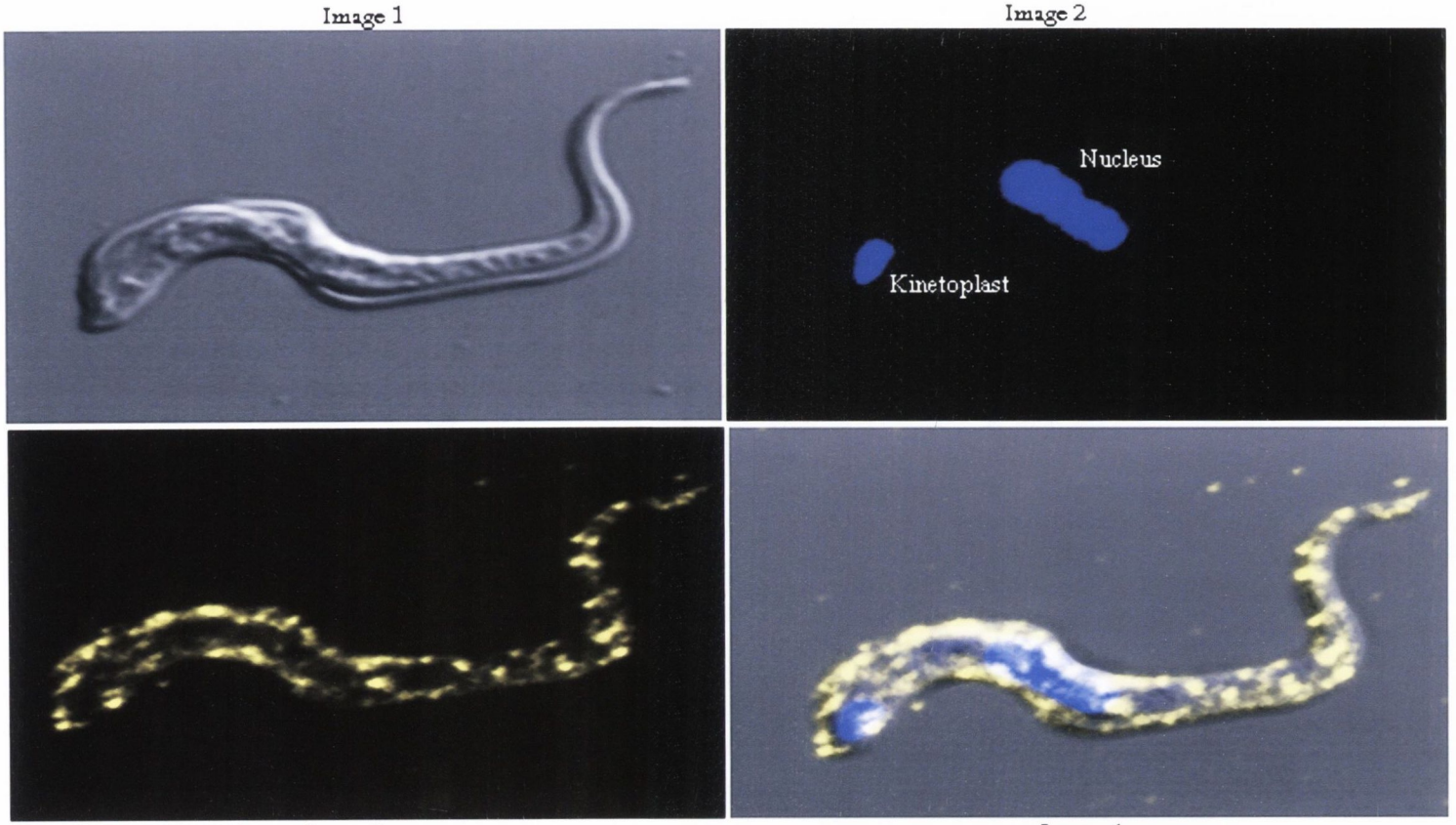

Plate 3.8, panel D. Confocal images of the cellular distribution of tubulin on bloodstream form trypanosomes fixed at 37°C in the absence of tritonX-100. Image 1 - Phase image of cell, image 2 - nucleus & kinetoplast, image 3 – tubulin, image 4 - merge of 1, 2 & 3.

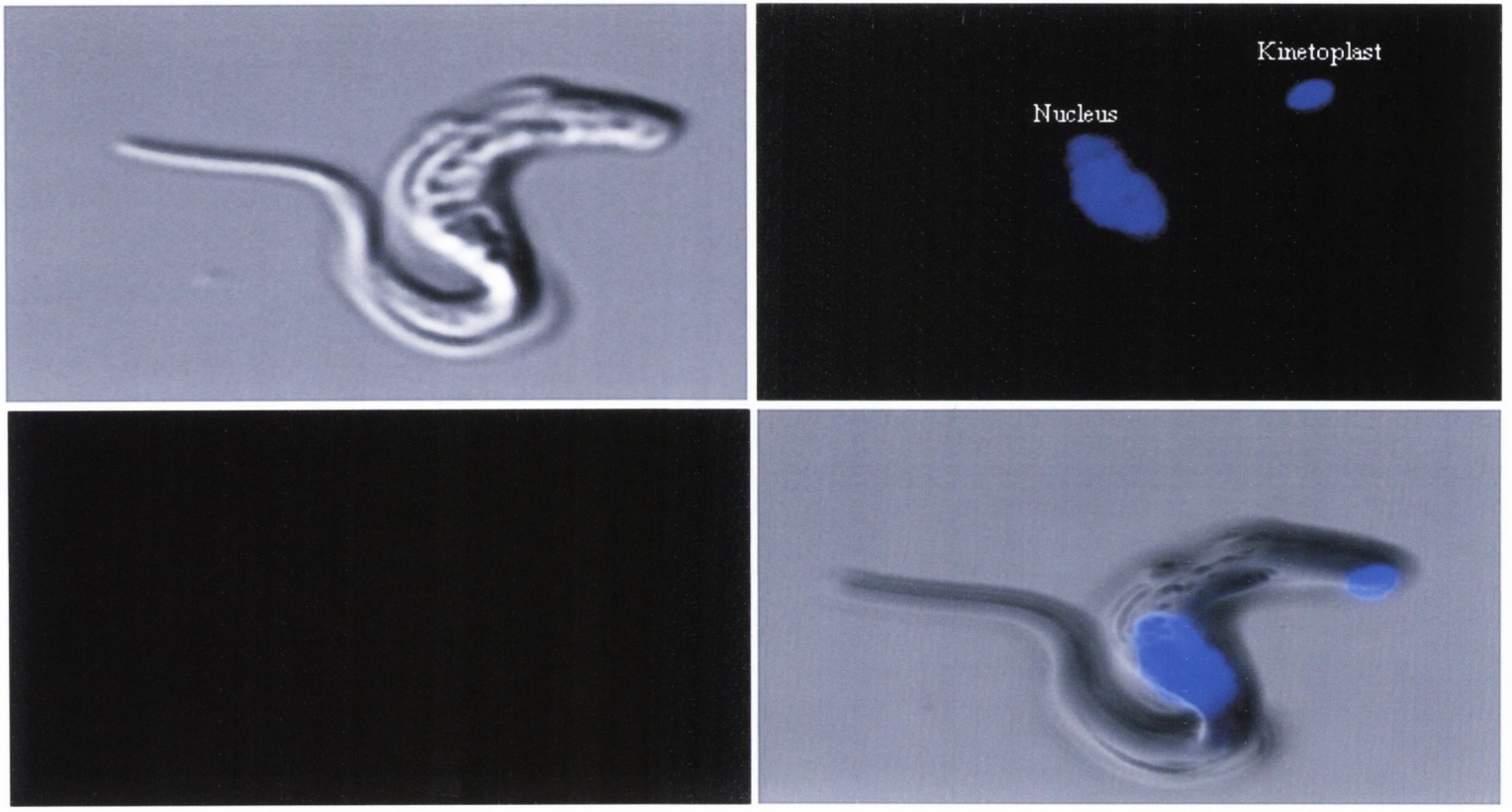

Plate 3.9. Confocal images of the cellular distribution of GPI-PLC (Panel A), VSG (Panel B), ISG70 (Panel C) and tubulin (Panel D) on bloodstream form trypanosomes fixed at 37°C in the presence of Triton X-100.

Bloodstream form trypanosomes (5 x 10^7 cells/ml) were fixed as described in Section 2.1.51, blocked with BSA (5% w/v) for 1 hr at room temperature and following washing incubated with either anti-GPI-PLC antibody (1/1000 dilution), anti-VSG antibody (1/1000 dilution), anti-α-tubulin (1/350 dilution of mouse monoclonal antibody, Clone DM1A) or anti-ISG70 antibody (1/1000 dilution) overnight at room temperature. The cells were washed and binding of primary antibodies to the cells was detected by incubating the cells with a Cy3 conjugated anti-rabbit IgG antibody (1/500 dilution) for the anti-VSG, anti-GPI-PLC and anti-ISG70 antibody detection. The anti-α-tubulin was detected with Alexa 488 anti-mouse IgG (1/2000 dilution). These were all incubated for 1 hr at room temperature. The cells were washed and mounted onto slides as described in section 2.1.53. **Panel A** shows the localization of GPI-PLC on bloodstream form cells fixed at 37°C (+ 0.1 % Tx-100). **Panel B** shows the localization of VSG on bloodstream form trypanosomes fixed at 37°C (+0.1 % Tx-100). **Panel C** shows the localization of ISG-70 on bloodstream form trypanosomes fixed at 37°C (+ 0.1 % Tx-100) and **Panel D** shows the localization of tubulin on bloodstream form trypanosomes fixed at 37°C (+ 0.1 % Tx-100). An Olympus FV-1000 confocal microscope was used to collect images. The laser power was at 1 % and the Kalman filter was used during data collection. Each panel of plate 3.9 displays four images.

Image 1 of each panel displays a phase-contrast image of the cell.

Image 2 displays the location of the nucleus and kinetoplast.

Image 3 displays the protein of interest.

Image 4 displays a merge of images 1, 2 & 3.

Plate 3.9, panel A. Confocal images of the cellular distribution of the GPI-PLC on bloodstream form trypanosomes fixed at 37°C in the presence of tritonX-100. Image 1 – Phase image of cell, image 2 – nucleus & kinetoplast, image 3 – GPI-PLC, image 4 – merge of 1, 2 & 3.

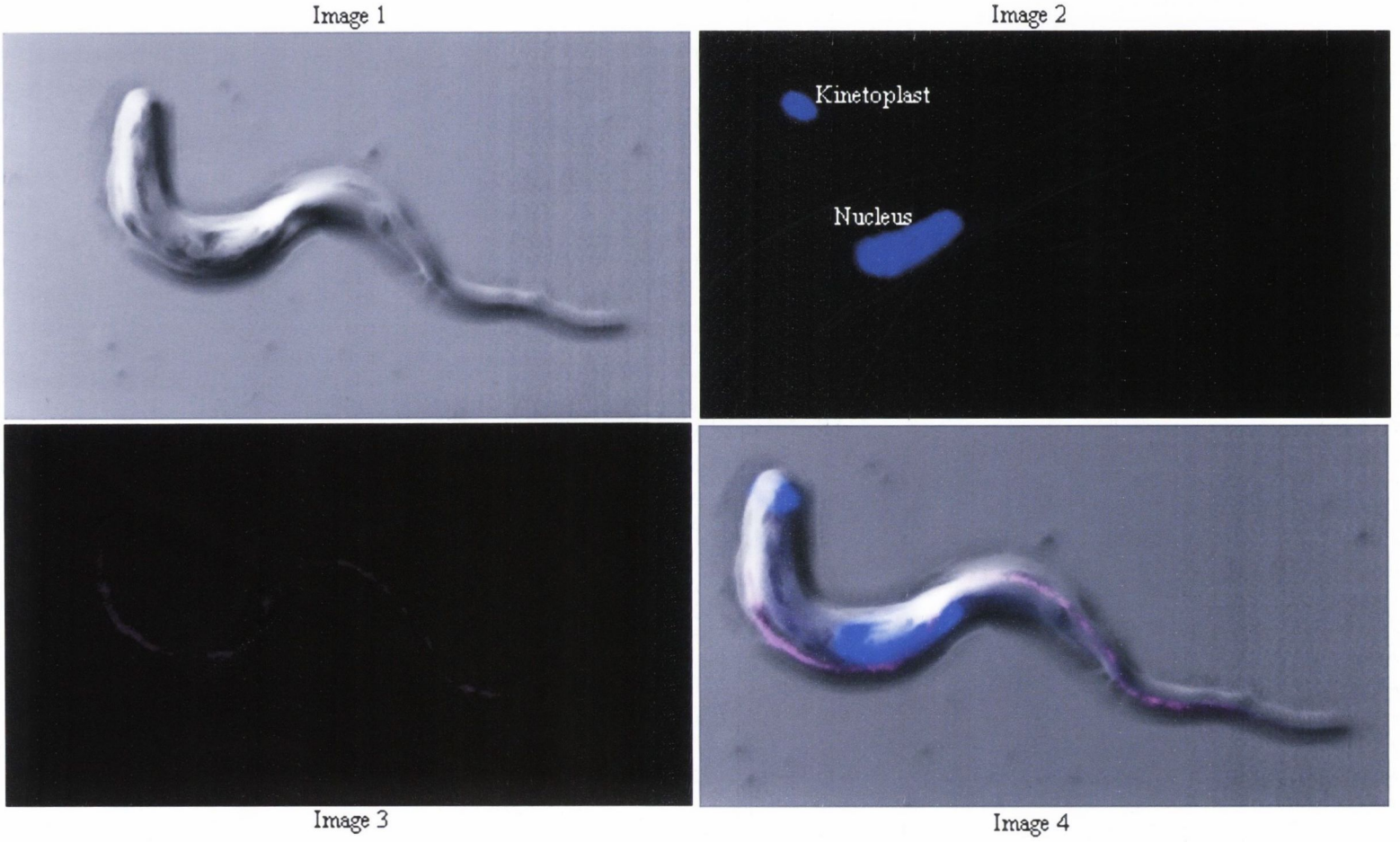

Plate 3.9, panel B. Confocal images of the cellular distribution of the VSG on bloodstream form trypanosomes fixed at 37°C in the presence of tritonX-100. Image 1 – Phase image of cell, image 2 – nucleus & kinetoplast, image 3 – VSG, image 4 – merge of 1, 2 & 3.

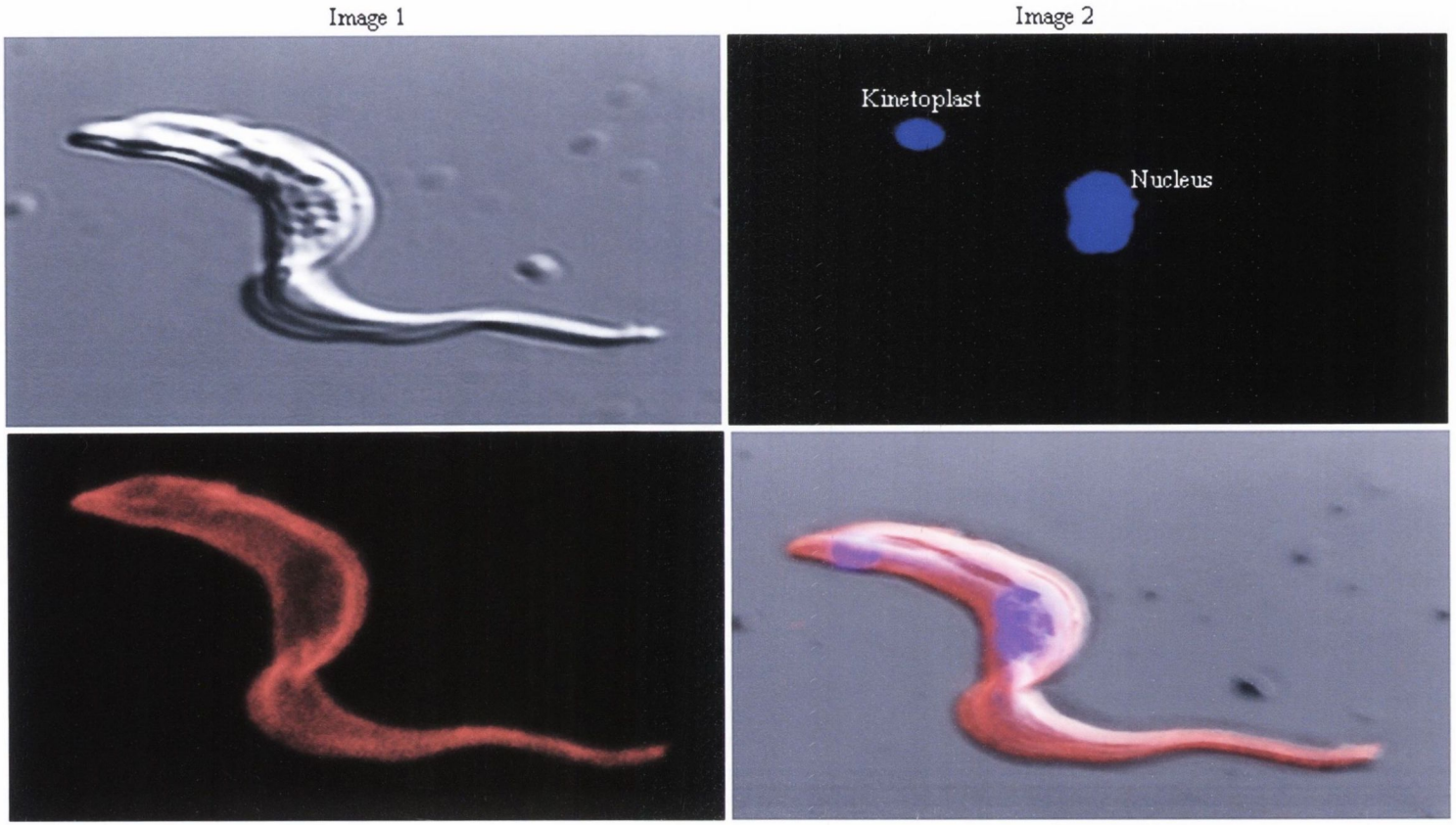

Plate 3.9, panel C. Confocal images of the cellular distribution of the ISG-70 on bloodstream form trypanosomes fixed at 37°C in the presence of tritonX-100. Image 1 – Phase image of the cell, image 2 – nucleus & kinetoplast, image 3 – ISG-70, image 4 – merge of 1, 2 & 3.

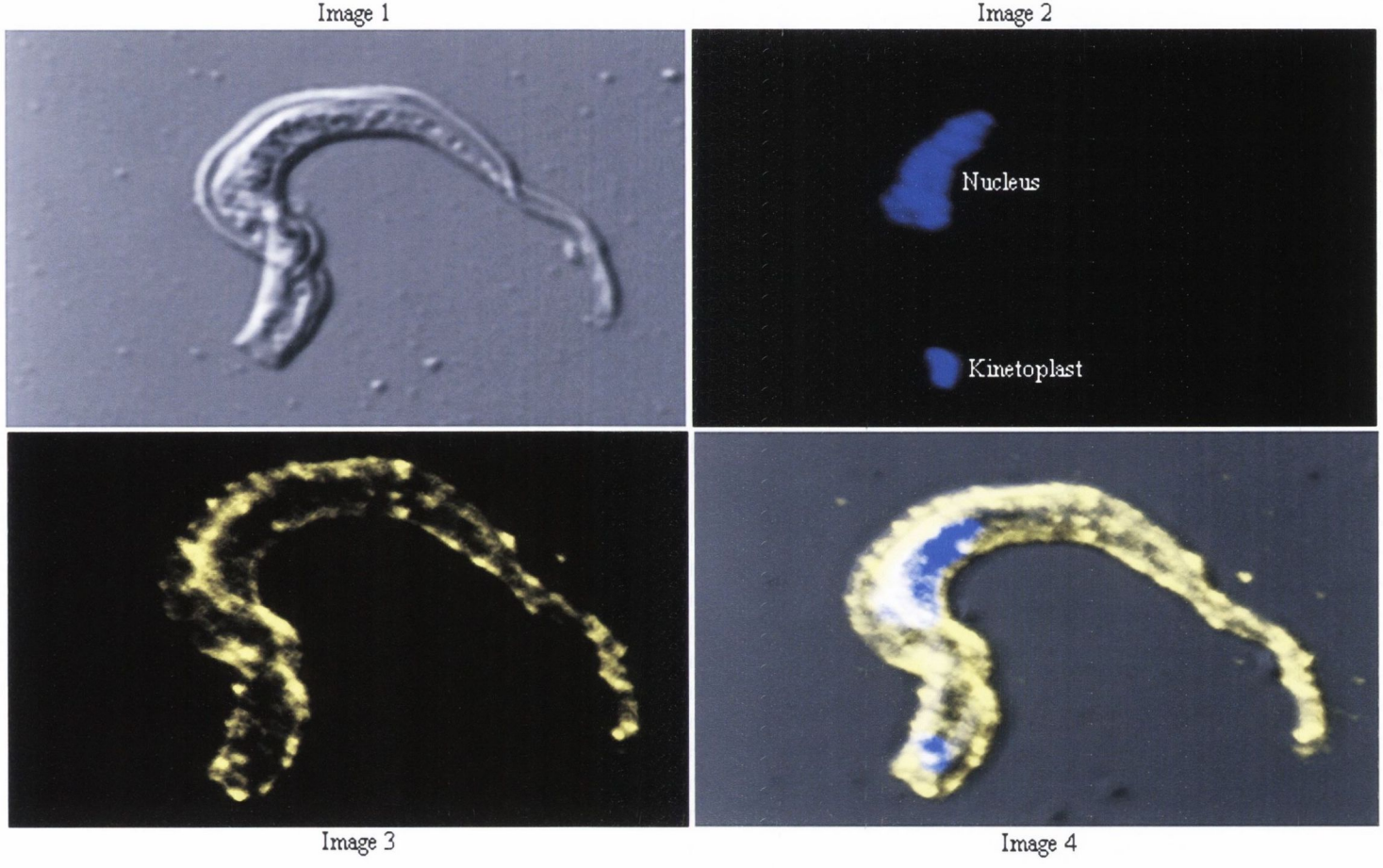

Plate 3.9, panel D. Confocal images of the cellular distribution of tubulin on bloodstream form trypanosomes fixed at 37°C in the presence of tritonX-100. Image 1 – Phase image of cell, image 2 – nucleus & kinetoplast, image 3 – tubulin, image 4 – merge of 1, 2 & 3

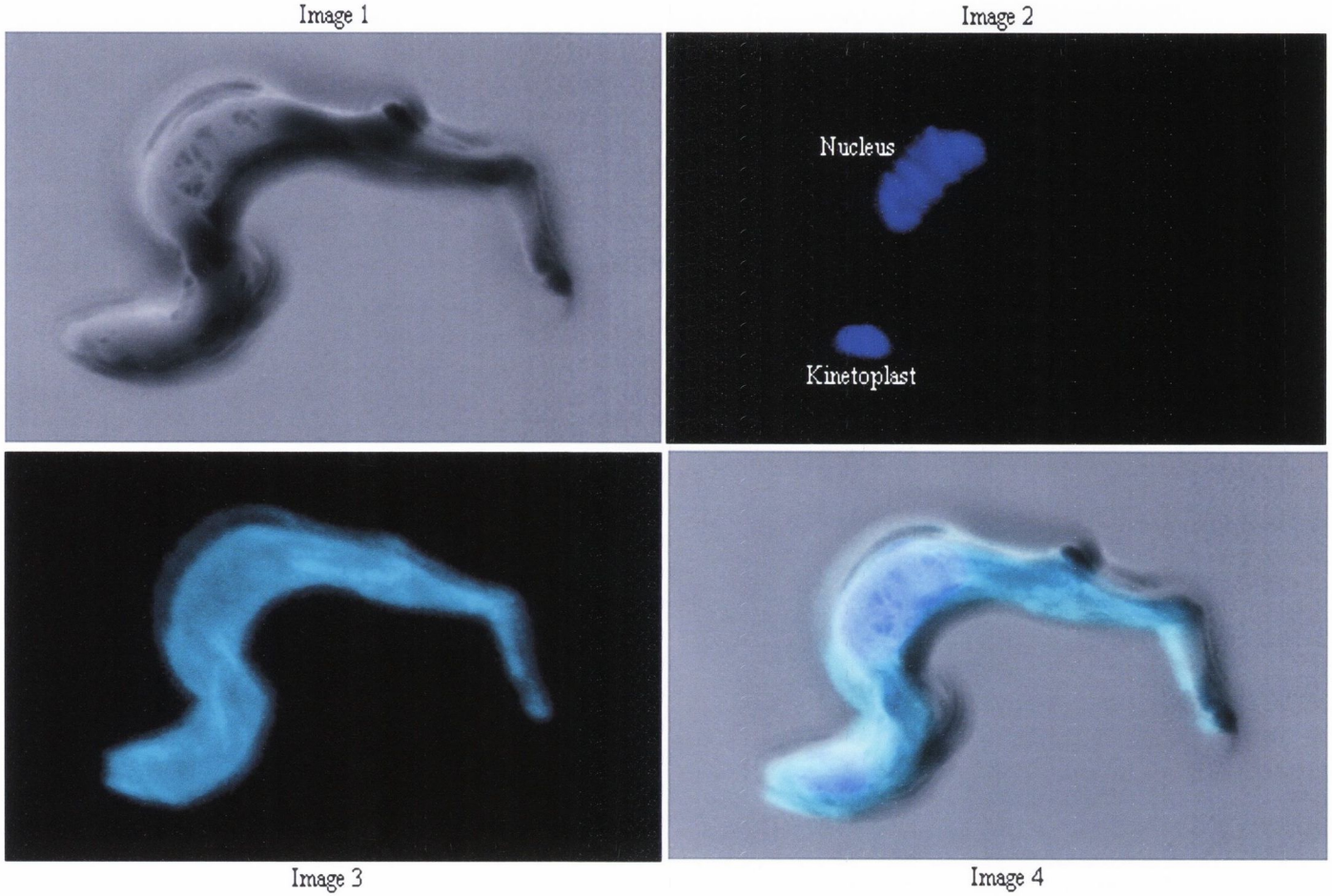

transformation from slender to stumpy forms of *T. brucei* is accompanied by the acquisition of a tolerance or resistance to extracellular external acidic and proteolytic stress, in terms of GPI-PLC mediated surface coat release (Nolan *et al.*, 2000). The possibility that the location of the GPI-PLC is different in short stumpy forms compared to its location in slender forms was investigated. Stumpy forms of S42 trypanosomes were fixed according to the procedure described in the methods section (2.1.51). GPI-PLC was detected using FITC-labelled anti-GPI-PLC in stumpy cells that had been fixed at 0°C (Plate 3.10). The GPI-PLC was found to have the same pattern of fluorescence in short stumpy trypanosomes as in long thin forms (Plate 3.10).

It can be concluded from these results that the GPI-PLC is located on the outer surface of the plasma membrane together with the ISG-70, because the presence of a detergent to permeabilize the plasma membrane was not required for the antibody to access the antigen as was the case with tubulin. It can also be concluded that the GPI-PLC is shielded by the VSG because antibody access to the GPI-PLC is blocked by fixation at 37°C, where the rapid motion of the VSG allows it to be cross-linked above the surface of the GPI-PLC while the more rigid orientation of the VSG at 0°C permits cross-linking of adjacent VSG molecules but not across the surface of the GPI-PLC (See discussion for further elaboration of this explanation). In addition, there is no change in the distribution of the GPI-PLC between long slender forms and stumpy forms of bloodstream form trypanosomes.

3.2.3. Localization of GPI-PLC and tubulin in bloodstream form trypanosomes.

In order to verify that the GPI-PLC was not localized to the inner face of the plasma membrane, the following experiment was carried out. Bloodstream form trypanosomes were prepared for confocal microscopy as described previously (see Chapter 2, section 2.1.53). The monoclonal antibody, DM1A (used in this study) recognizes α-tubulin (Blose *et al.*, 1984). Staining bloodstream trypanosomes with DM1A reveals the location of the trypanosomal microtubular network. The distribution of tubulin was found to produce an intense fluorescence due to the massive numbers and homogenous distribution of the subpellicular microtubules. The flagellum is seen as a fluorescent wavy line along the side of the cell body, indicating the microtubules of the flagellar axoneme (Plate 3.11, image 3). The GPI-PLC was found distributed between these two regions of microtubules lying closer to the flagellar axoneme than to the cell body (Plate 3.11, image

Plate 3.10. Cellular distribution of GPI-PLC in stumpy forms of S42 trypanosomes.

Stumpy forms of S42 trypanosomes (5 x 10^7 cells/ml) were fixed as described in Section 2.1.51, blocked with BSA (5% w/v) for 1 hr at room temperature and following washing incubated with anti-GPI-PLC antibody (1/1000 dilution) overnight at room temperature. The cells were washed and binding of primary antibody to the cells was detected by incubating the cells with FITC conjugated anti-IgG antibody (1/2000 dilution). This was incubated for 1 hr at room temperature. The cells were washed and mounted onto slides as described in section 2.1.53. Plate 3.10 shows two images.

Image 1 displays a phase-contrast image of stumpy cells.

Image 2 displays the location of the GPI-PLC in stumpy cells.

Plate 3.10. Cellular distribution of GPI-PLC in stumpy forms of S42

Image 1

Image 2

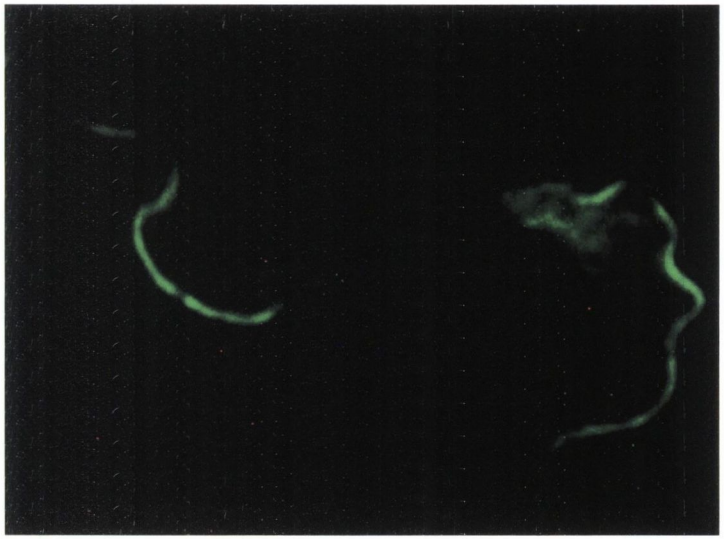

4), and at no point were the two fluorescent dyes co-localised. Furthermore, it is apparent from the low power view of trypanosomes stained with both anti-α-tubulin and anti-GPI-PLC IgG (Plate 3.11, image 1) that the GPI-PLC is not located on the cell body in those cells where the flagellum is pulled away from the cell. This observation is further emphasized in the high power view (Plate 3.11, image 4) where it is obvious that the GPI-PLC is distributed along the line of the flagellum, indicating that the GPI-PLC is not localized to the cell body but to the flagellar membrane complex. These results led to the conclusion that the GPI-PLC is not located on the inner face of the plasma membrane and is not located on the cell body.

3.2.4. Localization of GPI-PLC and the plasma membrane in bloodstream form trypanosomes.

The following experiment was conducted in order to confirm that the GPI-PLC is an extracellular protein. The plasma membrane of bloodstream forms of T. brucei consists of three distinct but contiguous domains: the pellicular membrane, the flagellar membrane and the flagellar pocket membrane. Labelling trypanosomes with a Cy-3 membrane protein marker detects all three domains. Bloodstream form trypanosomes (5 x 10^7 cells/ml) were incubated with a Cy-3 marker (Amersham) that reacts with amines on proteins and oligonucleotides for 10 min at 0°C and subsequently prepared for confocal microscopy as described previously (Chapter 2, section 2.1.53). The cellular distribution of the GPI-PLC is shown in Plate 3.12, image 2. The fluorescence of the GPI-PLC in image 2 indicates that this particular trypanosome is biflagellate. The fluorescence distribution of the GPI-PLC begins where the flagellum leaves the cell body (the flagellar pocket) and is aligned along the length of the flagellum, terminating just posterior to the most distal tip of the flagellum. The Cy-3 dye has labelled both the plasma membrane of the cell body and the flagellar membrane (Plate 3.12, image 3). When the images of the GPI-PLC and the plasma membrane fluorescence are merged the resulting image suggests that the GPI-PLC is located on the membrane of both flagella (Plate 3.12, image 4). These results indicate that the GPI-PLC is distributed in a patchy string-like fashion along the membrane of the flagellum. Consequently, the GPI-PLC is an extracellular protein.

Plate 3.11. Confocal images of the cellular distribution of GPI-PLC and tubulin on bloodstream form trypanosomes fixed at 0°C in the presence of Tx-100.

Bloodstream form trypanosomes (5 x 10^7 cells/ml) were fixed as described in Section 2.1.51, blocked with BSA (5% w/v) for 1 hr at room temperature and following washing incubated with anti-GPI-PLC antibody (1/1000 dilution) and anti-α-tubulin (1/350 dilution of mouse monoclonal antibody, Clone DM1A) overnight at room temperature. The cells were washed and binding of primary antibodies to the cells was detected by incubating the cells with Cy3 conjugated anti-rabbit IgG antibody (1/500 dilution) for the anti-GPI-PLC antibody detection. The anti-α-tubulin was detected with Alexa 488 anti-mouse IgG (1/2000 dilution). These were incubated for 1 hr at room temperature. The cells were washed and mounted onto slides as described in section 2.1.53. An Olympus FV-1000 Confocal microscope was used to collect images. The laser power was at 1 % and the Kalman filter was used during data collection. Four images are displayed on the opposite page.

Image 1 displays a phase contrast view of the cell with a low power view inset.

Image 2 displays the localization of the GPI-PLC on bloodstream form trypanosomes (magenta).

Image 3 displays the localization of tubulin on bloodstream form trypanosomes (cyan).

Image 4 displays a merge of 1, 2 & 3.

Plate 3.11. Confocal images of the cellular distribution of GPI-PLC and tubulin on bloodstream form trypanosomes fixed at 0°C in the presence of Tx-100. Image 1- phase contrast view of cell with low power view inset, image 2 – GPI-PLC, image 3 – tubulin, image 4 – a phase image merged with images 2 & 3.

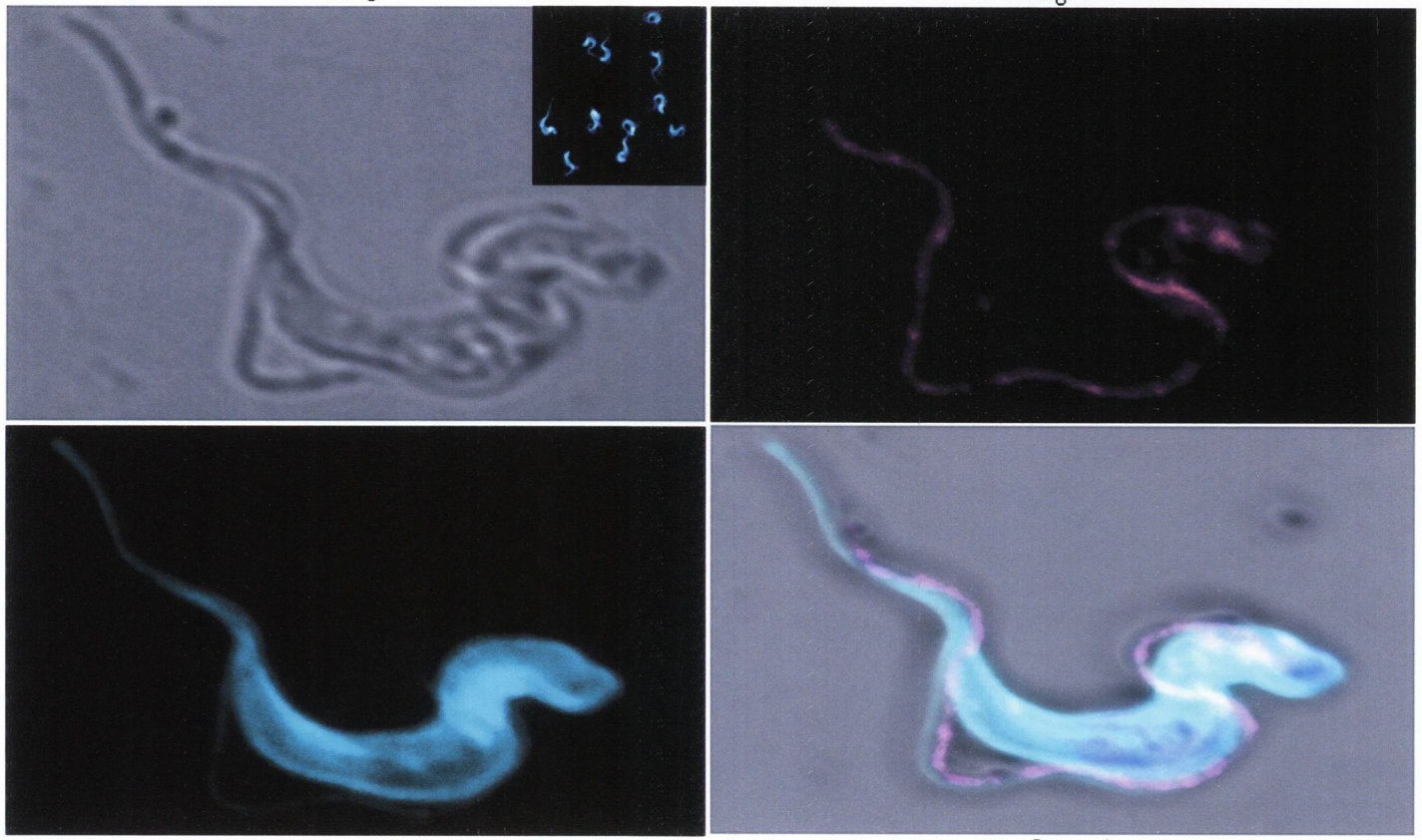

Plate 3.12. Localization of the GPI-PLC and a Cy3 plasma membrane marker in bloodstream form trypanosomes.

Bloodstream form trypanosomes (5 x 10^7 cells/ml) were incubated with Cy3 mono-reactive dye™ (Amersham) for 10 min at 4°C. The cells were washed (x2) and fixed for 10 min on ice (Section 2.1.51). The cells were then mounted onto poly-L-lysine coverslips and blocked with BSA (5% in PBS) for one hour at room temperature. Anti-GPI-PLC IgG (1/1000 dilution) was added in BSA/PBS (5% w/v) and incubated overnight at room temperature. The cells were washed and binding of anti-GPI-PLC IgG was detected using Alexa-488 anti-IgG (1/2000 dilution). The cells were incubated with this for 1 hour at room temperature. The coverslips were then prepared for confocal microscopy as described in methods (Section 2.1.53). An Olympus FV-1000 confocal microscope was used to collect images. The laser power was at 1 % for detection and the Kalman filter was used during data collection. Four images are shown on the opposite page.

Image 1 displays a phase contrast view of the cell with a low power view inset.

Image 2 displays the cellular distribution of the GPI-PLC (magenta).

Image 3 displays the plasma membrane of the trypanosome using the Cy-3 membrane protein marker (green).

Image 4 displays a merge of 1, 2 & 3.

Plate 3.12. Localization of the GPI-PLC and a Cy3 plasma membrane marker in bloodstream form trypanosomes. Image 1 displays a phase contrast view of the cell with low power view inset. Image 2 displays the GPI-PLC (magenta). Image 3 displays the membrane marker (green) and image 4 is a phase image merged with images 2 & 3.

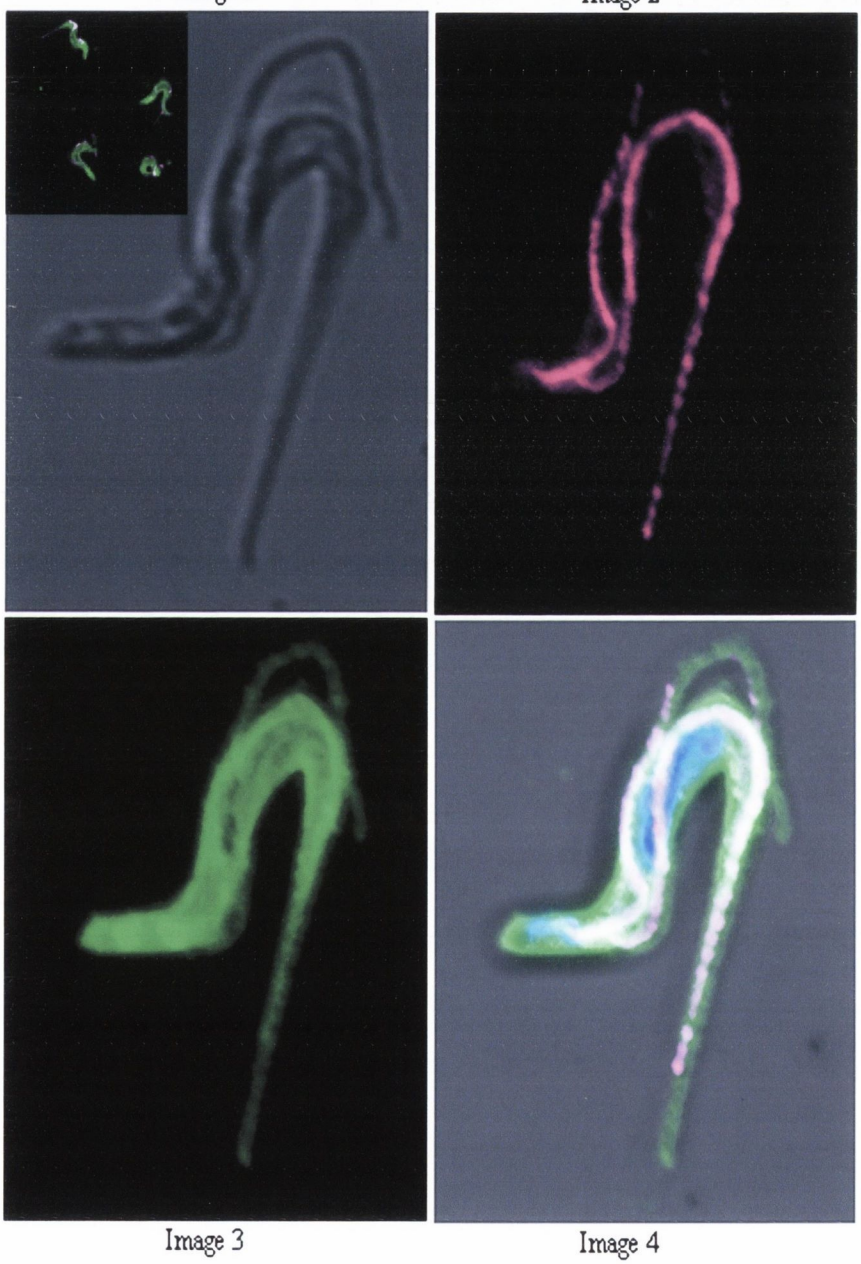

3.2.5. Localization of the GPI-PLC and the para-flagellar rod (PFR) in bloodstream form trypanosomes.

The para-flagellar rod is a large structure found within the flagellum of bloodstream form trypanosomes. It is present from the point where the flagellum exits the flagellar pocket and runs alongside the axoneme of the flagellum right to the distal tip (Bastin *et al.*, 2000). The PFR is physically connected to the axoneme *via* fibres attaching the proximal domain to the microtubule doublets four through 7 (Bastin *et al.*, 2000). The crescent shape of the para-flagellar rod and its location in trypanosomes prompted us to determine the localization of the GPI-PLC at the same time as the localization of the para-flagellar rod was being determined.

Bloodstream form trypanosomes (5×10^7 cells/ml) were fixed at 0°C for 10 minutes and prepared for confocal microscopy as described previously (Chapter 2 section 2.1.53). The pattern of staining using anti-PFR-A revealed detection of the flagellum from the flagellar pocket to the flagellar tip (Plate 3.13, image 3 & 4), as seen by many workers in the past (Kohl *et al.*, 1999 & Bastin, 2000 #158). The GPI-PLC is distributed from a point in the flagellar pocket to an area just posterior to the tip of the flagellum (Plate 3.13, image 2 & 4). The GPI-PLC is located immediately adjacent to the inside of the rod on the same side as the cell body (Plate 3.13, image 4). Along the length of the flagellum the localization of the GPI-PLC is clearly distinct from that of the PFR. The merged image (image 4) shows that the two proteins can be resolved into two non-overlapping patterns. This distribution is particularly striking when the flagellum appears to cross from one side of the cell body to the other side of the cell body; *e.g.* when the flagellum, running along the top of the cell body falls on one side so that it first lies to the right of the cell body and then, to the left of the cell body. In each case the para-flagellar rod is furthest from the cell body and the GPI-PLC is closest to the cell body (Plate 3.13, image 4). This result indicates that the GPI-PLC is not located in the same position as the PFR.

3.2.6. Localization of GPI-PLC and the flagellar attachment zone (FAZ) in bloodstream form trypanosomes.

The FAZ is found in the cytoplasm and immediately adjacent to the para-flagellar rod on the cell body side of bloodstream form trypanosomes as seen in fluorescent studies carried out in the past (Kohl *et al.*, 1999). These fluorescent images prompted us to

Plate 3.13. Confocal images showing the localization of the GPI-PLC and the paraflagellar rod in bloodstream forms of *T. brucei*.

Bloodstream form trypanosomes (5 x 10^7 cells/ml) were fixed as described in Section 2.1.51, blocked with BSA (5% w/v) for 1 hr at room temperature and following washing incubated with anti-GPI-PLC antibody (1/1000 dilution) and monoclonal anti-PFR antibody (L8C4, recognises exclusively PFR-A) (1/50 dilution) overnight at room temperature. The cells were washed and binding of primary antibodies to the cells was detected by incubating the cells with Cy3 conjugated anti-rabbit IgG antibody (1/500 dilution) for the anti-GPI-PLC antibody detection and Alexa 488 anti-mouse IgG for the anti-PFR antibody detection. These were incubated for 1 hr at room temperature. The cells were washed and mounted onto slides as described in section 2.1.53. An Olympus FV-1000 confocal microscope was used to collect images. The laser power was at 1 % for detection of Cy3 and 5 % for detection of Alexa 488 and the Kalman filter was used during data collection. Four images are on display.

Image 1 displays a phase-contrast image of a trypanosome.

Image 2 shows the location of the GPI-PLC (magenta).

Image 3 shows the location of the para-flagellar rod (green).

Image 4 displays a merge of 1,2 & 3.

Plate 3.13. Confocal images showing the localization of the GPI-PLC and the paraflagellar rod in bloodstream forms of *T. brucei*. Image 1 displays a phase image of the cell. Image 2 displays the GPI-PLC (magenta). Image 3 displays the PFR (green) and image 4 displays a merge of 1, 2 & 3.

determine whether the GPI-PLC was located in the same compartment as the FAZ, due to the results displayed in Plate 3.13, where we found the GPI-PLC distributed immediately adjacent to the PFR on the cell body side of the trypanosome. Bloodstream form trypanosomes (5 x 10^7 cells/ml) were fixed and prepared for confocal microscopy as described previously (Chapter 2, section 2.1.53). The pattern of fluorescence using anti-FAZ antibodies revealed detection of the region between the cell body and the flagellum (Plate 3.14, image 3). The GPI-PLC is distributed in the usual patchy string-like fashion (Plate 3.14, image 2) along the outer side of the FAZ (Plate 3.14, image 4). The distribution of both the FAZ and the GPI-PLC begins in the flagellar pocket region, just anterior to the kinetoplast (Plate 3.14, image 4). When the fluorescent images of the GPI-PLC and the FAZ are merged it is apparent that the GPI-PLC is not located in the same compartment as the FAZ (Plate 3.14, image 4). The GPI-PLC appears to be located immediately adjacent to the outer side of the FAZ on the same side as the flagellum. Combining the information gained from the results in Plate 3.13 and Plate 3.14 one can conclude that the GPI-PLC lies between the flagellar attachment zone (FAZ) and the para-flagellar rod (PFR) in a patchy string-like distribution. Therefore, in this case when the flagellum lies on its side, the FAZ is closest to the cell body and the GPI-PLC is furthest from the cell body (Plate 3.14, image 4). The only structure that lies between the FAZ and the para-flagellar rod is the restricted area of the flagellar plasma membrane. Consequently, I conclude that the GPI-PLC is located in this structure.

3.2.7. Localization of the GPI-PLC and the FAZ in bloodstream form trypanosomes labelled with a Cy-3 membrane marker and where the flagellum is positioned away from the cell body.

Bloodstream form trypanosomes (5 x 10^7 cells/ml) were incubated with a Cy-3 marker (Amersham) and prepared for confocal microscopy as described previously (chapter 2, section 2.1.53). These labelled cells were subsequently probed with anti-FAZ antibody (Plate 3.15) and anti-GPI-PLC antibodies (Plate 3.16). These images are presented in order to show with more clarity that firstly, the GPI-PLC and the FAZ are not in the same location in bloodstream form trypanosomes and secondly, to show that the GPI-PLC is localized to the flagellar membrane of bloodstream form trypanosomes while the FAZ remains with the cell body. The trypanosomes in the high powered views of Plate 3.15 and Plate 3.16 (images 2, 3 & 4) have been specially selected because they

Plate 3.14. Confocal images showing the localization of the GPI-PLC and the flagellar attachment zone (FAZ) in bloodstream forms of *T. brucei*.

Bloodstream form trypanosomes (5 x 10^7 cells/ml) were fixed as described in Section 2.1.51, blocked with BSA (5% w/v) for 1 hr at room temperature and following washing incubated with anti-GPI-PLC antibody (1/1000 dilution) and monoclonal anti-FAZ antibody (L3B2, a kind gift from Keith Gull, Oxford) (1/5 dilution) overnight at room temperature. The cells were washed and binding of primary antibodies to the cells was detected by incubating the cells with Cy3 conjugated anti-rabbit IgG antibody (1/500 dilution) for the anti-GPI-PLC antibody detection and Alexa 488 anti-mouse IgG for the anti-FAZ antibody detection. These were incubated for 1 hr at room temperature. The cells were washed and mounted onto slides as described in section 2.1.53. An Olympus FV-1000 confocal microscope was used to collect images. The laser power was at 1 % for detection of Cy3 and 5 % for detection of Alexa 488 and the Kalman filter was used during data collection. Four images are on display.

Image 1 displays a phase-contrast image of a trypanosome.

Image 2 shows the location of the GPI-PLC (magenta).

Image 3 shows the location of the flagellar attachment zone (cyan).

Image 4 displays a merge of images 1, 2 & 3.

Plate 3.14. Confocal images showing the localization of the GPI-PLC and the flagellar attachment zone (FAZ) in bloodstream forms of *T. brucei*. Image 1 displays a phase image of the cell, image 2 displays the GPI-PLC, image 3 displays the FAZ and image 4 displays a merge of 1, 2 & 3.

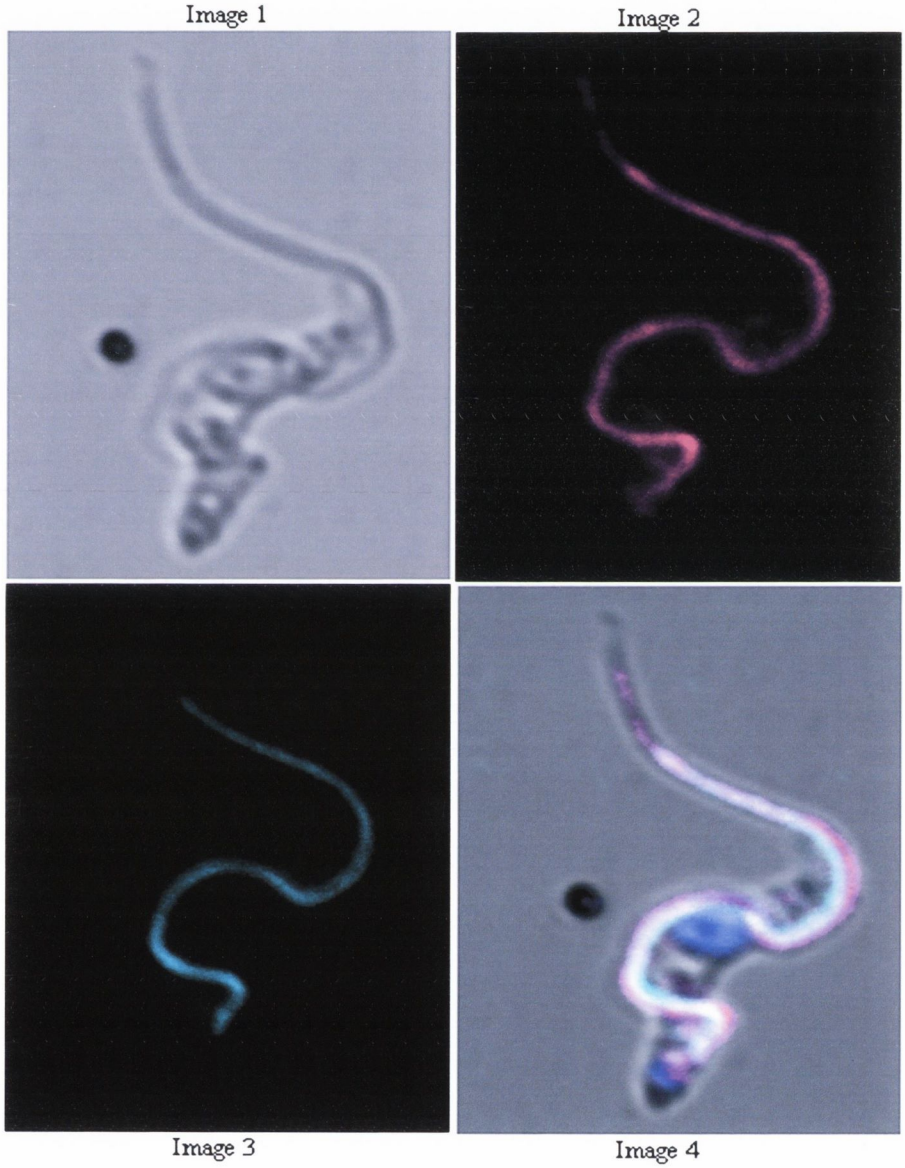

have been damaged by having their flagellum and surrounding membrane torn from its attachment to the cell body with its surrounding plasma membrane. These images distinguish clearly between the distribution of the GPI-PLC and the FAZ in bloodstream form trypanosomes. Clearly, the FAZ remains attached to the cell body (Plate 3.15, images 2, 3 & 4). The images of Plate 3.16 (images 2, 3 & 4) demonstrate unequivocally that the GPI-PLC is not located on the cell body but is aligned along the flagellum in the usual patchy string-like distribution. Furthermore, it can be seen that the GPI-PLC is not distributed all over the flagellar membrane. Rather, it occupies a position on this membrane that is immediately adjacent to the cell body.

3.2.8. Localization of the GPI-PLC in intact bloodstream form trypanosomes following release of the VSG.

An experiment was conducted in order to determine whether the GPI-PLC moved away from the flagellar membrane during release of the VSG from intact bloodstream form trypanosomes. The VSG was released from intact trypanosomes by incubating cells in hyperosmotic buffer (to prevent rupture) containing 2-deoxy-D-glucose (10 mM) at 37°C for 45 min (see section 2.1.19 in the methods section, Fig 2.6 a & b & Fig 2.7). These de-energized cells were then prepared for confocal microscopy as described in section 2.1.53 and subsequently probed with anti-GPI-PLC IgG. The GPI-PLC was detected by Cy3-labelled anti-IgG (Plate 3.17). The distribution of the GPI-PLC in trypanosomes that have lost their VSG coat and are still intact is the same as it is in fully energized trypanosomes. These results suggest that the GPI-PLC does not move from its location in the flagellar membrane in order to cleave the GPI anchor of the VSG in bloodstream form trypanosomes. In addition to the confocal microscopy analysis, trypanosomes were also analysed by SDS-PAGE and subsequent western blotting (Fig 3.3). This result informs us that the VSG is released from the trypanosomes (Fig 3.3, A) and exposure of the CRD epitope indicates this release is due to GPI cleavage by the action of the GPI-PLC on the GPI anchor of the VSG (Fig 3.3, B). Consequently, for VSG release to have occurred the VSG must have diffused within the plane of the membrane to the position of the GPI-PLC; and the GPI-PLC did not move to the position of each molecule of VSG in turn.

Plate 3.15. Location of the FAZ in bloodstream form trypanosomes labelled with a Cy-3 plasma membrane marker.

Bloodstream form trypanosomes (5 x 10^7 cells/ml) were fixed as described in Section 2.1.51, blocked with BSA (5% w/v) for 1 hr at room temperature and following washing incubated with monoclonal anti-FAZ antibody (1/5 dilution) overnight at room temperature. The cells were washed and binding of primary antibodies to the cells was detected by incubating the cells with Alexa 488 anti-mouse IgG for the anti-FAZ antibody detection. These were incubated for 1 hr at room temperature. The cells were washed and mounted onto slides as described in section 2.1.53. Four images are on display.

Image 1 shows a phase contrast view of the cell with a low power view inset.

Image 2 shows a single trypanosome at high power labelled with the Cy-3 membrane marker (green).

Image 3 shows a single trypanosome at high power labelled with anti-FAZ IgG (orange).

Image 4 displays a merge of 1, 2 & 3.

Plate 3.15. Location of the FAZ in bloodstream form trypanosomes labelled with a Cy-3 plasma membrane marker. Image 1 displays a phase contrast view with low power view inset. Image 2 displays the plasma membrane (green). Image 3 displays the FAZ (orange) and image 4 displays a phase image merged with images 2 & 3.

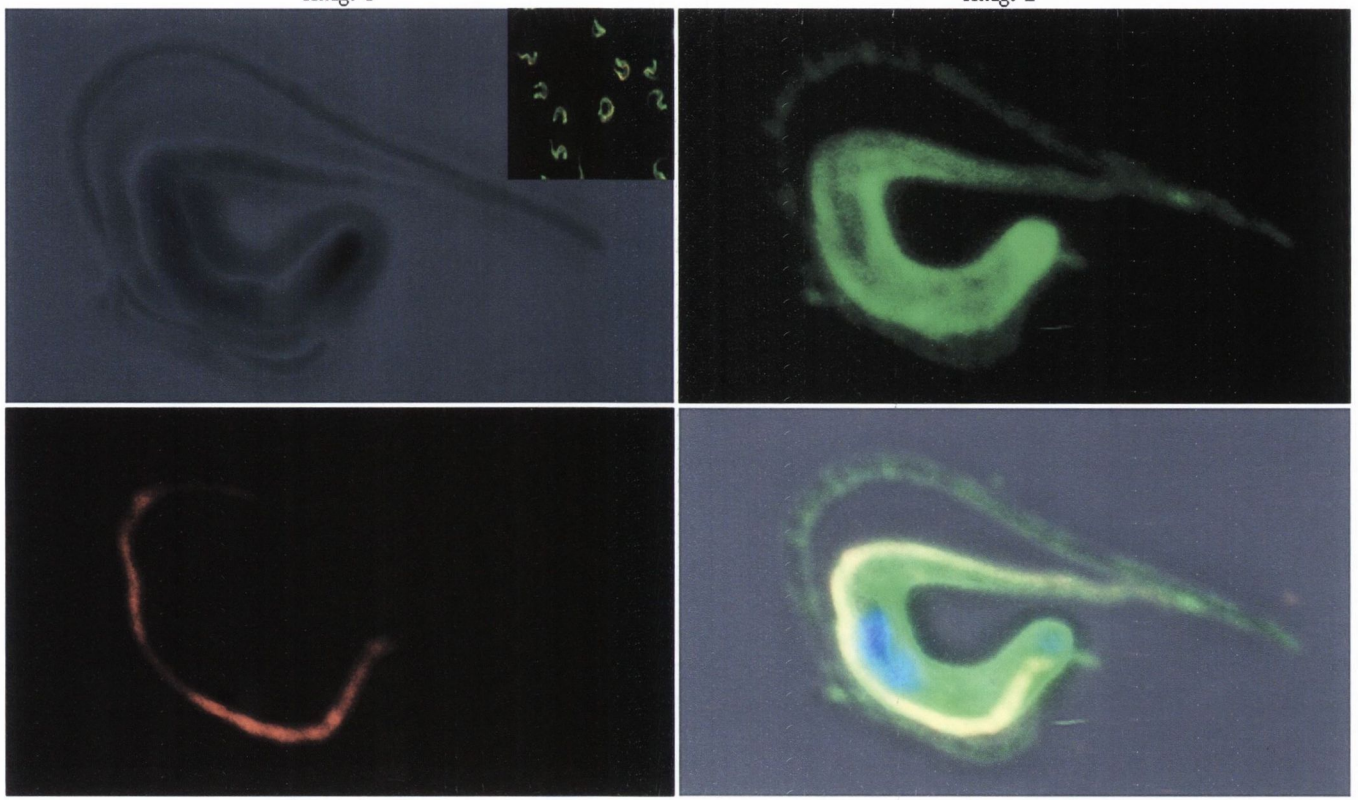

Plate 3.16. Location of the GPI-PLC in bloodstream form trypanosomes labelled with a Cy-3 plasma membrane marker.

Bloodstream form trypanosomes (5 x 10^7 cells/ml) were fixed as described in Section 2.1.51, blocked with BSA (5% w/v) for 1 hr at room temperature and following washing incubated with anti-GPI-PLC antibody (1/1000 dilution) overnight at room temperature. The cells were washed and binding of primary antibodies to the cells was detected by incubating the cells with Cy3 conjugated anti-rabbit IgG antibody (1/500 dilution) for the anti-GPI-PLC antibody detection. These were incubated for 1 hr at room temperature. The cells were washed and mounted onto slides as described in section 2.1.53. Four images are on display.

Image 1 shows a phase contrast view of the cell with a low power view inset.

Image 2 shows a single trypanosome at high power labelled with anti-GPI-PLC IgG (magenta)

Image 3 shows a single trypanosome at high power labelled with the Cy-3 membrane marker (green).

Image 4 displays a merged of 1, 2 & 3.

Plate 3.16. Location of the GPI-PLC in bloodstream form trypanosomes labelled with a Cy-3 plasma membrane marker. Image 1 displays a phase contrast view with a low power view inset. Image 2 displays the GPI-PLC (magenta). Image 3 displays the membrane marker (green). Image 4 displays a phase image merged with 2 & 3.

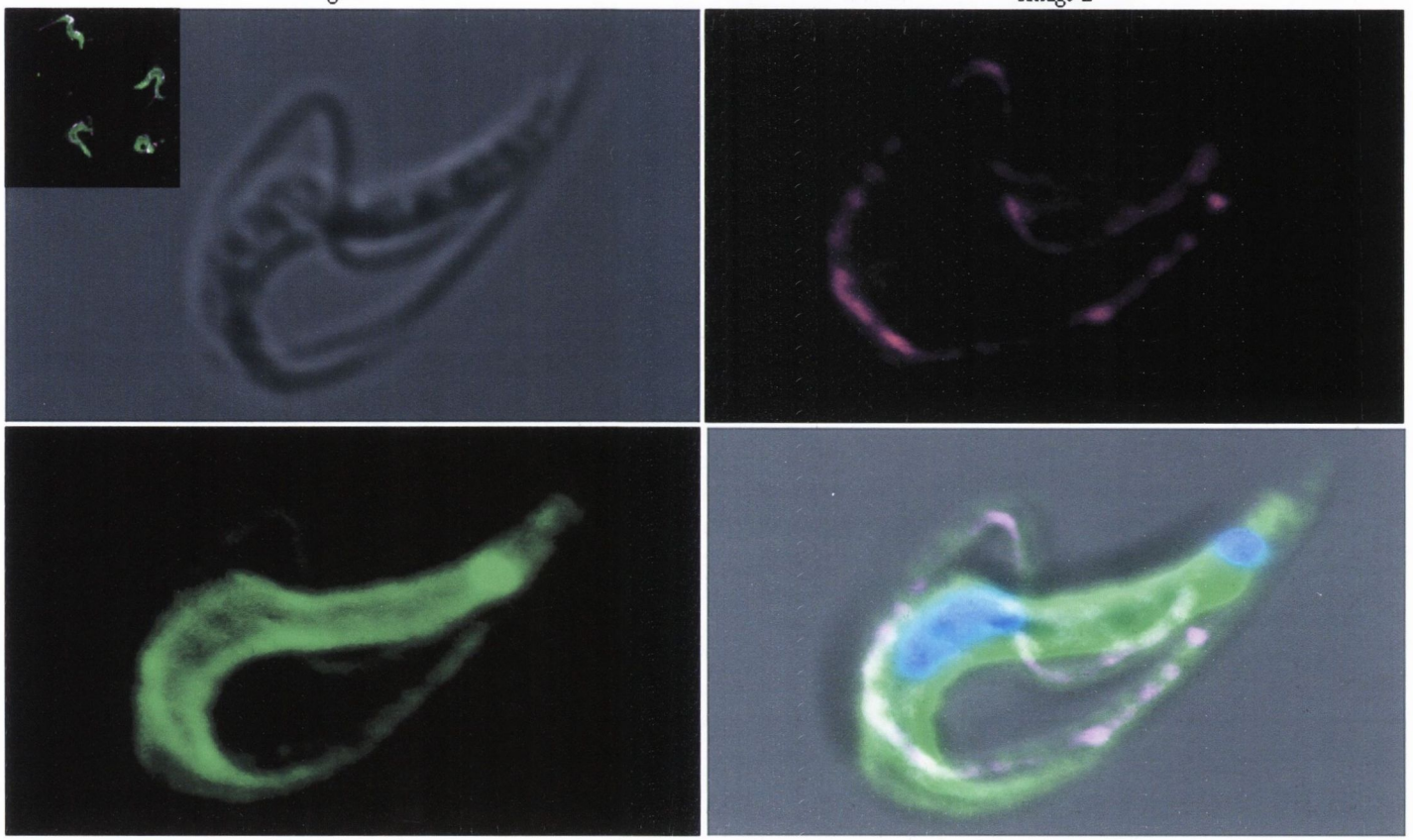

Plate 3.17. Localization of the GPI-PLC in intact bloodstream form trypanosomes following release of the VSG.

Bloodstream form trypanosomes were de-energized according to the methods section (2.1.19) and subsequently fixed as described in Section 2.1.51, blocked with BSA (5% w/v) for 1 hr at room temperature and following washing incubated with anti-GPI-PLC antibody (1/1000 dilution) overnight at room temperature. The cells were washed and binding of primary antibodies to the cells was detected by incubating the cells with Cy3 conjugated anti-rabbit IgG antibody (1/500 dilution). These were incubated for 1 hr at room temperature. The cells were washed and mounted onto slides as described in section 2.1.53. An Olympus F V-1000 confocal microscope was used to collect images. The laser power was at 1 % for detection and the Kalman filter was used during data collection.

Panel A displays two images of a fully energized bloodstream form trypanosome. **Panel B** displays two images of a trypanosome following a 45 minute incubation under de-energizing conditions where the VSG coat is released from intact bloodstream from trypanosomes by the action of the GPI-PLC.

Image 1 displays the distribution of the GPI-PLC (magenta) and the nucleus and kinetoplast (blue).

Image 2 displays a phase-contrast image merged with image 1.

Plate 3.17. Localization of the GPI-PLC in intact bloodstream form trypanosomes following release of the VSG. **Panel A** -energized cell displaying the GPI-PLC (magenta) and the nucleus and kinetoplast (blue). **Panel B** –de-energized cell displaying the GPI-PLC (magenta) and the nucleus and kinetoplast (blue).

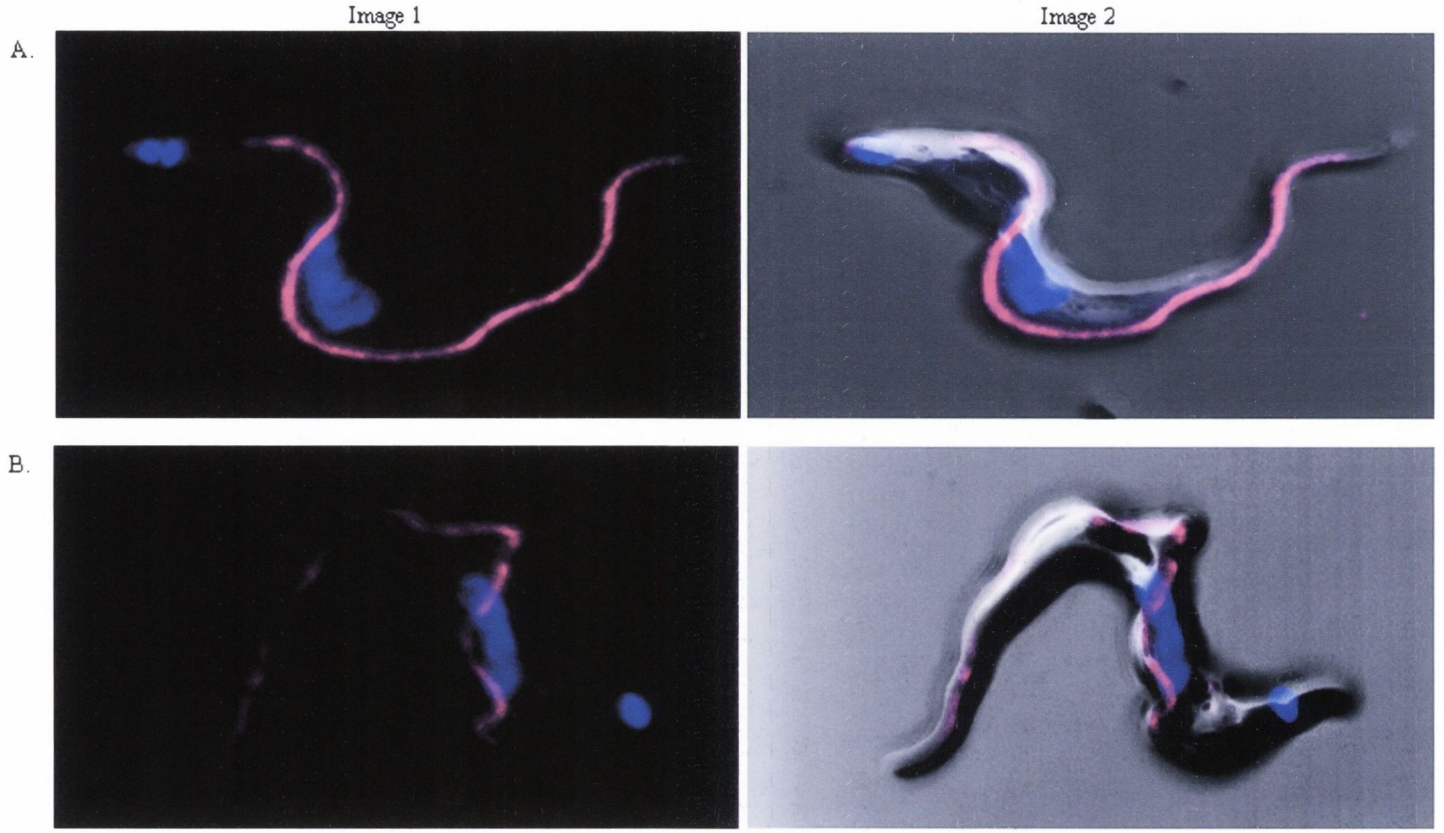

3.3. Discussion.

The results presented in this chapter provide a consistent picture of the localization of GPI-PLC in bloodstream forms of *T. brucei*. The enzyme is found on the outer surface of the cell body in the flagellar membrane. This result is in stark contrast to what other researchers have found in the past. Firstly in 1987, it was reported by workers that GPI-PLC activity was found within or enclosed by membranes of the flagellar pocket as well as in the Golgi fraction, primarily due to its co-localization with acid phosphatase, an enzyme found in the flagellar pocket, lysosomes, and in the Golgi apparatus of trypanosomes (Grab *et al.*, 1987). These results were not confirmed when in 1989 another group reported that the GPI-PLC was not associated with the inner or outer face of the plasma membrane including the flagellar pocket region. They did however explain how the other group found the enzyme in the flagellar pocket (Bolow *et al.*, 1989). Essentially, the method used by the first group (Grab *et al*), sub-cellular fractionation, was criticized by Bulow *et al.* (1989) on the basis that this approach disrupts the parasites and, consequently may lead to fusion of the membrane containing GPI-PLC with the flagellar pocket membrane, thereby allowing for co-localization of acid phosphatase and GPI-PLC. Bulow *et al.* (1989), using immunofluoresence and immunoelectron microscopy reported that the GPI-PLC was associated preferentially with the cytoplasmic face of intracellular vesicles. This location separates the enzyme from its major substrate, the VSG and raised the question of how they might interact. The next group to report data on the localization of the GPI-PLC were investigating the differentiation process in bloodstream forms of *T. brucei*. They reported that the GPI-PLC is present on the extracellular side of the plasma membrane in intact short stumpy cells using a surface biotinylation assay (Gruszynski *et al.*, 2003). This location places the enzyme and its substrate on the same side of the plasma membrane, and according to this group the GPI-PLC has a role in releasing the VSG during differentiation of bloodstream forms to procyclic forms. This group were, however, unable to detect the GPI-PLC on the cell surface by immunofluoresence. The most recent account of GPI-PLC localization in bloodstream forms of *T. brucei* has reported that the protein is translocated from glycosomes to the endoplasmic reticulum and that this translocation is important for the cleavage of GPI's (Subramanya and Mensa-Wilmot, 2006)

The results in this chapter provide evidence that the GPI-PLC in bloodstream forms of *T. brucei* has an extracellular localization. At no point throughout this study was the GPI-PLC found in the flagellar pocket, Golgi apparatus, on the cytoplasmic face of intracellular vesicles, in glycosomes or in the ER. By means of immunofluoresence

studies the GPI-PLC was found on the outer surface of the plasma membrane together with the VSG and the ISG-70, both of which are extracellularly disposed proteins. The fact that a detergent is required to access tubulin, a marker adjacent to the inner surface of the plasma membrane, and is not required to access the GPI-PLC indicates that the GPI-PLC is not located inside the permeability barrier of the plasma membrane. Furthermore, the GPI-PLC is shielded by the VSG because the distribution of the GPI-PLC was only clearly present on those trypanosomes that were fixed at 0°C and not 37°C. This phenomenon can be explained by the motion of the VSG molecules in the plane of the plasma membrane at different temperatures (Fig 3.4). When trypanosomes are incubated at 37°C the VSG molecules are in constant motion within the membrane. If a solution of paraformaldehyde fixative, also at 37°C is added to these trypanosomes, the VSG molecules will cross-link in an even distribution forming a lattice of cross-linked VSG over the entire surface of the cell. This lattice forms a barrier to underlying and interdigitated antigens below the surface of the VSG, thereby making it difficult for antibodies to approach antigens located in this region. This barrier is reasoned to account for failure to observe the GPI-PLC in trypanosomes fixed at 37°C whether or not detergent was present. When trypanosomes are incubated at 0°C there is a decrease in the motion of the VSG molecules within the plane of the membrane and they become more or less stationary and somewhat condensed in their lateral distribution. If a solution of paraformadehyde fixative, also at 0°C is added to these cells, the fixative will cross-link VSG molecules to adjacent VSG molecules within the membrane but not across the top of underlying proteins, which they cannot reach at 0°C due to their decreased thermal flexing and motion. In this situation gaps would be present in the lattice where the VSG molecules are too far apart to cross-link (Fig 3.4) without the flexing and moving that can occur at 37°C. Although the ISG-70 is also shielded by the VSG, IgG anti-ISG-70 appears to have access to its antigen under all conditions of fixation. This observation can be explained by the fact that ISG-70 has a molecular weight of 70,000 (Jackson *et al.*, 1993) and is larger than the GPI-PLC (Mr 39,000). Therefore, ISG-70 may extend upwards away from the lipid bilayer and into the external phase a greater distance than the GPI-PLC. Consequently, the VSG molecules may not shield the ISG-70 as well as it shields the GPI-PLC and, as a result, the anti-ISG-70 antibody may detect its antigen with more ease than the anti-GPI-PLC detects its antigen. Even though the GPI-PLC and the ISG-70 are both exposed to the exterior and at least partially hidden by the VSG, ISG-70 has a patchy distribution over the entire outer leaflet of the plasma

membrane (Jackson *et al.*, 1993) while the GPI-PLC is located in the flagellar membrane adjacent to the cell body and parallel to but separate from the FAZ.

We have shown that the GPI-PLC does not change its location in the flagellar membrane when intact long slender trypanosomes release their VSG upon de-energization. This result suggests that the VSG travels to the GPI-PLC in order to be released and that the GPI-PLC remains stationary and does not travel to the VSG. This phenomena may also explain the release of the VSG from intact bloodstream forms during treatment with Ca^{2+} and the calcium ionophore, A23187 (Bowles and Voorheis, 1982, Voorheis, 1982 #63). In this report it was shown that Ca^{2+} and a calcium ionophore together initiate the release of ~ 80 % of the VSG from the plasma membrane within 10 minutes, without simultaneous rupture of the cell and suggests that the GPI-PLC may require activation *in vivo* where cells are in a normal, viable fully energized state.

It is frequently stated that the GPI-PLC releases the VSG from bloodstream form trypanosomes by hydrolyzing the GPI anchor of the VSG and releasing a soluble form (sVSG) of the VSG, which retains the GPI core glycan. However, it would be more correct to state that rather than hydrolysis, involving nucleophilic attack of water or hydrolysis on the phosphorus in the phosphate attached to the 1-position of the inositol, release occurs by "inositolysis" because nucleophilic attack on the phosphorus of this phosphate occurs from the 2-hydroxyl of the inositol to produce an inositol 1,2 phosphodiester, generating a strained trans-fused double ring system (Ferguson and Cross, 1984). GPI-anchor cleavage occurs in three situations during the bloodstream form stage of the life cycle: firstly, upon cell lysis (Cardoso de Almeida and Turner, 1983) secondly, in normal growth of long slender trypanosomes where VSG is slowly shed into the medium with a half-life of ~32 hr (Seyfang *et al.*, 1990 & Bulow, 1989 #237) and third during differentiation of bloodstream stage trypanosomes (Rolin *et al.*, 1998). The release of the VSG or the GPI-anchored peptide after proteolysis in these instances can be more readily visualized if the enzyme and its substrate on the same side of the bilayer in the same membrane.

The flagellar membrane is part of the plasma membrane in *T. brucei* along with the pellicular membrane and the flagellar pocket membrane. All three domains are covered by the VSG. Consequently this newly recognized localization for the GPI-PLC places it on the same side of the plasma membrane as its major substrate, the VSG, thereby facilitating access of the enzyme to the GPI anchor. Several of the reports already published have described an internal location for the GPI-PLC; thereby presenting a topological barrier to

VSG release by GPI hydrolysis. However, if both enzyme and substrate are located in the same compartment and release is not constantly occurring, it is clear that the enzyme must be regulated. In this case, either activation of the enzyme *in vivo* by some mechanism would be required or some inhibitory mechanism must be inactivated to initiate release.

There are at least two types of proteins localised only to the flagellar membrane: a flagellar calcium-binding protein (FCaBP) in *T. cruzi* (Engman *et al.*, 1989) and one isoform of a glucose transporter in *Leishmania enrietti* (Piper *et al.*, 1995). The latter is a good example of differential targeting: isoform 1 (ISO1) is localised to the flagellar membrane, whereas isoform 2 (ISO2) is found on the pellicular membrane. The two proteins only differ by their cytosolic amino-terminal end. The fact that both isoforms are found in the flagellar pocket suggests that sorting occurs after they reach the plasma membrane. The flagellar FCaBP of *T. cruzi* appears to be localised to the flagellum by a different pathway than that used by ISO-1. The FCaBP associates with the flagellar membrane via its N-terminal myristate and palmitate moieties in a calcium-modulated, conformation-dependent manner (Godsel and Engman, 1999).

The means by which the GPI-PLC attaches to the membrane are unclear (Carrington *et al.*, 1998). The extracellular localization of the GPI-PLC is not due to classic secretion, because the enzyme does not have an N-terminal signal sequence or any other overtly hydrophobic domains (Hereld *et al.*, 1986). However, the GPI-PLC in *T. brucei* is post-translationally modified by thioacylation (Paturiaux-Hanocq *et al.*, 2000). This thioacylation involves a group of cysteine residues in the C-terminal region of the polypeptide. It was found that both palmitic and myristic acid were incorporated in metabolic labelling experiments with significantly more palmitate acid than myristate incorporated. It was found that the thioacylation of the GPI-PLC was not an absolute requirement for catalytic activity nor was it solely responsible for the hydrophobic behaviour of the protein. However, it was proposed that the thioacylation might have a regulatory role in modulating access of the GPI-PLC to the GPI anchor of the VSG. Could this thioacylation possibly be responsible for the flagellar membrane attachment of the GPI-PLC and its flagellar localization just as acylation of the FcaBP directs it to the flagellar membrane in *T. cruzi*? There is an emerging consensus that reversible thioacylation is involved in the functional regulation of several plasma membrane proteins and the processes mediated by them (Mumby, 1997 & Milligan, 1995 #242). In addition to mediating attachment to a membrane, it might also be that subsequent additional thioacylation at an additional site on the enzyme may produce the conformational change

required to bring the enzyme active site in contact with the position of the phosphodiester substrate *in vivo* when detergent is not present. Alternatively, selective cleavage of one of the thioesters may perform this role. It is interesting to note that Ca^{2+} has been reported to be involved in the regulation of some membrane proteins, acting at some point in the mechanism of their reversible thioacylation (Godsel and Engman, 1999).

4.1. Introduction.

The GPI-PLC was found to be located on the surface of both long-thin and short-stumpy bloodstream form trypanosomes as determined by immunofluorescent techniques (Chapter 3). In order to confirm these results and provide additional evidence as to its location, a second technique for locating the GPI-PLC was employed. Surface labelling of bloodstream form trypanosomes was performed in an attempt to corroborate the immunofluorescent results. Previously, the GPI-PLC was reported to be located on the surface of intact short stumpy trypanosomes by means of a surface biotinylation assay (Gruszynski *et al.*, 2003). This same group attempted to verify the presence of the GPI-PLC on the cell surface by immunofluorescence techniques. However, these attempts were unsuccessful.

In the experiments described here sulfo-NHS-biotin, a membrane impermeable biotinylating reagent was employed to label the surface proteins of bloodstream form trypanosomes. *N* -Hydroxysulfosuccinimide (sulfo-NHS) esters of biotin are the most popular type of biotinylation reagent. NHS-activated biotins react efficiently with any primary amine that they contact in pH 7-9 buffers to form stable amide bonds. Proteins, including antibodies, generally have several available primary amines *e.g.* the ε-amino group in the side chain of each lysine residue and the α-amino group at the N-terminus of each polypeptide. The sulfo-NHS ester reagents are water soluble, enabling reactions to be performed in the absence of organic solvents such as DMSO or DMF. Because these molecules dissolve readily in polar solutions and carry a negative charge on the sulfonate group, they cannot penetrate the cell membrane. As long as the cell remains intact, only primary amines exposed on the surface will be biotinylated with sulfo-NHS-biotin reagents. GPI-PLC contains 14 lysine residues, sufficient primary amines to react extensively with sulfo-NHS-biotin if they are exposed on the outer surface of trypanosomes. Lactoperoxidase-catalyzed radio-iodination was another technique employed to determine the location of the GPI-PLC. This technique has been used successfully in the past to localize proteins on the cell surface of bloodstream form trypanosomes (Jackson *et al.*, 1993). ^{125}I provides robust and sensitive labelling of those cell surface proteins that contain tyrosine and histidine residues. The GPI-PLC contains 12 tyrosine residues and 12 histidine residues. Consequently, labeling the surface of trypanosomes with ^{125}I should permit detection of the GPI-PLC with ease, if these residues of the protein are exposed externally.

In this chapter bloodstream form trypanosomes, both monomorphic (MITat 1.2) and pleomorphic (ILTat 1.1) were surface labelled with sulfo-NHS-Biotin and Iodine-125. In addition, purified recombinant GPI-PLC was labeled with NHS-Biotin at pH 8.5 and pH 9.3, under conditions of protein denaturation and after transfer onto PVDF membrane. However, the biotinylation assays failed to confirm the surface location of the GPI-PLC but did lead to the discovery of a new property of the GPI-PLC, *i.e.* neither recombinant GPI-PLC or that expressed naturally in bloodstream forms could react with sulfo-NHS-biotin, whether native or in the presence of denaturing agents.

4.2. Results.

4.2.1. Immunoprecipitation of proteins from surface biotinylated trypanosomes.

Bloodstream forms of *T. brucei* were surface biotinylated and proteins were specifically immunoprecipitated using antibodies to proteins known to be located at the inner and outer surfaces of the plasma membrane. ISG-70 was immunoprecipitated from detergent lysates with anti-ISG-70 antibody as a control for the outer surface of the plasma membrane and tubulin was immunoprecipitated from detergent lysates with anti-α-tubulin antibody as a control for proteins located on the cytoplasmic side of the inner membrane of trypanosomes. In both cases the immunoprecipitates were subjected to SDS-PAGE, transferred to nylon membranes and probed with specific IgG antibodies and detected with peroxidase-conjugated secondary antibodies.

4.2.1. (a) Investigating the use of different lysis buffers during the preparation of biotinylated cell lysates and their effect on the immunoprecipitation of GPI-PLC from bloodstream forms of T. brucei.

Bloodstream forms of *T. brucei* were biotinylated with sulfo-NHS-biotin as described in the Methods section (2.1.21). Lysates were then made from these labelled cells using a variety of lysis buffers. The composition of these buffers is shown in the legend of Fig 4.1. It was found that when lysis buffer I (tris/NP40/CHAPS) and lysis buffer III (tris/triton-X100) were used to make cell lysates from biotinylated trypanosomes the GPI-PLC was successfully immunoprecipitated from the cells (Fig 4.1, A1, lane 1 & B1, lane 1). Furthermore, lysis buffer I (tris/NP40/CHAPS) allowed for the maximum

immunoprecipitation of GPI-PLC (Fig 4.1, A1, lane 1). When lysis buffer II (HEPES/Tween) and buffer IV (TES/CHAPS) were used to make cell lysates the GPI-PLC was not immunoprecipitated with anti-GPI-PLC IgG (Fig 4.1, A1, lane 2 & B1, lane 2). Consequently, Buffer I (tris/NP40/CHAPS) was used in the preparation of all lysates in subsequent experiments.

Following immunoprecipitation of proteins from surface-biotinylated cell lysates, samples were separated by SDS-PAGE and transferred to nitrocellulose membranes. The membranes were probed with Streptavidin-HRP in order to detect the proteins that were biotinylated on the surface of trypanosomes. The results show that the GPI-PLC does not become biotinylated indicating either that it is not located on the surface of the trypanosome (Fig 4.1, A2, lane 1 & 3 & B2, lane 1 & 3) or that all of the lysines in the GPI-PLC are unavailable for reaction with sulfo-NHS-biotin. However, the results of the immunofluorescent work strongly points toward an outer surface localisation for the GPI-PLC (Chapter 3). The proteins that do become biotinylated and therefore are present on the surface of bloodstream form trypanosomes are shown as protein bands between the 45 and 66 kDa markers (Fig 4.1, A2 & B2, lanes 2 & 4). These bands most likely represent ISG-70 when anti-ISG-70 is employed for the immunoprecipitation and VSG as the single major contaminant when either anti-ISG-70 or anti-GPI-PLC are used for Immunoprecipitations. VSG appears as a contaminant because of its high copy number (1.12×10^7 copies / cell) compared to ISG-70 (5.1×10^4 copies / cell) and the GPI-PLC (3×10^4 copies / cell).

4.2.1. (b) Surface biotinylation of proteins in bloodstream forms of T. brucei.

To explore further the apparent extracellular location of the GPI-PLC, surface biotinylation of proteins was performed with MITat 1.2 trypanosomes grown in rats and isolated by the procedure of Lanham (1968). Trypanosomes remained fully viable throughout the biotinylation procedure as assessed by microscopic observation of their motility, and the inner membrane marker, α-tubulin, was used as a control for cell integrity. This tubulin marker of the cellular interior was shown to be specifically immunoprecipitated by anti-α-tubulin antibody (Fig 4.2, B1, lane 3). However, the tubulin did not become biotinylated (Fig 4.2, B2, lane 3) indicating that the integrity of the plasma membrane was maintained throughout the assay. ISG-70 was used as a positive control for surface biotinylation of proteins, and a robust signal was evident for

Fig 4.1. The effect of different lysis buffers on the immunoprecipitation of GPI-PLC from bloodstream forms of *T. brucei*. Bloodstream populations of MITat 1.2 (5 x 10^7 cells/ml) were surface biotinylated using Sulfo-NHS-LC-biotin (Section 2.1.21). Cell lysates (1 x 10^9 cells/ml) were made using four different lysis buffers (I, II, III or IV) and subjected to specific immunoprecipitation with anti-GPI-PLC (Section 2.1.23). Immunoprecipitates were separated by SDS-PAGE, electrotransferred to PVDF membrane, blotted with the corresponding antibody (1) or HRP-Streptavidin (2) and developed by chemiluminesence.

Lysis Buffer I:	50 mM Tris, pH 7.5 containing 0.1% NP40, 0.5% CHAPS, 150 mM NaCl.
Lysis Buffer II:	50 mM Hepes, pH 7.5 containing 150 mM NaCl, 1 mM EDTA, 2.5 mM EGTA, 10 % glycerol, 0.1% Tween.
Lysis Buffer III:	50 mM Tris, pH 7.5 containing 250 mM NaCl, 5 mM EDTA, 0.1% Tx-100.
Lysis Buffer IV:	50 mM TES, pH 7.5 containing 150 mM NaCl & 0.1% CHAPS

A1: (Probed with anti-GPI-PLC IgG (1/1000 dilution of stock, followed by 1/30,000 dilution of HRP-anti-rabbit IgG).
Lane 1: Immunoprecipitation of GPI-PLC (equivalent to 2 x 10^8 cells) from cell lysates using buffer I as lysis buffer.
Lane 2: Supernatant (2 x 10^8 cell equivalents) following immunoprecipitation with anti-GPI-PLC IgG using buffer I as lysis buffer.
Lane 3: Immunoprecipitation of GPI-PLC (equivalent to 2 x 10^8 cells) from cell lysates using buffer II as the lysis buffer.
Lane 4: Supernatant (2 x 10^8 cell equivalents) following immunoprecipitation with anti-GPI-PLC IgG using buffer II as lysis buffer.

A2:
Blot from A1 above was run in duplicate and this blot (A2) was probed with streptavidin-HRP (1/30,000 dilution, 1 hr, RT). The identity of the lanes is the same as in A1.

Panel B
B1: (Probed with anti-GPI-PLC IgG (1/1000 dilution of stock, followed by 1/30,000 dilution of HRP-anti-rabbit IgG).
Lane 1: Immunoprecipitation of GPI-PLC (equivalent to 2 x 10^8 cells) from cell lysates using buffer III as lysis buffer.
Lane 2: Supernatant (2 x 10^8 cell equivalents) following immunoprecipitation with anti-GPI-PLC IgG using buffer III as lysis buffer.
Lane 3: Immunoprecipitation of GPI-PLC (equivalent to 2 x 10^8 cells) from cell lysates using buffer IV as lysis buffer.
Lane 4: Supernatant (2 x 10^8 cell equivalents) following immunoprecipitation with anti-GPI-PLC IgG using buffer IV as lysis buffer.

B2:
Blot from B1 above was run in duplicate and this blot (B2) was probed with streptavidin-HRP (1/30,000 dilution, 1 hr, RT). The layout of the lanes is the same as in B1.

Fig 4.1. The effect of different lysis buffers on the immunoprecipitation of GPI-PLC from bloodstream forms of *T. brucei*.

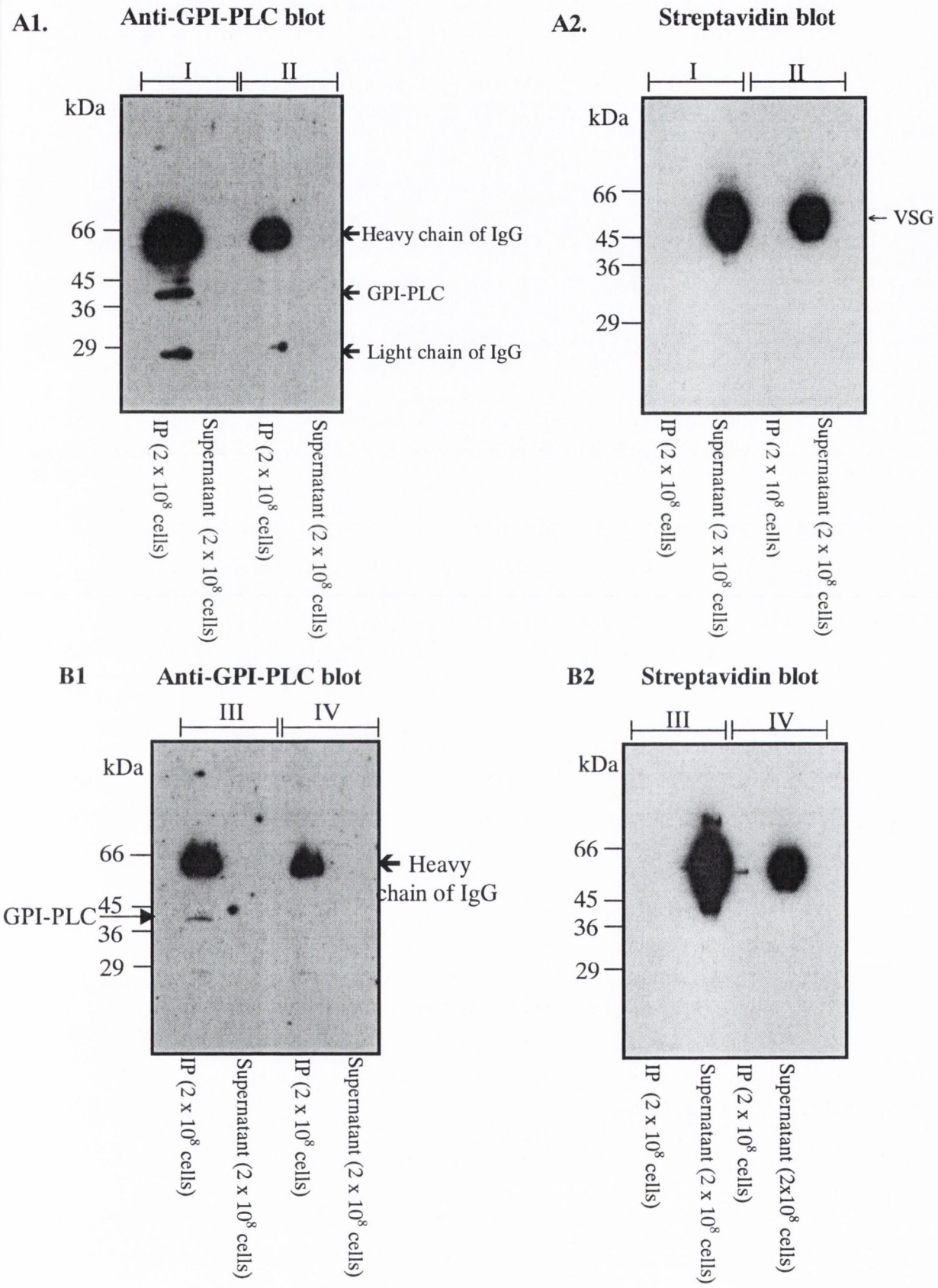

Figure 4.2. Surface biotinylation of proteins in bloodstream forms of MITat 1.2 trypanosomes.
Bloodstream populations of MITat 1.2 (5 x 10^7 cells/ml) were surface biotinylated using Sulfo-NHS-LC-biotin (Section 2.1.21). Cell lysates (1 x 10^9 cells/ml) were subjected to specific immunoprecipitation with anti-GPI-PLC (G), anti-tubulin (T) or anti-ISG70 (I) antibodies (Section 2.1.23). Immunoprecipitates were separated by SDS-PAGE, electrotransferred to PVDF membrane, blotted with the corresponding antibody (1) or HRP-Streptavidin (2) and developed by chemiluminesence. The predicted electrophoretic mobility of each protein is indicated on the right with the corresponding abbreviation.

Panel A.
A1: (Probed with anti-GPI-PLC IgG (1/1000 dilution of stock, followed by 1/30,000 dilution of HRP-PA from calbiochem).
Lane 1: GPI-PLC $^-$ mutant trypanosome cell lysates (2 x 10^7 cells)
Lane 2: Immunoprecipitated protein (equivalent to 2 x 10^8 cells) from GPI-PLC $^-$ mutant trypanosomes using anti-GPI-PLC IgG.
Lane 3: Supernatant (2 x 10^8 cell equivalents) following immunoprecipitation by anti-GPI-PLC IgG.
Lane 4: Wild type trypanosome cell lysates (2 x 10^7 cells)
Lane 5: Immunoprecipitated protein (equivalent to 2 x 10^8 cells) from wild type trypanosomes using anti-GPI-PLC IgG.
Lane 6: Supernatant (2 x 10^8 cell equivalents) following immunoprecipitation with anti-GPI-PLC IgG.

A2:
Blot from A1 above was run in duplicate and this blot (A2) was probed with streptavidin-HRP (1/30,000 dilution, 1 hr, RT). The identity of the lanes is the same as in A1.

Panel B.
B1: (Probed with rat anti-alpha tubulin IgG (1/1000 dilution of stock from Abcam, followed by 1/2,000 dilution of HRP-anti-rat IgG from stock).
Lane 1: Wild type trypanosome cell lysates (2 x 10^7 cells)
Lane 2: Supernatant (2 x 10^8 cell equivalents) following immunoprecipitation by anti-tubulin IgG.
Lane 3: Immunoprecipitated protein (equivalent to 2 x 10^8 cells) from wild type trypanosomes using anti-tubulin IgG.

B2:
Blot from B1 above was run in duplicate and this blot (B2) was probed with streptavidin-HRP (1/30,000 dilution, 1 hr, RT). The identity of the lanes is the same as in B1.

Panel C.
C1: (Probed with rabbit anti-ISG70 IgG (1/1000 dilution of stock, followed by 1/30,000 dilution of HRP-PA from Calbiochem).
Lane 1: Wild type trypanosome cell lysates (2 x 10^7 cells)
Lane 2: Supernatant (2 x 10^8 cell equivalents)following immunoprecipitation by anti-ISG70 IgG.
Lane 3: Immunoprecipitated protein (equivalent to 2 x 10^8 cells) from wild type trypanosomes using anti-ISG70 IgG.

C2:
Blot from C1 above was run in duplicate and this blot (C2) was probed with streptavidin-HRP (1/30,000 dilution, 1 hr, RT). The layout of the lanes is the same as in C1.

Figure 4.2. Surface biotinylation of proteins in bloodstream forms of MITat 1.2 trypanosomes.

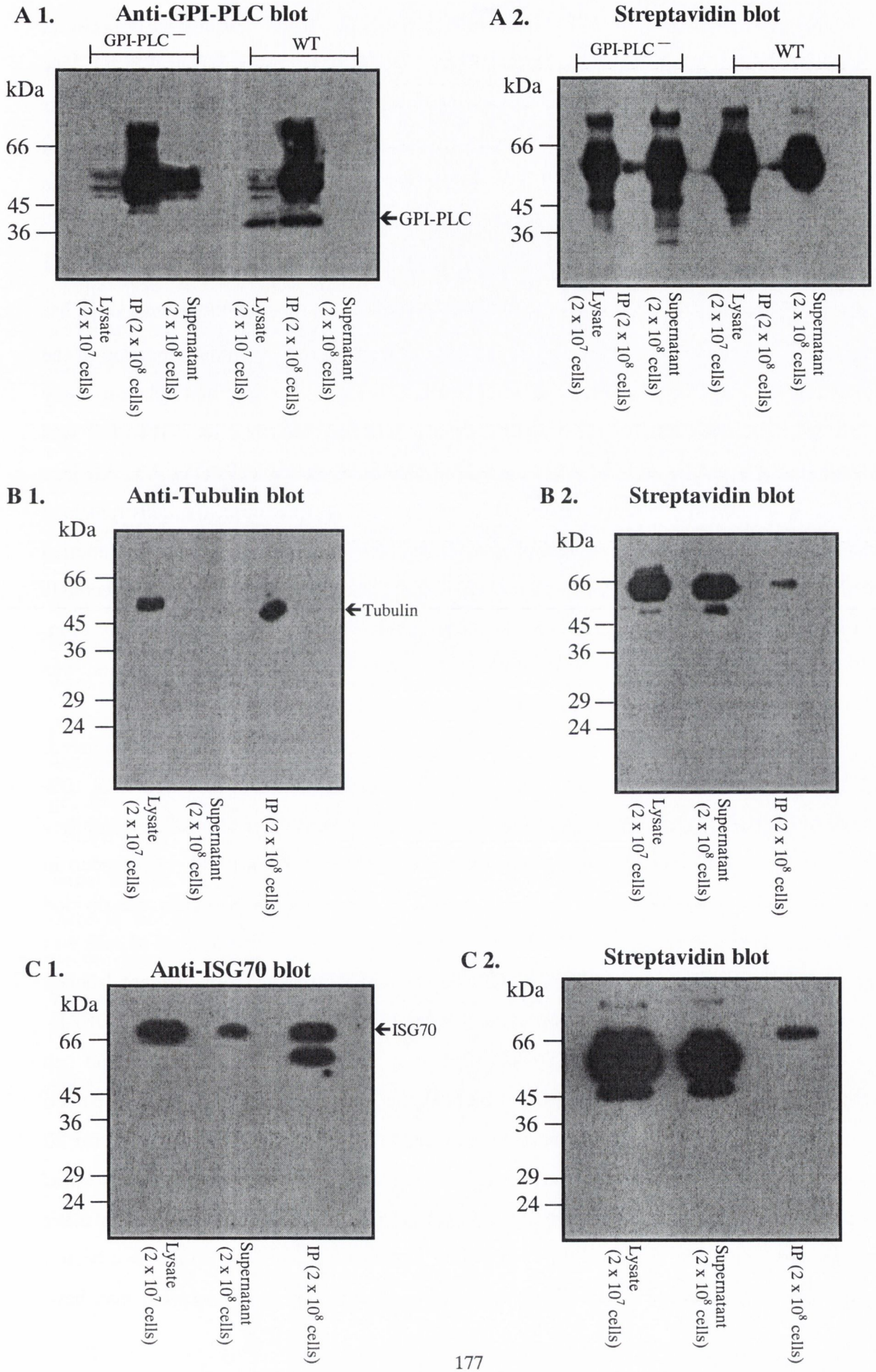

the immunoprecipitated ISG-70 (Fig 4.2, C1 & C2 lane 3). The GPI-PLC was specifically immunoprecipitated by anti-GPI-PLC antibody (Fig 4.2, A1, lane 5) from wild type parent strain trypanosomes but not from the GPI-PLC $^{-}$ mutant trypanosomes (Fig 4.2, A1, lane 2). However, the GPI-PLC did not become biotinylated (Fig 4.2, A2, lane 5). The blots also detected other surface labelled proteins that have molecular weights (45 – 66 kDa) higher than that of the GPI-PLC. These correspond to the VSG and ISG-70 in all three cases (Fig 4.2, A2, lanes 1, 3, 4 & 6, B2 & C2, lanes 1 & 2).

This same experiment was conducted using pleomorphic populations of ILTat 1.1 trypanosomes. These cells were predominantly (>80%) stumpy in morphology. It has previously been reported that stumpy populations of trypanosomes contain a portion of the total cellular pool of GPI-PLC on their surface using a surface biotinylation assay (Gruszynski *et al.*, 2003). The results shown here indicate that the GPI-PLC was immunoprecipitated by anti-GPI-PLC antibody from these stumpy cells (Fig 4.3, A1, lane 2) but did not become biotinylated (Fig 4.3, A2, lane 2). Furthermore, the cells remained viable and intact during the process as assessed by their motility and because the internal marker, tubulin, was not biotinylated (Fig 4.3, B2, lane 2) but was effectively immunoprecipitated (Fig 4.3, B1, lane 2). The positive control for surface biotinylation, ISG-70, was immunoprecipitated by anti-ISG-70 antibody (Fig 4.3, C1, lane 2) and was also found to be biotinylated as expected (Fig 4.3, C2, lane 2).

Surface biotinylation of trypanosomes cultured *in vitro* was also investigated. MITat 1.2 cells were grown at 37°C in HMI-9 culture medium supplemented with 10% foetal calf serum. When the trypanosomes reached a cell density of 1 x 10^6 cells/ml they were removed from the medium by centrifugation (1500 ***g*** x 5 min) and resuspended in TSB buffer (for composition see Table 2.1.), pH 8.0. The suspension of cells was divided into three separate tubes, each tube with an equal number of cells. The first set of cells was directly biotinylated with sulfo-NHS-biotin. In this procedure the biotin reagent labelled all cells and any cell debris that was present. The second set was passed through a DEAE-52 column, pre-equilibrated in TSB buffer, in order to remove any dead cells and cell debris and then surface labelled with the biotinylating reagent. The third set was passed through the DEAE-52 column and subsequently energized by stirring gently at 37°C for 20 minutes in TSB buffer, pH 8 and then surface biotinylated. This experiment was performed to investigate whether or not the GPI-PLC found on the surface of trypanosomes by other investigators (Gruszynski *et al.*, 2003) following biotinylation reactions could have been a result of the presence of dead cells in the mixture or cells where the location may have

been different due to de-energization during isolation of the trypanosomes from the culture medium and preparation for the experiment or even due to cell lysis. The GPI-PLC was immunoprecipitated with anti-GPI-PLC antibody effectively (Fig 4.4 Panel A, lane 1,3 & 5) in all cases but did not become biotinylated under any of the three conditions (Fig 4.4 Panel B, lane 1, 3 & 5). It was clear from these experiments that the GPI-PLC did not become biotinylated in dead/damaged cells or in cells that were viable following the DEAE-52 purification and a short energization step. It is also evident that the culturing of trypanosomes in HMI-9 medium did not expose the GPI-PLC to reaction with sulfo-NHS-biotin. The results presented so far for the surface labelling of trypanosomes with biotin pose two important questions: Firstly, do these results imply that the GPI-PLC is not a surface protein? Secondly, is the GPI-PLC actually reacting with the biotin reagent?

4.2.2. Surface biotinylation of proteins in plasma membranes prepared from bloodstream forms of T. brucei.

An experiment was conducted to test whether the GPI-PLC could be labelled with more ease if the region in the cell where it is located is isolated and then subjected to reaction with sulfo-NHS-biotin. Plasma membranes containing the attached cytoskeleton were prepared according to the method of Voorheis (1978) (Section 2.1.28). The purified plasma membrane fraction was surface biotinylated (Section 2.1.21) and lysates were made using lysis buffer I (see Fig 4.1). The biotinylated lysates were separated on a 15 % SDS gel and subsequently transferred to PVDF membrane. The membrane was probed with anti-GPI-PLC (Fig 4.5, lane 1) and HRP-streptavidin (Fig 4.5, lane 2). There is a strong signal for the GPI-PLC protein itself (Fig 4.5, lane 1) when probed with anti-GPI-PLC, but there is no corresponding band detected when the same sample is probed with HRP-streptavidin (Fig 4.5, lane 2). The easy detection of other proteins at higher molecular weight that became biotinylated under these conditions validates the efficacy of both the biotinylating reagent and the HRP-streptavidin detection system. One can conclude from this data that the GPI-PLC is present but is not reacting with the biotinylating reagent.

Figure 4.3. Surface biotinylation of proteins in pleomorphic forms of ILTat 1.1 trypanosomes.
Pleomorphic populations of ILTat 1.1 (5 x 10^7 cells/ml) were surface biotinylated using Sulfo-NHS-LC-biotin (Section 2.1.21). Cell lysates (1 x 10^9 cells/ml) were subjected to specific immunoprecipitation with anti-ISG70 (I), anti-tubulin (T) or anti-GPI-PLC (G) antibodies (Section 2.1.23). Immunoprecipitates were separated by SDS-PAGE, electrotransferred to PVDF membrane, blotted with the corresponding antibody (1) or HRP-Streptavidin (2) and developed by chemiluminesence. The predicted electrophoretic mobility of each protein is indicated on the right with the corresponding abbreviation. Each lane contains 2 x 10^8 cell equivalents.

Panel A. (Probed with anti-GPI-PLC IgG (1/1000 dilution of stock, followed by 1/30,000 dilution of HRP-PA from Calbiochem).
A1:
Lane 1: Cell lysates (2 x 10^7 cells)
Lane 2: Immunoprecipitated protein (equivalent to 2 x 10^8 cells) from ILTat 1.1 trypanosomes using anti-GPI-PLC IgG.
Lane 3: Supernatant (2 x 10^8 cell equivalents) following immunoprecipitation by anti-GPI-PLC IgG.

A2:
Blot from A1 above was run in duplicate and this blot (A2) was probed with streptavidin-HRP (1/30,000 dilution, 1 hr, RT). The layout of the lanes is the same as in A1.

Panel B.
B1: (Probed with rat anti-alpha tubulin IgG (1/1000 dilution of stock from Abcam, followed by 1/2,000 dilution of HRP-anti-rat IgG from stock).
Lane 1: Cell Lysates (2 x 10^7 cells)
Lane 2: Immunoprecipitated protein (equivalent to 2 x 10^8 cells) from ILTat 1.1 trypanosomes.
Lane 3: Supernatant (2 x 10^8 cell equivalents) following immunoprecipitation by anti-tubulin IgG.

B2:
Blot from B1 above was run in duplicate and this blot (B2) was probed with streptavidin-HRP (1/30,000 dilution, 1 hr, RT). The identity of the lanes is the same as in B1.

Panel C.
C1: (Probed with anti-ISG70 IgG (1/1000 dilution of stock, followed by 1/30,000 dilution of HRP-PA from Calbiochem).
Lane 1: Cell Lysates (2 x 10^7 cells)
Lane 2: Immunoprecipitated protein (equivalent to 2 x 10^8 cells) from wild type trypanosomes using anti-ISG70 antibody.
Lane 3: Supernatant (2 x 10^8 cell equivalents) following immunoprecipitation by anti-ISG70 antibody.

C2:
Blot from C1 above was run in duplicate and this blot (C2) was probed with streptavidin-HRP (1/30,000 dilution, 1 hr, RT). The layout of the lanes is the same as in C1.

Figure 4.3. Surface biotinylation of proteins in pleomorphic forms of ILTat 1.1 trypanosomes.

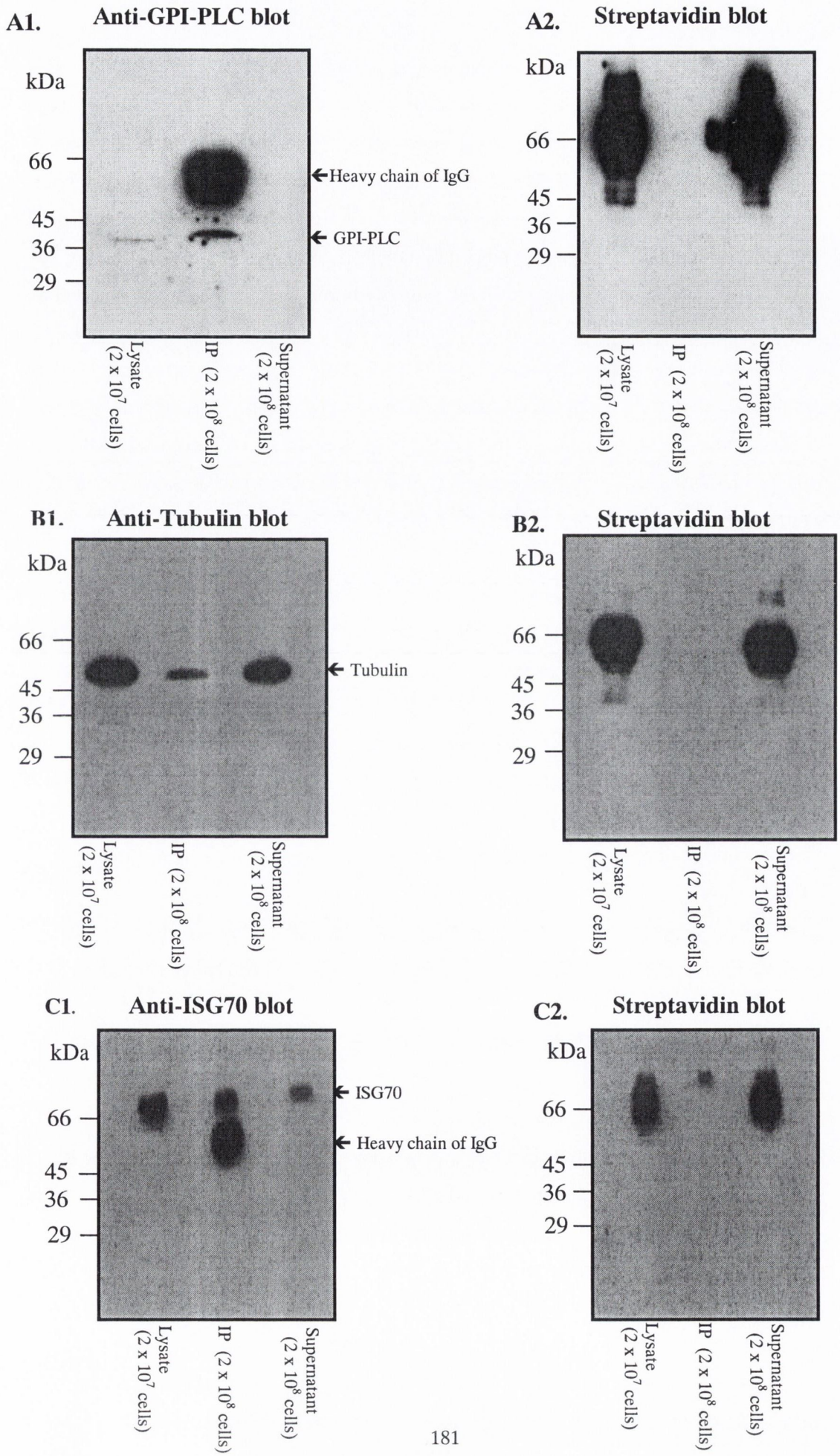

Figure 4.4. Surface biotinylation of proteins in cell cultured forms of MITat 1.2 trypanosomes.

MITat 1.2 trypanosomes grown in cell culture media (1 x 10^6 cells/ml) were washed into TSB buffer (Table 2.1) and divided into three tubes. Trypanosomes were either directly surface biotinylated using Sulfo-NHS-LC-biotin (Section 2.1.21), lanes 1 +2, or purified on a DEAE-52 column pre-equilibrated with TSB and then surface biotinylated, lanes 3 + 4 or following the DEAE-52 elution energised by incubating at 37°C for 20 min and subsequently surface biotinylated, lanes 5 + 6. Cell lysates (1 x 10^8 cells/ml) were made with the surface biotinylated cells and these lysates were subjected to specific immunoprecipitation with anti-GPI-PLC antibodies (Section 2.1.23). Immunoprecipitates were separated by SDS-PAGE, electrotransferred to PVDF membrane, blotted with the corresponding antibody (1) or HRP-Streptavidin (2) and developed by chemiluminesence. The predicted electrophoretic mobility of GPI-PLC is indicated on the right with the corresponding abbreviation. Each lane contains 2 x 10^8 cell equivalents.

Panel A. (Probed with anti-GPI-PLC IgG (1/1000 dilution of stock, followed by 1/30,000 dilution of HRP-PA from Calbiochem).

Lane 1: Immunoprecipitated protein (equivalent to 2 x 10^8 cells) from cultured trypanosomes biotinylated directly following removal from culture media using anti-GPI-PLC IgG.
Lane 2: Supernatant (2 x 10^8 cell equivalents) following immunoprecipitation with anti-GPI-PLC IgG.
Lane 3: Immunoprecipitated protein (equivalent to 2 x 10^8 cells) from cultured trypanosomes purified on a DEAE-52 column prior to surface biotinylation using anti-GPI-PLC IgG.
Lane 4: Supernatant (2 x 10^8 cell equivalents) following immunoprecipitation with anti-GPI-PLC IgG.
Lane 5: Immunoprecipitated protein (equivalent to 2 x 10^8 cells) from cultured trypanosomes purified on a DEAE-52 column and subsequently energized at 37°C for 20 min prior to surface biotinylation using anti-GPI-PLC IgG.
Lane 6: Supernatant (2 x 10^8 cell equivalents) following immunoprecipitation with anti-GPI-PLC IgG.

Panel B.

Blot from A above was run in duplicate and this blot (B) was probed with streptavidin-HRP (1/30,000 dilution, 1 hr, RT). The identity of the lanes is the same as in A.

Figure 4.4. Surface biotinylation of proteins in cell cultured forms of MITat 1.2 trypanosomes.

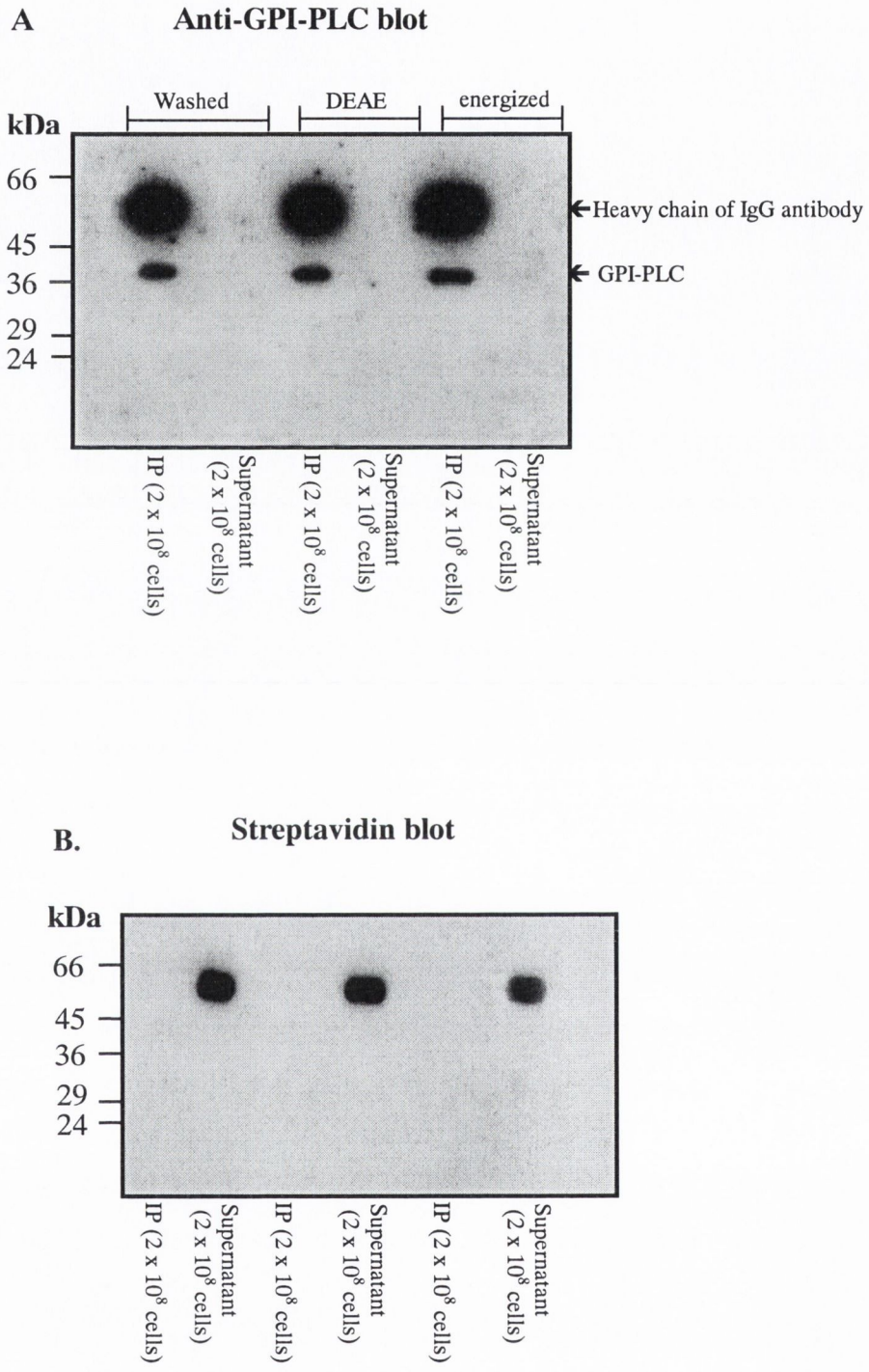

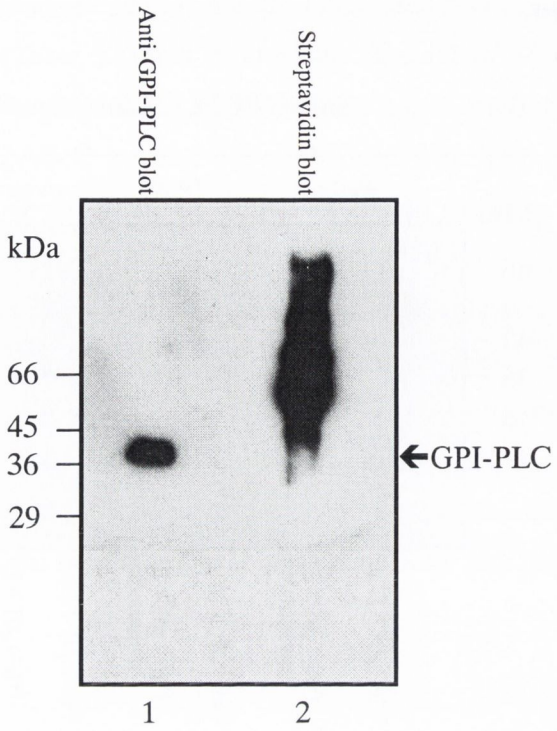

Figure 4.5. Biotinylation of plasma membranes from bloodstream forms of T. brucei.

Purified plasma membranes, equivalent to 2 x 10^8 cells (see Methods Section 2.1.28) were biotinylated with Sulfo-NHS-LC-Biotin (Section 2.1.21). Lysates (equivalent to 2 x 10^8 cells) were separated by SDS-PAGE, electrotransferred to PVDF membrane, blotted with anti-GPI-PLC antibody (lane 1) or HRP-Streptavidin (lane 2) and developed by chemiluminesence. Each lane contains 2 x 10^8 cell equivalents.

4.2.3. Biotinylation of purified recombinant GPI-PLC.

To test whether the GPI-PLC itself could react with the biotinylating reagent, purified recombinant GPI-PLC was labelled with NHS-biotin. Recombinant GPI-PLC was purified as described in the Methods chapter (Section 2.1.29) and labelled with NHS-biotin. The purified GPI-PLC (200 μg) was first exchanged into $NaHCO_3$, (50 mM, pH 8.5) for the labelling reaction. A stock solution of NHS-biotin (10 mM) was freshly prepared in dimethylformamide. NHS-biotin was then added to the GPI-PLC to give a 20-fold molar excess of NHS-biotin to protein. The reaction was conducted at room temperature for 30 min, after which any unbound NHS-biotin was inactivated by the addition of glycine (5 mM, final concentration). The whole sample was then subjected to immunoprecipitation with anti-GPI-PLC antibody. The immunoprecipitates were separated by SDS-PAGE, electrotransferred to PVDF membrane and blotted with anti-GPI-PLC antibody (Fig 4.6, A) or HRP-Streptavidin (Fig 4.6, B). The results of this experiment confirmed the previous conclusion; the GPI-PLC does not react with sulfo-NHS- biotin (Fig 4.6, B). There is a protein present – centred at ~ 66 kDa, in the purified recombinant protein mixture that does react with the NHS-biotin (Fig 4.6, B) but not with anti-GPI-PLC (Fig 4.6, A). This band was present following the purification of the GPI-PLC and could not be removed (Fig 2.9) with the techniques employed at this stage of my studies.

4.2.4. Biotinylation of recombinant GPI-PLC following transfer from SDS-PAGE to PVDF membrane.

The possibility that all the lysine residues in the GPI-PLC are hidden due to the folding of the protein was considered. Consequently, the GPI-PLC was separated on an SDS gel and subsequently transferred to PVDF membrane. Purified VSG was used as a positive control in this case. The PVDF membrane itself was then subjected to the biotinylation reaction and after washing probed with HRP-Streptavidin (LaRochelle and Froehner, 1986). The VSG was readily biotinylated (Fig 4.7, B lane 1) indicating that the labelling reaction was successful. However, the GPI-PLC was not labelled (Fig 4.7, B lane 2). A corresponding SDS gel stained with Coomassie blue showed the presence of both proteins (Fig 4.7, A, lane 2 & 3).

Figure 4.6. Immunoprecipitation of biotinylated recombinant GPI-PLC-His tagged.

Purified recombinant GPI-PLC (200 μg / 600 μl; section 2.1.29) was exchanged into $NaHCO_3$, pH 8.5 for the biotinylation reaction. A stock solution of NHS-biotin (10 mM) was prepared in dimethylformamide. NHS-biotin was then added to the GPI-PLC to give a 20-fold molar excess of NHS-biotin to protein. The labelling reaction was allowed to proceed at room temperature for 30 minutes, after which any unbound NHS-biotin was inactivated by the addition of glycine (5 mM). Following this procedure, the GPI-PLC was specifically immunoprecipitated with anti-GPI-PLC antibody (Section 2.1.23.). Immunoprecipitates were separated by SDS-PAGE, electrotransferred to PVDF membrane, blotted with anti-GPI-PLC antibody (lane 1) or HRP-Streptavidin (lane 2) and developed by chemiluminesence. The predicted electrophoretic mobility of GPI-PLC is indicated on the right.

Figure 4.6. Immunoprecipitation of biotinylated recombinant GPI-PLC-His tagged.

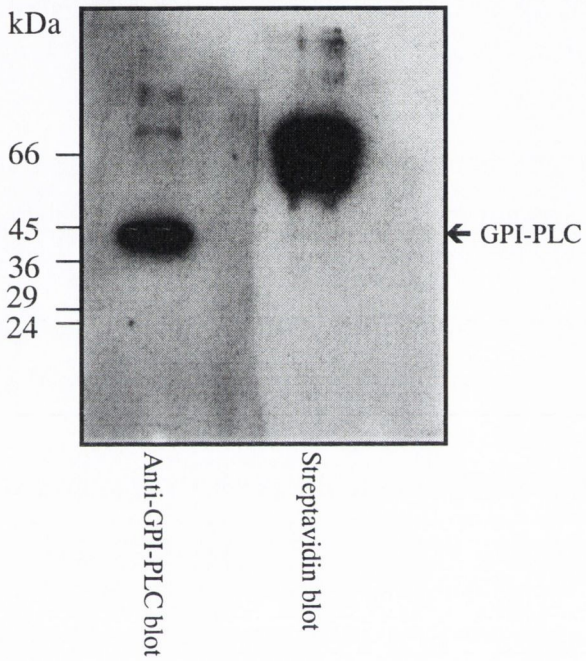

Figure 4.7. Biotinylation of Recombinant GPI-PLC-His tagged on PVDF membrane following transfer from SDS-PAGE.

Purified recombinant GPI-PLC (see Section 2.1.29) and purified MITat 1.1 VSG were subjected to gel electrophoresis on a 15% SDS-PAGE gel (Panel A) and subsequently transferred to PVDF membrane. Following transfer the membrane was washed in PBS buffer (x2) (see Table 2.1). Sulfo-NHS-Biotin (3 mg/ml) was then added and the membrane was incubated with this reagent for 20 minutes at room temperature with constant gentle agitation. It was finally washed in PBS containing glycine (5 mM) and transferred to TBST containing 5 % marvel for blocking. Biotinylated proteins were detected using HRP conjugated Streptavidin (1/30,000 dilution from stock) for 1 hour at room temperature (Panel B).

Panel A. (SDS-PAGE)

Lane 1: Low range molecular weight markers (Sigma)

Lane 2: Purified MITat 1.1 VSG (20 μg)

Lane 3: Purified recombinant GPI-PLC (5 μg)

Panel B. (Western blot of panel A following biotinylation of PVDF membrane)

Lane 1: Purified MITat 1.1 VSG (20 μg)

Lane 2: Purified recombinant GPI-PLC (5 μg)

Figure 4.7. Biotinylation of recombinant GPI-PLC-His tagged on PVDF membrane following transfer from SDS-PAGE.

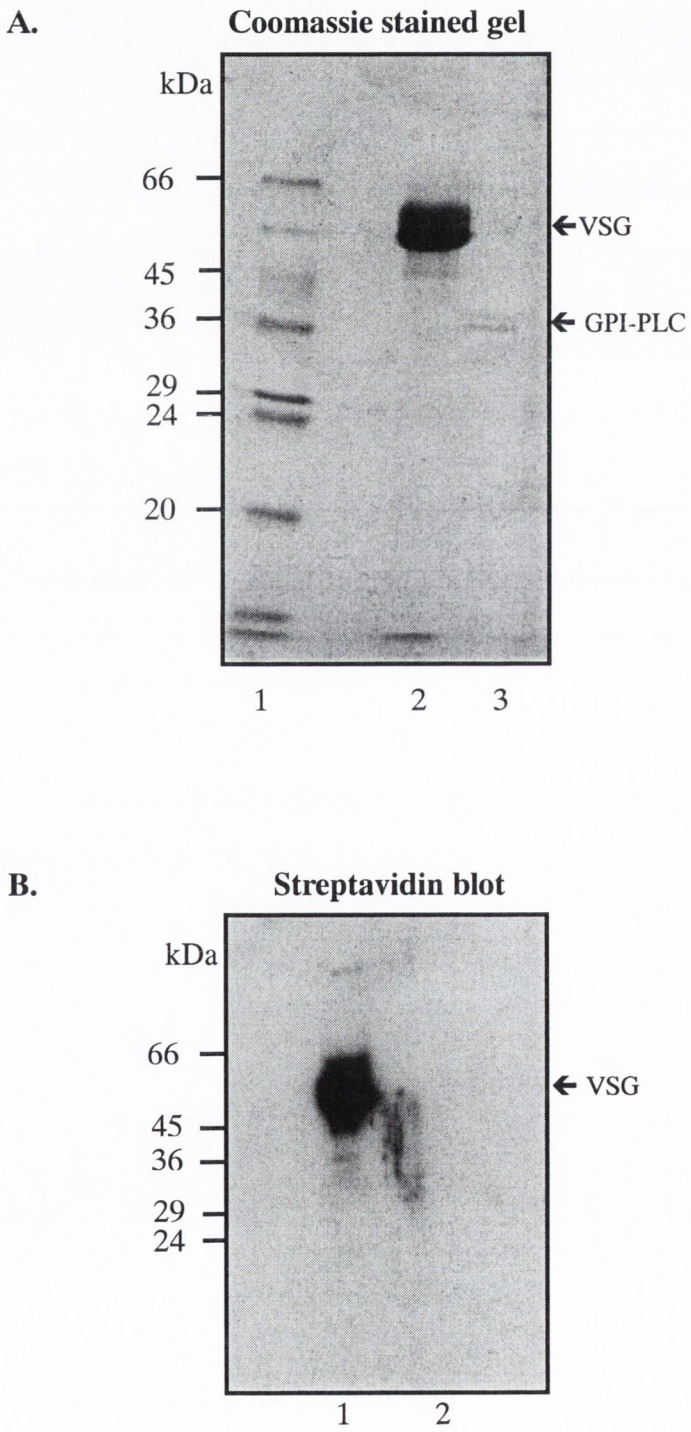

4.2.5. Biotinylation of purified recombinant GPI-PLC at elevated pH.

Lysine residues are more reactive at higher pH and therefore the hypothesis that the lysines of the GPI-PLC were abnormally pK-shifted to higher pH was tested to determine whether the GPI-PLC could be labelled with NHS-biotin successfully at higher pH (pH 9.3). The biotinylation was conducted as described previously after which any unbound NHS-biotin was inactivated by the addition of Glycine (5 mM, final concentration). Following this procedure, the GPI-PLC was specifically immunoprecipitated with anti-GPI-PLC antibody (Section 2.1.23.) and the immunoprecipitates separated by SDS-PAGE, electrotransferred to PVDF membrane, blotted with anti-GPI-PLC antibody (Fig 4.8, A) or HRP-streptavidin (Fig 4.8, B) and the blots developed by chemiluminesence. The GPI-PLC still did not become biotinylated.

4.2.6. Biotinylation of purified recombinant GPI-PLC in the presence of the protein denaturant, urea.

The following experiment was conducted in order to rule out the possibility that the GPI-PLC refolds after transfer to the PVDF membrane or remains folded at pH 9.3. Purified recombinant GPI-PLC (200 μg / 600 μl) was exchanged into $NaHCO_3$, pH 8.5 for the biotinylation reaction and was incubated in the presence or absence of urea (8 M final concentration) at room temperature for 30 minutes with constant agitation. The protein was then biotinylated in the presence or absence of urea as described. Following this procedure, a sample of the recombinant GPI-PLC was subjected to electrophoresis on a 15 % (w/v) acrylamide SDS gel, electrotransferred to PVDF membrane, blotted with anti-GPI-PLC antibody (Fig 4.9, A) or HRP-streptavidin (Fig 4.9, B) and developed using the chemiluminesence protocol. The GPI-PLC still did not become biotinylated in the presence of urea (8 M). Consequently, it seems likely that either these conditions fail to unfold the GPI-PLC or that all the lysines are blocked. This last possibility was investigated further using mass spectrometry and will be discussed later (see Chapter 6).

4.2.7. Surface labelling of bloodstream form trypanosomes with Iodine-125.

Because the lysines of the GPI-PLC proved unreactive, for whatever reason, additional experiments were conducted using the tyrosine residues of the GPI-PLC as targets for surface labelling in order to provide additional evidence that might help define

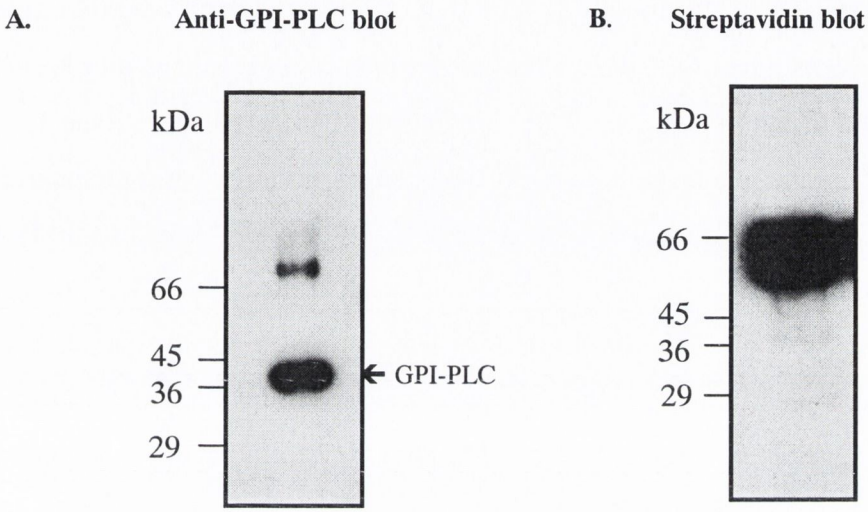

Fig. 4.8. Biotinylation of Recombinant GPI-PLC at elevated pH.

Purified recombinant GPI-PLC (200 μg / 600 μl) was exchanged into Na_2CO_3, pH 9.3 for the biotinylation reaction. A stock solution of NHS-biotin (10 mM) was prepared in dimethylformamide. NHS-biotin was then added to the GPI-PLC to give a 20-fold molar excess of NHS-biotin to protein. The labelling reaction was allowed to proceed at room temperature for 30 minutes, after which any unbound NHS-biotin was inactivated by the addition of glycine (5 mM, final concentration). Following this procedure, the GPI-PLC was specifically immunoprecipitated with anti-GPI-PLC antibody (Section 2.1.23.). Immunoprecipitates were separated by SDS-PAGE, electrotransferred to PVDF membrane, blotted with anti-GPI-PLC antibody (A) or HRP-Streptavidin (B) and developed by chemiluminesence. The predicted electrophoretic mobility of GPI-PLC is indicated on the right.

Fig 4.9. Biotinylation of Recombinant GPI-PLC following treatment with urea.

Purified recombinant GPI-PLC (200 μg / 600 μl) was exchanged into Na_2CO_3, pH 8.5 for the biotinylation reaction. This was incubated in the presence (lane 1, A & B) or absence (lane 2, A & B) of urea (8 M final concentration) at room temperature for 30 minutes with constant agitation. A stock solution of NHS-biotin (10 mM) was prepared in dimethylforamide. NHS-biotin was then added to the GPI-PLC to give a 20-fold molar excess of NHS-biotin to protein. The labelling reaction was allowed to proceed at room temperature for 30 minutes, after which any unbound NHS-biotin was inactivated by the addition of glycine (5 mM, final concentration). Following this procedure, the samples of recombinant GPI-PLC (+/- urea) were separated on a 15 % (w/v) SDS gel, electrotransferred to PVDF membrane, blotted with anti-GPI-PLC antibody (A) or HRP-Streptavidin (B) and developed by chemiluminesence. The predicted electrophoretic mobility of GPI-PLC is indicated on the right.

Panel A (Western blot probed with IgG anti GPI-PLC antibody)

Lane 1: Recombinant GPI-PLC biotinylated in the presence of urea

Lane 2: Recombinant GPI-PLC biotinylated in the absence of urea

Panel B (Western blot probed with HRP-streptavidin)

Lane 1: Recombinant GPI-PLC biotinylated in the presence of urea

Lane 2: Recombinant GPI-PLC biotinylated in the absence of urea

Fig 4.9. Biotinylation of Recombinant GPI-PLC following treatment with urea.

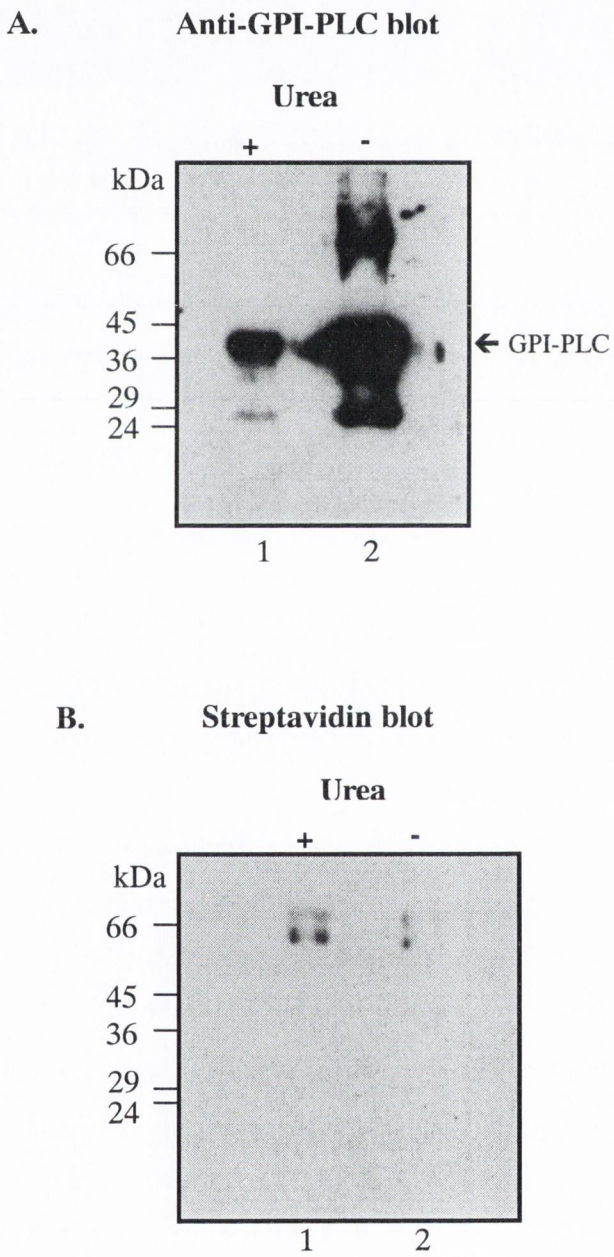

the cellular position of the GPI-PLC. Enzymatic surface radio iodination was carried out (Section 2.1.20) and lysates were specifically immunoprecipitated with anti-GPI-PLC antibody and with pre-immune serum. The pre-immune serum was used as a negative control. The immunoprecipitates were separated on SDS gels, which were stained with Coomassie blue and dried for subsequent development of the autoradiogram. The gels were exposed to X-ray film for either 9 days (Fig 4.10) or 15 days (Fig 4.11) at – 80°C. The anti-GPI-PLC antibody successfully immunoprecipitated the GPI-PLC as is evident in Fig 4.10. An intense band, which migrated in SDS-PAGE at the molecular weight (39 kDa) of the GPI-PLC (Fig 4.10, lane 1) was not present in the GPI-PLC $^{-}$ mutant strain (Fig 4.10, lane 2) as expected. When the pre-immune serum was used to immunoprecipitate radio iodinated proteins from the surface of trypanosomes there is a very weak signal below the 66kDa marker (Fig 4.11, lane 1). This band most likely corresponds to the VSG. A small amount of the VSG co-precipitates with the GPI-PLC (Fig 4.11 lane 2 & 3), which was not surprising considering its presence in bloodstream form trypanosomes at a 340 fold molar excess over that of the GPI-PLC. This result establishes that the GPI-PLC is at least partially exposed to the outer surface of bloodstream form trypanosomes.

4.3. Discussion.

The object of labelling bloodstream form trypanosomes with sulfo-NHS-Biotin and Iodine-125 was to confirm the localization of the GPI-PLC as seen by immunofluorescent studies. These immunofluorescent studies (Chapter 3) revealed that the GPI-PLC was located on the cell surface while surface biotinylation assays failed to detect the GPI-PLC on the surface of bloodstream forms of *T. brucei*. To resolve this dilemma, further investigation of the biotinylation technique was conducted using purified recombinant GPI-PLC. Initial experiments indicated that the recombinant enzyme did not react with the biotinylating reagent. This result could explain why the GPI-PLC was not identified as a cell surface protein when trypanosomes were labelled with sulfo-NHS-Biotin. To validate this result and confirm that the GPI-PLC does not react with the biotinylating reagent, the recombinant protein was labelled under a series of different conditions. Firstly, the recombinant GPI-PLC was biotinylated at higher pH (pH 9.3) rather than the conventional pH of 8.5 more generally used for this reaction. Secondly, the recombinant GPI-PLC was biotinylated on PVDF membrane after it had been electrophoresed by SDS-PAGE and,

finally, the recombinant protein was biotinylated in the presence of the protein denaturant, urea. All three of these experiments gave the same result. The GPI-PLC is unable to react with the biotinylating reagent sulfo-NHS-biotin and hence, the GPI-PLC cannot be detected as a surface protein by the method of cell surface biotinylation.

The fact that the GPI-PLC cannot be biotinylated is very unusual given that the native protein in *T. brucei* contains 14 lysine residues. This observation suggests that either all of the lysine residues are modified and, therefore, prevented from reacting with the biotinylating reagent, or that the GPI-PLC is folded in such a stable conformation that the protein cannot be denatured with urea or SDS and that, consequently, the lysine residues are hidden and, therefore, not exposed to the biotinylating reagent. Mass spectrometric analysis of the GPI-PLC revealed that at least 10 of the 15 lysines present in the peptides produced from trypsin digestion of the recombinant protein both 'in gel' and 'in solution' were not modified. The recombinant GPI-PLC has one additional lysine compared to the protein expressed in bloodstream form trypanosomes. Of the 10 lysines detected in unmodified form in the recombinant protein 7 were detected in the peptides produced by trypsin digestion of the GPI-PLC (Fig 4.12). An additional 3 lysines were found to be located in peptides not detected by mass spectrometry, but to be located immediately N-terminal to a peptide that was detected. Consequently, in these 3 cases trypsin cleavage must have occurred on the C-terminal side of these lysines, suggesting strongly that they were unmodified. This result accounts for 2/3 of all the lysine residues in the sequence. However, it seems curious that the sulfo-NHS-biotin cannot react with any of the free amines on these unmodified lysines. One would not expect such an unusual result *i.e.* no biotinylation of the GPI-PLC, when there is no modification to 2/3 of the target lysine. This result raises questions concerning the location of the lysine residues within the GPI-PLC itself and also questions the nature of the folding of the GPI-PLC.

A possible explanation for the failure of sulfo-NHS-biotin to react with the lysine residues may be due to the fact that they are not exposed and are buried in the hydrophobic core of the GPI-PLC protein. Amino acids such as lysine have not traditionally been classed as non-polar, yet they are frequently found in the interior of proteins where they are usually involved in salt bridges. Lysine also has a non-polar neck, located between the α-carbon and the ε-amino, that can interact with non-polar side chains (Fernandez and Scheraga, 2003) in the hydrophobic core of proteins. As long as the ε-NH_3^+ group is neutralized by salt-bridge formation or hydrogen bonding the lysine side chain may be considered as non-polar as methionine, and more so than leucine or isoleucine, whose side

Figure 4.10. Immunoprecipitation of GPI-PLC from bloodstream forms of MITat 1.2 trypanosomes labelled with Iodine-125.

Bloodstream populations of MITat 1.2 (1 x 10^8 cells), GPI- PLC $^-$ mutant trypanosomes and the parent strain, were surface iodinated using carrier-free $Na^{125}I$ (1 mCi) (Section 2.1.20). Cell lysates were subjected to specific immunoprecipitation with anti-GPI-PLC antibody (Section 2.1.23). Immunoprecipitates were separated by SDS-PAGE on a 15 % gel. The gel was stained with Coomassie and prepared for autoradiography (Section 2.1.14). After 9 days exposure the above film was developed in an X-ray film processor (Fuji).

Lane 1: Immunoprecipitated protein (equivalent to 2 x 10^8 cells) from wild type trypanosomes using anti-GPI-PLC IgG.

Lane 2: Immunoprecipitated protein (equivalent to 2 x 10^8 cells) from GPI-PLC $^-$ mutant trypanosomes using anti-GPI-PLC IgG.

Figure 4.10. Immunoprecipitation of GPI-PLC from bloodstream forms of MITat 1.2 trypanosomes labelled with Iodine-125.

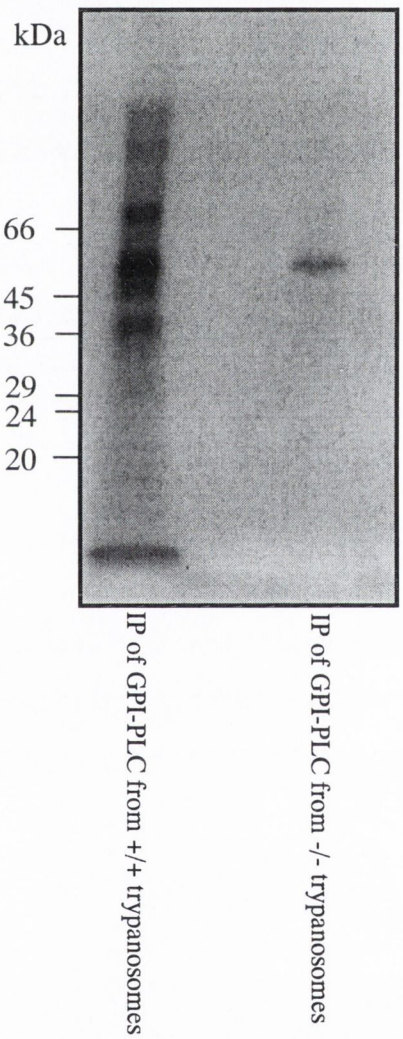

Figure 4.11. Immunoprecipitation of GPI-PLC from surface iodinated bloodstream forms of MITat 1.2 trypanosomes.

Bloodstream populations of MITat 1.2 (1 x 10^8 cells) were surface iodinated using carrier-free $Na^{125}I$ (1 mCi) (Section 2.1.20). Cell lysates were subjected to specific immunoprecipitation with pre-immune serum and anti-GPI-PLC antibody (Section 2.1.23). Immunoprecipitates were separated by SDS-PAGE on a 15 % gel. The gel was stained with Coomassie blue and prepared for autoradiography (Section 2.1.14). After 15 days exposure the above film was developed in an X-ray film processor (Fuji).

Lane 1: Immunoprecipitated protein (equivalent to 1 x 10^8 cells) from iodinated trypanosomes using pre-immune serum.

Lane 2: Immunoprecipitated protein (equivalent to 1 x 10^8 cells) from iodinated trypanosomes using anti-GPI-PLC IgG (5 μl of antibody).

Lane 3: Immunoprecipitated protein (equivalent to 1 x 10^8 cells) from iodinated trypanosomes using anti-GPI-PLC IgG (100 μl of antibody).

Figure 4.11. Immunoprecipitation of GPI-PLC from surface iodinated bloodstream forms of MITat 1.2 trypanosomes.

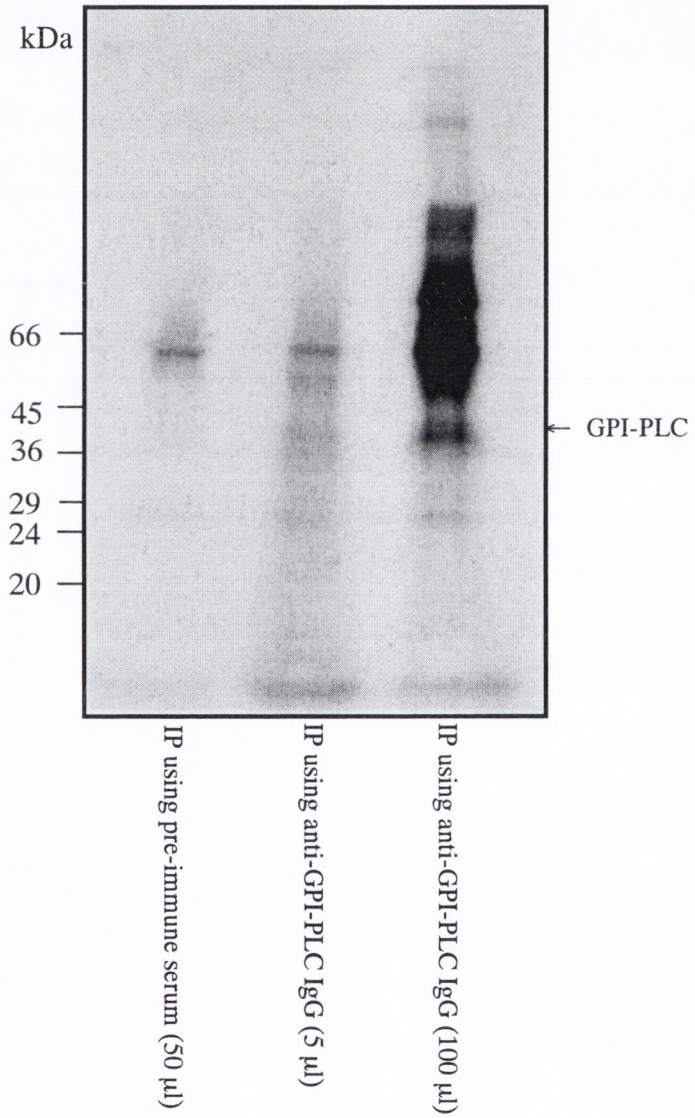

finally, the recombinant protein was biotinylated in the presence of the protein denaturant, urea. All three of these experiments gave the same result. The GPI-PLC is unable to react with the biotinylating reagent sulfo-NHS-biotin and hence, the GPI-PLC cannot be detected as a surface protein by the method of cell surface biotinylation.

The fact that the GPI-PLC cannot be biotinylated is very unusual given that the native protein in *T. brucei* contains 14 lysine residues. This observation suggests that either all of the lysine residues are modified and, therefore, prevented from reacting with the biotinylating reagent, or that the GPI-PLC is folded in such a stable conformation that the protein cannot be denatured with urea or SDS and that, consequently, the lysine residues are hidden and, therefore, not exposed to the biotinylating reagent. Mass spectrometric analysis of the GPI-PLC revealed that at least 10 of the 15 lysines present in the peptides produced from trypsin digestion of the recombinant protein both 'in gel' and 'in solution' were not modified. The recombinant GPI-PLC has one additional lysine compared to the protein expressed in bloodstream form trypanosomes. Of the 10 lysines detected in unmodified form in the recombinant protein 7 were detected in the peptides produced by trypsin digestion of the GPI-PLC (Fig 4.12). An additional 3 lysines were found to be located in peptides not detected by mass spectrometry, but to be located immediately N-terminal to a peptide that was detected. Consequently, in these 3 cases trypsin cleavage must have occurred on the C-terminal side of these lysines, suggesting strongly that they were unmodified. This result accounts for 2/3 of all the lysine residues in the sequence. However, it seems curious that the sulfo-NHS-biotin cannot react with any of the free amines on these unmodified lysines. One would not expect such an unusual result *i.e.* no biotinylation of the GPI-PLC, when there is no modification to 2/3 of the target lysine. This result raises questions concerning the location of the lysine residues within the GPI-PLC itself and also questions the nature of the folding of the GPI-PLC.

A possible explanation for the failure of sulfo-NHS-biotin to react with the lysine residues may be due to the fact that they are not exposed and are buried in the hydrophobic core of the GPI-PLC protein. Amino acids such as lysine have not traditionally been classed as non-polar, yet they are frequently found in the interior of proteins where they are usually involved in salt bridges. Lysine also has a non-polar neck, located between the α-carbon and the ε-amino, that can interact with non-polar side chains (Fernandez and Scheraga, 2003) in the hydrophobic core of proteins. As long as the ε-NH_3^+ group is neutralized by salt-bridge formation or hydrogen bonding the lysine side chain may be considered as non-polar as methionine, and more so than leucine or isoleucine, whose side

MFGGVKWSPQSWMSDTRSSIEKKCIGQVYMVGAHNAGTHGIQMFSPFGLDAPEKLRSLPPYVTFLLRFLTVGVSSRWGRCQNLSIRQLLDHGVRYL
WSPQSWMSDTRSSIEKKCIGQVYMVGAHNAGTHGIQMFSPFGLDAPEK SLPPYVTFLLRFLTVGVSSR QLLDHGVRYL

DLRMNISPDQENKIYTTHFHISVPLQEVLKDVKDFLTTPASANEFVILDFLHFYGFNESHTMKRFVEELQALEEFYIPTTVSLTTPLCNLWQSTRR
DLRMNISPDQENKIYTTHFHISVPLQEVLK *

IFLVVRPYVEYPYARLRSVALKSIWVNQMELNDLLDRLEELMTRDLEDVSIGGVPSKMYVTQAIGTPRNNDFAVAACCGACPGSHPDLYSAAKHKN
IFLVVRPYVEYPYAR SIWVNQMELNDLLDRLEELMTRDLEDVSIGGVPSKMYVTQAIGTPRNNDFAVAACCGACPGSHPDLYSAAK

PHLLKWFYDLNVNGVMRGERVTIRRGNNTHGNILLLDFVQEGTCTVKGVDKPMNAVALCVHLNTNQTARS
WFYDLNVNGVMRGERVTIR *

Fig 4.12. Sequence of the recombinant GPI-PLC with trypsin digested peptides shown in colour beneath the sequence.

Following analysis of MBP-PLC with Nanospray, the data files produced were put through the Mascot search engine and the amino acid sequence of the peptides was determined. All the lysine residues (K) not found within a peptide produced from trypsin cleavage are in red. * denotes a part of the sequence where trypsin will not cleave. No cleavage occurs when a proline residue is on the carboxyl side of the cleavage site.

* denotes a part of the sequence where cleavage is slower due to the presence of an acidic residue (aspartic acid, D) on the carboxyl side of lysine.

chains may not be ideal for optimum hydrophobic packing (Dyson *et al.*, 2006). These interactions strengthen hydrogen bonds and electrostatic interactions between charged groups both by reducing the entropy of otherwise freely rotating polar or charged side chains and creating a water diminished non-polar environment (Fernandez and Scheraga, 2003). Salt bridge and salt link are colloquial terms for the pH-dependent, non-covalent bond between oppositely charged residues that are sufficiently close to each other to experience electrostatic attraction. Salt bridges which can be considered a special form of hydrogen bond, are composed of negative charges from Asp, Glu, Tyr, Cys and the C-terminal carboxylate group, and of positive charges from His, Lys, Arg and the N-terminal amino group (Fig 4.13). Since the side chain charge of these residues depends on pH, the free energy contributions of salt bridges to protein stability are pH dependent.

If all, or even the majority of the lysine residues, are involved in salt bridges in the hydrophobic core of the GPI-PLC this could explain why sulfo-NHS-biotin could not react with their primary amine. If the lysine residues were all in salt bridges, then their ε-amino group would be "blocked" to reaction with a derivatizing reagent.

In addition to surface biotinylation assays bloodstream form trypanosomes were surface labelled with Iodine-125. This labelling technique proved successful, indicating that the tyrosine and, possibly the histidine residues, of the GPI-PLC are exposed on the surface of trypanosomes. This result also confirms the immunofluorescent results in chapter three, that the GPI-PLC is at least partially exposed to the outer surface of bloodstream form trypanosomes.

Previously, the GPI-PLC was reported to be located on the surface of intact short stumpy trypanosomes by means of a surface biotinylation assay (Gruszynski *et al.*, 2003). The antibody used to immunoprecipitate the GPI-PLC from biotinylated trypanosomal lysates in this study was the VSG-lipase-specific murine monoclonal antibody, 2A6-6 (Hereld *et al.*, 1988). Attempts, by this group, to verify the presence of the GPI-PLC on the cell surface by immunofluoresence using the same antibody were unsuccessful. However, the most recent report on the localization of the GPI-PLC by immunofluoresence in bloodstream forms of *T. brucei*, has found that the GPI-PLC is located in glycosomes, (Subramanya and Mensa-Wilmot, 2006). The antibody used for this glycosomal localization is the same murine, monoclonal antibody, 2A6-6, used for the immunoprecipitation of biotinylated GPI-PLC from the surface of bloodstream trypanosomes (Gruszynski *et al.*, 2003). These results are contradictory; the first group report that the GPI-PLC is located on the surface of short-stumpy trypanosomes, whereas

Fig 4.13. Salt Bridges (Adapted from Virtual Chembook, Elmhurst College).
Amino acids interact with each other in a typical acid-base neutralization reaction to form a salt. The reaction is simply the transfer of the -H (positive ion) from the acid to the amine and the attraction of the resulting positive and negative charges. The acid group becomes negative, and the amine nitrogen becomes positive because of the positive hydrogen ion. For example in the graphic above - top, glycine (gly) and alanine (ala) may just interact in the zwitterion form by an attraction of the positive (amine) of the alanine and negative (carboxyl acid) charges to form the salt. A more important interaction for protein tertiary structure is the interaction of the acid and base "side chains". If the amino acid has an extra acid or amine on the "side chain", these are used in the salt formation. For example above in the second reaction, Aspartic acid (asp) has a side chain that forms a salt with the amine on the lysine (lys) side chain. The hydrogen ion (red) moves to the amine nitrogen resulting in the salt with the attraction of the positive and negative charges.

Fig 4.13. Salt Bridges (Adapted from Virtual Chembook, Elmhurst College).

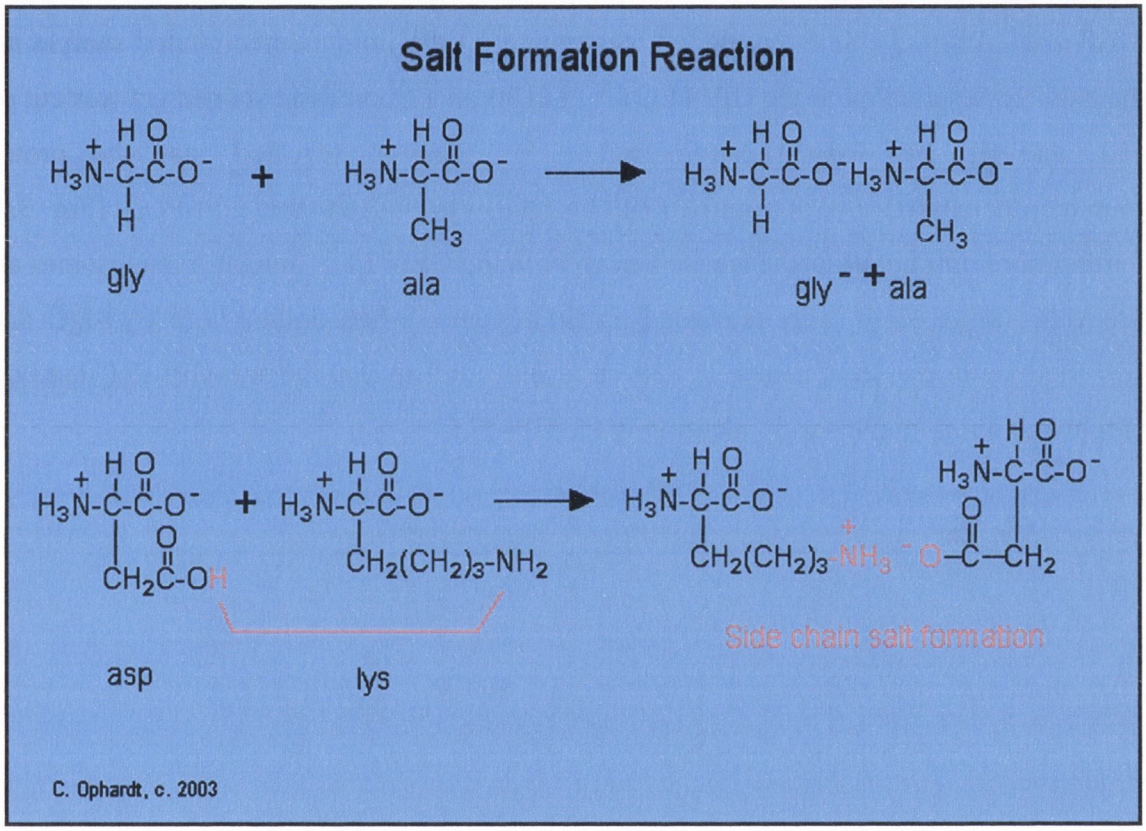

the second group report that the GPI-PLC is located in glycosomes and did not find it located on the surface of trypanosomes, even though both groups used the same VSG-lipase-specific murine monoclonal antibody, 2A6-6. These results question the specificity of the antibody for the GPI-PLC in bloodstream forms of *T. brucei*.

On the contrary however, the IgG anti-GPI-PLC antibody employed in this study immunoprecipitated the GPI-PLC in wild-type trypanosomes and did not immunoprecipitate a corresponding protein in GPI-PLC $^{-}$ mutant forms of *T. brucei*. In addition, the anti-GPI-PLC antibody was used to immunoprecipitate the GPI-PLC from a mixture of TEV cleaved MBP-PLC fusion protein, which contains uncleaved MBP-PLC, MBP and GPI-PLC. SDS-PAGE was performed on the immunoprecipitated sample and the band corresponding to the GPI-PLC (~ 39 kDa) on a Coomassie stained gel was cut out and analysed by mass spectrometry. This analysis revealed that the protein immunoprecipitated by the anti-GPI-PLC IgG was indeed the GPI-PLC (Fig 3.2). Furthermore, immunofluoresence studies on both the GPI-PLC $^{-}$ mutant trypanosomes and procyclic forms of *T. brucei* revealed no fluorescence when probed with Cy3-IgG anti-GPI-PLC antibody (see Chapter 3). These results confirm that the anti-GPI-PLC antibody employed in this study is truly identifying the GPI-PLC.

Chapter 5

The role of the GPI-PLC in the endo/exocytic cycle and also its involvement if any in disaggregation of T. brucei following aggregation with excess antibody

5.1. Introduction

The role of the GPI-PLC *in vivo* has been the topic of intense debate. It has been speculated that many processes may require the activity of the GPI-PLC. First, the trypanosome must replace the surface metacyclic VSG coat when first entering the mammalian bloodstream from the tsetse fly with a bloodstream form VSG coat and the GPI-PLC could be involved in the release of the metacyclic VSG immediately prior to or during its replacement with the first bloodstream form coat. Second, during antigenic variation, the entire VSG coat must be replaced by another antigenically distinct VSG about once every 8-10 days and the GPI-PLC could be involved in this process. Third, the VSG coat is replaced by a procyclin surface coat upon differentiation of the bloodstream form to the procyclic form trypanosome and the GPI-PLC could be conceived to be involved in the shedding of the VSG to make room for procyclin. Clearly, it was tempting to suggest that the GPI-PLC was involved in one or all of these three major VSG shedding events that are essential for the survival and life cycle completion of *T. brucei*. However, this hypothesis was investigated using a mutant trypanosomal cell line containing a double deletion mutation of the GPI-PLC, where the entire gene of both alleles was each replaced with separate and different selectable antibiotic resistant markers in procyclic form trypanosomes. The GPI-PLC $^{-}$ mutant trypanosomes were then successfully transmitted through the tsetse fly, recovered as bloodstream form cells, and were shown to be capable of antigenic variation. In addition, the GPI-PLC $^{-}$ mutant bloodstream form trypanosomes have been demonstrated to differentiate into procyclic forms *in vitro* and *in vivo*, completing the life cycle, with apparent normal kinetics (Webb *et al.*, 1997). Thus, it seems that the GPI-PLC is not essential for completion of the life cycle of *T. brucei* and is not required for either antigenic variation or transition of metacyclic forms into bloodstream form or bloodstream forms into procyclic forms.

There is at least one other physiological process in bloodstream form trypanosomes that might involve the GPI-PLC, the process of active disaggregation from anti-VSG-mediated aggregates of bloodstream form trypanosomes. Consequently, the possible involvement of the GPI-PLC in this disaggregation mechanism was investigated in the present study. The phenomenon of disaggregation was first reported in 1900 by Laveran & Mesnil and then again by these workers in 1901. Their observation was also confirmed by Francis (1903). No other reports or even confirmation of the phenomenon had appeared in the literature until, it was independently observed by Lowry (O'Beirne *et al.*, 1998). These workers found that disaggregation was strictly energy dependent and required normal

endosomal activity. In addition, disaggregation was not due to the separation of immunoglobulin chains and conversion to monomers by either disulfide reduction or disulfide exchange reactions. Furthermore, gross proteolytic cleavage of the immunoglobulins attached to the surface of the parasite was not detected. It was also observed, that gross cleavage or release of the VSG from the surface of the cell did not occur during disaggregation. Finally, the mechanism of disaggregation was found to be a regulated process, independent of Ca^{2+} movements but dependent upon the activity of protein kinase C or related kinases and inhibited by the activity of protein kinase A as evidenced by the effects of a panel of inhibitors and cAMP analogues on the process of disaggregation. While all of this evidence strengthened the case for a regulated physiological process that led to disaggregation and eliminated several possible mechanisms, it did not identify any specific protein or enzyme responsible for the process itself. Consequently, the present study began with the goal of testing the possibility that the GPI-PLC might be involved in the mechanism of disaggregation (O'Beirne *et al.*, 1998). Bloodstream form trypanosomes were probed at different time points throughout the process of disaggregation with antibodies against the CRD epitope of the VSG in order to determine if the CRD became exposed, even transiently during the disaggregation process. It is known that the CRD of the VSG only becomes accessible to antibody when the VSG is cleaved at the GPI anchor by the GPI-PLC (Carrington *et al.*, 1998). Consequently if the CRD became positive during disaggregation, then the GPI-PLC must somehow be involved in this process.

Another possible physiological role for the GPI-PLC was to release the GPI-linked transferrin receptor with the bound ligand from its membrane attachment following its endocytosis to the endosome. In fact, it had been observed that mutant GPI-PLC $^-$ trypanosomes were unable to exocytose degraded FITC-labelled transferrin following receptor-mediated endocytosis, in stark contrast to their wild-type counterparts (Brabazon, E, Ph.D. Thesis, 1999). Evidence will be presented which shows that the GPI-PLC $^-$ mutant trypanosomes behave exactly as their wild-type parents, endocytosing both VSG and transferrin and also exocytosing them. There was no alteration in the cycle of endo/exocytosis detected in the GPI-PLC- mutant cell line and the reason for the previous finding was determined to be related to the bioenergetic status of the mutant cells. The first double deletion mutant of the GPI-PLC, which was used by Brabazon (1999), was produced in an ANTat strain, which only gives 10^6-10^7 cells/ml, making the isolation of cells a lengthy procedure during which ATP levels can fall and thereby inhibit cellular

processes. A second GPI-PLC double deletion mutant, that was used in the present study, was produced directly in the bloodstream forms of a MITat 1.2 strain. Consequently, the yield of cells was greatly improved (10^9 cells/ml), making cell isolation a rapid procedure. In addition, I have introduced a short (15 min) stirred incubation of cells at 37°C at low cell concentration (5 x 10^7 /ml) in isosmotic buffer supplemented with glucose, immediately before beginning the experiment to ensure that the cells were properly energized and had recovered from the isolation procedure before use.

5.2. Results

5.2.1 The GPI-PLC in bloodstream forms of T. brucei is essential for the release of the VSG from water-lysed cells.

The exposure of the cross-reacting determinant following hypotonic lysis of the cells was determined for both wild-type and mutant GPI-PLC $^-$ trypanosomes. SDS-PAGE revealed that sVSGs have an apparent molecular weight 800-2000 Daltons higher than mfVSG (Cardoso de Almeida and Turner, 1983) (Fig 5.1 & 5.2). The change in mobility of the membrane bound form of the VSG upon conversion to the released form observed during SDS-PAGE is most likely due to the effect that the change in native charge has on binding to SDS molecules (Jackson and Voorheis, 1985). When the mVSG is cleaved at the GPI-anchor during hypotonic lysis of cells, the resulting sVSG has an extra negative charge associated with it. Consequently, the increased negativity of the released form of the VSG displaces more than stochiometric amounts of negatively charged SDS molecules, causing the sVSG to migrate more slowly than the mfVSG during electrophoresis. The action of the GPI-PLC on the GPI-anchor of the VSG results in the release of dimyristyl glycerol and the formation of an inositol 1,2 cyclic phosphate (Hereld *et al.*, 1986). The appearance of this residual anchor can be visualised by western blotting with anti-CRD antibody (Carrington *et al.*, 1998). Fig 5.1, lane 2 shows that the VSG in the GPI-PLC $^-$ mutant trypanosomes remained anti-CRD negative, confirming the results from other laboratories (Carrington *et al.*, 1998); (Cardoso De Almeida *et al.*, 1999).

Fig 5.1. Release of VSG and detection of CRD epitope upon water lysis of the wild-type parent strain of the GPI-PLC $^-$ mutant trypanosomes at 37°C.

GPI-PLC $^-$ mutant trypanosomes and its parent strain at a concentration of 5 x 10^8 cells/ml, following washing with TES buffer, pH 7.4, were resuspended in 100 µl TES, containing protease inhibitors (Table 2.3) at 0°C. Subsequently 900 µl H_2O, containing protease inhibitors, was added at 37°C and the cells were incubated at 37°C for 10min. Following this incubation 2 x 10^7 cells (40 µl) were added directly to an equal amount of SDS-PAGE sample buffer (x2). 2.5 x 10^6 cells (20 µl) were loaded per well and SDS-PAGE carried out as described in Section 2.1.13. The above gel was western blotted using the anti-CRD IgG (1/100 dilution) as the primary antibody.

Plate A: Coomassie stained gel (10 %)

Lane 1: Wild-type trypanosomes water lysed

Lane 2: GPI-PLC $^-$ mutant trypanosomes water lysed

Plate B: Gel in Plate A western blotted using anti-CRD IgG antibody (1/100 dilution).

Lane 1 & 2 as in Gel.

A. **Coomassie stained gel**

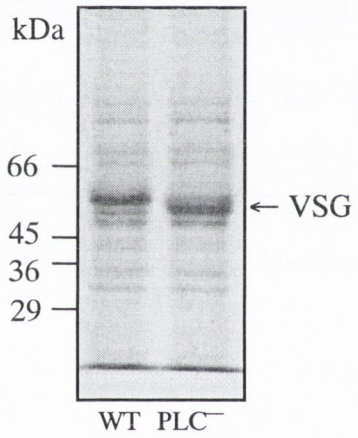

B. **Anti-CRD blot**

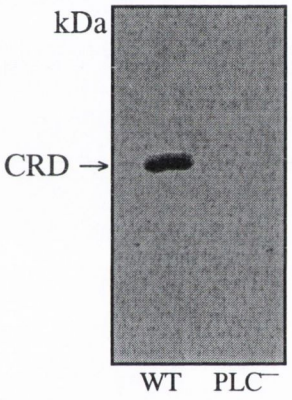

Fig 5.2. Change in molecular weight of the variant surface glycoprotein when it is converted from mfVSG to sVSG upon water lysis of bloodstream form trypanosomes.

Bloodstream form trypanosomes at a concentration of 5 x 10^8 cells/ml, following washing with TES buffer, pH 7.4, were resuspended in 100 µl TES, containing protease inhibitors (Table 2.3) at 0°C. Subsequently 900 µl H_2O, containing protease inhibitors, was added at 37°C and the cells were incubated at 37°C for 10min. Following this incubation 2 x 10^7 cells (40 µl) were added directly to an equal amount of SDS-PAGE sample buffer (x2). 2.5 x 10^6 cells (20 µl) were loaded per well and SDS-PAGE carried out as described in Section 2.1.13. The above gel was western blotted using the anti-VSG IgG (1/1000 dilution) as the primary antibody.

Plate A: Coomassie stained gel (10 %)

Lane 1: Bloodstream form trypanosomes untreated

Lane 2: Bloodstream form trypanosomes water lysed

Plate B: Gel in Plate A western blotted using anti-VSG IgG antibody (1/1000 dilution).

Lane 1 & 2 as in Gel.

Fig 5.2. Change in molecular weight of the variant surface glycoprotein when it is converted from mfVSG to sVSG upon water lysis of bloodstream form trypanosomes.

A. **Coomassie stained gel**

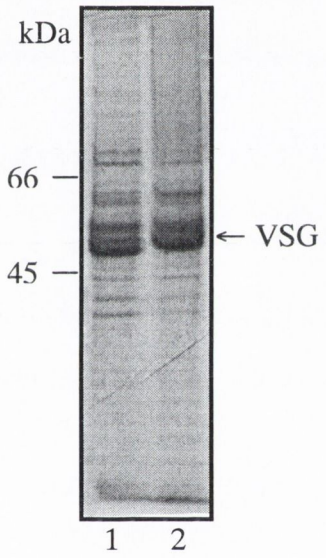

B. **Anti-VSG IgG blot**

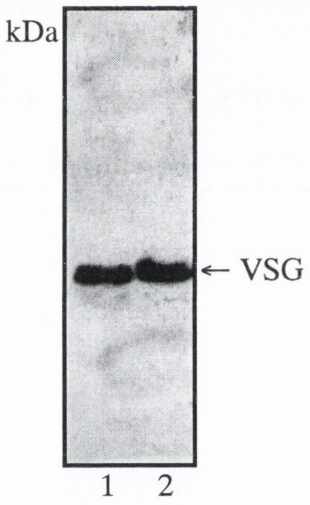

5.2.2. GPI-PLC is not involved in the disaggregation of trypanosomes or the cycle of endocytosis and exocytosis of either transferrin or surface immune complexes.

Fig 5.3 shows a time-course of disaggregation for wild-type and GPI-PLC $^-$ mutant cells. Both sets of cells were incubated at 37°C in TES buffer, pH 7.4 for 15 minutes with constant gentle stirring. Following this incubation, anti-VSG IgM (5 μg/ml) was added to each set of cells. At various times, samples were removed and cells were counted microscopically. Both the wild–type and GPI-PLC $^-$ mutant trypanosomes had the same time-course of disaggregation. The $t_{½}$ was between 10-15 min and the time course was complete in just over 30 minutes for both the wild-type and GPI-PLC $^-$ mutant cells. The fact that the GPI-PLC $^-$ mutant cells disaggregate informs us that the GPI-PLC is not essential for the process of disaggregation. Furthermore, the fact that the time course of the process is unaltered in GPI-PLC $^-$ mutant cells compared to the wild-type suggests that it is not simply replaced by a slower "fail-safe" mechanism in the deletion mutant cells.

One potential mechanism (Fig 5.4) that would account for the observed disaggregation in both the wild-type and GPI-PLC $^-$ mutant trypanosomes is that the VSG-antibody complexes were shed from the cells into the surrounding medium thereby permitting disaggregation. The results of O'Beirne *et al.*, 1998 indicate that no gross release of the VSG occurs during disaggregation but the possibility still exists that a small percentage of the total surface coat may have been released. Since this possibility may indeed reflect the true situation it was required that these experiments be repeated to unequivocally determine that release of the VSG from cells that are disaggregating, if it occurs, is below the level of detection.

MITat 1.2 wild-type and mutant GPI-PLC $^-$ trypanosomes were incubated in the presence of IgM anti-VSG antibody and samples removed at various times, subjected to SDS PAGE, transferred onto nitrocellulose and probed with anti-CRD antibody. These samples were examined for the release of the VSG at various time points throughout the process of disaggregation (Fig 5.5, Gel A & Gel B). There was no release of the VSG observed at any point during the process of disaggregation and the CRD did not become exposed (Fig 5.5, Blot A & Blot B).

Finally, the possibility that some but not all of the VSG within surface immune complexes was cleared by a different mechanism at a different point in the VSG was considered. In this case the CRD may not have become positive but cleavage at a different point could have exposed the C-terminal domain of the VSG, which is not normally exposed in healthy live cells. The very close packing nature of the VSG coat means that

the C-terminal of the protein is afforded protection and only becomes accessible to antibodies when the VSG has been released into solution and until that moment it is only the very top of the N-terminal domain that is exposed to the host immune system. Exposure of the C-terminal domain could arise without release of the VSG if the cleavage process was terminated in any particular cell as soon as it became free of the aggregate. Clearly, any two aggregated cells will have some but not necessarily all of their bound anti-VSG IgM attached to both cells. It would be sufficient for disaggregation if the antibody cross - linked from just one cell in a two cell aggregate were cleaved from its GPI anchor. Consequently, it was possible that not all VSG molecules in an aggregate were cleaved during disaggregation. This possibility was investigated.

MITat 1.1 wild-type trypanosomes were incubated in the presence and the absence of anti-VSG IgM and samples removed at $t_{½}$ of disaggregation. These samples were subjected to SDS PAGE, transferred onto nitrocellulose and probed with anti-C-terminal antibody. These samples were examined for the release of the VSG at the half point ($t_{1/2}$) of disaggregation (Fig 5.6, Gel A). There was no release of the VSG observed and the C-terminal domain of the VSG did not become exposed (Fig 5.6, Blot B).

In order to confirm the results already obtained by SDS PAGE and western blotting, cells that had been incubated with/without aggregating amounts of IgM anti-VSG antibody were probed with IgG anti-CRD antibody, IgG anti-C-terminal antibody and IgG anti-VSG antibody immediately following disaggregation. Subsequently the cells were fixed and prepared for confocal microscopy as described in methods (Section 2.1.53). Unfixed cells incubated with aggregating IgM anti-VSG antibody and IgG anti-CRD or IgG anti-C-terminal domain antibody displayed no fluorescence (Plate 5.2 B & C). Unfixed cells incubated with aggregating IgM anti-VSG antibody and IgG anti-VSG antibody displayed fluorescent capping of the VSG (Plate 5.2, D). The images obtained for those cells incubated without IgM and with IgG anti-CRD, IgG anti-C-terminal domain antibody or IgG anti-VSG antibody, show the same pattern of fluorescence (Plate 5.1 A-D). These results further substantiate the fact that the GPI-PLC is not involved in the mechanism of disaggregation in bloodstream form trypanosomes.

In addition to the above experiments to discover whether there was any cleavage of the VSG molecules during the process of disaggregation, a separate test was carried out to determine if any of the VSG of one cell in an aggregate of cells moved to another cell during disaggregation. In order to do this, two sets of cells were labelled separately with either FITC-DHPE (FITC-labelled dipalmitoyl phosphatidyl ethanolamine) or Cy3-DHPE

Figure 5.3. Time course of disaggregation for MITat 1.2 WT parent strain of GPI-PLC $^-$ mutant trypanosomes and GPI-PLC $^-$ mutant trypanosomes.

WT (panel A) and GPI-PLC $^-$ mutant trypanosomes (panel B) ($2x10^7$ cells/ml) were incubated in isosmotic TES buffer, pH 7.4 at 37°C with constant gentle stirring for 15 min. Following this energising incubation an aggregating concentration of anti-VSG IgM (5 μg/ml) in TES buffer, pH 7.4 was added. Samples (10 μl) were withdrawn from the incubation medium at the times indicated and the number of free, unaggregated cells counted microscopically. The percentage of cells was determined as described in methods. Data are the mean +/- the standard deviation of triplicate measurements and where no error bar is shown, the error is smaller than the symbol used.

Figure 5.3. Time course of disaggregation for MITat 1.2 WT parent strain of GPI-PLC $^-$ mutant trypanosomes and GPI-PLC $^-$ mutant trypanosomes.

A.

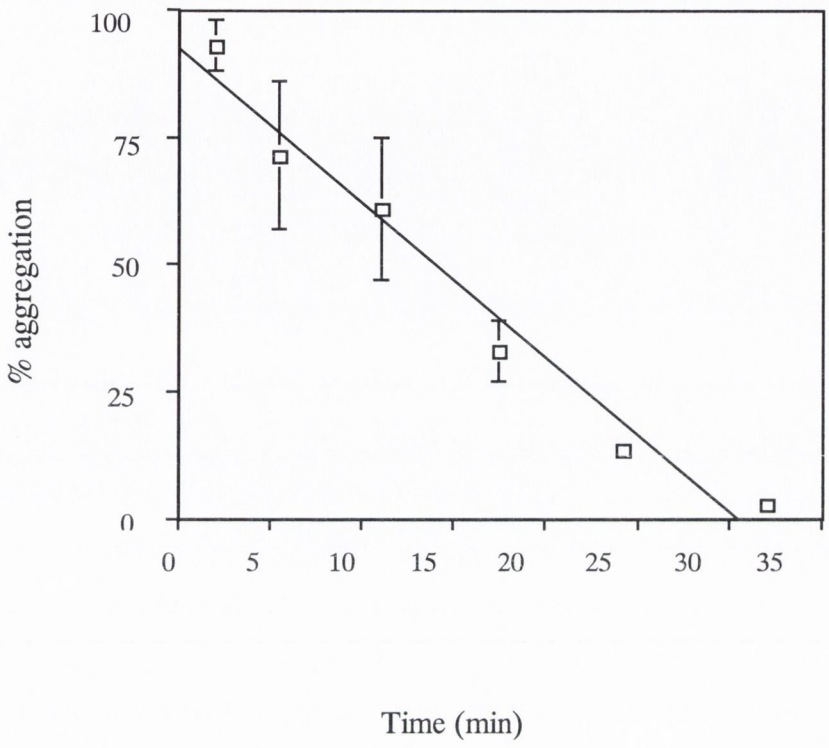

B.

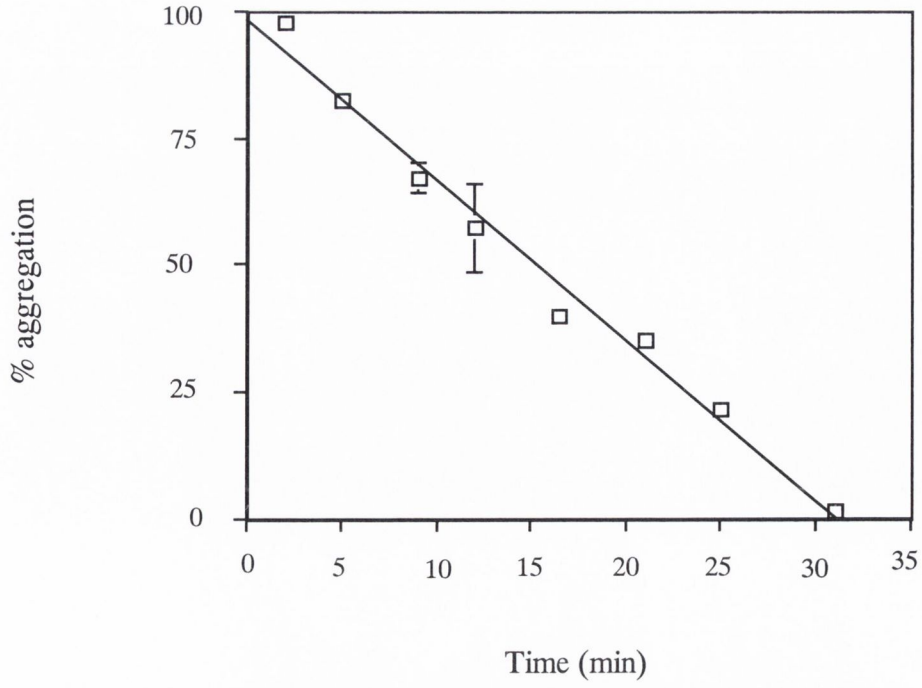

Fig 5.4. The GPI anchor of the Variant Surface Glycoprotein in trypanosomes. The diagram depicts the cleavage sites of the GPI-PLC, the GPI-PLD and protease, 3 possible mechanisms of disaggregation in bloodstream forms of *T. brucei*.

Addition of anti-VSG IgM antibody (0.36 mg/ml) leads to aggregation of bloodstream forms of T. brucei (2 x 10^7 cells/ml). Aggregated cells disaggregate by an unknown mechanism. There are two possible cleavage sites on the GPI anchor of the VSG and a third cleavage site in the hinge region that forms the link between the C-terminal and the N-terminal of the VSG; any of these cleavages could be causing the aggregated cells to disaggregate.

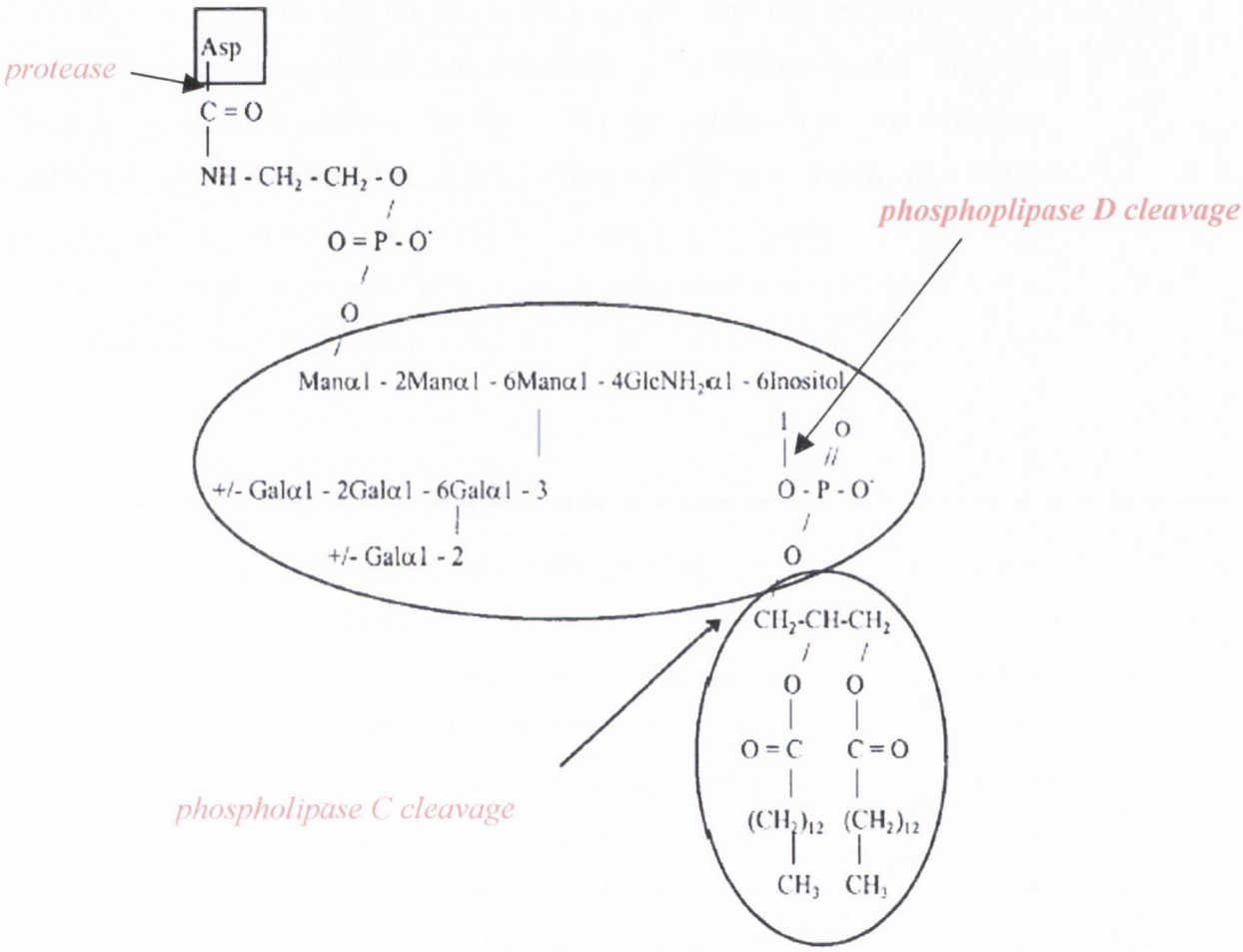
protease
Asp
C = O
NH - CH2 - CH2 - O
O = P - O-
O
Manα1 - 2Manα1 - 6Manα1 - 4GlcNH2α1 - 6Inositol
+/- Galα1 - 2Galα1 - 6Galα1 - 3
+/- Galα1 - 2
phosphoplipase D cleavage
O - P - O-
O
CH2-CH-CH2
O = C
C = O
(CH2)12
CH3
phospholipase C cleavage

Figure 5.5. SDS-PAGE of cells during the course of aggregation/disaggregation.

Wild-type trypanosomes and GPI-PLC $^-$ mutant trypanosomes (2x 10^7cells/ml) were incubated in separate chambers in TES buffer, pH 7.4 at 37°C with constant gentle stirring for 15 min. Purified IgM antibody (5 μg/ml) was then added to the incubation medium and the cells were allowed to aggregate. At the times indicated samples (200μl) were withdrawn and centrifuged (13,000 **g**, 20 seconds). The pellets were resuspended in 60μl (1 x 10^7 cells) of sample buffer. Two lanes were loaded with control samples, one with wild-type cells treated with H_2O and the other with GPI-PLC $^-$ mutant cells treated with water (see Section 2.1.18). The samples were subjected to gel electrophoresis on a 10% SDS-PAGE gel. The gel was then western blotted using anti-CRD IgG (1/100 dilution) as the primary antibody.

Gel A.

Lane 1:	Wide-range molecular weight markers
Lane 2:	Wild-type whole cells not treated
Lane 3:	GPI-PLC $^-$ mutant cells not treated
Lane 4:	Wild-type cells at 0 time
Lane 5:	GPI-PLC $^-$ mutant cells at 0 time
Lane 6:	Wild-type cells at 2 min
Lane 7:	GPI-PLC $^-$ mutant cells at 2 min
Lane 8:	Wild-type cells at 5 min
Lane 9:	Wild-type cells treated with H_2O
Lane 10:	GPI-PLC $^-$ mutant cells treated with H_2O

Blot A.

Western blot of gel A probed with anti-CRD IgG antibody. Layout of blot is the same as in gel A.

Figure 5.5. SDS-PAGE of cells during the course of aggregation/disaggregation (A).

Gel A.

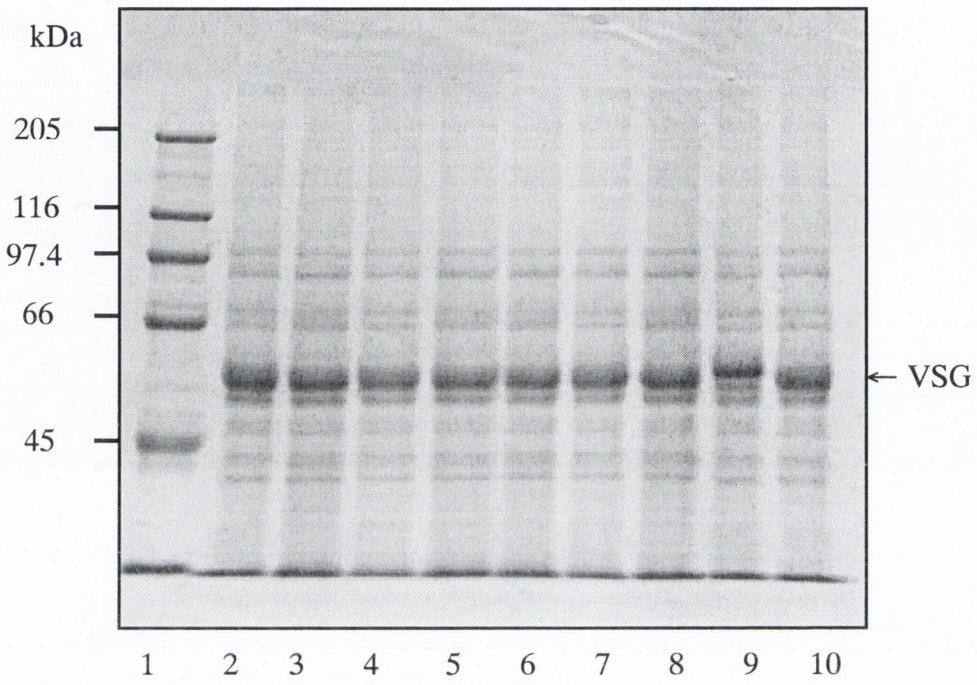

Blot A.

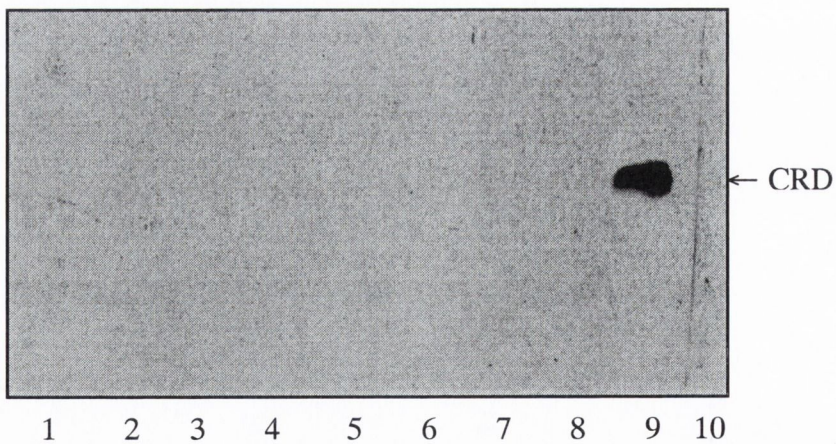

Figure 5.5. SDS-PAGE of cells during the course of aggregation/disaggregation.

Wild-type trypanosomes and GPI-PLC $^-$ mutant trypanosomes (2x 10^7cells/ml) were incubated in separate chambers in TES buffer, pH 7.4 at 37°C with constant gentle stirring for 15 min. Purified IgM antibody (5 μg/ml) was then added to the incubation medium and the cells were allowed to aggregate. At the times indicated samples (200μl) were withdrawn and centrifuged (13,000 **g**, 20 seconds). The pellets were resuspended in 60μl (1 x 10^7 cells) of sample buffer. Two lanes were loaded with control samples, one with wild-type cells treated with H_2O and the other with GPI-PLC$^-$ mutant cells treated with water (see Section 2.1.18). The samples were subjected to gel electrophoresis on a 10% SDS-PAGE gel. The gel was then western blotted using anti-CRD IgG (1/100 dilution) as the primary antibody

Gel B.

Lane 1	Wide-range molecular weight markers
Lane 2	Wild-type whole cells at 10 min
Lane 3	GPI-PLC $^-$ mutant cells at 10 min
Lane 4	Wild-type cells at 15 min
Lane 5	GPI-PLC $^-$ mutant cells at 15 min
Lane 6	Wild-type cells at 20 min
Lane 7	GPI-PLC $^-$ mutant cells at 20 min
Lane 8	Wild-type cells at 30 min
Lane 9	GPI-PLC $^-$ mutant cells at 30 min
Lane 10	Wild-type cells at 45 min
Lane 11	GPI-PLC $^-$ mutant cells at 45 min
Lane 12	Wild-type cells at 60 min

Blot B.

Western blot of gel B probed with anti-CRD IgG antibody. Layout of blot is the same as in gel B.

Figure 5.5. SDS-PAGE of cells during the course of aggregation/disaggregation (B).

Gel B.

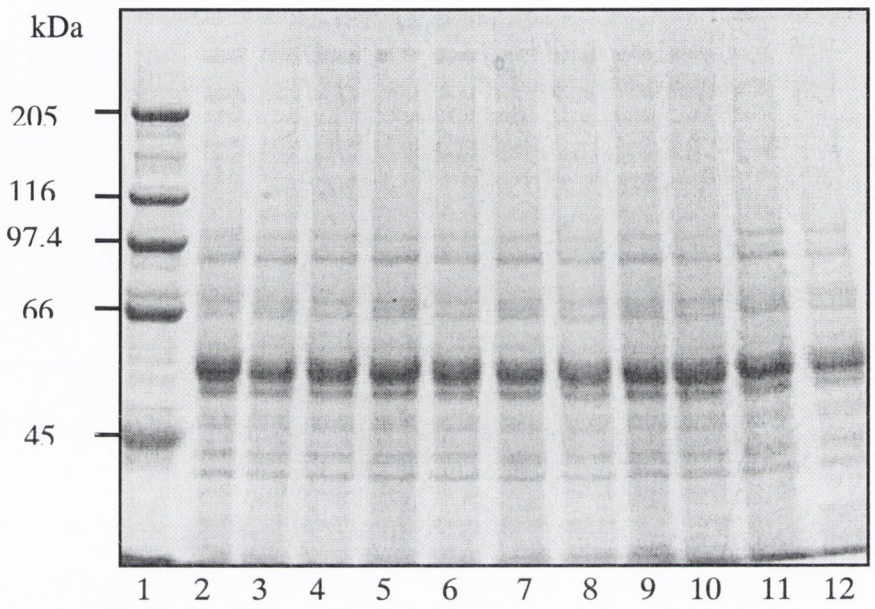

Blot B.

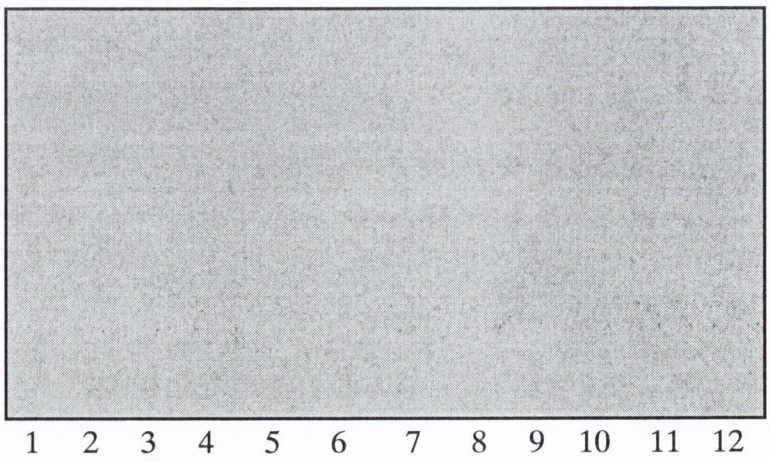

Fig 5.6. SDS-Polyacrylamide gel electrophoresis of bloodstream form trypanosomes incubated in the presence or the absence of aggregating amounts of anti-VSG IgM antibody.

MITat 1.1 trypanosomes were incubated at a concentration of 2 x 10^7 cells/ml in TES buffer, pH 7.4 at 37°C with constant gentle stirring for 15 min. Purified IgM antibody (5 μg/ml) was then added to the incubation medium and the cells were allowed to aggregate. At $t_{1/2}$ samples (200μl) were withdrawn and centrifuged (13,000 **g**, 20 seconds). The pellets were resuspended in 60μl (1 x 10^7 cells) of sample buffer. The samples were subjected to gel electrophoresis on a 10%, (w/v) SDS-PAGE gel.

B. The above gel was western blotted using the anti-C-terminal domain IgG (1/500 dilution) as the primary antibody.

Lane 1. Cells ($t_{1/2}$) incubated in the absence of aggregating amounts of IgM antibody

Lane 2. Cells ($t_{1/2}$) incubated in the presence of aggregating amounts of IgM antibody

Lane 3. Bloodstream form trypanosomes treated with H_2O

Fig 5.6. SDS-Polyacrylamide gel electrophoresis of bloodstream form trypanosomes incubated in the presence or the absence of aggregating amounts of anti-VSG IgM antibody.

A. Coomassie stained gel **B. Anti-C-terminal blot**

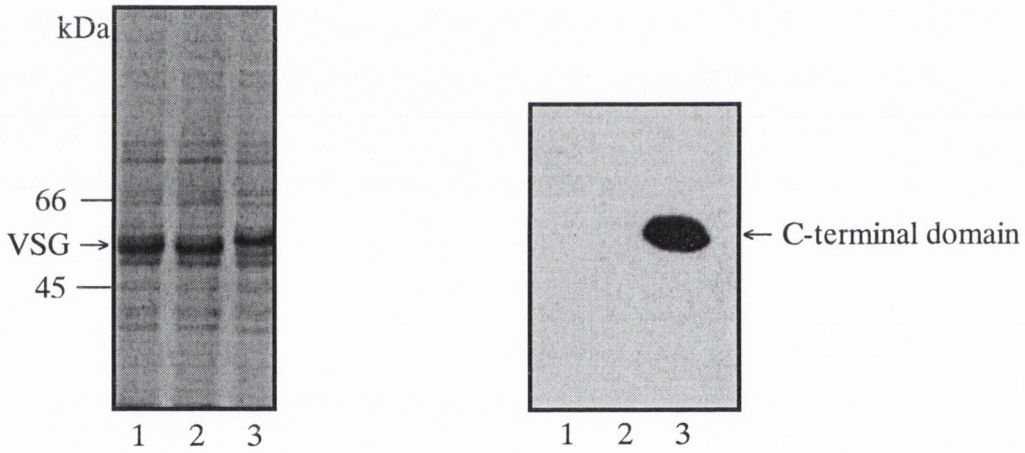

Plate 5.1. Addition of IgG anti-C-terminal domain antibody, anti-CRD antibody and anti-VSG antibody to unfixed cells at 0°C with no aggregating IgM anti-VSG antibody present.

Bloodstream forms of T. brucei (MITat 1.1) were incubated (2 x 10^7 cells/ml) in isosmotic TES buffer (pH 7.5) for 15 minutes at 37°C. The cells were washed into ice-cold TES buffer and incubated with anti-C-terminal, anti-CRD or anti-VSG IgG antibody (1/100 dilution) at 0°C for 30 minutes. Cells were washed free of any unbound antibody and subsequently fixed by the addition of an equal volume of ice-cold paraformaldehyde (3 %, w/v) at 0°C for 10 minutes. Binding of primary antibody to the cells was detected with a Cy3 conjugated anti-rabbit IgG (red fluor). Cells were prepared for confocal microscopy as described in methods (section 2.1.53). Panels A-D show confocal images of cells incubated with no antibody (A), cells incubated with anti-C-terminal IgG (B), cells incubated with anti-CRD IgG (C) and cells incubated with anti-VSG IgG (D). Each panel displays a phase-contrast image of the cell, the protein of interest (red) and a merge of image 1 & 2 with the nucleus and kinetoplast (stained blue).

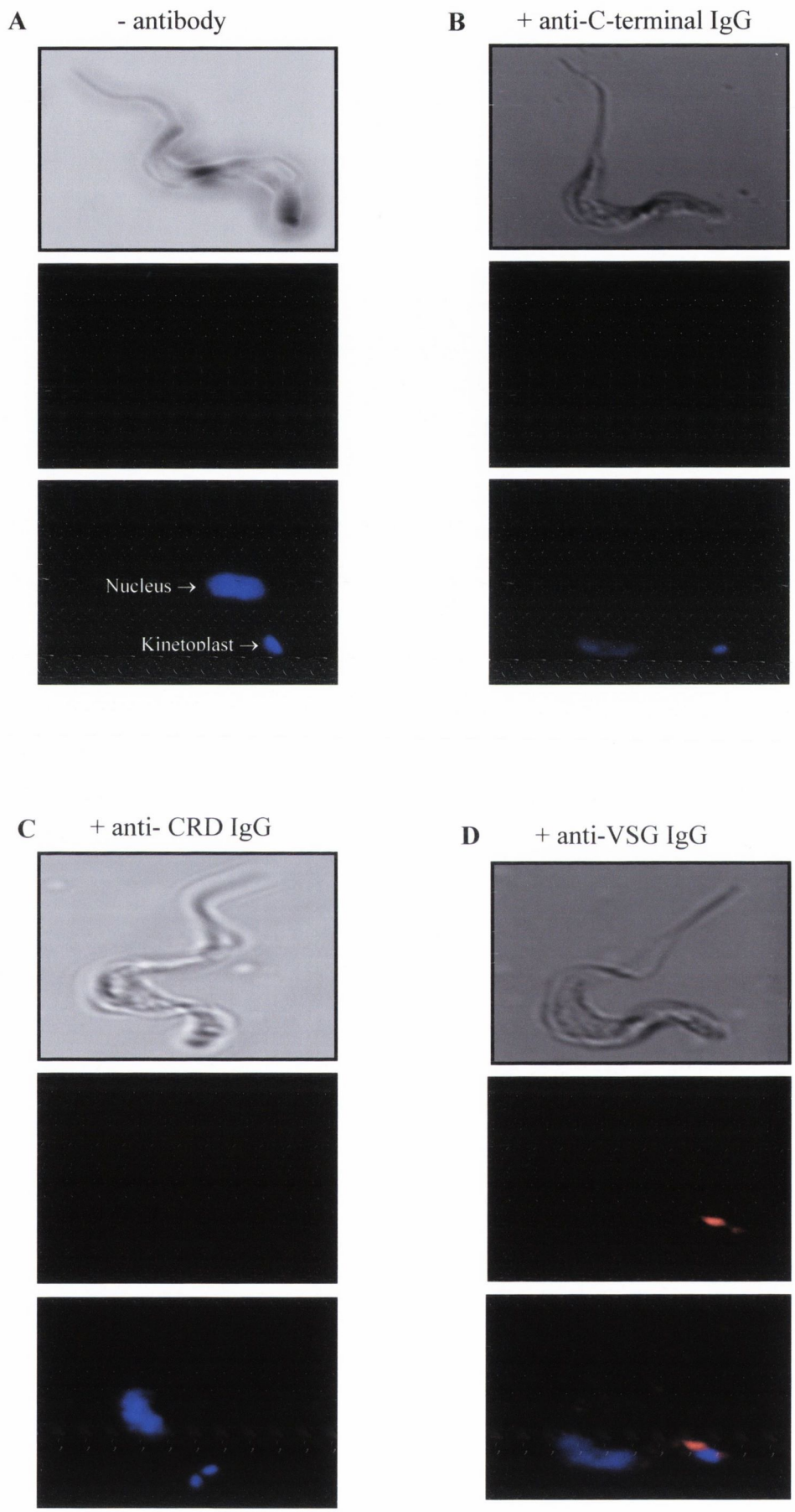
A
- antibody
B
+ anti-C-terminal IgG
Nucleus →
Kinetoplast →
C
+ anti- CRD IgG
D
+ anti-VSG IgG

Plate 5.2. Addition of IgG anti-C-terminal domain antibody, anti-CRD antibody and anti-VSG antibody to unfixed cells at 0°C with aggregating amounts of IgM anti-VSG antibody present.

Bloodstream forms of T. brucei (MITat 1.1) were incubated (2 x 10^7 cells/ml) in isosmotic TES buffer (pH 7.5) for 15 minutes before incubation with an aggregating amount of IgM anti-VSG antibody (5 μg/ml) for 20 minutes at 30°C, at which time the cells were fully disaggregated. Following this incubation the cells were washed into ice-cold TES buffer and incubated with anti-C-terminal, anti-CRD or anti-VSG IgG antibody (1/100 dilution) at 0°C for 30 minutes. Cells were fixed by the addition of an equal volume of ice-cold paraformaldehyde (3 % w/v) at 0°C for 10 minutes. Binding of primary antibody to the cells was detected with a Cy3 conjugated anti-rabbit IgG (red fluor). Cells were prepared for confocal microscopy as described in methods (section 2.1.53). Panels A-D show confocal images of cells following aggregation/disaggregation of trypanosomes with IgM anti-VSG antibody. Panel A shows images of cells incubated with no antibody following aggregation/disaggregation. Panel B shows images of cells incubated with anti-C-terminal IgG, panel C shows images of cells incubated with anti-CRD IgG and panel D shows images of cells incubated with anti-VSG IgG following aggregation/disaggregation with IgM anti-VSG antibody. Each panel displays a phase-contrast image of the cell, the protein of interest (red) and a merge of images 1 & 2 with the nucleus & kinetoplast (stained blue).

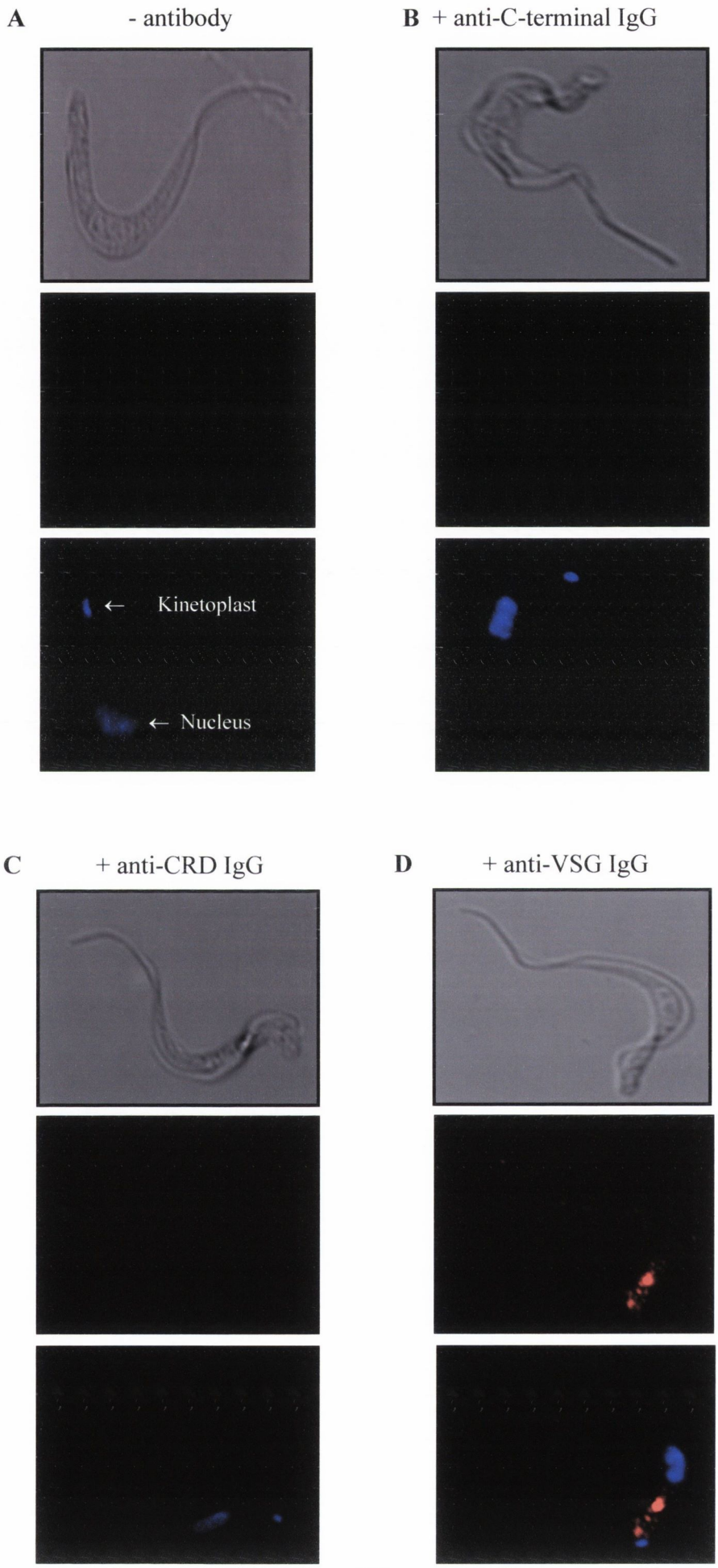
A
- antibody
B
+ anti-C-terminal IgG
← Kinetoplast
← Nucleus
C
+ anti-CRD IgG
D
+ anti-VSG IgG

(Cy3-labelled dipalmitoyl phosphatidyl ethanolamine) at 0°C for 30 minutes. The cells were then washed free of unbound label, combined, brought up to 30°C and incubated in the presence or absence of IgM anti-VSG antibody for 30 minutes. Following this incubation, cells were removed, washed and fixed for confocal microscopy. Plate 5.3 (A & B) shows that there was no transfer of VSG from one cell to another whether cells were incubated with IgM anti-VSG antibody (A) or without IgM anti-VSG antibody (B).

Normal endosomal/lysosomal functioning is required during the mechanism of disaggregation and this points to a mechanism that involves the endocytic/exocytic cycle in some way that is not yet defined (O'Beirne *et al.*, 1998). However, it is clear that even if surface immune complexes are eventually endocytosed, this step cannot occur until any antibody connections that exist between trypanosomes are eliminated. Preliminary experiments were carried out on the endocytic/exocytic cycle of wild-type and GPI-PLC $^-$ mutant trypanosomes. Fig 5.7 shows a typical experiment in which MITat 1.2 trypanosomes were incubated with FITC labelled anti-VSG antibody at 4°C and, following washing, further incubated at 30°C to allow receptor mediated endocytosis to occur. Fig 5.9 shows the same type of experiment but here the trypanosomes are incubated with FITC-labelled transferrin. In all cases, the typical pattern of endocytosis is observed, *i.e.* an initial decrease in fluorescence due to quenching of the fluorescence of the probe upon entering the acidic endosomal compartment of the trypanosome, followed by an increase and overshoot in fluorescence due to proteolysis and exocytosis of the cleaved, FITC-labelled IgG or transferrin into the extracellular medium. The same endo/exocytic cycle for FITC labelled transferrin and FITC labelled anti-VSG antibody was observed in the GPI-PLC $^-$ mutant trypanosomes (Fig 5.8 & 5.10) indicating that the GPI-PLC is not involved in the cycle of endocytosis and exocytosis of either transferrin or surface immune complexes as previously thought (Brabazon, E, Ph.D. Thesis, 1999).

5.2.3 The effects of Sulfydryl blocking reagent on the mechanism of disaggregation in bloodstream form trypanosomes.

Preliminary experiments were carried out into the mechanism of disaggregation in *Trypanosoma brucei.* The effect of iodoacetic acid and iodoacetamide on disaggregation was investigated. It was reported that disaggregation was not due to the separation of immunoglobulin chains and conversion to monomers by either disulfide reduction or disulfide exchange reactions (O'Beirne *et al.*, 1998). However, the possibility remained

Plate 5.3. Addition of FITC-labelled and Cy3-labelled dipalmitoyl phosphatidyl ethanolamine to bloodstream forms of *T. brucei* in the absence or presence of aggregating amounts of IgM anti-VSG antibody.

Bloodstream forms of T. brucei (MITat 1.1) were incubated (2 x 10^7 cells/ml) in isosmotic TES buffer (pH 7.5) for 15 minutes at 30°C with constant gentle stirring. The cells were then washed with ice-cold TES buffer and incubated with FITC-DHPE or Cy3-DHPE for 30 minutes on ice. Following this incubation the cells were washed (x2) to remove unbound label and the two sets of labelled cells were combined. These combined cells were brought up to 30°C and incubated for a further 30 minutes in the absence or presence of aggregating amount of IgM anti-VSG antibody (5 μg/ml). After 30 minutes the cells were washed in an excess of ice-cold TES buffer and subsequently fixed with *p*-formaldehyde (3 %, w/v) at 0°C for 10 minutes. The cells were then prepared for confocal microscopy as described in methods (section 2.1.53). Confocal images of FITC & Cy3-labelled trypanosomes following incubation without IgM anti-VSG antibody are shown in **A**. Confocal images of FITC & Cy3-labelled trypanosomes following incubation with IgM anti-VSG antibody are shown in **B**.

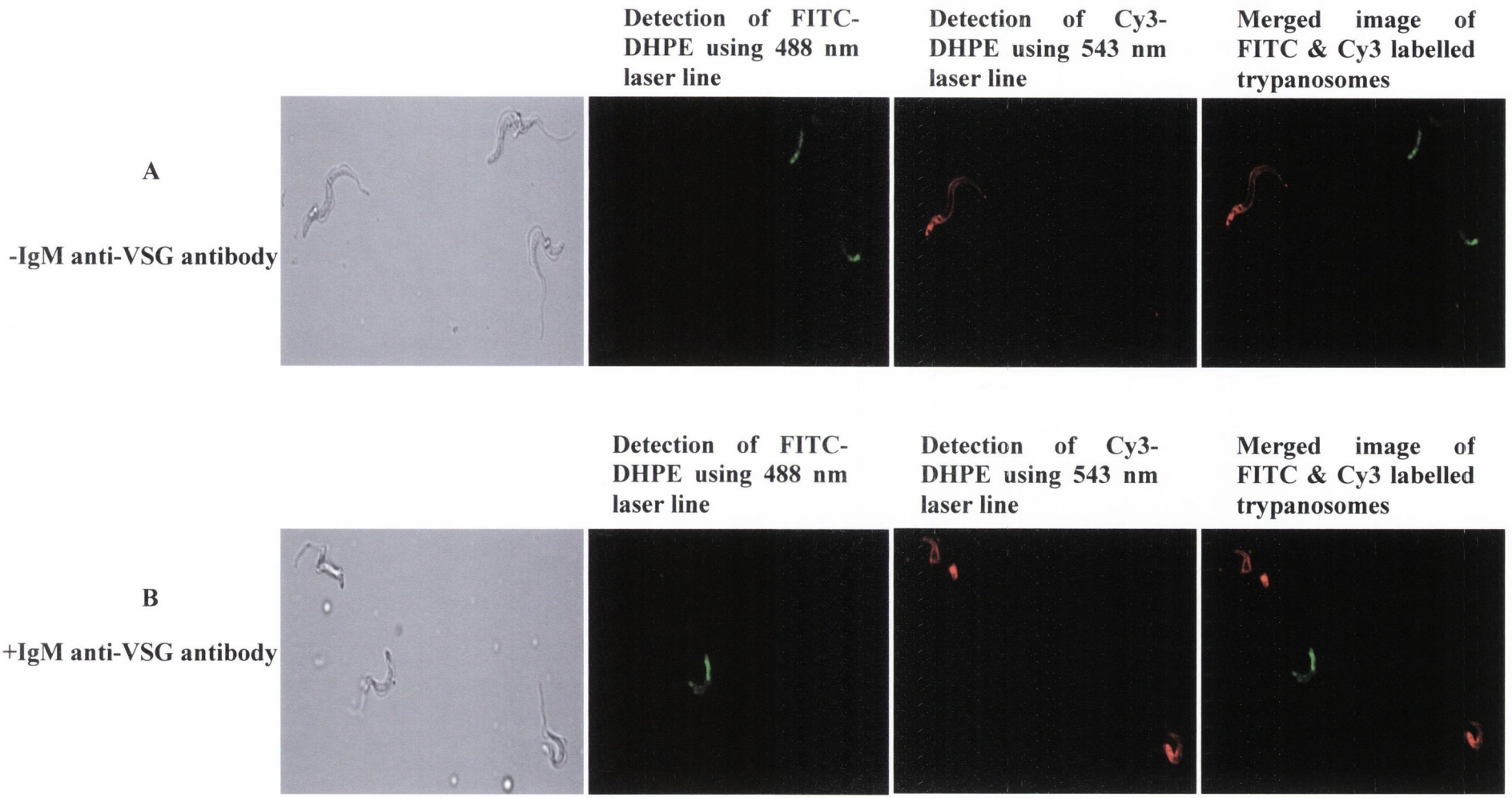
Detection of FITC-DHPE using 488 nm laser line
Detection of Cy3-DHPE using 543 nm laser line
Merged image of FITC & Cy3 labelled trypanosomes
A
-IgM anti-VSG antibody
Detection of FITC-DHPE using 488 nm laser line
Detection of Cy3-DHPE using 543 nm laser line
Merged image of FITC & Cy3 labelled trypanosomes
B
+IgM anti-VSG antibody

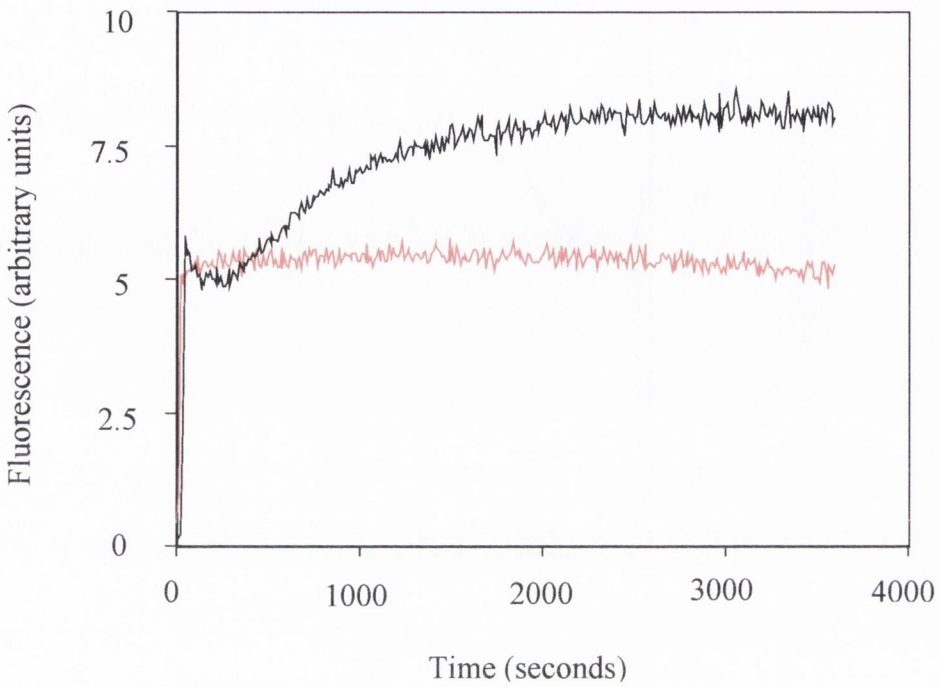

Figure 5.7. Endo-Exocytosis of FITC labelled anti-VSG antibody in the wild-type parent strain of the GPI-PLC $^-$ mutant trypanosomes.

Wild-type trypanosomes (2 x 10^8 cells/ml) were incubated in the presence (black trace) or absence (red trace) of FITC labelled anti-VSG IgG (60µg/2 x 10^8 cells in a final volume of 1 ml) at 4°C for 30 min. The cells were washed (x2) to remove any unbound anti-VSG IgG and incubated at 37°C (3 x 10^7 cells/ml; 3 ml final volume) with constant gentle stirring. The fluorescent intensity was monitored continuously with the excitation wavelength at 476 nm and the emission wavelength at 515 nm. Both excitation and emission slit widths were set at 5 nm and the integration time was one second. All incubations were carried out in a glucose-rich, isosmotic TES buffer, pH 7.4.

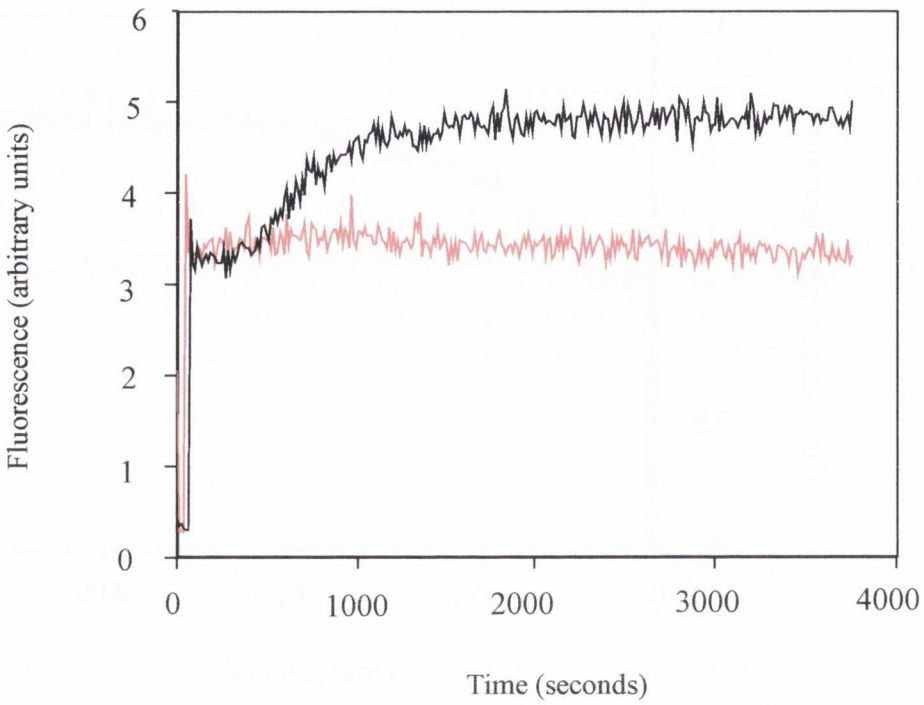

Figure 5.8. Endo/Exocytosis of FITC labelled anti-VSG antibody in GPI-PLC $^-$ mutant trypanosomes.

GPI-PLC $^-$ mutant trypanosomes (2 x 10^8 cells /ml) were incubated in the presence (black trace) or absence (red trace) of FITC labelled anti-VSG antibody (60µg/2 x 10^8 cells in a final volume of 1 ml) at 4°C for 30 min. The cells were washed (x2) to remove any unbound anti-VSG IgG and incubated at 37°C (3 x 10^7 cells/ml; 3 ml final volume) with constant gentle stirring. The fluorescent intensity was monitored continuously with the excitation wavelength at 476 nm and the emission wavelength at 515 nm. Both excitation and emission slit widths were set at 5 nm and the integration time was one second. All incubations were carried out in a glucose-rich, isosmotic TES buffer, pH 7.4.

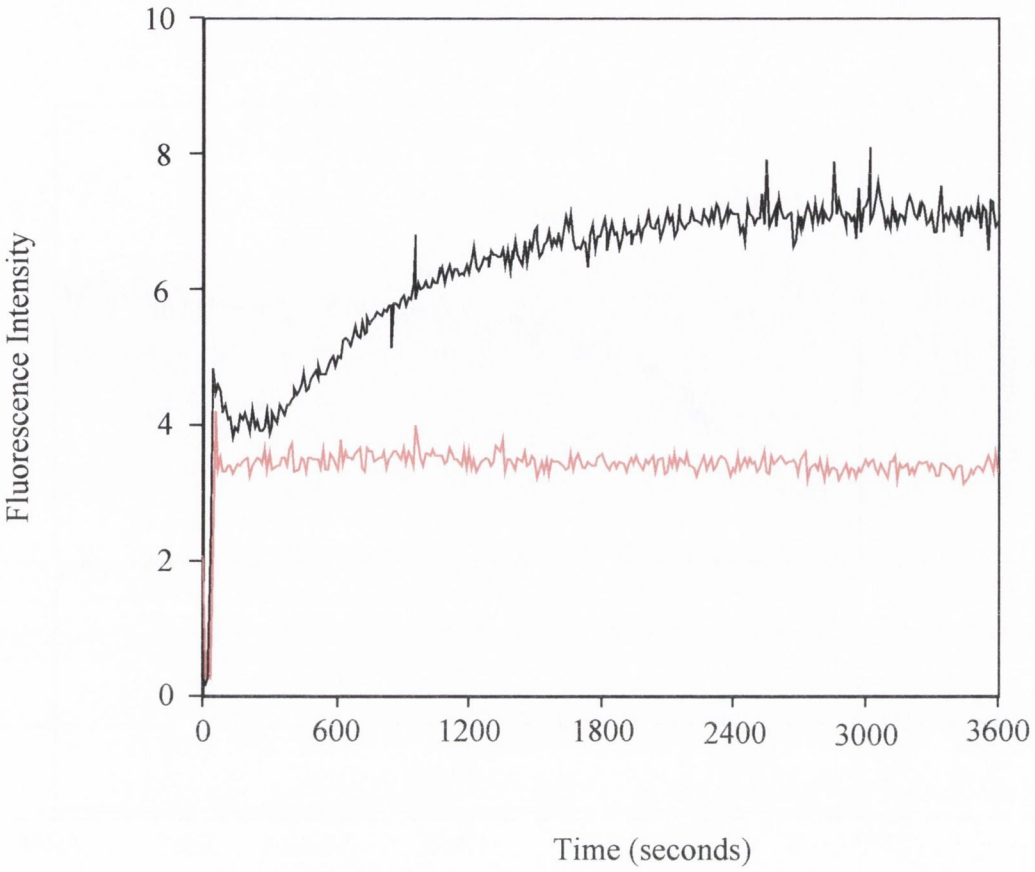

Figure 5.9. Endo-Exocytosis of FITC labelled transferrin in the wild-type parent strain of the GPI-PLC $^-$ mutant trypanosomes.

Wild-type trypanosomes (2 x 10^8 cells/ml) were incubated in the presence (black trace) or absence (red trace) of FITC labelled transferrin (100 µg/2 x 10^8 cells in a final volume of 1 ml) at 4°C for 30 min. The cells were washed (x2) to remove any unbound FITC-labelled transferrin and incubated at 37°C (3 x 10^7 cells/ml; 3 ml final volume) with constant gentle stirring. The fluorescent intensity was monitored continuously with the excitation wavelength at 476 nm and the emission wavelength at 515 nm. Both excitation and emission slit widths were set at 5 nm and the integration time was one second. All incubations were carried out in a glucose-rich, isosmoticTES buffer, pH 7.4.

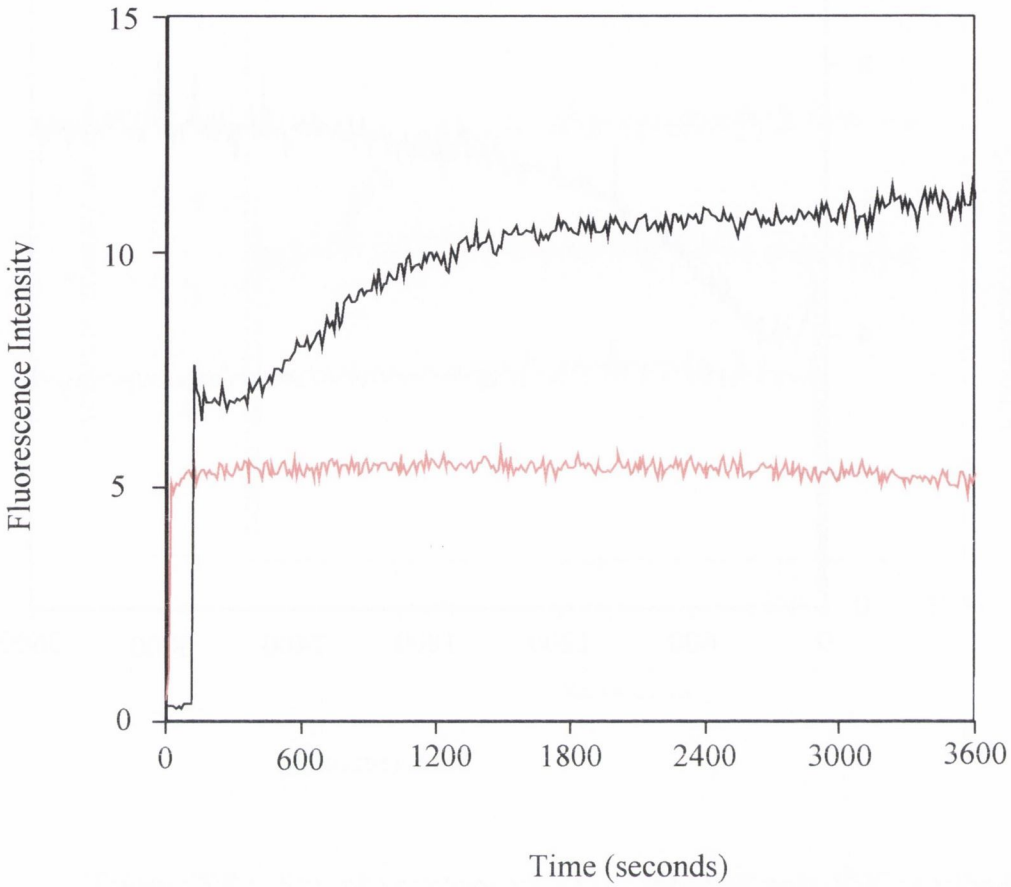

Figure 5.10. Endo/Exocytosis of FITC labelled transferrin in GPI-PLC $^-$ mutant trypanosomes.

GPI-PLC $^-$ mutant trypanosomes (2 x 10^8 cells /ml) were incubated in the presence (black trace) or absence (red trace) of FITC labelled transferrin (100 µg/2 x 10^8 cells in a final volume of 1 ml) at 4°C for 30 min. The cells were washed (x2) to remove any unbound FITC-labelled transferrin and incubated at 37°C (3 x 10^7 cells/ml; 3 ml final volume) with constant gentle stirring. The fluorescent intensity was monitored continuously with the excitation wavelength at 476 nm and the emission wavelength at 515 nm. Both excitation and emission slit widths were set at 5 nm and the integration time was one second. All incubations were carried out in a glucose-rich, isosmotic TES buffer, pH 7.4.

that a disulfide exchange reaction within the VSG molecule had occurred that "scrambled" the disulfide pairs altering the conformation of the VSG, and reducing the affinity of the VSG for the antibody. Iodoacetic acid and iodoacetamide are alkylating agents; the reaction of thiols (-SH) with both can be rapid and is irreversible under all conditions; so the modified species are stable. During disulfide exchange reactions, free thiols are formed transiently. If iodoacetic acid or iodoacetamide is present at this time, it will react with the free thiols and therefore prevent completion of the disulfide interchange reaction. If indeed, disulfide exchange reactions are required for disaggregation of aggregated cells then the reaction of iodoacetic acid or iodoacetamide with free thiols will block disaggregation.

It was observed that disaggregation was inhibited when MITat 1.1 cells were incubated with anti-VSG IgM (5 μg/ml) in the presence of iodoacetic acid (5 μM) (Fig 5.11). The fact that such a small amount of this substance could have such a huge effect on the cells was surprising. To ensure that the cells remained in good shape and that their respiration was not being affected as a result of the reaction, their oxygen consumption was measured. MITat 1.1 trypanosomes were incubated at 37°C in a final stirred volume of 4 ml in an O_2 electrode chamber. The experiment was initiated by the addition of IgM antibody in the presence of iodoacetic acid. It was found that the O_2 consumption decreased by 50% in the presence of iodoacetic acid (Fig 5.12). It was concluded after this result that iodoacetamide might be a better candidate than iodoacetic acid. It was found that iodoacetamide also inhibited disaggregation in bloodstream form trypanosomes (Fig 5.13 & 5.14). However, 50μM iodoacetamide was required compared to the 5 μM of iodoacetic acid used previously. Furthermore, iodoacetamide (50 μM) was found to have no effect on the O_2 consumption of trypanosomes during the course of dissaggregation (Fig 5.15). Consumption of O_2 was measured for 25 minutes; the time course for disaggregation is 20 minutes. The effect of iodoacetamide on the O_2 consumption of cells alone (-IgM) was also measured over the same time course without any change in O_2 consumption (Fig 5.15).

To determine whether iodoacetamide had an irreversible effect on the disaggregation of bloodstream form trypanosomes, the following experiment was undertaken. Firstly, cells (2×10^7 /ml) in TES buffer (pH 7.4) were incubated in the presence of aggregating amounts of anti-VSG antibody at 37°C for 15 min, with constant gentle stirring. Following this, the cells were added to ice-cold TES buffer, pH 7.4 (x3) and centrifuged (9,000 rpm, 2 min). The resulting pellet was resuspended in TES buffer,

Fig. 5.11 The effect of iodoacetic acid on the cycle of aggregation-disaggregation that occurs when bloodstream forms of *T. brucei* are incubated with purified IgM anti-VSG antibodies.

Bloodstream forms of *T. brucei* (MITat 1.1) were incubated (4×10^7 cells/ml) for 15 min in isosmotic TES buffer (pH 7.5, 37°C). The experiment was initiated by the addition of IgM antibody (5μg/ml final incubation; stock antibody solution, 1.9 mg ml^{-1}) to the incubation medium, either in the absence (■) or presence (♦) of iodoacetic acid (5μM, final incubation; stock solution, 5mM). At the times indicated samples were withdrawn from the incubation medium and the percentage of aggregated cells was determined as described in methods. The experiment was repeated eight times on three separate occasions and gave similar results on each occasion. The data in the figure is a representative result drawn form one of these experiments.

Fig. 5.11 The effect of iodoacetic acid on the cycle of aggregation-disaggregation that occurs when bloodstream forms of *T. brucei* are incubated with purified IgM anti-VSG antibodies.

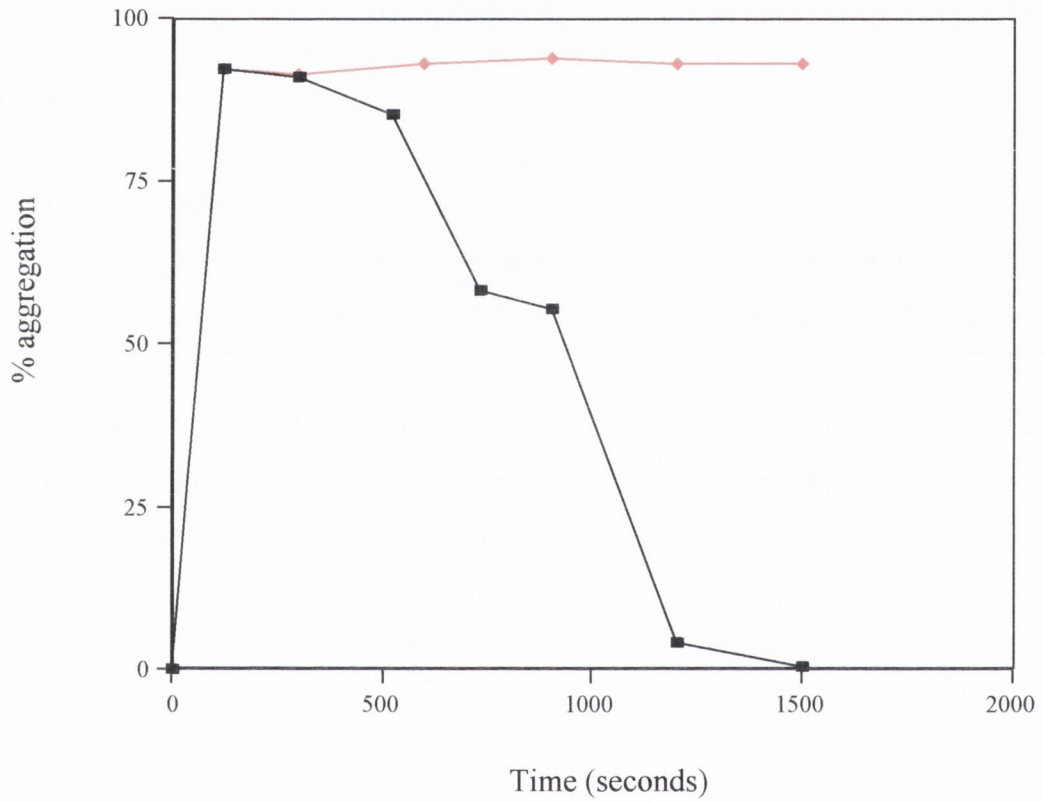

Fig 5.12. The effect of iodoacetic acid on glucose supported aerobic respiration of bloodstream forms of *T. brucei*.

Bloodstream forms of *T. brucei* (MITat 1.1) were incubated (2×10^7 ml^{-1}) in isosmotic TES buffer (pH 7.5) at 37°C in a final stirred volume of 4 ml. The experiment was initiated by the addition of IgM antibody (5 μg/ml final incubation; stock antibody solution, 1.9 mg ml^{-1}) to the incubation medium, either in the absence or presence of iodoacetic acid (5 μM, final incubation; stock solution, 1 mM). O_2 consumption was measured during (in-flight) disaggregation. Results represent the mean ± SD of three separate experiments.

Fig 5.12. The effect of iodoacetic acid on glucose supported aerobic respiration of bloodstream forms of *T. brucei*.

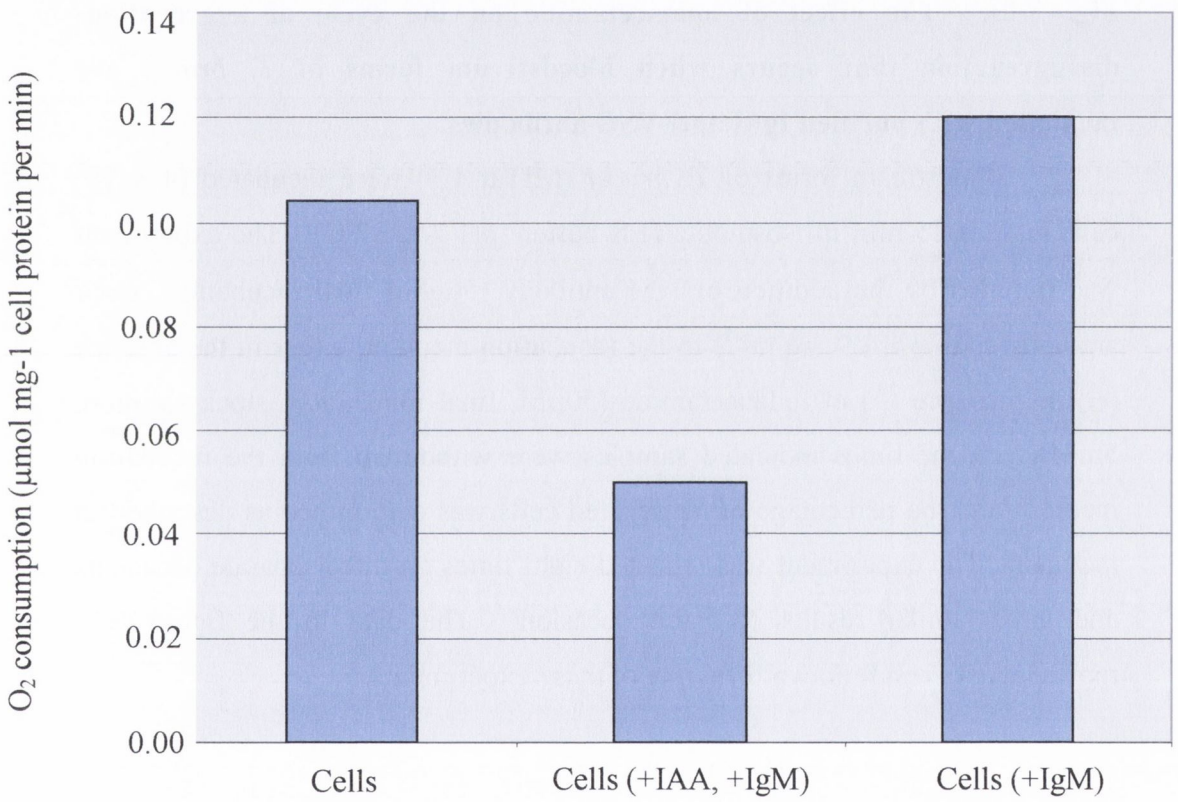

Fig. 5.13. The effect of iodoacetamide on the cycle of aggregation-disaggregation that occurs when bloodstream forms of *T. brucei* are incubated with purified IgM anti-VSG antibodies.

Bloodstream forms of *T. brucei* (MITat 1.1) were incubated (4 x 10^7 cells/ml) for 15 min in isosmotic TES buffer (pH 7.5, 37°C). The experiment was initiated by the addition of IgM antibody (5μg/ml final incubation; stock antibody solution, 1.9 mg ml^{-1}) to the incubation medium, either in the absence (□) or presence (◊) of iodoacetamide (50μM, final incubation; stock solution, 5mM). At the times indicated samples were withdrawn from the incubation medium and the percentage of aggregated cells was determined as described in methods. The experiment was repeated eight times on three separate occasions and gave similar results on each occasion. The data in the figure is a representative result drawn form one of these experiments.

Fig. 5.13. The effect of iodoacetamide on the cycle of aggregation-disaggregation that occurs when bloodstream forms of *T. brucei* are incubated with purified IgM anti-VSG antibodies.

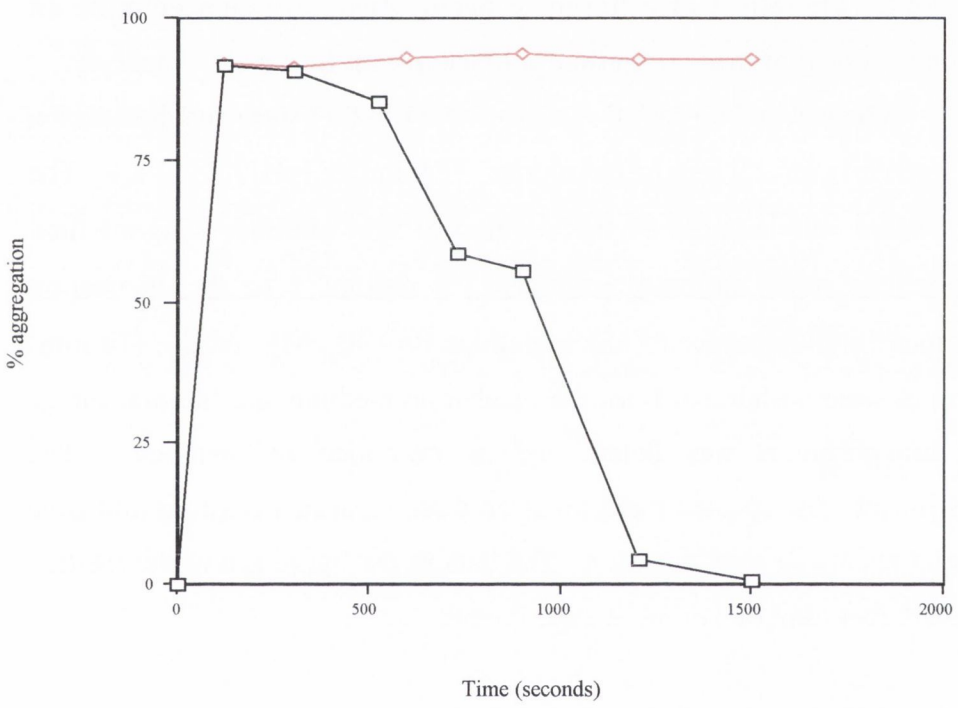

Fig 5.14. The effect of different concentrations of iodoacetamide on the mechanism of disaggregation in bloodstream forms of *T. brucei*.

Bloodstream forms of *T. brucei* (MITat 1.1) were incubated (4 x 10^7 cells/ml) for 15 min in isoosmotic TES buffer (pH 7.5, 37°C). The experiment was initiated by the addition of IgM antibody (5μg/ml final incubation; stock antibody solution, 1.9 mg ml^{-1}) to the incubation medium, in the presence of iodoacetamide (0 – 40 μM). At $t_{1/2}$ (10 min) samples were withdrawn from the incubation medium and the percentage of disaggregation was determined as described in methods. The experiment was repeated three times on three separate occasions and gave similar results on each occasion. The data in the figure is a representative result drawn form one of these experiments.

Fig 5.14. The effect of different concentrations of iodoacetamide on the mechanism of disaggregation in bloodstream forms of *T. brucei*.

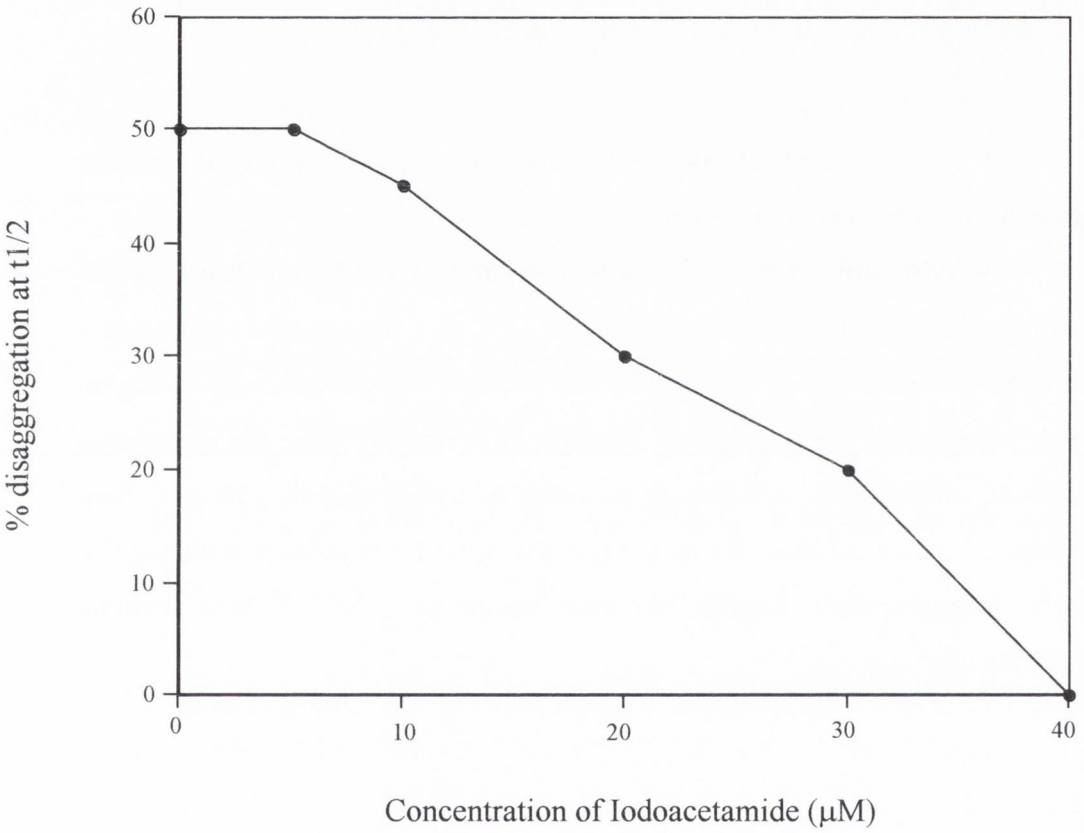

Fig 5.15. The effect of iodoacetamide on glucose supported aerobic respiration of bloodstream forms of *T. brucei*.

Bloodstream forms of *T. brucei* (MITat 1.1) were incubated (2 x 10^7 ml^{-1}) in isosmotic TES buffer (pH 7.5) at 37°C in a final stirred volume of 4 ml. The experiment was initiated by the addition of IgM antibody (5 μg/ml final incubation; stock antibody solution, 1.9 mg ml^{-1}) to the incubation medium, either in the absence or presence of iodoacetamide (50 μM, final incubation; stock solution, 5 mM). O_2 consumption was measured during (in-flight) disaggregation. Results represent the mean ± SD of three separate experiments.

Fig 5.15. The effect of iodoacetamide on glucose supported aerobic respiration of bloodstream forms of *T. brucei*.

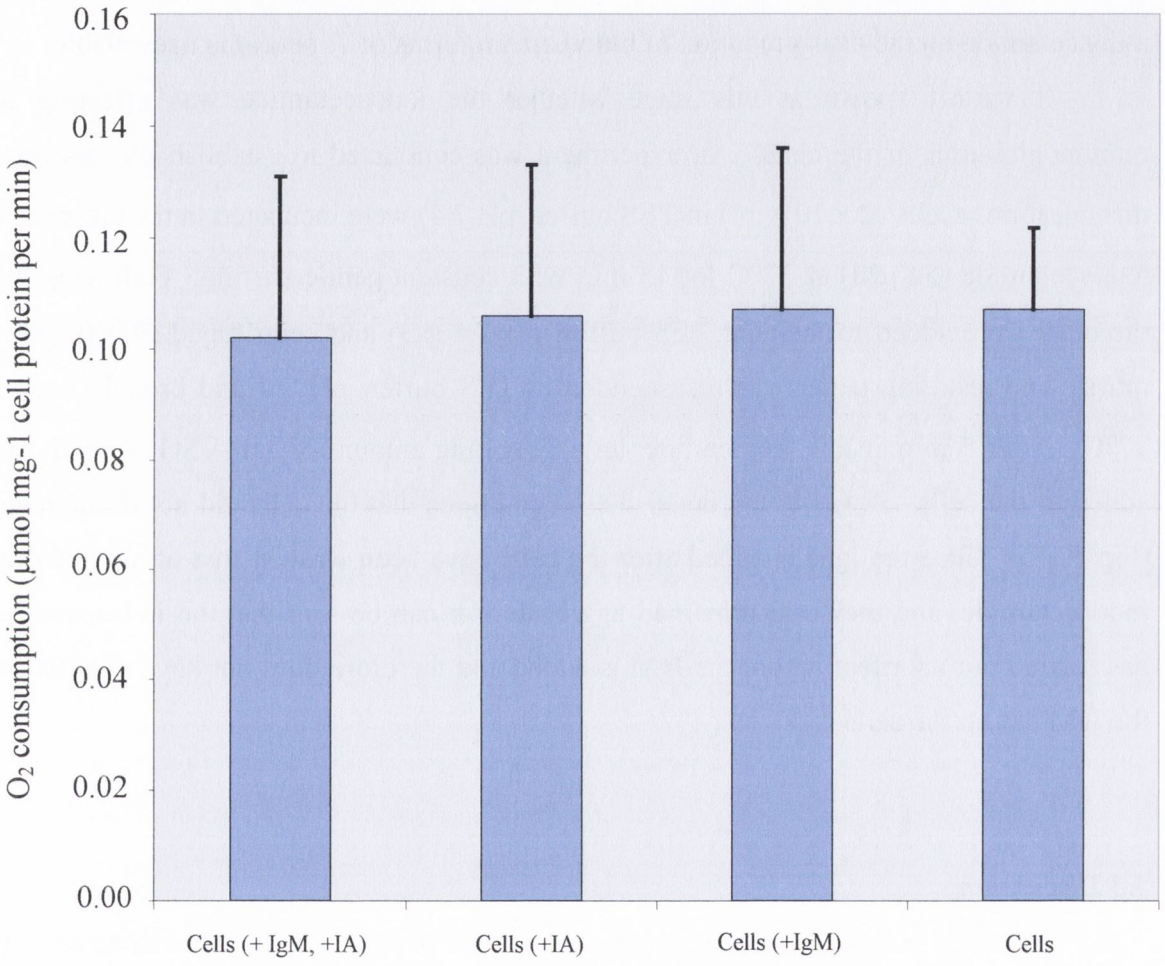

pH 7.4 and brought back to 37°C. It was observed that the cells disaggregated with a half time of 15 minutes. Second, cells (2 x 10^7 /ml) in TES buffer (pH 7.4) were incubated in the presence of aggregating amounts of anti-VSG antibody and iodoacetamide (50 μM) at 37°C for 15 min, with constant gentle stirring. Following this, the cells were added to ice-cold TES buffer, pH 7.4 (x3) and centrifuged (9,000 rpm, 2 min). The resulting pellet was resuspended in TES buffer, pH 7.4 and brought back to 37°C. It was observed that the cells remained aggregated indefinitely (Fig 5.16). This suggests that the effect of iodoacetamide on the disaggregation of bloodstream forms of *T. brucei* is irreversible.

It wasn't known at this stage whether the iodoacetamide was affecting the immunoglobulins or the cells. An experiment was conducted to establish the answer to this question. Cells (2 x 10^7 /ml) in TES buffer (pH 7.4) were incubated in the presence of iodoacetamide (50 μM) at 37°C for 15 min with constant gentle stirring. Following this, the cells were added to ice-cold TES buffer, pH 7.4 (x3) and centrifuged (9,000 rpm, 2 min). The resulting pellet was resuspended in TES buffer, pH 7.4 and brought back to 37°C. After 5 min at this temperature, an aggregating amount of anti-VSG antibody was added to the cells. It was found under these conditions that the cells did not disaggregate (Fig 5.17). Since the IgM is added after the cells have been washed free of any unbound iodoacetamide, and they still remained aggregated, it can be said that the iodoacetamide has carried out its affect before the IgM is added and therefore does not have an affect on the IgM but on the cells.

5.3 Discussion

A number of different processes were studied in this chapter in order to reveal a possible function for the GPI-PLC in bloodstream form trypanosomes *in-vivo*. The function of the GPI-PLC in *T. brucei* has been the cause of much speculation, as the enzyme has an activity that could theoretically facilitate the rapid shedding of the protective VSG coat. There are roughly 3 x 10^4 molecules of this enzyme per cell (Hereld *et al.*, 1986). At an estimated turnover rate of 100 – 700 mfVSG molecules per minute under assay conditions (Hereld *et al.*, 1986) there is sufficient GPI-PLC to release the entire coat in a few minutes, as occurs on hypotonic lysis of trypanosomes. The VSG is the only substrate present in amounts sufficient to account for the quantity of enzyme present. The VSG and the GPI-PLC show the same developmentally regulated expression, being found in bloodstream but not in procyclic trypanosomes (Carrington *et al.*, 1989).

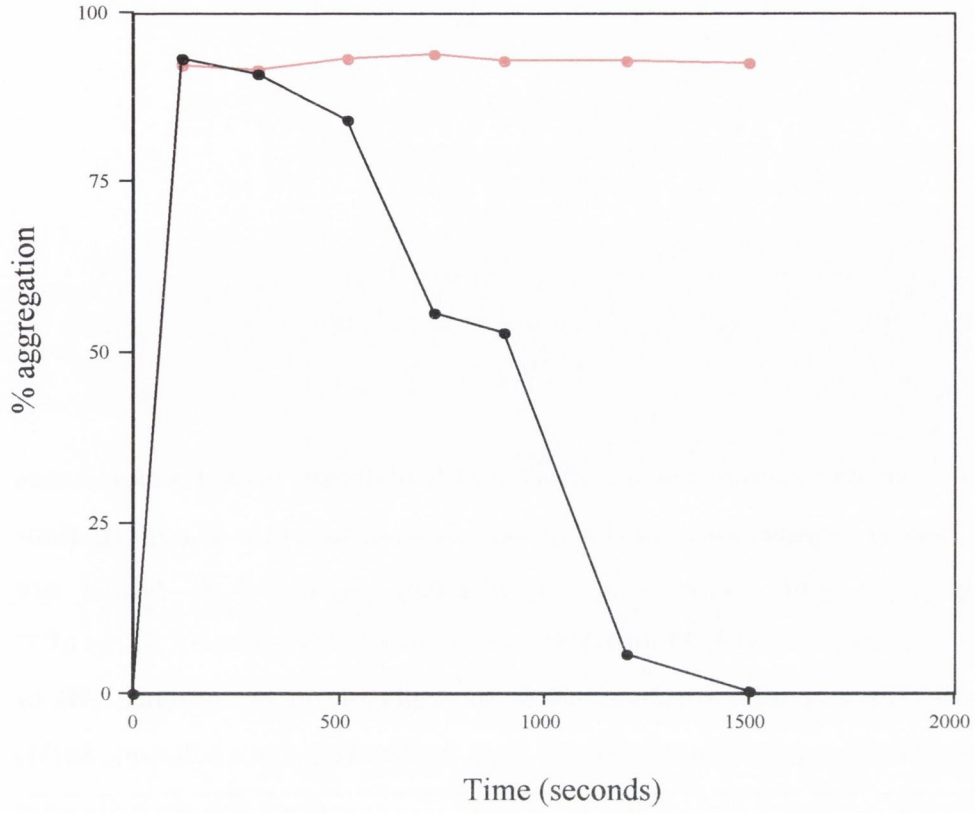

Fig. 5.16. Iodoacetamide has an irreversible affect on the cycle of aggregation-disaggregation that occurs when bloodstream forms of *T. brucei* are incubated with purified IgM anti-VSG antibodies.

Bloodstream forms of *T. brucei* (MITat 1.1) were incubated (4 x 10^7 cells/ml) with IgM antibody (5μg/ml final incubation; stock antibody solution, 1.9 mg ml^{-1}) in the absence (•) or presence (•) of iodoacetamide (50μM, final incubation; stock solution, 5mM) for 15 min in isosmotic TES buffer (pH 7.5, 37°C). Following this the cells were added to an excess of ice-cold Tes buffer and centrifuged. The resulting pellets were resuspended in TES buffer and brought back to 37°C. At the times indicated samples were withdrawn from the incubation medium and the percentage of aggregated cells was determined as described in methods. The experiment was repeated three times on three separate occasions and gave similar results on each occasion. The data in the figure is a representative result drawn form one of these experiments.

Fig. 5.17. Iodoacetamide has an affect on bloodstream form trypanosomes rather than the aggregating IgM antibody during the cycle of aggregation-disaggregation that occurs when bloodstream forms of *T. brucei* are incubated with purified IgM anti-VSG antibodies. Bloodstream forms of *T. brucei* (MITat 1.1) were incubated (4 x 10^7 cells/ml) in the absence (■) or presence (■) of iodoacetamide (50μM, final incubation; stock solution, 5mM) for 15 min in isosmotic TES buffer (pH 7.5, 37°C). Following this the cells were added to an excess of ice-cold TES buffer and centrifuged. The resulting pellets were resuspended in TES buffer and brought back to 37°C. After 5 minutes at this temperature IgM antibody (5μg/ml final incubation; stock antibody solution, 1.9 mg ml^{-1}) was added. At the times indicated samples were withdrawn from the incubation medium and the percentage of aggregated cells was determined as described in methods. The experiment was repeated three times on three separate occasions and gave similar results on each occasion. The data in the figure is a representative result drawn form one of these experiments.

Fig. 5.17. Iodoacetamide has an affect on bloodstream form trypanosomes rather than the aggregating IgM antibody during the cycle of aggregation-disaggregation that occurs when bloodstream forms of *T. brucei* are incubated with purified IgM anti-VSG antibodies.

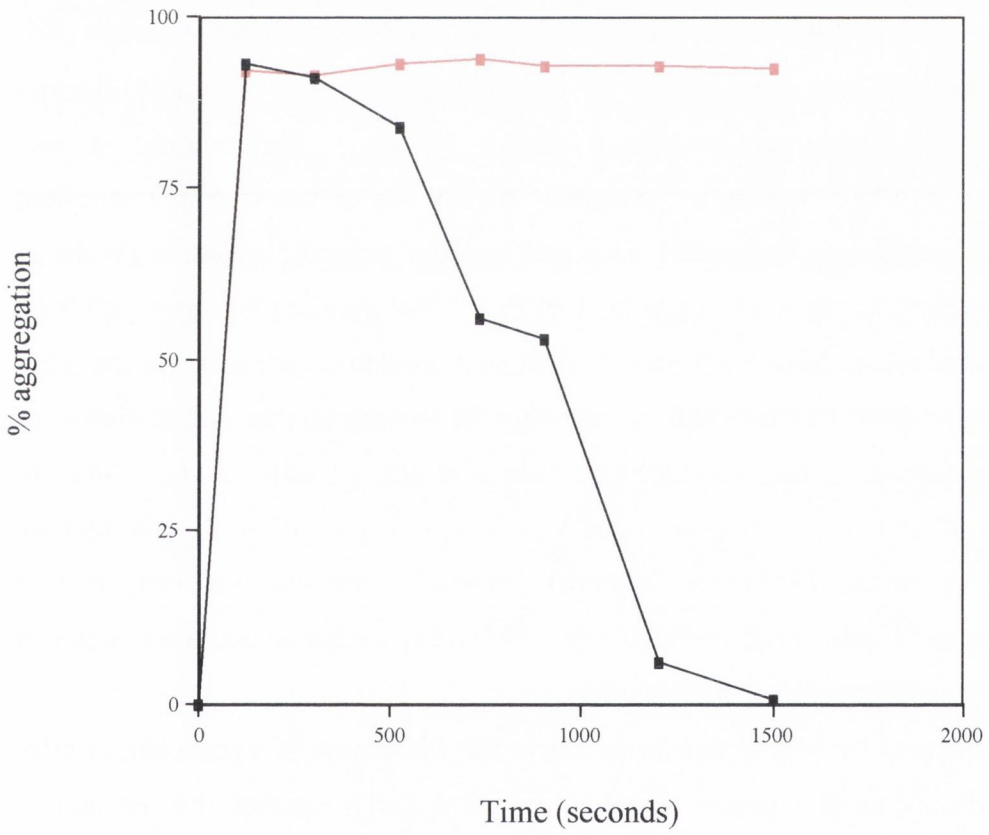

The most direct approach to revealing the function of the GPI-PLC was to use a GPI-PLC null mutant in parallel experiments with the wild type trypanosomes. In the present study it was demonstrated that the release of the VSG does not occur in GPI-PLC $^-$ mutant trypanosomes that lack the gene for the GPI-PLC. The CRD epitope did not become exposed upon hypotonic lysis of mutant trypanosomes and the mfVSG was not converted to sVSG (Fig 5.1). Thus it is clear that in wild type cells VSG release is mediated through the action of the GPI-PLC. This confirms previous results from different laboratories (Rolin *et al.*, 1996, Cardoso de Almeida, 1983). This experiment provides the evidence that there is no other enzyme that metabolises the GPI-anchor on a substantial scale.

The normal cellular function of the GPI-PLC is unknown despite intensive study. The enzyme does not appear to be essential for normal differentiation to procyclic forms (Webb *et al.*, 1997), when the surface VSG is released by proteolytic cleavage (Bulow *et al.*, 1989 & Ziegelbauer, 1993) and replaced by a small family of GPI-PLC resistant GPI-anchored proteins that are characterised by glutamate-proline-rich (EP) and glycine-proline-glutamate-glutamate-threonine-rich (GPEET) repeats. Furthermore, it was revealed that the GPI-PLC $^-$ mutant trypanosomes are capable of maintaining a persistent infection in immunologically competent mice and undergo antigenic variation (Webb *et al.*, 1997). This result clearly showed that the GPI-PLC is not required for the switch from metacyclic to bloodstream form VSG or for subsequent antigenic variation. On the other hand, it has been reported that GPI-PLC is necessary for the accelerated differentiation of pleomorphic trypanosomes that is induced by mild acid stress (Rolin *et al.*, 1998). In addition, since constitutive GPI-PLC-mediated VSG release is part of the parasite biology (Shapiro, 1986 & Black, 1982) and improper control of the enzyme hampers GPI metabolism (Mensa-Wilmot *et al.*, 1994 & Garg, 1997) it is anticipated that interference in GPI-PLC control could impair parasite viability.

The mechanism by which transferrin enters the cytoplasm of trypanosomes after binding to a GPI-anchored receptor is not clear, particularly whether the receptor is released from a membrane and how the occupancy of the receptor is signalled across the plasma membrane. It has been proposed that the GPI-PLC may be involved in the hydrolysis of the GPI-anchor of the transferrin receptor and therefore have a role in the endocytosis of the transferrin into trypanosomes. The process of endocytosis and exocytosis of both FITC labelled transferrin and FITC labelled anti-VSG IgG was examined in wild-type and GPI-PLC $^-$ mutant trypanosomes. Both sets of cells revealed

the same pattern of endo/exocytosis for the transferrin and anti-VSG antibody using a fluorometric assay (Fig 5.7, 5.8, 5.9 & 5.10). These results suggest that the GPI-PLC is not involved in the process of endocytosis or exocytosis in bloodstream form trypanosomes.

The process of disaggregation in bloodstream form trypanosomes following aggregation with anti-VSG antibody is an attractive process for the GPI-PLC to have a potential role. The mechanism by which trypanosomes disaggregate is not known. We proposed that the GPI-PLC be involved in cleaving the GPI anchor of the VSG in aggregated trypanosomes thereby allowing them to disaggregate. If the GPI-PLC performed this function then the CRD epitope would become exposed. Initial experiments provided us with the answer immediately. The GPI-PLC $^{-}$ mutant trypanosomes disaggregated with the same time-course of disaggregation as the wild type cells, indicating that the GPI-PLC is not required for the process. In addition, the VSG was not released from cells at any point during the process and the CRD did not become exposed. Given that the CRD-epitope did not become exposed upon disaggregation we explored the theory that the GPI anchor of the VSG was being cleaved by another mechanism. Fig 5.4 shows the other possible cleavage sites on the GPI-anchor of the VSG. We considered the possibility that the GPI-PLD might have a role in the process of disaggregation. Phospholipase D (PLD) hydrolyzes the phosphodiester bond of the glycerolipid phosphatidylcholine, resulting in the production of phosphatidic acid and free choline. If trypanosomes were using this enzyme to cleave the GPI anchor of the VSG the CRD epitope would not become exposed but the C-terminal domain would be detected. This domain is never detected in living cells when probed with an anti-C-terminal domain antibody. When this was investigated it was shown that detection of the C-terminal domain remained negative as it is in living cells indicating that GPI-PLD is not involved in disaggregation of bloodstream forms of *T. brucei*. These results indicated that the VSG GPI-anchor was not being cleaved at any point where the CRD epitope or the C-terminal domain would be exposed and it was not being transferred from one cell to another when disaggregation was taking place. How do bloodstream form trypanosomes disaggregate and evade the host immune system after they have become aggregated with the hosts' antibodies? What is the mechanism of disaggregation?

The phenomenon of disaggregation has been investigated by many workers in the past (Laveran & Mesnil, 1900, 1901 & 1907; Francis, 1903 and O'Beirne 1998) and as yet no mechanism for the process has been proposed. While all of the evidence from these

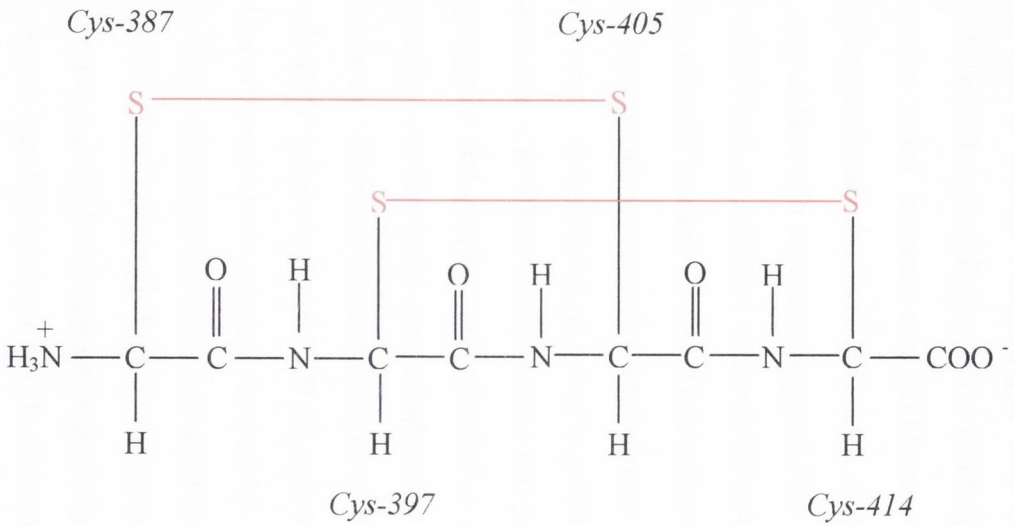

Fig 5.18. An example of disulfide bond formation between cysteine residues in the C-terminal region of the mature form of MITat 1.1 VSG

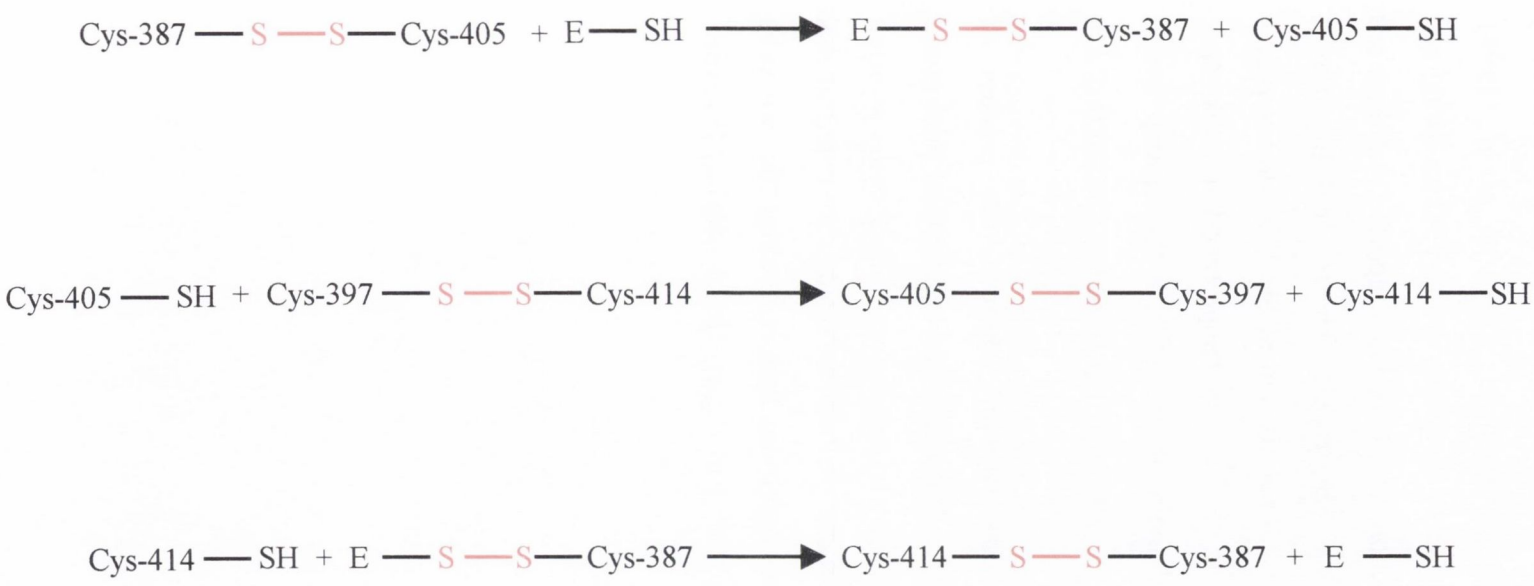

Fig 5.19. Mechanism for the enzyme catalyzed disulfide interchange reaction in the C-terminal region of the mature form of MITat 1.1 VSG. Protein disulfide isomerase catalyses disulfide interchange reactions. PDI itself contains two active site Cys residues, which must be in the –SH form for the isomerase to be active. The enzyme catalyses the random cleavage and reformation of a protein's disulfide bonds thereby interchanging them as the protein progressively attains thermodynamically more favourable conformations.

workers strengthened the case for a regulated physiological process that led to disaggregation and eliminated several possible mechanisms, it did not identify any specific protein or enzyme responsible for the process itself. It was reported that disaggregation was not due to the separation of immunoglobulin chains and conversion to monomers by either disulfide reduction or disulfide exchange reactions (O'Beirne *et al.*, 1998). However, could it possibly be due to the exchange of disulfides in the VSG molecule and hence, the conversion of the VSG dimers to monomers? It has been reported that there are no free thiols in the C-terminal domain of the VSG (Biggs, MSc Thesis, 2000) therefore it can be concluded that the free thiols in the C-terminal domain of the VSG do not play a role in the disaggregation of cells. However, if disulfide exchange reactions took place within the C-terminal domain or any other domain of the VSG, a thiol group would become available transiently for the reaction with the sulfydryl-blocking reagent (see Fig 5.18 & 5.19).

The sulfhydryl blocking reagent, iodoacetamide, inhibited the process of disaggregation completely. Consequently, this result implies that an essential thiol group is involved in the disaggregation of bloodstream form trypanosomes. The specific location of this thiol group is as yet unknown but from the preliminary results presented in this chapter it is on the cell and not on the immunoglobulin that is binding the two cells together. The role of the protein disulfide isomerase, particularly the glycosylated enzyme, requires further study.

Chapter 6

Cloning, purification and characterization of the MBP-TbGPI-PLC fusion protein.

6.1. Introduction

Chapter four described how the GPI-PLC in bloodstream from trypanosomes and the purified recombinant GPI-PLC did not react with the biotinylating reagent, sulfo-NHS-biotin. This result led to further studies on the recombinant protein to determine why the protein could not be labeled with the biotinylating reagent. The GPI-PLC was expressed with maltose binding protein as a fusion protein. The pMAL-2 vectors provide a method for expressing and purifying a protein produced from a cloned gene or open reading frame. The cloned gene is inserted downstream from the malE gene of *E. coli*, which encodes maltose-binding protein (MBP), resulting in the expression of an MBP fusion protein. The method uses the strong "tac" promoter and the malE translation initiation signals to give high-level expression of the cloned sequences, and a one-step purification of the fusion protein using MBP's affinity for maltose. The pMAL-2 vectors also contain the sequence coding for the recognition site of a specific protease, located just 5´ to the polylinker insertion sites. This construct allows MBP to be cleaved from the protein of interest after purification. The pMAL-c2 (a kind gift from Amir Khan, department of Biochemistry, Trinity College Dublin) vector used in this study encodes the site for TEV (Tobacco Etch Virus) protease. TEV protease recognizes a linear epitope of the general form E-Xaa-Xaa-Y-Xaa-Q-(G/S), with cleavage occurring between Q and G or Q and S. The most commonly used sequence is ENLYFQG.

This chapter describes the cloning, expression, purification and characterization of the MBP-TbGPI-PLC fusion protein.

6.2. Results.

6.2.1. Cloning of the MBP-TbGPI-PLC

6.2.1.(a) PCR amplification of GPI-PLC from trypanosoma brucei

Primers were designed with standard criteria using cDNA sequence data for the GPI-PLC. The cDNA clone was used as template DNA. *Bam*H1 (NEB) and *Xho*1 (NEB) restriction sites were incorporated into the ends of each primer in order to facilitate ligation of the ORF into the vector at a later stage.

GPI-PLC forward primer:

5' AGG GAT CCTTTGGTGTAAAGTGGTCACCGCAG 3'

Note: *Bam*H1 site underlined

GPI-PLC reverse primer:

5' AGC AAC TCG AGTTATGACCTTGCGGTTTGGTTGGT 3'

Note: *Xho*1 site underlined

Using standard cycling conditions (Chapter 2, Table 2.6), GPI-PLC was amplified by PCR and then separated by electrophoresis on a 1 % (w/v) agarose gel and stained with ethidium bromide to verify the successful amplification of the gene before proceeding (Fig 6.1 A).

6.2.1. (b) Restriction digestion of GPI-PLC product.

The silica spin column purified GPI-PLC PCR product (50 µl) and pMAL-c2 vector were digested with 1 unit of *Bam*H1 and *Xho*1 in separate reactions using standard conditions. Digested fragments were removed by spin column purification and dissolved in 50 µl of deionised water. Both the cut vector and cut insert were further purified by gel purification to increase the efficiency of vector insert recombination. A sample of these purified DNA fragments were separated by agarose gel electrophoresis prior to ligation to determine their relative concentration (Fig 6.1.B).

6.2.1.(c) Ligation of GPI-PLC into pMAL-c2 and transformation of DH5α.

Digested GPI-PLC was ligated into the digested pMAL-c2 expression vector under standard conditions using a molar ratio of 5:1 insert to vector. Competent DH5α cells were generated and transformed with 5 µl of ligation reaction under standard conditions.

6.2.1. (d) Analysis of transformants and selection of clones.

Six putative positive clones were selected and grown overnight in a 10 ml LB broth in the presence of ampicillin to maintain selection. Plasmids were extracted from these by

miniprep preparation and digested using 1 unit of *Bam*H1 and *Xho*1 to determine whether they contained the GPI-PLC gene (Fig 6.1 C).

6.2.2. Expression of recombinant MalE-TbGPI-PLC in bacteria.

Competent BL21 cells were generated and transformed with MBP-TbGPI-PLC following maxipreparation of the cloned products above. Following transformation, glycerol stocks were prepared and fresh plates were restreaked and incubated overnight. Cultures were then grown using a single colony from the overnight growth and induced with 50 μM IPTG overnight at 18°C (Fig 6.2). It was found after many attempts that the lower temperature of 18°C compared with 37°C and lower IPTG concentration (originally 1mM was used) allowed for better expression of MBP-TbGPI-PLC in the BL21 cells (data not shown).

6.2.3. Purification of MBP-TbGPI-PLC from BL21 cells.

Bacterial cells were lysed using a French press in the presence of lysozyme and protease inhibitors. Following lysis and centrifugation the supernatant (Fig 6.2, lane 4) was loaded onto an amylose column (1 ml), equilibrated with column buffer (20 mM Tris, pH 7.4; 200 mM NaCl, 1 mM EDTA, 10 mM β-mercaptoethanol). MBP binds amylose, which is a maltose polymer, with high affinity allowing a one-step purification in most cases. Following washing of the column with column buffer (1 L) the MBP-TbGPI-PLC was specifically eluted with column buffer containing maltose (10 mM) (Fig 6.3 & 6.4). Maltose competes with amylose for binding to MBP. From the gels in Fig 6.4 it is clear that there are still other bands present even after extensive washing of the amylose column and specific elution of the MBP-TbGPI-PLC with maltose. In order to purify the MBP-TbGPI-PLC fusion protein further, after elution a number of different purification systems were tested. The purification systems tested were, **1.** Hydroxylapatite chromatography, **2.** Chromatofocusing on Polybuffer exchanger PBE-94, **3.** Gel filtration on Sephacryl S-200. The procedure finally adopted was gel filtration on Sephacryl S-200.

Fig 6.1. Cloning of GPI-PLC from trypanosoma brucei.

A. PCR amplification of GPI-PLC. 5 μl of PCR product run on a 1 % agarose gel. GPI-PLC PCR product is approximately 1,000 bps in size.

B. GPI-PLC after digestion and gel purification. 1 μl of purified digest was run on a 1 % agarose gel in order to ensure recovery and integrity of product prior to ligation.

C. Test digestion of Clones following ligation of GPI-PLC and pMAL-c2. 10 μl of minipreps from putative positive clones 4 – 9 were digested with *Bam*H1 and *Xho*1 for 1 hour at 37°C and run on a 1 % agarose gel. 1 kB marker run as standard. Linearised pMALc2 is approximately 6,000 bps and GPI-PLC is at 1,000 bps.

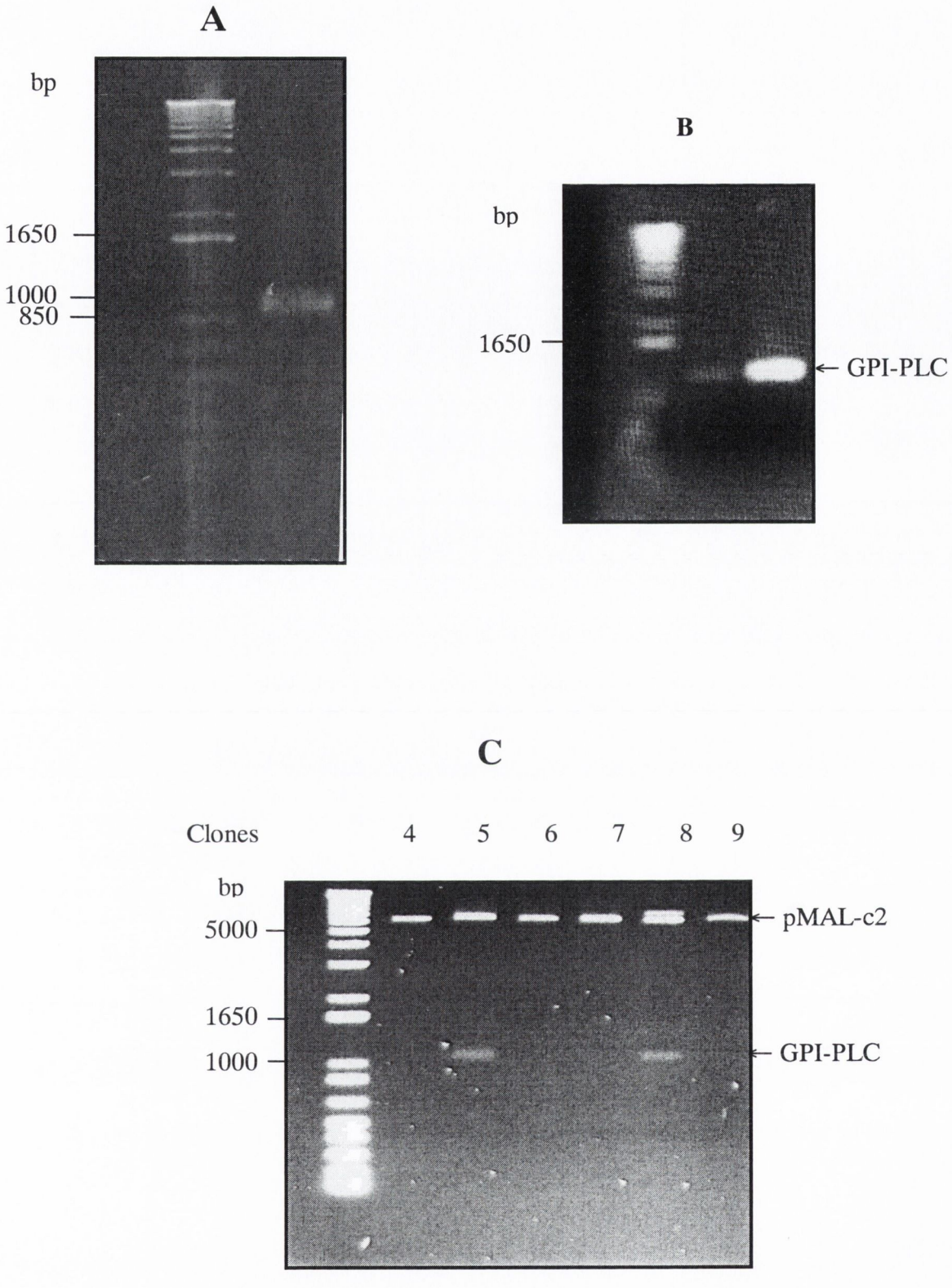
A
bp
1650
1000
850
B
bp
1650
GPI-PLC
C
Clones
4
5
6
7
8
9
bp
5000
1650
1000
pMAL-c2
GPI-PLC

Figure 6.2. Induction of protein MBP-TbGPI-PLC expression at 18°C.

Cultures (500 ml) were grown at 37°C until an optical density of 0.3-0.5 at A_{600} nm was reached. The cultures were then transferred to 18°C and after 1 hour isopropyl-1-thiol-β-D-galactopyranoside was added to a final concentration of 50 μM and cultures incubated overnight at 18°C.

Cells were harvested and resuspended in 0.01-0.02 volumes of column buffer (20 mM Tris, pH 7.4; 200 mM NaCl, 1 mM EDTA, 10 mM β-Mercaptoethanol), prior to lysis by French Press. 20 μl of each sample was loaded on a 15%, (w/v) SDS PAGE gel.

Lane 1: Low Molecular Weight Markers (Sigma)

Lane 2: Pre-induction

Lane 3: Post-induction

Lane 4: cell lysate-pellet

Lane 5: cell lysate-supernatant (sample loaded onto amylose resin)

Figure 6.2. Induction of protein MBP-TbGPI-PLC expression at 18°C.

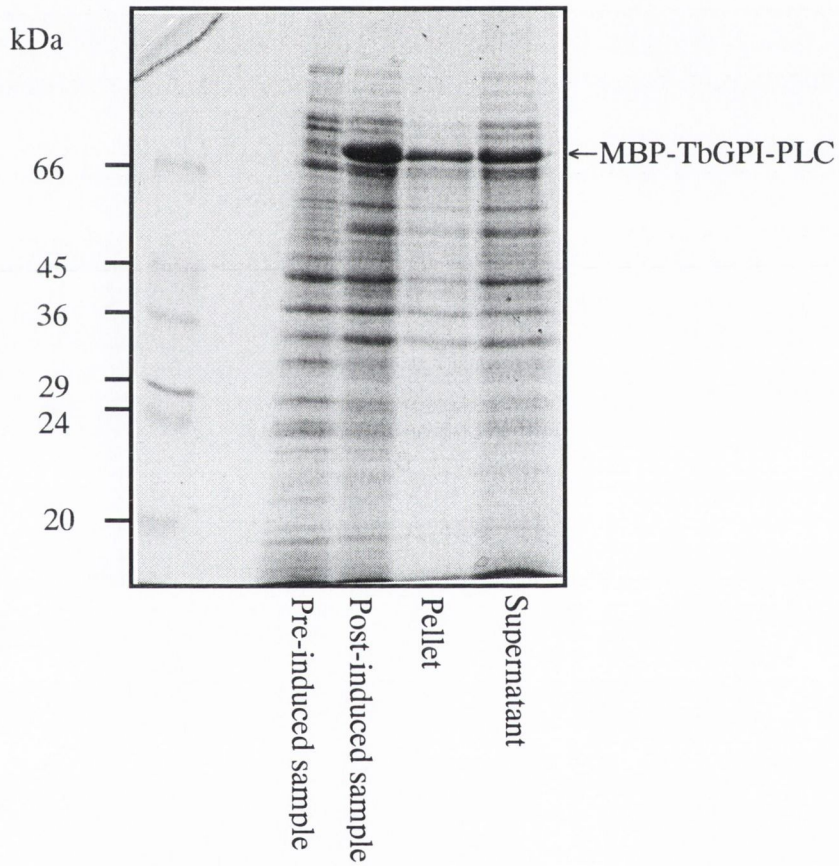

Fig 6.3. Elution profile of the MBP-TbGPI-PLC on amylose resin.

Crude extract (30 ml) from BL21 cells expressing MBP-TbGPI-PLC was passed over a 1 ml column of amylose resin pre-equilibrated with column buffer (20 mM Tris, pH 7.4; 200 mM NaCl, 1 mM EDTA, 10 mM β-mercaptoethanol) at 4°C. The column was washed with column buffer (1 L) and protein was eluted with the above buffer plus 10mM maltose. Fractions were analysed for protein content by measuring the absorbance of each fraction at 280 nm. A graphical representation of the elution profile of MBP-TbGPI-PLC from the amylose column is shown on the opposite page.

Fig 6.3. Elution profile of the MBP-TbGPI-PLC on amylose resin.

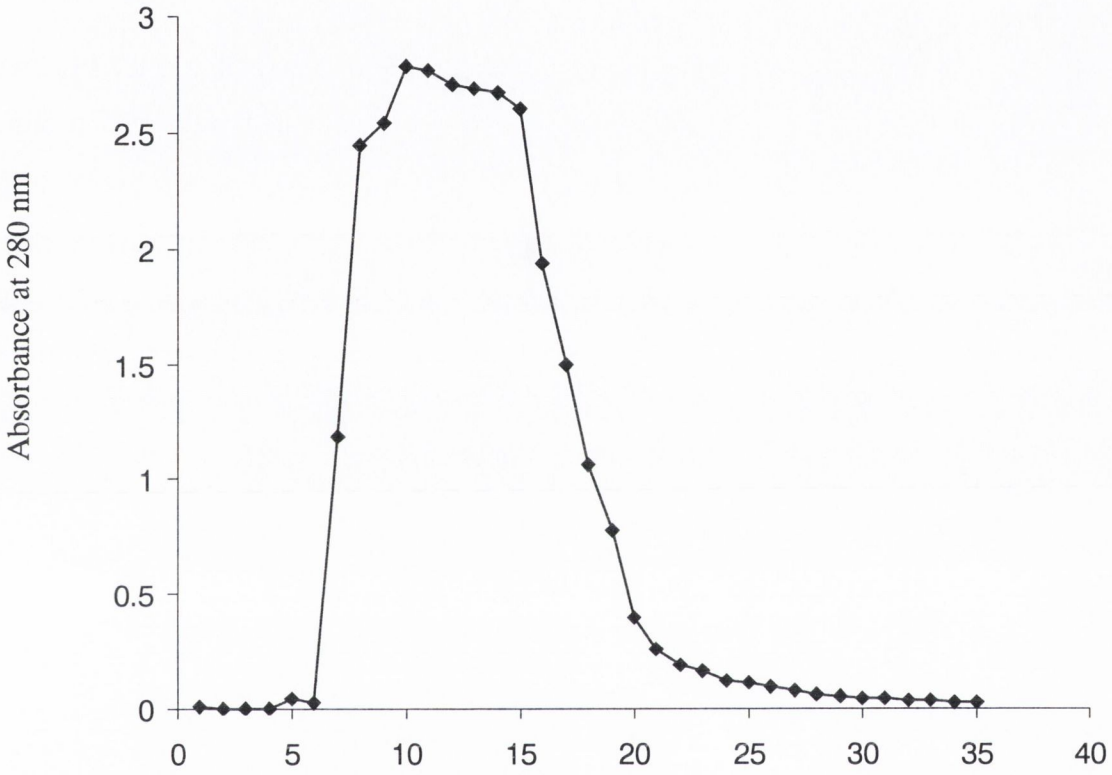

Fig 6.4. Purification of the MBP-TbGPI-PLC fusion protein on amylose resin.

Crude extract (30 ml) from BL21 cells expressing MBP-TbGPI-PLC was passed over a 1 ml column of amylose resin pre-equilibrated with column buffer (20 mM Tris, pH 7.4; 200 mM NaCl, 1 mM EDTA, 10 mM β-mercaptoethanol) at 4°C. The column was washed with column buffer (1 L) and protein was eluted with the above buffer plus 10mM maltose. All fractions were analysed by gel electrophoresis on a 15%, (w/v) SDS-PAGE gel. Each lane represents 20μl of a 1 ml sample.

Gel A:

Lane 1:	Low Molecular weight markers (Sigma)
Lanes 2 – 12:	Eluted fractions 7 – 17 (20 μl of 1 ml fraction)

Gel B:

Lane 1:	Low Molecular weight markers (Sigma)
Lanes 2 – 10:	Eluted fractions 18 – 26 (20 μl of 1 ml fraction)
Lane 11:	Combined fractions 7 – 26 (20 μl of 21 ml fraction)

Fig 6.4. Purification of the MalE-TbGPI-PLC fusion protein on amylose resin.

A.

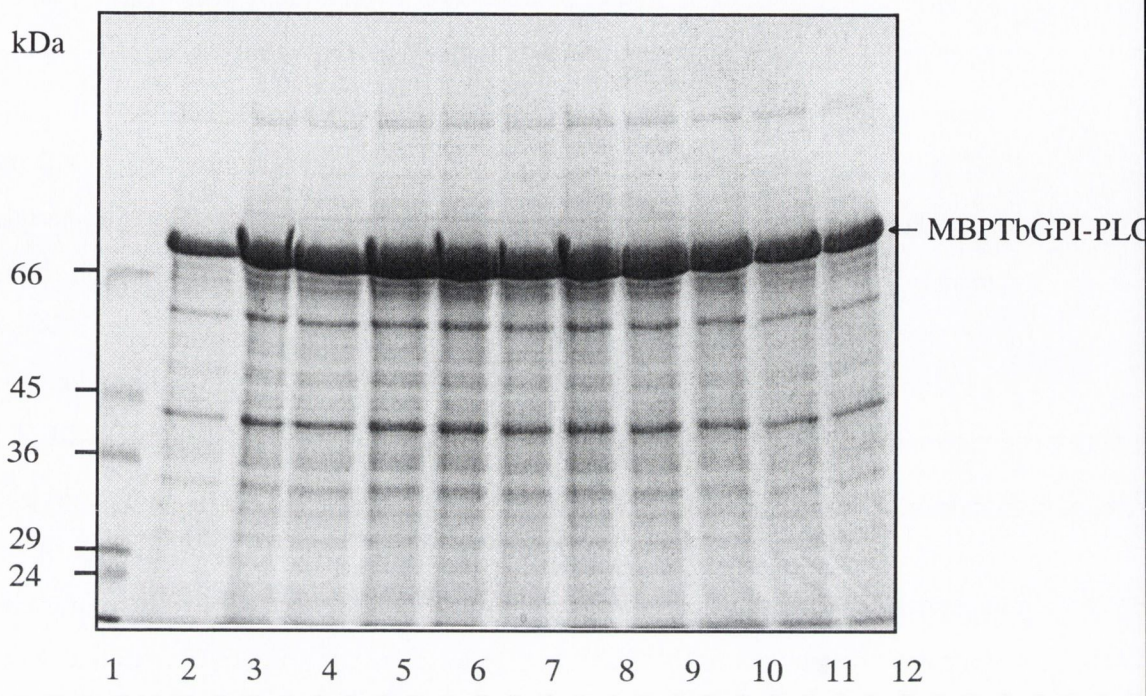

B.

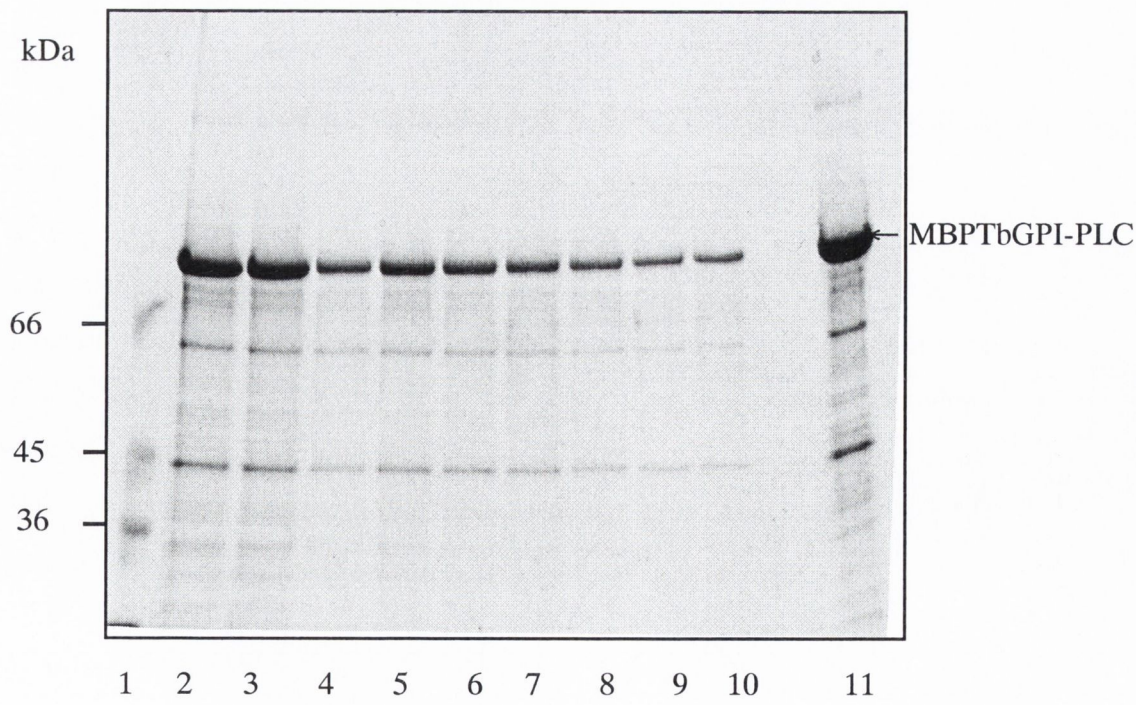

6.2.4. Removal of maltose from TEV cleaved MBP-TbGPI-PLC fusion protein by hydroxyapatite chromatography and domain separation by rebinding MBP to amylose.

Maltose must first be removed from the cleaved fusion protein mixture so that when it is passed back through the amylose resin the MBP will stick. In this study hydroxyapatite chromatography was utilized to remove the maltose. This method removes maltose from the cleavage mixture, but not the TEV protease or any trace contaminants. In addition, any MBP that has been denatured or otherwise damaged will not bind to the amylose column. The procedure was carried out at room temperature to avoid precipitation of phosphate buffer. When this method was used to purify the GPI-PLC from the MBP-TbGPI-PLC fusion protein the result was disappointing. When the cleaved MBP-TbGPI-PLC fusion was loaded onto the hydroxyapatite column and then eluted with high salt only the residual MBP and some uncleaved MBP-TbGPI-PLC fusion protein came off the column and the GPI-PLC itself remained bound to the resin (data not shown) and could not be removed even with high salt (0.5 M or 1 M sodium phosphate) or high pH (pH 10). Therefore the amylose column could not be used to purify the GPI-PLC after it had been cleaved from the MBP-TbGPI-PLC fusion protein. It was decided that the fusion protein itself would be purified and analysis of the enzymatic properties of the recombinant GPI-PLC would be done using the MBP-TbGPI-PLC fusion protein.

6.2.5. Chromatofocusing of MBP-TbGPI-PLC on Polybuffer™ exchanger PBE-94 using Polybuffer™ 74.

Chromatofocusing with Polybuffer™ and PBE allows separation of proteins according to their isoelectric point (pI) in a column chromatographic system characterized by self-generated pH gradients, which eliminate the need for a gradient making apparatus and produce sharp, well separated bands with very high resolution. Polybuffer™ 74 is an amphoteric buffer designed for chromatofocussing in the range pH 4 – 7. The three main species in the MBP-TbGPI-PLC fusion protein eluted from the amylose column are MBP-TbGPI-PLC (pI: 5.9), MBP (pI: 4.7) and GPI-PLC (pI: 9.4).

A column (0.65 cm x 11 cm) of Polybuffer™ exchanger PBE-94 was equilibrated in the starting buffer (25 mM Imidazole, pH 7.4). The MBP-TbGPI-PLC fusion protein from the amylose column was also equilibrated with starting buffer by gel filtration on Sephadex G-25. To initiate elution on the Polybuffer™ exchanger, 5 ml of Polybuffer™ 74 (pH 4; 1:8, Polybuffer™ 74:H2O; Amersham) was applied to the column first followed

by the MBP-TbGPI-PLC fusion protein. Proteins were then eluted with Polybuffer™ 74. It is clear from the gels shown in Fig 6.5 that the chromatofocusing step has removed the majority of contaminants that were present following elution from the amylose resin. The MBP-TbGPI-PLC fusion is the major protein band in each fraction.

The Polybuffer™ 74 was removed from all fractions by gel filtration on Sephadex G-75 that had been equilibrated with column buffer (20 mM Tris, pH 7.4; 200 mM NaCl, 1 mM EDTA, 10 mM β-mercaptoethanol). Fig 6.6 shows a gel containing different volumes of the final product in column buffer before and after concentration in a vivaspin membrane filter (M.W. cut-off 5000). The sample is composed of MBP-TbGPI-PLC fusion protein that is approximately 90 % pure.

6.2.6. Gel filtration of MBP-TbGPI-PLC on Sephacryl S-200.

In order to achieve further purification of the MBP-TbGPI-PLC fusion protein from the chromatofocussing step a gel filtration column was employed. In Fig 6.6 a band just below the fusion protein that runs at approximately 60 kDa can be observed as well as a band corresponding to the MBP (42 kDa) and corresponding to the GPI-PLC (39 kDa). The S-200 column was calibrated by running samples of known molecular weight, blue dextran (2,000 kDa), BSA (66 kDa), ovalbumin (45 kDa) and cytochrome C (12.4 kDa) (Fig 6.7). The MBP-TbGPI-PLC from the amylose elution was eluted from the S-200 column with column buffer containing N-octylglucoside (0.1 %, w/v). The MBP-TbGPI-PLC eluted at a volume corresponding to its molecular weight, 84 kDa. Each fraction was analyzed by SDS-PAGE to determine the purity of the MBP-TbGPI-PLC fusion protein (Fig 6.8). Fractions 35 – 50 were combined, because these fractions contained only the MBP-TbGPI-PLC fusion protein. This combined sample was used for further analysis by mass spectrometry. Unfortunately not all S-200 elutions gave such excellent results as the trial shown and in some trials the protein band at ~60 kDa co-purified with the MBP-TbGPI-PLC. In these cases, concentration of the eluted material and re-chromatography (x3) on S-200 improved the purification.

Fig 6.5. Chromatofocusing of the MBP-TbGPI-PLC fusion protein on PBE-94 with Polybuffer 74.

A column (0.65 cm x 11cm) of Polybuffer exchanger PBE-94 was equilibrated in starting buffer (25 mM Imidazole, pH 7.4). The MBP-TbGPI-PLC fusion protein from the amylose column was also equilibrated with starting buffer by gel filtration on Sephadex G-25. To initiate elution on the Polybuffer exchanger, 5 ml of Polybuffer 74 (pH 4; 1:8, Polybuffer 74:H_2O; Amersham) was applied to the column first, followed by the MBP-TbGPI-PLC fusion protein. Proteins were then eluted with Polybuffer 74. Fractions (1 ml) were collected and the pH of each fraction measured immediately. The samples were analysed for protein content by gel electrophoresis on 15 %(w/v) SDS-PAGE gels.

Gel A.

Fractions eluted in the pH range 6.17 – 5.34.

Gel B.

Fractions eluted in the pH range 5.28 – 4.72.

Gel C.

Fractions eluted in the pH range 4.68 – 4.32.

Gel D.

Fractions eluted in the pH range 4.29 – 4.09.

Fig 6.5. Chromatofocusing of the MBP-TbGPI-PLC fusion protein on PBE-94 with Polybuffer 74.

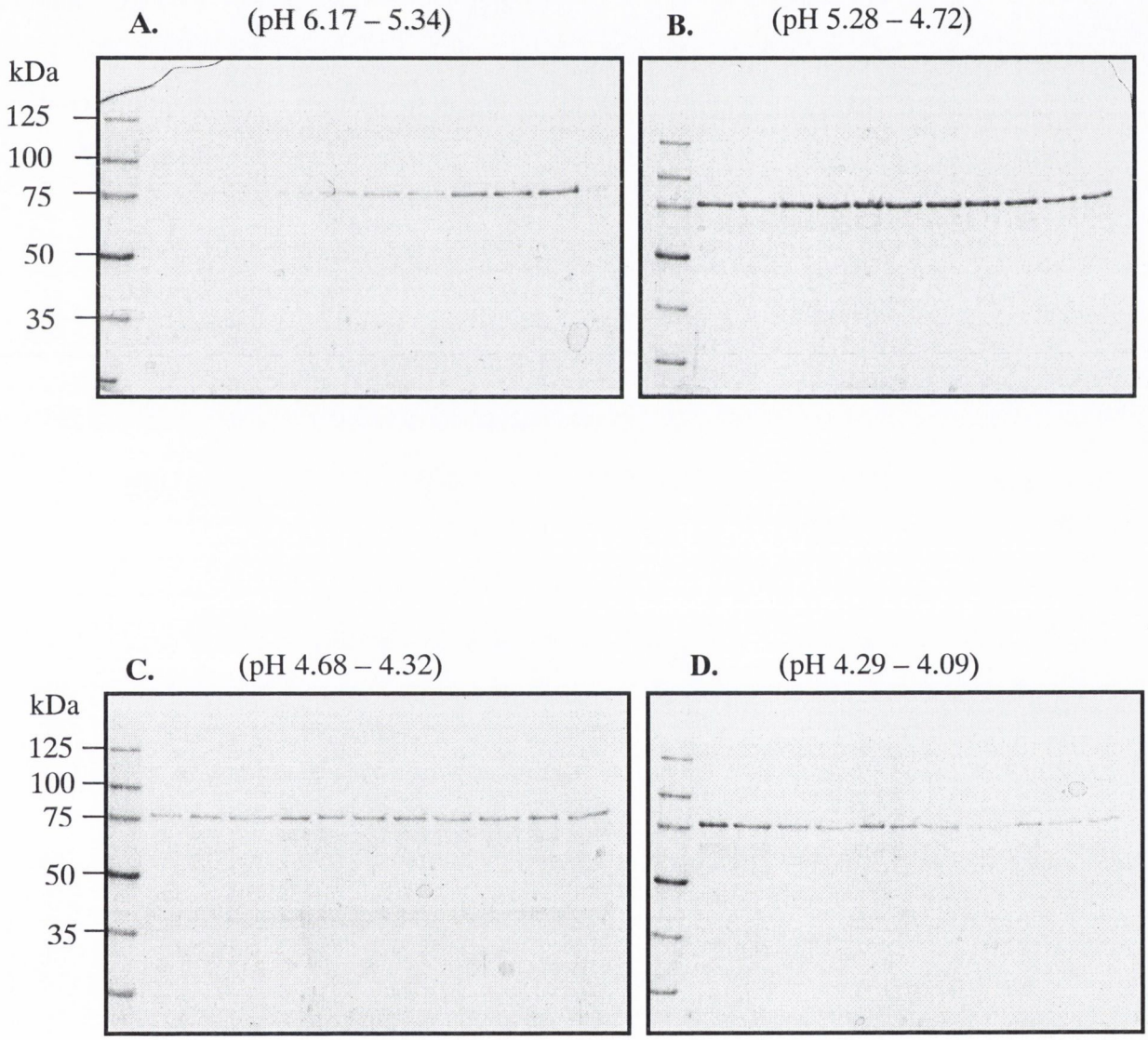

Fig 6.6. Polyacrylamide gel electrophoresis of MBP-TbGPI-PLC following chromatofocusing on PBE-94.

MBP-TbGPI-PLC eluted from the chromatofocusing step (all fractions containing MBP-PLC in Fig 6.5) was concentrated in a vivaspin membrane filter (M.W. cut-off 5000) and samples were then analysed by SDS-PAGE.

Lane 1: Molecular weight markers
Lane 2: MBP-TbGPI-PLC before concentration (5 μl)
Lane 3: MBP-TbGPI-PLC before concentration (10 μl)
Lane 4: MBP-TbGPI-PLC before concentration (20 μl)
Lane 5: MBP-TbGPI-PLC after concentration (5 μl)
Lane 6: MBP-TbGPI-PLC after concentration (10 μl)
Lane 7: MBP-TbGPI-PLC after concentration (20 μl)

Fig 6.6. Polyacrylamide gel electrophoresis of MBP-TbGPI-PLC in following chromatofocusing on PBE-94.

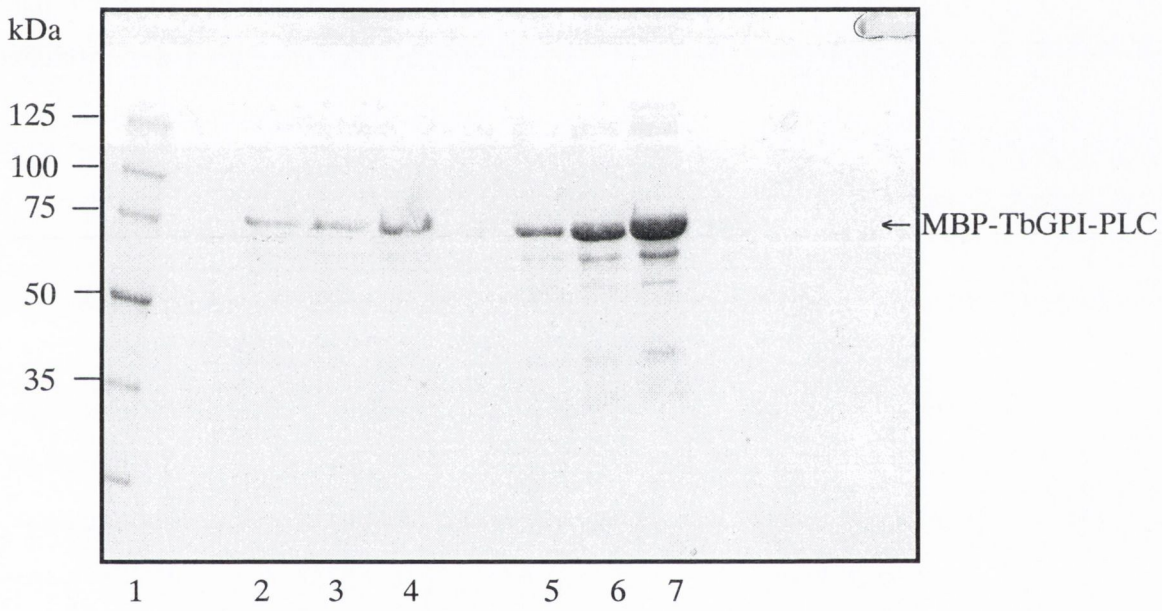

Figure 6.7. Elution profile of MBP-TbGPI-PLC and molecular weight markers from Sephacryl S-200.

The molecular weight markers shown in the table below were applied separately to a Sephacryl S-200 column (internal diameter 1.1 cm, height 90 cm), eluted with column buffer (20 mM Tris, pH 7.4; 200 mM NaCl, 1mM EDTA) containing 0.1 %, (w/v) N-octylglucoside and protease inhibitors [0.1 mM TLCK, 0.3 mM PMSF and leupeptin0.1 %(w/v)] and detected spectrophotometrically as outlined. The elution volume of each marker, corresponding to the maximum concentration of solute (V_e) was estimated to the nearest 0.5 ml from the elution diagram, by extrapolating both sides of the

Marker/ MBP-TbGPI-PLC	Molecular Weight (kDa)	Elution Volume (ml)	Method of Detection
Blue Dextran (1)	2,000	35 ml	Absorbance at 660 nm
MBP-TbGPI-PLC (2)	84	39ml	Absorbance at 280 nm
BSA (3)	66	51 ml	Absorbance at 280 nm
Ovalbumin (4)	45	63 ml	Absorbance at 280 nm
Cytochrome C (5)	12.4	81 ml	Absorbance at 550nm

Figure 6.7. Elution profile of MBP-TbGPI-PLC and molecular weight markers from Sephacryl S-200.

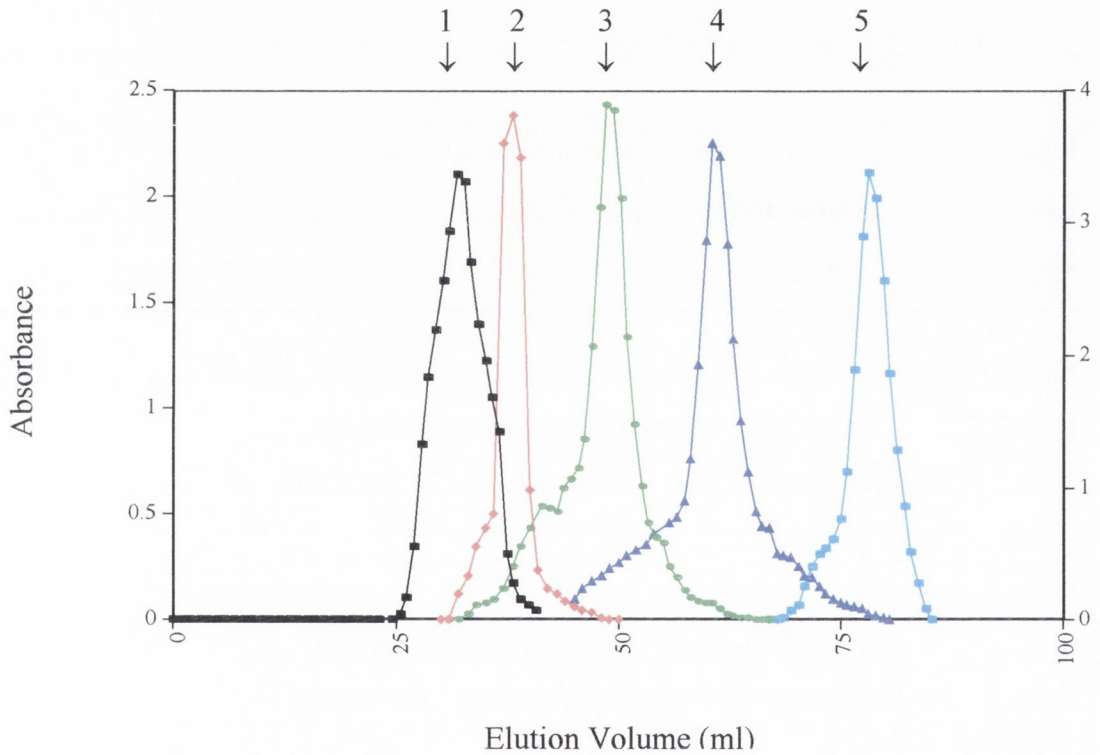

Figure 6.8. Further purification of MBP-TbGPI-PLC on Sephacyrl S - 200.

Eluted fractions containing MBP-TbGPI-PLC from the amylose column were combined and concentrated to give a final volume of 10 ml. The whole sample was applied to a Sepahacryl S – 200 column (internal diameter 1.1 cm, height 90 cm) pre-equilibrated with column buffer (20 mM Tris, pH 7.4; 200 mM NaCl, 1mM EDTA) containing 0.1%, (w/v) N-octylglucoside and protease inhibitors [0.1 mM TLCK, 0.3 mM PMSF and leupeptin 0.1 %(w/v)]. The protein was eluted in the same buffer and fractions (1 ml) were collected at a rate of 0.125 ml/min. All fractions were analysed by gel electrophoresis on a 15%, (w/v) SDS-PAGE gel. Each lane represents 20µl of a 1 ml sample.

Gel A:

Lane 1: Sigma Low range molecular weight markers

Lane 2: Sample applied to the column.

Lane 3 – 11: Fractions 22 – 30 of Sephacryl S – 200 elution

Gel B:

Lane 1: Sigma Low range molecular weight markers

Lane 2 – 12: Fractions 31 – 41 of Sephacryl S – 200 elution

Gel C:

Lane 1: Sigma Low range molecular weight markers

Lane 2 – 10: Fractions 42 – 50 of Sephacryl S – 200 elution

A.

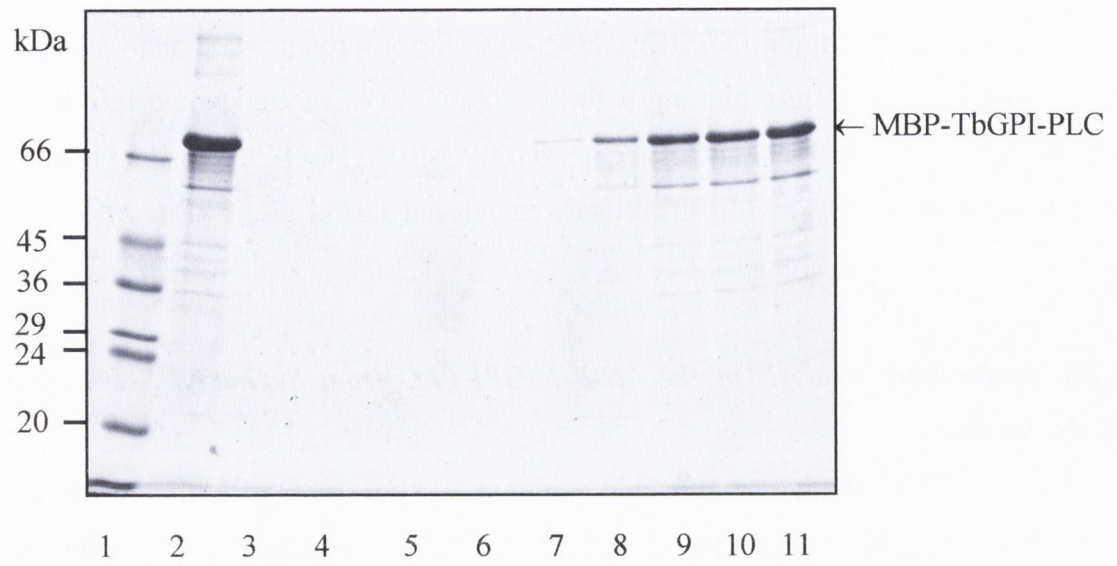
kDa
66
45
36
29
24
20
← MBP-TbGPI-PLC
1 2 3 4 5 6 7 8 9 10 11

B.

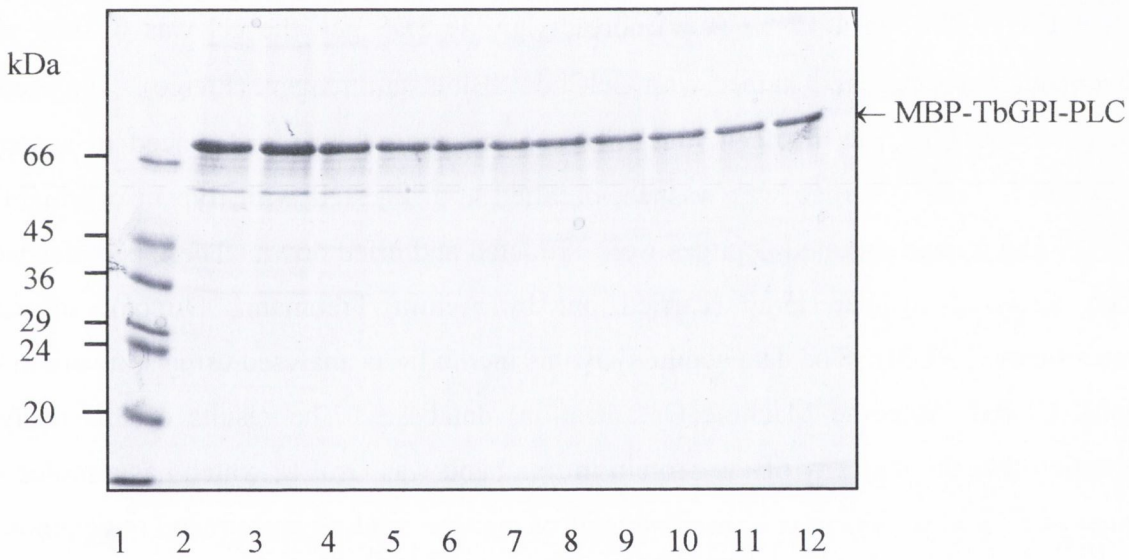
kDa
66
45
36
29
24
20
← MBP-TbGPI-PLC
1 2 3 4 5 6 7 8 9 10 11 12

C.

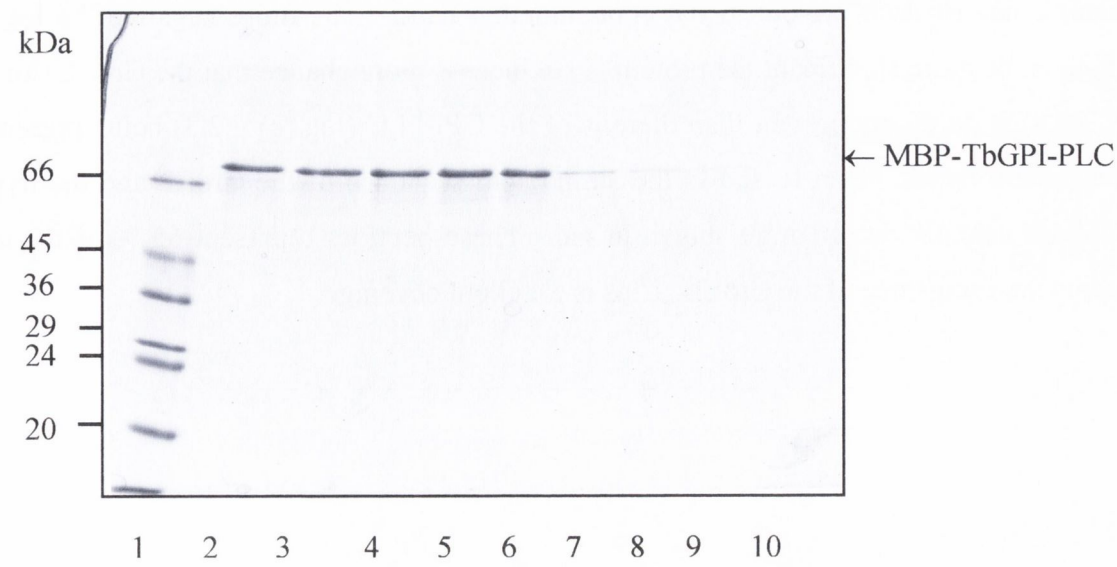
kDa
66
45
36
29
24
20
← MBP-TbGPI-PLC
1 2 3 4 5 6 7 8 9 10

6.2.7. Analysis of the MBP-TbGPI-PLC from Sephacryl S-200 elution by Western Blotting.

Fractions containing the MBP-TbGPI-PLC fusion protein were analysed by SDS-PAGE followed by western blotting with IgG anti-GPI-PLC antibody and IgG anti-MBP antibody (Fig 6.9). Both antibodies recognized the MBP-TbGPI-PLC fusion protein at 84 kDa. In addition, the IgG anti-MBP antibody recognized a band at ~60 kDa.

6.2.8. Preliminary analysis of the MBP-TbGPI-PLC from Sephacryl S-200 by Mass Spectrometry.

The contaminating band that ran at 60 kDa on SDS-PAGE and was present in approximately 80 % of all purified MBP-TbGPI-PLC preparations was sequenced by Mass Spectrometry to determine its identity. Following electrophoresis of the purified MBP-TbGPI-PLC on a 15 %, (w/v) polyacrylamide SDS gel, the gel was washed with deionized water (x3) and stained with GelCode™Blue stain reagent (Pierce). The protein band at ~60 kDa was then cut out with a clean sharp blade and placed in a sterile eppendorf. The gel slice was washed, desalted and digested with trypsin overnight at 37°C. The trypsin digested peptides were extracted and dried down. These peptides were then anlaysed by nanospray (carried out by Achim Treumann, Director of mass spectrometry, RCSI). The data acquired by this method was analysed using software in the gpm (Global Proteome Machine Organization) database. The results of this analysis revealed that the majority of the protein in this band was GroEL, which has a molecular mass of 57.3 kDa. There is a small amount of maltose binding protein and trace amounts of GPI-PLC also present. The log (e) values in Table 6.1 inform us of the relative significance of each protein in the contaminating band. The more negative the log (e) value is the more significant the protein is *i.e.* there is more chance that the GroEL (log (e) – 207.8) is definitely present than there is of the GPI-PLC (log (e) – 2.3) being present in the protein band. Fig 6.10 shows the amino acid sequence of the GroEL and the tryptic peptides actually detected are shown in red. These peptides represent 65 % of the total amino acid sequence of the GroEL. This is excellent coverage.

Log (e)	**Mr**	**Protein**
- 207.8	57.3	Chaperonin GroEL (E. Coli K12)
- 25.3	43.4	Maltose Binding protein
- 2.3	40.6	GPI-PLC

Table 6.1. Proteins present in the contaminating band (57.3 kDa), which co-purifies with the MBP-TbGPI-PLC fusion protein.

Following electrophoresis of the purified MBP-TbGPI-PLC on a 15 %, (w/v) polyacrylamide SDS gel, the gel was washed with deionized water (x3) and stained with GelCode™Blue stain reagent (Pierce). The protein band at ~60 kDa was then cut out with a clean sharp blade and placed in a sterile eppendorf. The gel slice was washed, desalted and digested with trypsin overnight at 37°C. The trypsin-digested peptides were extracted and dried down. These peptides were analysed by nanospray and the data acquired was subsequently analysed using the gpm (Global proteome machine organization) database. This table represents the proteins present in the band at ~ 60 kDa and the log (e) values inform us of the relative significance of each protein in the contaminating band. The more negative the log (e) value is the more significant the protein is i.e. there is more chance that the GroEL (log (e) – 207.8) is definitely present than there is of the GPI-PLC (log (e) – 2.3) being present in the protein band.

Fig 6.9. Analysis of MBP-TbGPI-PLC fusion protein by gel electrophoresis and western blotting.

Fractions (26 – 31) from Sephacryl S-200 elution (see Fig 6.10) containing the MBP-TbGPI-PLC fusion and the contaminant protein at ~60 kDa were analysed by electrophoresis on 15 %, (w/v) polyacrylamide gels (A) and subsequent transfer to nitrocellulose. The nitrocellulose membranes were probed with either (B) IgG anti-GPI-PLC antibody (1/1000 dilution) or (C) IgG anti-MBP antibody (1/2000 diltuion).

Fig 6.9. Analysis of MBP-TbGPI-PLC fusion protein by gel electrophoresis and western blotting.

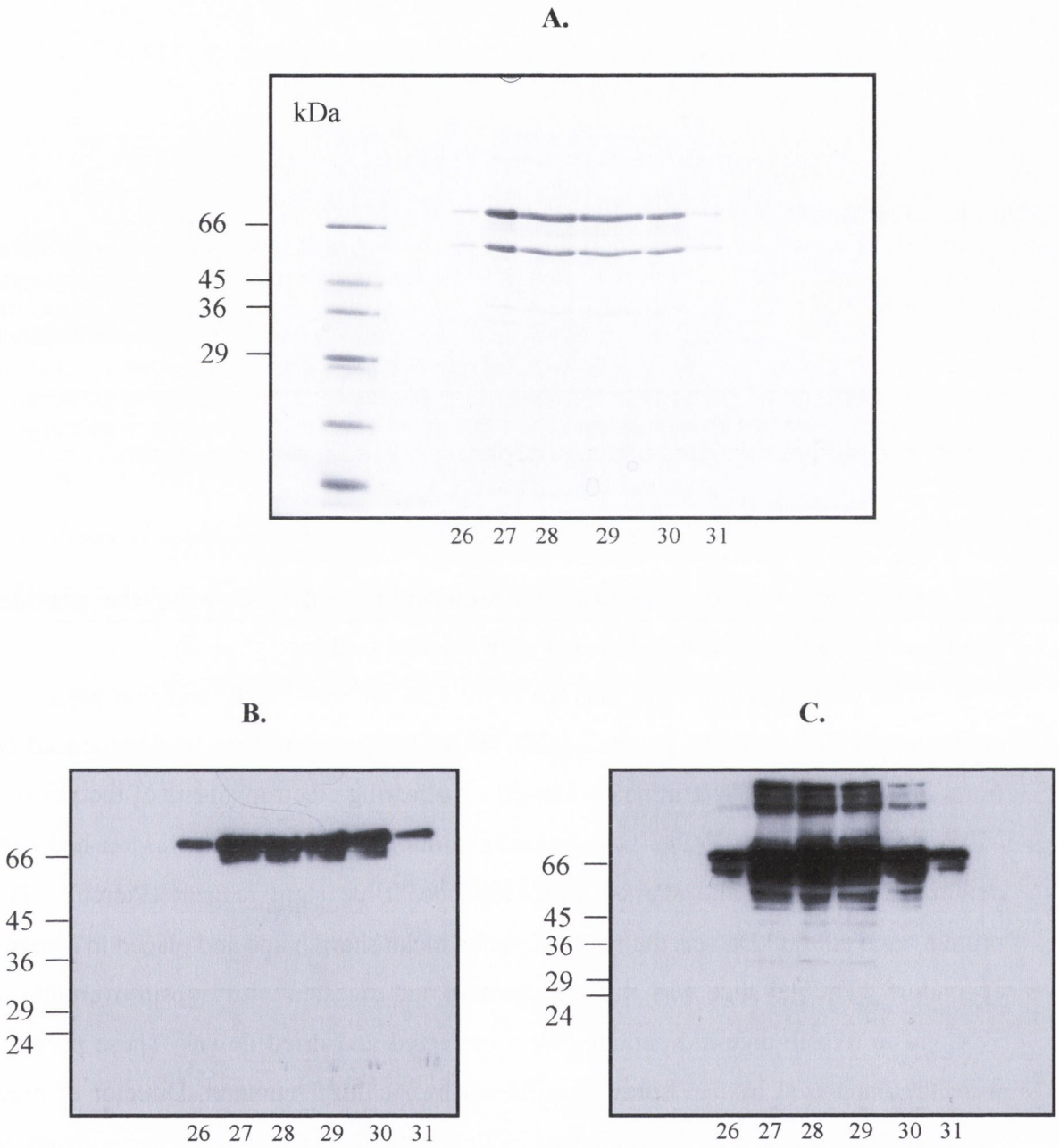

>**Chaperonin GroEL**
maakdvkfgndarvkmlrgvnvladavkvtlgpkgrnvvldksfgaptitkdgvsvareieledkfenmg
aqmvkevaskandaagdgtttatvlaqaiiteglkavaagmnpmdlkrgidkavtaaveelkalsvpcsd
skaiaqvgtisansdetvgkliaeamdkvgkegvitvedgtglqdeldvvegmqfdrgylspyfinkpet
gavelespfilladkkisniremlpvleavakagkplliiaedvegealatlvvntmrgivkvaavkapg
fgdrrkamlqdiatltggtviseeigmelekatledlgqakrvvinkdtttiidgvgeeaaiqgrvaqir
qqieeatsdydreklqervaklaggvavikvgaatevemkekkarvedalhatraaveegvvagggvali
rvaskladlrgqnedqnvgikvalrameaplrqivlncgeepsvvantvkggdgnygynaateeygnmid
mgildptkvtrsalqyaasvaglmittecmvtdlpkndaadlgaaggmggmggmggmm

Fig 6.10. Amino Acid Sequence of Chaperonin GroEL showing the peptides produced when the protein is digested with trypsin (red).

The contaminating band that ran at 60 kDa on SDS-PAGE and was present in approximately 80 % of all purified MBP-TbGPI-PLC preparations was sequenced by Mass Spectrometry to determine its identity. Following electrophoresis of the purified MBP-TbGPI-PLC on a 15 %, (w/v) polyacrylamide SDS gel, the gel was washed with deionized water (x3) and stained with GelCode™Blue stain reagent (Pierce). The protein band at ~60 kDa was then cut out with a clean sharp blade and placed in a sterile eppendorf. The gel slice was washed, desalted and digested with trypsin overnight at 37°C. The trypsin-digested peptides were extracted and dried down. These peptides were then anlaysed by nanospray (carried out by Achim Treumann, Director of mass spectrometry, RCSI). The data acquired by this method was analysed using software in the gpm (Global Proteome Machine Organization) database. The peptides actually detected are shown in red. These peptides represent 65 % of the total amino acid sequence of the GroEL. This is excellent coverage.

6.2.9. Investigating the use of different concentrations of N-octylglucoside on the cleavage of the MBP-TbGPI-PLC with TEV protease

Purification of the MBP-TbGPI-PLC required the presence of the non-ionic detergent N-octylglucoside, in order to maintain the protein in a soluble form. In fact the purified MBP-TbGPI-PLC precipitated if stored for more than 12 hours at 4°C in the absence of detergent, even if the protein was initially in a dilute solution. Although, concentrations of N-octylglucoside (1.25 %) prevented the MBP-TbGPI-PLC from precipitating, it also prevented the TEV protease from cleaving the MBP-TbGPI-PLC fusion protein. A review of the literature revealed that detergents with higher CMC values had been reported (Mohanty *et al.*, 2003) to have inhibitory effects on the activity of TEV and the CMC value of N-octylglucoside is particularly high (19 mM).

Consequently the concentration of N-octylglucoside was varied in the range 0-1 %, w/v in order to determine the lowest concentration of the detergent that would keep the protein in solution and the highest concentration that would allow cleavage with TEV protease. MBP-TbGPI-PLC purified using the Sephacryl S-200 gel filtration column was mixed with TEV protease overnight at room temperature in the presence of varying concentrations of N-octylglucoside (Fig 6.11). It was found that N-octylglucoside (0 – 0.6 % w/v) allowed cleavage of MBP-TbGPI-PLC with TEV protease (Fig 6.11) and that 0.5 % was the lowest concentration that could be used to keep the protein in solution. It was decided from this data to use N-octylglucoside at a concentration of 0.5 % as it allowed TEV cleavage to proceed without any of the MBP-TbGPI-PLC precipitating.

6.2.10. Effect of temperature on the cleavage of MBP-TbGPI-PLC fusion protein with TEV protease.

According to the literature (Kellermann and Ferenci, 1982) the most successful way to purify a protein of interest that is part of an MBP-fusion protein following affinity purification of the fusion protein on amylose is to cleave the purified MBP-fusion protein with TEV protease and then pass the cleaved material through the amylose column a second time. Any uncleaved MBP-fusion protein and the cleaved MBP will bind to the amylose resin and the protein of interest will travel through the column in the void volume.

TEV protease cleavage of MBP-TbGPI-PLC was tested at different temperatures and for different periods of time to ensure the best possible cleavage of the fusion protein. The optimum conditions for cleavage with TEV protease were found to be incubation

Figure 6.11. Effect of the detergent N-octylglucoside (nog) on the activity of TEV protease with MBP-TbGPI-PLC.

Purified MBP-TbGPI-PLC (1 ml) was taken and divided equally between 11 tubes (90 µl each). The detergent N-octylglucoside (nog) was added to the respective tubes at a final concentration of between 0 –1 %. These were incubated with gentle shaking overnight at RT in the presence of TEV protease (5 µg). Following this, samples (20 µl) were taken and resuspended in equal volumes of 2x sample buffer. These were subjected to SDS-PAGE on a 15 %, (w/v) acrylamide gel.

Lane 1: MBP-TbGPI-PLC cleaved with TEV in the absence of nog
Lane 2: MBP-TbGPI-PLC cleaved with TEV in the presence of 0.1 % nog
Lane 3: MBP-TbGPI-PLC cleaved with TEV in the presence of 0.2 % nog
Lane 4: MBP-TbGPI-PLC cleaved with TEV in the presence of 0.3 % nog
Lane 5: MBP-TbGPI-PLC cleaved with TEV in the presence of 0.4 % nog
Lane 6: MBP-TbGPI-PLC cleaved with TEV in the presence of 0.5 % nog
Lane 7: MBP-TbGPI-PLC cleaved with TEV in the presence of 0.6 % nog
Lane 8: MBP-TbGPI-PLC cleaved with TEV in the presence of 0.7 % nog
Lane 9: MBP-TbGPI-PLC cleaved with TEV in the presence of 0.8 % nog
Lane 10: MBP-TbGPI-PLC cleaved with TEV in the presence of 0.9 % nog
Lane 11: MBP-TbGPI-PLC cleaved with TEV in the presence of 1 % nog

Figure 6.11. Effect of the detergent N-octylglucoside (nog) on the activity of TEV protease with MBP-TbGPI-PLC.

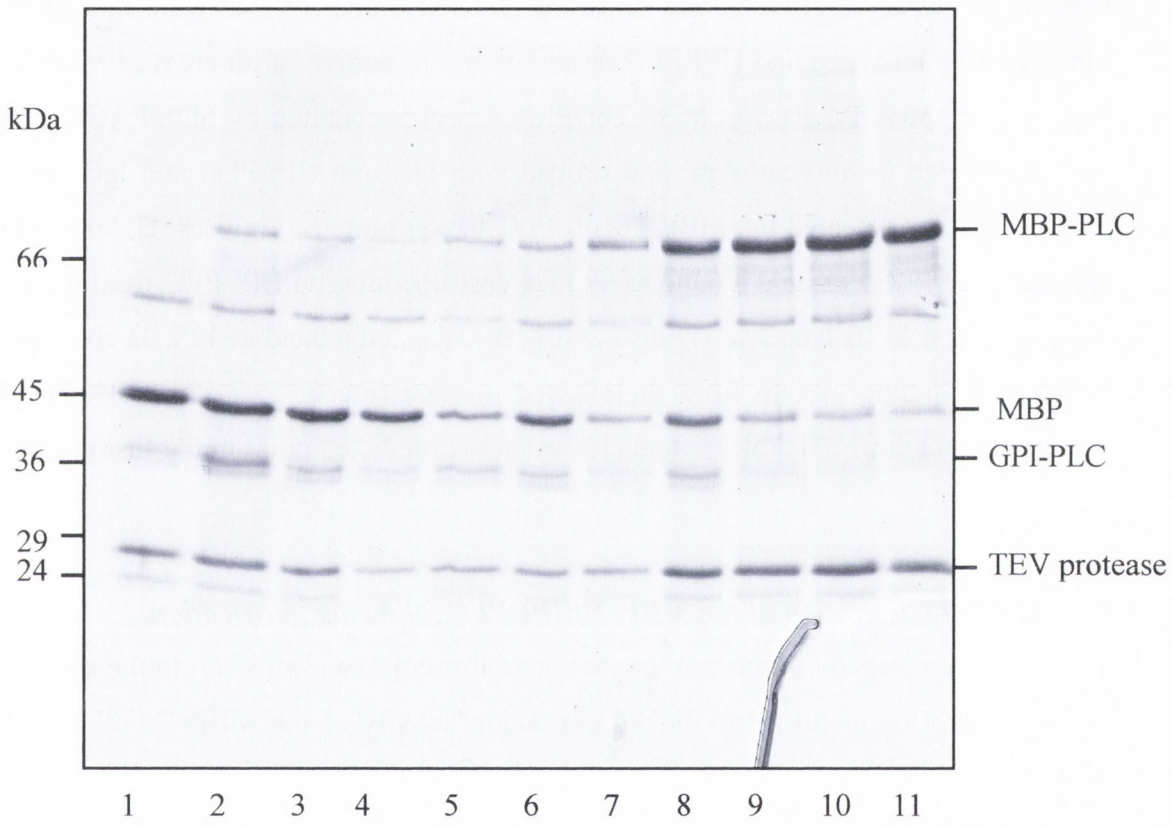

overnight at either room temperature (Fig 6.12, Gel A, lane 11) or at 30°C (Fig 6.12, Gel B, lane 5). When incubation of MBP-TbGPI-PLC with TEV protease was conducted at 4°C the cleavage was always incomplete (Fig 6.12, Gel A, lanes 1 - 5 respectively). For all subsequent cleavage reactions the samples were incubated overnight at room temperature.

6.2.11. Analysis of the products of TEV cleavage of the MBP-TbGPI-PLC fusion protein by Western blotting.

The TEV cleaved MBP-TbGPI-PLC was analyzed by western blotting to ensure that the products of cleavage that migrated at 42 kDa and 39 kDa were indeed maltose binding protein (MBP) and GPI-PLC respectively. A sample of un-cleaved MBP-TbGPI-PLC fusion and TEV cleaved MBP-TbGPI-PLC were separated by SDS-PAGE. The gel was transferred to nitrocellulose and probed with IgG anti-GPI-PLC and IgG anti-MBP. Both antibodies detected the MBP-TbGPI-PLC fusion protein (Fig 6.13, B, lane 1-4). The IgG anti-GPI-PLC detected a band at 39 kDa corresponding to GPI-PLC from the cleaved mixture (Fig 6.13, B lane 2). The IgG anti-MBP detected a band at 42 kDa corresponding to maltose binding protein from the cleaved mixture (Fig 6.13, B, lane 4). This result confirmed that the TEV protease had cleaved at the predicted point in the fusion protein.

6.2.12. Characterization of the MBP-TbGPI-PLC following purification.

The conversion of the membrane bound form of VSG (mfVSG) to the soluble form (sVSG) was used as an assay for the enzymatic activity of the MBP-TbGPI-PLC fusion protein.

GPI-PLC $^-$ mutant trypanosomes (5 x 10^8 cells) were incubated either without addition or with MBP-TbGPI-PLC fusion protein or MBP-TbGPI-PLC that had been cleaved with TEV protease. The activity of the recombinant MBP-TbGPI-PLC fusion protein, expressed in different host bacteria, was analysed. Incubation of GPI-PLC $^-$ mutant trypanosomes with MBP-TbGPI-PLC purified from BL21, orgami and AD494 bacterial cells in the presence or absence of Tx-100 (0.2 %) for 5 minutes at room temperature caused the release of the VSG, initiating a shift in molecular weight on SDS-PAGE (lane 3 of all the gels in Fig 6.14). Release never occurred in the absence of triton-x-100 nor in the absence of the MBP-TbGPI-PLC fusion protein. This result suggests that the MBP-TbGPI-PLC cleaves the GPI anchor of the VSG, releasing dimyristoyl glycerol

Fig 6.12. Effect of temperature on the cleavage of MBP-TbGPI-PLC with TEV protease.

MBP-TbGPI-PLC was purified from BL21 crude extract as described in section 2.15. Following this a sample (1 ml) was taken and incubated with 10 µl of purified TEV protease (see section 2.16) at 4°C, room temperature or 30°C. Samples (20 µl) were taken at the time points outlined below and resuspended in equal volumes of 2x sample buffer. The samples were subjected to SDS-PAGE on a 15 %, (w/v) acrylamide gel.

Gel A.

MBP-TbGPI-PLC incubated with TEV protease at 4°C and RT

Lane 1: Low Molecular weight markers (Sigma)
Lane 2: Sample incubated for 1 hr at 4°C
Lane 3: Sample incubated for 2 hrs at 4°C
Lane 4: Sample incubated for 3 hrs at 4°C
Lane 5: Sample incubated for 4 hrs at 4°C
Lane 6: Sample incubated O/N at 4°C
Lane 7: Sample incubated for 1 hr at RT .
Lane 8: Sample incubated for 2 hrs at RT.
Lane 9: Sample incubated for 3 hrs at RT.
Lane 10: Sample incubated for 4 hrs at RT.
Lane 11: Sample incubated for O/N at RT.

Gel B.

MalE-TbGPI-PLC incubated with TEV protease at 30°C

Lane 1: Sample incubated for 1 hr at 30°C.
Lane 2: Sample incubated for 2 hrs at 30°C.
Lane 3: Sample incubated for 3 hrs at 30°C.
Lane 4: Sample incubated for 4 hrs at 30°C.
Lane 5: Sample incubated O/N at 30°C.

Fig 6.12. Effect of temperature on the cleavage of MBP-TbGPI-PLC with TEV protease.

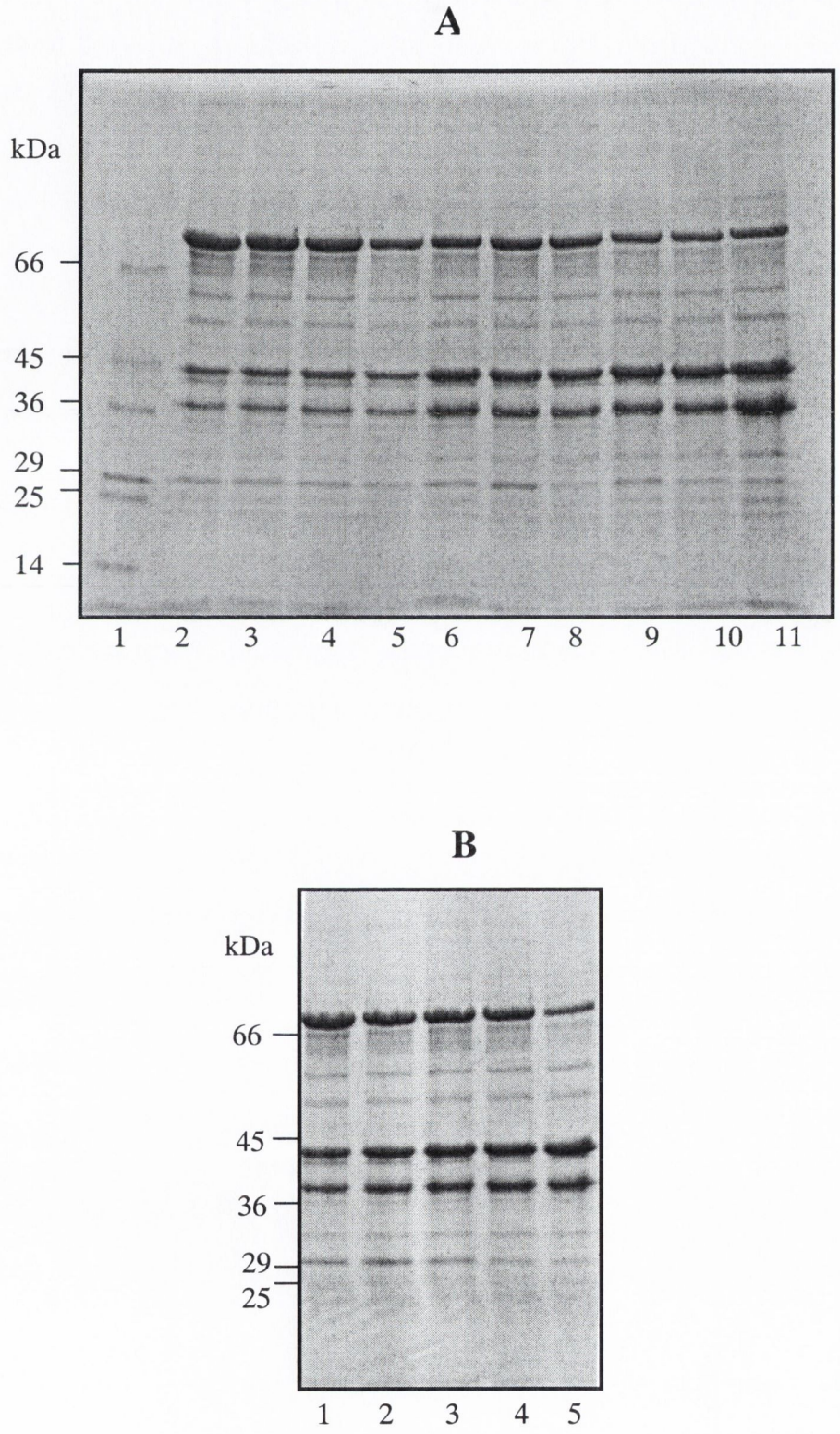

Figure 6.13. Analysis of the cleaved MBP-TbGPI-PLC fusion protein by SDS-PAGE and Western Blotting.

MBP-TbGPI-PLC was purified from BL21 crude extract as described in section 2.1.42. Following this, a sample (0.1 ml) was taken and incubated in the presence (+) or absence (-) of purified TEV protease (20 μl) (see section 2.1.46) O/N at RT. Samples (20 μl) were taken and resuspended in equal volumes of 2x sample buffer. These were separated by SDS-PAGE on a 15 %, (w/v) acrylamide gel, transferred to PVDF membrane and immunoblotted with (Panel B, lanes 1 + 2) IgG anti-GPI-PLC (1/1000 dilution of stock antibody) and (Panel B, lanes 3 + 4) anti-MBP IgG (1/20,000 dilution of antiserum from *NEB*).

Panel A (SDS-PAGE)

Lane 1: Low range molecular weight markers (*Sigma*)

Lane 2: MBP-TbGPI-PLC uncleaved

Lane 3: MBP-TbGPI-PLC cleaved with TEV

Lane 4: Prestained markers (*NEB*)

Lane 5: MBP-TbGPI-PLC uncleaved

Lane 6: MBP-TbGPI-PLC cleaved with TEV

Lane 7: Low range molecular weight markers (*Sigma*)

Panel B (Western Blot)

Lanes 1+ 2: Lanes 2 + 3 from panel A probed with IgG anti-GPI-PLC antibody

Lanes 3 + 4: Lanes 5 + 6 from panel A probed with IgG anti-MBP antibody

Figure 6.13. Analysis of the cleaved MBP-TbGPI-PLC fusion protein by SDS-PAGE and Western Blotting.

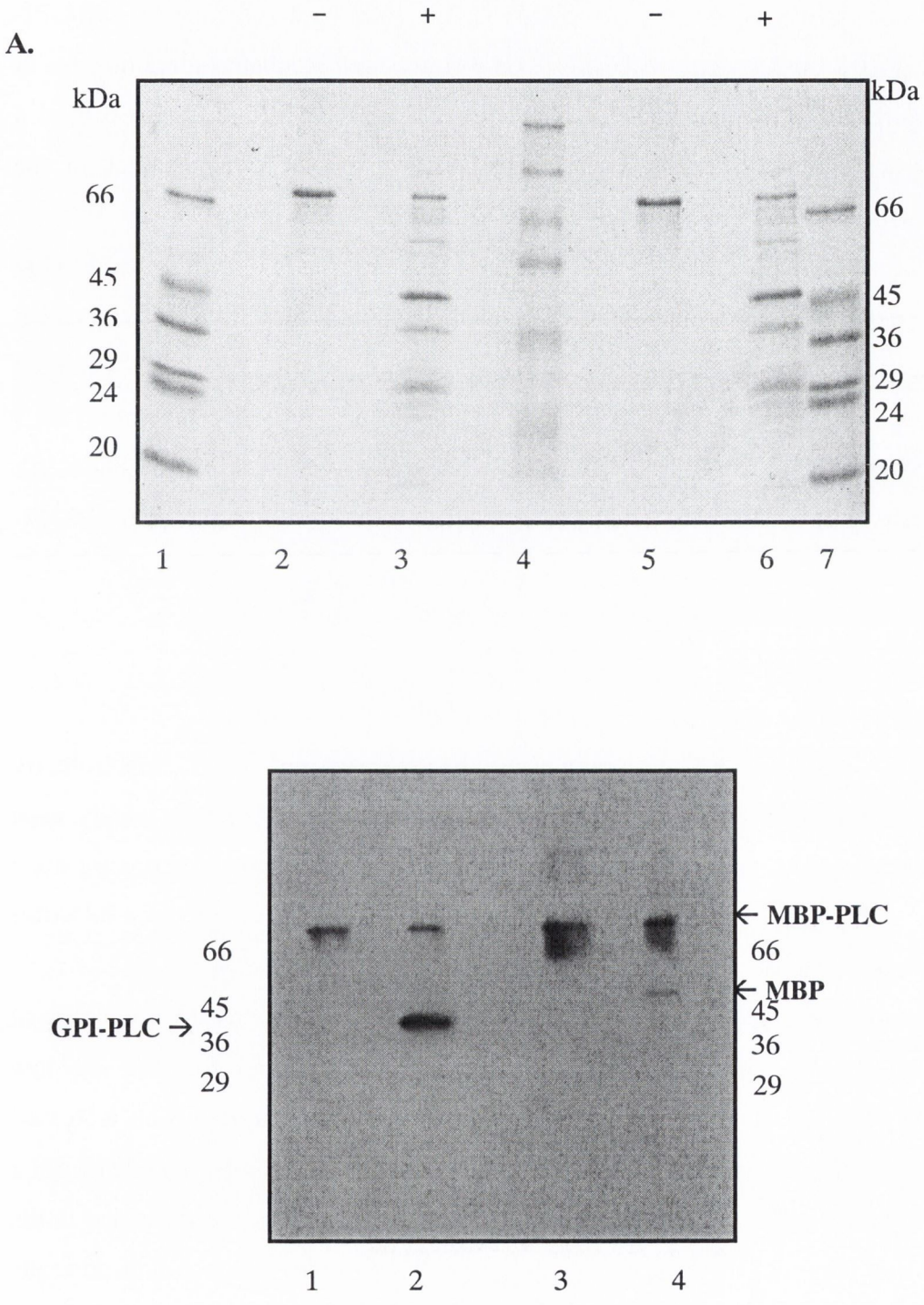

and forming soluble VSG (sVSG), just as the native GPI-PLC cleaves the GPI anchor in wild-type trypanosomes during hypotonic lysis (See Chapter 5, Fig 5.1 & 5.2).

The activity of the TEV cleaved MBP-TbGPI-PLC fusion protein on the GPI anchor of VSG in GPI-PLC $^-$ mutant trypanosomes was also investigated. The MBP-TbGPI-PLC was cleaved with TEV protease overnight at room temperature. A sample of the cleaved mixture in the presence or absence of Tx-100 (0.2 %) was incubated with GPI-PLC $^-$ mutant trypanosomes (5 x 10^8 cells). This reaction was incubated for 5 minutes at room temperature. It was found that the TEV cleaved MBP-TbGPI-PLC also caused a shift in molecular weight of the VSG from GPI-PLC $^-$ mutant trypanosomes in the presence of Tx-100 (0.2 %) (Fig 6.14, Gel A, B & C lane 5).

The action of the MBP-TbGPI-PLC fusion protein on the GPI anchor of the VSG in plasma membranes prepared from GPI-PLC $^-$ mutant trypanosomes was also examined. When the plasma membranes (equivalent to 5 x 10^8 cells) from GPI-PLC $^-$ mutant trypanosomes were mixed with MBP-TbGPI-PLC fusion protein at room temperature for 5 minutes in the presence of Tx100 (0.2 %) the mfVSG was converted to sVSG (Fig 6.15). Again, no activity was observed in the absence of either triton-x-100 or the MBP-TbGPI-PLC.

6.2.13. Analysis of MBP-TbGPI-PLC by MALDI-TOF

Matrix-assisted laser desorption/ionization time-of-flight mass spectrometry (MALDI-TOFMS) introduced in 1988 (Karas and Hillenkamp, 1988) is a widely used technique for mass spectrometric analysis of biological samples. It provides precise mass determination of proteins, high mass range, high sensitivity and relative tolerance to buffer components compared to other MS techniques.

An attempt was made to detect the mass ion of the MBP-TbGPI-PLC by means of nanospray, which is a development of ESI (Electrospray ionisation) for spraying very low amounts of very low concentration samples (nmol/mL). The technique has an increased tolerance to high aqueous solvents and salt contamination. Spectra can be obtained from a pg of material with very little prior clean up required. This increased performance is the result of lowering the inner diameter of the spray needle and reducing potentials normally used in ESI. Although nanospray has a high tolerance to salt the buffer of the purified MBP-TbGPI-PLC was changed from column buffer (20 mM Tris, pH 7.4; 200 mM NaCl, 1 mM EDTA, 10 mM β-mercaptoethanol) to ammonium bicarbonate (50 mM) by gel

Figure 6.14. Investigation into the activity of MBP-TbGPI-PLC expressed and purified from three different bacterial hosts, namely AD494, BL21 and Origami.

GPI-PLC$^-$ mutant trypanosomes at a concentration of 5 x 10^8 cells/ml, following washing with TES buffer (30 mM Tris-chloride replacing 30 mM TES), pH 7.4, were incubated in the presence or absence of the MBP-TbGPI-PLC fusion (40 μg) or the TEV cleaved MBP-TbGPI-PLC (40 μg) purified from either AD494, BL21 or origami expressions (Section 2.x), +/- Tx-100 (0.2%, (w/v)) at RT for 5 mins. Samples (6μl) were withdrawn and added to SDS sample buffer (x1). The samples were subjected to gel electrophoresis on a 10%, (w/v) SDS-PAGE gel.

Gel A.

Lane 1: GPI-PLC$^-$ mutant cells alone

Lane 2: GPI-PLC$^-$ mutant cells treated with MBP-TbGPI-PLC fusion from AD494 E. Coli

Lane 3: GPI-PLC$^-$ mutant cells treated with MBP-TbGPI-PLC fusion from AD494 E. Coli + Tx-100 (0.2%)

Lane 4: GPI-PLC$^-$ mutant cells + TEV cleaved MBP-TbGPI-PLC from AD494 E. Coli

Lane 5: GPI-PLC$^-$ mutant cells + TEV cleaved MBP-TbGPI-PLC from AD494 E. Coli + Tx-100 (0.2%)

Gel B.

Lane 1: GPI-PLC$^-$ mutant cells alone

Lane 2: GPI-PLC$^-$ mutant cells treated with MBP-TbGPI-PLC fusion from BL21 E. Coli

Lane 3: GPI-PLC$^-$ mutant cells treated with MBP-TbGPI-PLC fusion from BL21 E. Coli + Tx-100 (0.2%)

Lane 4: GPI-PLC$^-$ mutant cells + TEV cleaved MBP-TbGPI-PLC from BL21 E. Coli

Lane 5: GPI-PLC$^-$ mutant cells + TEV cleaved MBP-TbGPI-PLC from BL21 E. Coli + Tx-100 (0.2%)

Gel C.

Lane 1: GPI-PLC$^-$ mutant cells alone

Lane 2: GPI-PLC$^-$ mutant cells treated with MBP-TbGPI-PLC fusion from origami E. Coli,

Lane 3: GPI-PLC$^-$ mutant cells treated with MBP-TbGPI-PLC fusion from origami E. Coli + Tx-100 (0.2%)

Lane 4: GPI-PLC$^-$ mutant cells + TEV cleaved MBP-TbGPI-PLC from origami E. Coli

Lane 5: GPI-PLC$^-$ mutant cells + TEV cleaved MBP-TbGPI-PLC from origami E. Coli + Tx-100 (0.2%)

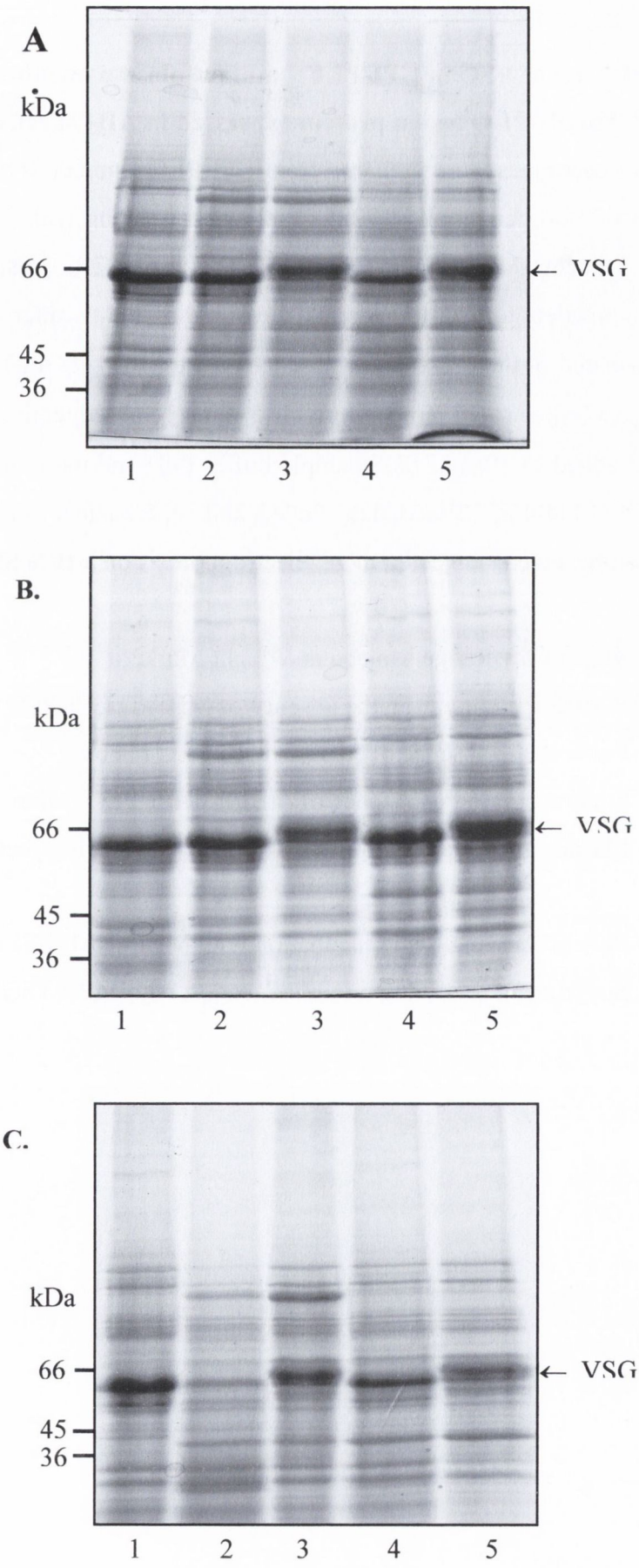
A
kDa
66
45
36
← VSG
1 2 3 4 5
B.
kDa
66
45
36
← VSG
1 2 3 4 5
C.
kDa
66
45
36
← VSG
1 2 3 4 5

Figure 6.15. Release of VSG in GPI-PLC$^-$ mutant plasma membranes upon cleavage with the MBP-TbGPI-PLC fusion protein expressed in AD494 cells.

Plasma membranes were prepared from GPI-PLC$^-$ mutant trypanosomes according to the protocol of Voorheis et al., (1978). Following washing with TES buffer (see Table 2.1; 30 mM Tris-chloride replacing 30 mM TES), pH 7.4, plasma membranes at a concentration equivalent to 5 x 10^8 cells/ml (measured by light scattering at 600 nm, see Fig 2.13) were incubated in the presence or absence of the MBP-TbGPI-PLC fusion (40 μg) + Tx-100 (0.2%, (w/v)) at room temperature for 5 mins. Subsequently, samples (20μl) were withdrawn and added to 10μl of SDS sample buffer (x3) and the remainder of the mixture was centrifuged (13,000 **g**, 20 seconds). Pellets and supernatants were analysed for release of VSG. All samples were subjected to gel electrophoresis on a 10% SDS-PAGE gel.

Lane 1: Sigma Low Range Molecular Weight Markers

Lane 2: Plasma membranes in the absence of MBP-TbGPI-PLC fusion

Lane 3: Pellet in the absence of MBP-TbGPI-PLC fusion

Lane 4: Supernatant in the absence of MBP-TbGPI-PLC fusion

Lane 5: Plasma membranes following 5 min incubation with MBP-TbGPI-PLC fusion at RT

Lane 6: Pellet following 5 min incubation with MBP-TbGPI-PLC fusion at RT

Lane 7: Supernatant following 5 min incubation with MBP-TbGPI-PLC fusion at RT

Figure 6.15. Release of VSG in GPI-PLC $^{-}$ mutant plasma membranes upon cleavage with the MBP-TbGPI-PLC fusion protein expressed in AD494 cells.

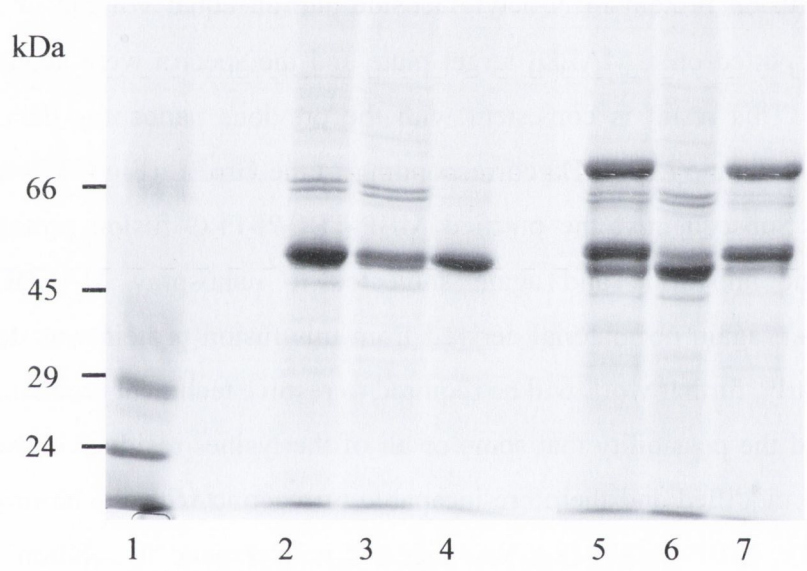

filtration on Sephadex G-25. The sample was given to Achim Treumann (Director of Mass Spectrometry, RCSI, Dublin) for analysis by nanoelectrospray. The nanospray analysis revealed different peaks corresponding to the molecular weights of the proteins present in the sample. There is a major peak at 57.3 kDa, which corresponds, to the GroEL in the sample (Fig 6.16). There was no other peak evident which might correspond to the MBP-TbGPI-PLC fusion (84 kDa) even when the range of acquisition was altered.

In parallel to this analysis a sample of the whole uncleaved MBP-TbGPI-PLC fusion protein was analyzed by MALDI-TOF. A sample (500 µl) of the MBP-TbGPI-PLC fusion protein purified by gel filtration on Sephacryl S-200 was freeze-dried and reconstituted in N-octylglucoside (20 mM). Octylglucoside is a neutral detergent that does not cause interference in MALDI mass spectrometric analysis (Cohen and Chait, 1996). A sample (2 µl) of the fusion protein in N-octylglucoside and an equal volume of matrix (sinapinic acid) were spotted on a MALDI target plate and the spectra were acquired as described previously. This result is consistent with the previous nanospray data. The graph depicts a major peak at 57.225 kDa corresponding to the GroEL (Fig 6.17) with no other peaks present. Subsequently, the purified MBP-TBGPI-PLC fusion protein was derivatized with acetic anhydride and again subjected to nanospray MALDI mass spectrometry. However, again no material derived from this fusion protein was detected (data not shown). Clearly, further work will be required to resolve technical problems.

We investigated the possibility that some or all of the lysines residues in the GPI-PLC sequence may be modified and therefore incapable of reacting with the biotinylation reagent (see Chapter 4). MBP-TbGPI-PLC was digested with trypsin 'in-solution'. This particular digestion was very kindly performed by Achim Treumann (Director of Mass Spectrometry, RCSI, Dublin). The log (e) values in Table 6.2 inform us of the relative significance of each protein in the MBP-TbGPI-PLC solution. This data indicates that the MBP-TbGPI-PLC fusion contains more or less equivalent amounts of MBP protein and GPI-PLC. The data in Fig 6.18 (a & b) depicts the peptides produced from trypsin digestion of the GPI-PLC from the MBP-TbGPI-PLC fusion protein. Eleven peptides were produced from the trypsin digestion. Fig 6.18 (a) shows the results of trypsin digestion from three separate experiments carried out in three different locations on three separate mass spectrometers. The data collected from Trinity College and RCSI are from trypsin digestion of the MBP-TbGPI-PLC fusion protein. The data collected from Glasgow identified the peptides, derived from the native GPI-PLC present in a mixture of proteins comprising the plasma membranes of bloodstream forms of *T. brucei*.

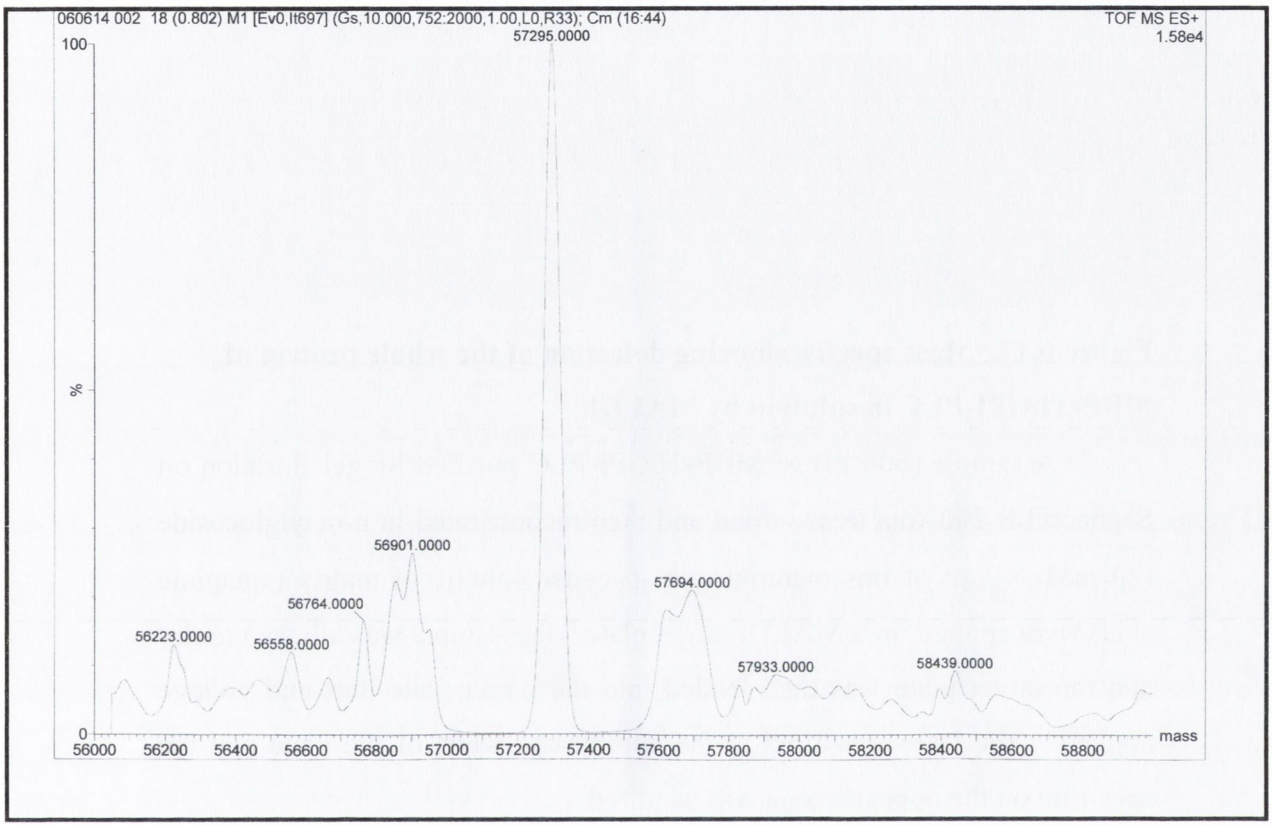

Fig 6.16. Nanoelectrospray-ES of MBP-TbGPI-PLC fusion protein.

Purified MBP-TbGPI-PLC was changed from column buffer (20 mM Tris, pH 7.4; 200 mM NaCl, 1 mM EDTA, 10 mM β-mercaptoethanol) to ammonium bicarbonate (50 mM) by gel filtration on Sephadex G-25. The sample was given to Achim Treumann (Director of Mass Spectrometry, RCSI, Dublin) for analysis by nanoelectrospray. The spectra shown on the opposite page depicts the molecular weights of the proteins detected from the nanospray analysis as peaks. There is a major peak present that corresponds to a molecular weight of 57.3 kDa, which is the GroEL.

Figure 6.17. Mass spectra showing detection of the whole protein of MBP-TbGPI-PLC in solution by MALDI.

A sample (500 µl) of MBP-TbGPI-PLC purified by gel filtration on Sephacryl S-200 was freeze-dried and then reconstituted in n-octylglucoside (20 mM). 2 µl of this material and an equal volume of matrix (sinapinic acid) were spotted on a MALDI target plate. The sample was allowed to dry and the target plate was then loaded into the target plate port and voltage applied. The laser was fired at the appropriate wells of the plate and the spectrum on the opposite page was acquired.

Figure 6.17. Mass spectra showing detection of the whole protein of MBP-TbGPI-PLC in solution by MALDI.

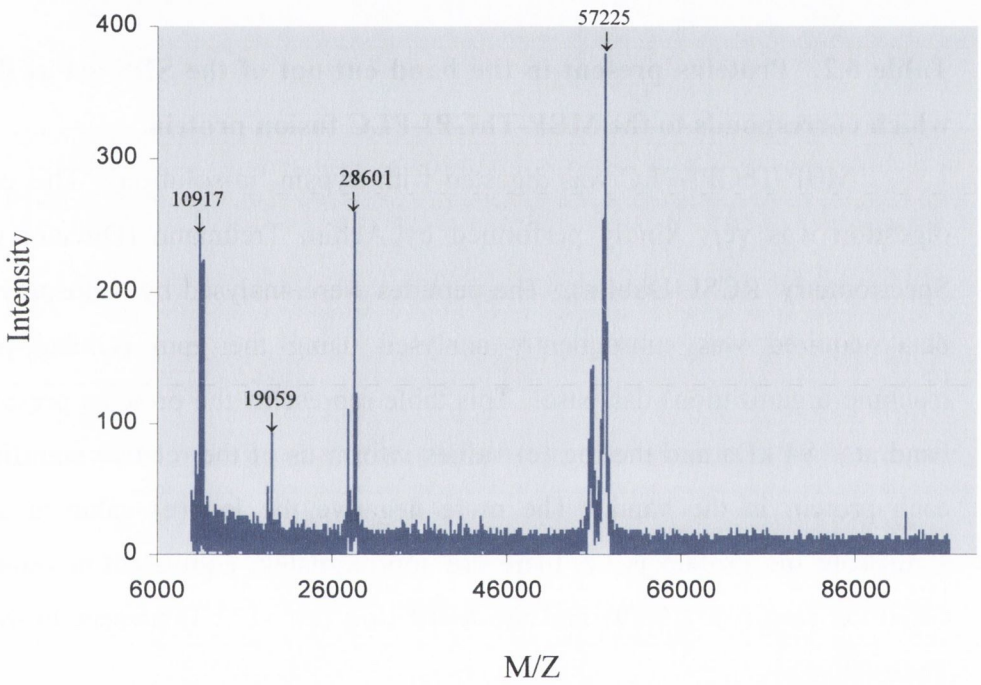

Log (e)	*Mr*	*Protein*
- 122.3	43.4	Maltose binding protein
- 93.9	40.6	GPI-PLC

Table 6.2. Proteins present in the band cut out of the SDS gel at (84 kDa) which corresponds to the MBP-TbGPI-PLC fusion protein.

MBP-TbGPI-PLC was digested with trypsin 'in-solution'. This particular digestion was very kindly performed by Achim Treumann (Director of Mass Spectrometry, RCSI, Dublin). The peptides were analysed by nanospray and the data acquired was subsequently analysed using the gpm (Global proteome machine organization) database. This table represents the proteins present in the band at ~ 84 kDa and the log (e) values inform us of the relative significance of each protein in the band. The more negative the log (e) value is the more significant the protein is i.e. there are approximately equivalent amounts of the GPI-PLC (log (e): - 93.9) and the MBP (log (e): -122.3) present in the MBP-TbGPI-PLC

Fig 6.18(a). Table of those peptides actually detected that are produced when the GPI-PLC is cleaved by trypsin digestion.

The data was collected from three separate experiments and analysis was carried out using mass spectrometry in three separate laboratories. The peptides detected are shown in colour with corresponding coloured ticks that specify the laboratory where each peptide was identified. The data collected from Trinity College and RCSI are from trypsin digestion of the MBP-TbGPI-PLC fusion protein. The data collected from Glasgow identified the peptides, derived from the native GPI-PLC present in a mixture of proteins comprising the plasma membranes of bloodstream forms of *T. brucei*.

Peptides produced from trypsin digestion of GPI-PLC	MALDI-TOF analysis performed in Trinity College Dublin	MALDI-TOF analysis performed at University of Glasgow	Nanospray analysis performed at RCSI, Dublin.
WSPQSWMSDTRSSIEKKCIGQVYMVGAHNAGTHGIQMFSPFGLDAPEK WSPQSWMSDTRSSIEKK	✓		
WSPQSWMSDTRSSIEKKCIGQVYMVGAHNAGTHGIQMFSPFGLDAPEK CIGQVYMVGAHNAGTHGIQMFSPFGLDAPEK			✓
SLPPYVTFLLRFLTVGVSSR SLPPYVTFLLR			✓
SLPPYVTFLLRFLTVGVSSR FLTVGVSSR		✓	
CQNLSIRQLLDHGVRYLDLRMNISPDQENKIYTTHFHISVPLQEVLK CQNLSIRQLLDHGVRYLDLR	✓		
CQNLSIRQLLDHGVRYLDLRMNISPDQENKIYTTHFHISVPLQEVLK MNISPDQENKIYTTHFHISVPLQEVLK			✓
IFLVVRPYVEYPYAR IFLVVRPYVEYPYAR	✓		
IFLVVRPYVEYPYAR IFLVVRPYVEYPYAR		✓	
IFLVVRPYVEYPYAR IFLVVRPYVEYPYAR			✓
SIWVNQMELNDLLDRLEELMTRDLEDVSIGGVPSKMYVTQAIGTPRNNDFAVAACCGACPGSHPDLYSAAK SIWVNQMELNDLLDRLEELMTR	✓		
SIWVNQMELNDLLDRLEELMTRDLEDVSIGGVPSKMYVTQAIGTPRNNDFAVAACCGACPGSHPDLYSAAK DLEDVSIGGVPSKMYVTQAIGTPR		✓	
SIWVNQMELNDLLDRLEELMTRDLEDVSIGGVPSKMYVTQAIGTPRNNDFAVAACCGACPGSHPDLYSAAK NNDFAVAACCGACPGSHPDLYSAAK			✓
WFYDLNVNGVMRGERVTIR WFYDLNVNGVMR			✓
WFYDLNVNGVMRGERVTIR GERVTIR	✓		

Fig 6.18(b). Sequence of the recombinant GPI-PLC with trypsin digested peptides shown in colour beneath the sequence.

The peptides from Fig 6.18 (a) are shown here aligned beneath the sequence of the recombinant GPI-PLC. All the lysine residues (K) not found within a peptide produced from trypsin cleavage are in red. * denotes a part of the sequence where trypsin will not cleave. No cleavage occurs when a proline residue is on the carboxyl side of the cleavage site.

* denotes a part of the sequence where cleavage is slower due to the presence of an acidic residue (aspartic acid, D) on the carboxyl side of lysine.

Fig 6.18(b). Sequence of the recombinant GPI-PLC with trypsin digested peptides shown in colour beneath the sequence.

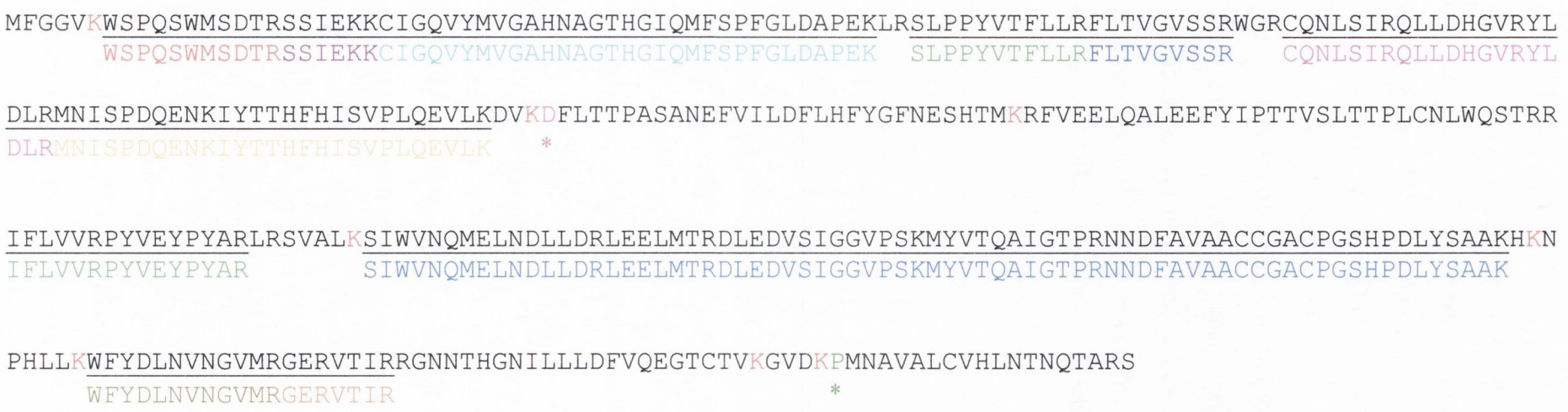

The GPI-PLC from the MBP-TbGPI-PLC fusion protein contains 15 lysine residues. From the information provided in Fig 6.18 (a & b), only seven lysine residues are present in the peptides produced from trypsin digestion. According to the data obtained there were no modifications present on any of these lysine residues. This analysis suggests that 47% of lysine residues are definitely not modified, and, therefore, one would expect these lysine residues to react with the biotinylation reagent. It could also be argued further, that the lysine residues present on the N-terminal side of a trypsin-digested peptide are not derivatized because trypsin would not cleave at this point if the lysines were modified. There are three such lysines present in the sequence and this could arguably increase the detection of unmodified lysines to ten. This analysis suggests that a minimum of 67 % of the lysine residues in the recombinant GPI-PLC are not modified and hence one would expect these to be reactive unless they are folded into the hydrophobic core of the protein or exist as salt bridges.

6.3. Discussion.

The purification of over expressed fusion proteins using bacterial expression systems is a useful tool for the study of many proteins. One problem that can occur is the formation of stable interactions between the expressed fusion protein and certain endogenous bacterial proteins, such as the molecular chaperone GroEL. Such interactions may result in the co-purification of contaminating bacterial proteins (Rohman and Harrison-Lavoie, 2000).

The purification of MBP-TbGPI-PLC was very straightforward and efficient with only one drawback, the co-purification of one other protein. This protein migrated at approximately 60 kDa on SDS-PAGE and could not be removed by any means of purification tested in this study. It was present in at least 80 % of all purifications from the post-induced sample to the Sephacryl S-200 samples. Purification on the amylose resin followed by gel filtration on S-200 would have produced a 100 % pure protein if the contaminant at 60 kDa did not co-purify with the MBP-TbGPI-PLC. Although, this protein was present throughout the purification its presence did not affect the activity of the GPI-PLC in the MBP-TbGPI-PLC fusion. The recombinant GPI-PLC produced, using the MBP fusion system, was capable of cleaving the GPI anchor of the VSG in GPI-PLC $^{-}$ mutant trypanosomes and the GPI anchor of VSG from GPI-PLC $^{-}$ mutant plasma membranes.

The Mass Spectrometry data gave us evidence that the majority of the protein in the band at ~60 kDa is the bacterial protein GroEL (Mr 57.3 kDa). GroEL and its cochaperonin GroES are two essential proteins in *E. coli* that assist in the folding of a large number of proteins. GroEL recognizes and binds to polypeptides predominantly by hydrophobic interactions. The interactions between polypeptides and GroEL are nucleotide dependent: ATP binding and hydrolysis in GroEL control the binding of polypeptide/ GroES and the folding/release of the polypeptide. It has been reported that by treating the clarified lysate with 2 mM ATP, 10 mM $MgSO_4$ before binding a GST-fusion to its resin can sometimes remove the contaminating bacterial protein. However, addition of ATP to the MBP-TbGPI-PLC fusion lysate before binding to the amylose resin did not remove the co purified GroEL (data not shown).

One method for the removal of co purifying GroEL from GST fusion proteins has been published which uses either an ATP- or ATP–GroES-wash step (Thain *et al.*, 1996). The addition of GroES can induce the release of GroEL from some proteins for which the addition of ATP alone is not sufficient for release. One potential drawback to this method is that GroES must either be purified or be purchased commercially. The latter option can be very expensive for anything other than small-scale purification. However, GroEL has been shown to be able to interact with a large proportion (~50%) of urea-denatured proteins in *E. coli* cell extracts (Viitanen *et al.*, 1992). A method has been developed which uses urea-denatured proteins to compete with the over-expressed proteins for binding to GroEL (Rohman and Harrison-Lavoie, 2000). Note that these methods for the removal of GroEL have only been tested for GST-fusion proteins and therefore, it is only assumed that they will work for other fusion proteins as well. The fact that GroEL co-purifies with the MBP-TbGPI-PLC but not with other MBP-fusion proteins strongly suggests that the GPI-PLC is folded with many if not most of its hydrophobic residues on the outside of the protein. This evidence is also consistent with the aggregating behaviour of the GPI-PLC when purified and the probable folding of positively charged residues to the interior. Such a folding mechanism would be inconceivable if not accompanied by the balanced inward folding of aspartate and glutamate residues to maintain electro-neutrality in such a small and confined space as the interior of a protein certainly is. Consequently, the presence of many salt bridges in the GPI-PLC of *T. brucei* must be considered and further work undertaken to test this hypothesis.

The analysis by Mass Spectrometry of the purified MBP-TbGPI-PLC was expected to give us some answers as to why the protein cannot be biotinylated. Firstly, we

attempted to determine the true mass of the MBP-TbGPI-PLC fusion protein using MALDI-TOF analysis. The mass accuracy depends on the type and performance of the analyser of the mass spectrometer, but most modern instruments should be capable of measuring masses to within 0.01% of the molecular mass of the sample, at least up to approximately 40,000 Da. When we attempted to get the true mass of the MBP-TbGPI-PLC fusion we found only one peak at 57 kDa, which corresponded to the co-purifying GroEL. The time-of-flight (TOF) analyser separates ions according to their mass (m)-to-charge (z) (m/z) ratios by measuring the time it takes for ions to travel through a field free region known as the flight, or drift, tube. The heavier ions are slower than the lighter ones. The MBP-TbGPI-PLC fusion has a theoretical molecular mass of 84 kDa and is possibly too heavy to fly and therefore cannot be detected.

Nanospray is a sensitive technique for the detection of proteins with high molecular masses and generally a mass accuracy of within 0.01 % of the molecular mass should be achievable. However, when this technique was used to determine the molecular mass of the MBP-TbGPI-PLC a peak corresponding to the contaminant was again detected but without an accompanying peak for the MBP-TbGPI-PLC fusion protein, confirming the MALDI-TOF analysis and indicating to us that Nanospray cannot detect the MBP-TbGPI-PLC fusion protein for some technical reason. Clearly, Coomassie stained gels have shown that the MBP-TbGPI-PLC was present in large amounts.

Chapter 7

General Discussion

7.1 Introduction

The GPI-PLC in bloodstream forms of *T. brucei* is a peculiar enzyme in many respects possessing several rather curious features. First, the enzyme behaves as an integral membrane protein during purification and subcellular fractionation (Bulow and Overath, 1986, Hereld, 1986 #61, Fox, 1986 #62 & Mensa-Wilmot, 1992 #66), even though the primary sequence does not contain any obvious hydrophobic stretches to account for this physical property. Second, this work has established that the GPI-PLC and the presumed substrate (the VSG) are both located in the same membrane. However, the enzyme is not required for any of the key VSG shedding events that are essential for the survival and life cycle completion of *T. brucei*. This raises two questions: how does the membrane-bound VSG access the active site of the GPI-PLC, and how is enzyme activity controlled to prevent 'futile' hydrolysis?

7.2 The GPI-PLC is located in the flagellar membrane of T. brucei

The main aim of this study was to clarify the localization of the GPI-PLC in bloodstream forms of *T. brucei*. Immunofluoresence studies provided evidence for an extracellular localization for the GPI-PLC in bloodstream forms of *T. brucei*. Experimental results do not support a localization in the flagellar pocket, Golgi apparatus, on the cytoplasmic face of intracellular vesicles, in glycosomes or in the ER, as other investigators have proposed (Grab *et al.*, 1987, Bulow, 1989 #191 & Subramanya, 2006 #159). By immunofluoresence the GPI-PLC was found on the outer side of the plasma membrane with the VSG and the ISG-70, two proteins known to have an extracellular localization (Vickerman, 1969 ; Jackson *et al.*, 1993). The fact that a detergent was required to access tubulin, an inner surface protein (Sherwin *et al.*, 1987), and not the GPI-PLC provides good evidence that the GPI-PLC is not inside the permeability barrier of the plasma membrane (Chapter 3). Furthermore, cell surface iodination revealed that at least some of the enzyme is localized in the outer leaflet of the plasma membrane bilayer (Chapter 4). The data also indicate that the GPI-PLC is exclusively located on the flagellar membrane rather than the pelicular membrane of the cell body or the flagellar pocket membrane. This location places the GPI-PLC and the VSG on the same side of the plasma membrane bilayer covering the flagellum, thereby indicating that both enzyme and substrate reside in close proximity making the cleavage reaction of the GPI-PLC on the GPI anchor a much more feasible process than previously thought. A previously accepted

consensus in the literature was that in growing bloodstream forms of *T. brucei,* endocytosed vesicles containing mfVSG fuse with GPI-PLC-containing vesicles and released sVSG would be recycled to the medium *via* the flagellar pocket (Bulow *et al.*, 1989). This report also postulated that during differentiation to procyclic cells, internalised mfVSG is preferentially processed to a proteolytic fragment, which would likewise be recycled to the surface (Bulow *et al.*, 1989). However, it is now known that upon differentiation of bloodstream forms to procyclic forms the VSG is released by two primary mechanisms: initially release is mediated by GPI cleavage and at later time points, mediated by proteolysis. These two modes of release are apparently independent, with each occurring at the cell surface (Gruszynski *et al.*, 2003) indicating that the VSG does not need to be internalised for GPI hydrolysis to occur.

The release of sVSG in dividing bloodstream trypanosomes in culture has a half-life of approximately 32 hours (Seyfang *et al.*, 1990 & Bulow, 1989 #237). This slow release of sVSG is curious given the proposed extracellular location of the GPI-PLC. The slow release was previously attributed to VSG endocytosis, subsequent fusion of the VSG with the GPI-PLC inside the cell and then exocytosis *via* the flagellar pocket, since earlier reports placed the enzyme on the inner face of intracellular vesicles (Bolow *et al.*, 1989). In this thesis it is proposed that the GPI-PLC remains in the flagellar membrane and the VSG travels to the enzyme for hydrolysis of the GPI anchor and subsequent release from the cell surface. The experimental evidence for this is that the GPI-PLC remained associated with the flagellar membrane during release of the VSG from intact trypanosomes (Chapter 3). That the release of the VSG is by the action of the GPI-PLC rather than by proteolysis was confirmed by the detection of the CRD epitope (see Chapter 3).

The activity of the GPI-PLC must be controlled. Otherwise the VSG would be shed from the membrane continuously. One possibility is that the enzyme is normally inactive, however, the regulatory factor(s) remains elusive. The GPI-PLC is an abundant protein, present at approximately 3 x 10^4 copies / cell, which represents 0.04 % of the total cellular protein (Hereld *et al.*, 1986). With an estimated turnover rate of 100-700 mf VSG molecules/min the VSG can be released (1.12 x 10^7 molecules/cell, 16 % total cellular protein) within a few minutes (Hereld *et al.*, 1986). It is difficult to accept that a parasite, particularly one as parsimonious as *T. brucei* harbours an abundant enzyme on its surface that at least according to the literature is not required for any of the life cycle processes

where the VSG is shed from the cell. However, it remains possible that we are simply ignorant of its true role at the present time.

It has been reported that the addition of Ca^{2+} and the calcium ionophore A23187 to intact bloodstream forms of *T. brucei* causes release of the VSG, thereby exposing the CRD epitope (Bowles and Voorheis, 1982). A23187 is a carboxylic antibiotic that selectively transfers calcium, magnesium, and other divalent cations across biological membranes. In these experiments sVSG was released from the cell surface, indicating that it was the GPI-PLC, which had cleaved the GPI anchor and thus implying that the GPI-PLC had been activated by some factor. The addition of Ca^{2+} alone had no affect on the cells and the release of sVSG only took place when both Ca^{2+} and the calcium ionophore were added to the incubation medium together (Voorheis *et al.*, 1982). It is known that the catalysis activity of the GPI-PLC itself is independent of Ca^{2+} *in vitro* (Fox *et al.*, 1986). This important observation suggests that the calcium activates some other factor possibly in the cytosol that either activates the GPI-PLC directly or triggers a sequence of events that in turn activates the GPI-PLC. Alternatively, Ca^{2+} may inactivate some inhibitory factor. In addition, when bloodstream forms of *T. brucei* were incubated with the glucose analogue, 2-deoxyglucose, sVSG was released and the cells remained intact (Voorheis *et al.*, 1982). This result again suggests that the GPI-PLC needs to be activated.

A number of proteins have been localized to the flagellum: an adenylate cyclase in *T. brucei* (Paindavoine *et al.*, 1992), a minor isoform of a glucose transporter that is specifically targeted to the flagellum membrane of *Leishmania enrietti* (Piper *et al.*, 1995), the flagellum calcium-binding protein (FcaBP) of *T. cruzi* (Engman *et al.*, 1989 & Godsel, 1999 #240) and the calflagins of *T. brucei* (Wu *et al.*, 1994). However, the exclusive flagellar location of adenylate cyclase reported by Paindavoine, *et al.* (1992) could not be repeated in our laboratory using the same antibodies used by these workers (O'Beirne & Voorheis, unpublished observation). The flagellum calcium-binding protein (FcaBP) and the calflagins are both specifically localized to the flagellar membrane (Engman *et al.*, 1989 & Godsel, 1999 #240). Both proteins associate with the flagellar membrane in a manner that depends on dual acylation at their N-termini. Mutations abrogating acylation confer a cytoplasmic localization, while mutations that allow myristoylation but not palmitoylation lead to a pellicular membrane localization (communication from 'The International Conference of Kinetoplastid Molecular Cell Biology', April 2007). It has been reported that the GPI-PLC is reversibly thioacylated (Paturiaux-Hanocq *et al.*, 2000). This thioacylation involves a group of three closely clustered cysteine residues located in

the C-terminal region of the polypeptide, but the exact number of cysteines actually acylated remains uncertain. It was found that both palmitic acid and myristic acid were incorporated in metabolic labelling experiments (Paturiaux-Hanocq *et al.*, 2000). This modification was found not to be an absolute requirement for catalytic activity but it was proposed that it might have some function in regulating enzyme access to the mfVSG (Paturiaux-Hanocq *et al.*, 2000). Accepting that the GPI-PLC and the VSG are located in the same membrane suggests that the GPI-PLC does not need to be modified by thioacylation in order to gain access to its substrate, but the possibility exists that thioacylation of the GPI-PLC is required for its association with the flagellar membrane, similar to the calflagins in *T. brucei*.

Myristoylation and palmitoylation are post-translational modifications found at the N-termini of some mammalian proteins. Myristate (14-carbon) is covalently attached by an amide linkage to an N-terminal glycine during its biosynthesis (Han and Martinage, 1992). Palmitate (16-carbon) is attached post-translationally *via* a thioester linkage, most commonly to a cysteine residue. There is no known amino acid sequence requirement for palmitoylation; however, in many instances, this modification occurs when the cysteine is located near a previously acylated amino acid residue (Hallak *et al.*, 1994 & Mumby, 1994 #249). Both myristoylation and palmitoylation are involved in the membrane associations of some proteins, such as G protein α-subunits and *src* tyrosine kinases (Resh, 1993 & Milligan, 1995 #251). Palmitoylation may also be involved in protein-protein interactions, as well as in the stabilization of membrane associations (Shenoy-Scaria *et al.*, 1993 & Wedegaertner, 1993 #253). It is interesting to note that the GPI-PLC possesses a similar pattern of clustered cysteine residues (CCXXC) to that found at the acylation site of some members of the α-subunit family of G-proteins (Linder *et al.*, 1993). The possibility therefore exists that thioacylation of the GPI-PLC in *T. brucei* leads to membrane association of the protein just as it does in the α-subunit of G proteins and *src* tyrosine kinases.

7.3 GPI-PLC is not involved in the disaggregation of trypanosomes or the cycle of endocytosis and exocytosis of either transferrin or surface immune complexes.

A number of processes were studied in this thesis in order to investigate the function of the GPI-PLC in bloodstream form trypanosomes *in vivo*. The function of the GPI-PLC in *T. brucei* has been the cause of much speculation, as the enzyme has an

activity that could theoretically facilitate the rapid shedding of the protective VSG coat. The VSG is the only substrate present in amounts sufficient to account for the quantity of GPI-PLC present. The VSG and the GPI-PLC show the same developmentally regulated expression found in bloodstream but not in procyclic trypanosomes (Carrington *et al.*, 1989). As a null mutant cell line was available, it seemed reasonable that a direct comparison between these cells and wild-type trypanosomes might give information on the function of the GPI-PLC. In the present study it was demonstrated that the release of the VSG does not occur in GPI-PLC $^{-}$ mutant trypanosomes. The CRD epitope did not become exposed upon hypotonic lysis of GPI-PLC $^{-}$ mutant trypanosomes and the mfVSG was not converted to sVSG. Thus it is clear that in wild type cells VSG release, when it occurs, is mediated through the action of the GPI-PLC. This observation confirms previous results from different laboratories (Rolin *et al.*, 1996, Cardoso de Almeida, 1983 #43). This experiment also provides the evidence that there is no other enzyme that metabolises the GPI-anchor on a substantial scale.

The normal cellular function of the GPI-PLC *in vivo* is unknown despite intensive study. The enzyme does not appear to be essential for normal differentiation to procyclic forms (Webb *et al.*, 1997), when the surface VSG is released mainly by proteolytic cleavage (Bulow *et al.*, 1989 & Ziegelbauer, 1993 #82). Furthermore, it was revealed that the GPI-PLC $^{-}$ mutant trypanosomes are capable of maintaining a persistent infection in immunologically competent mice and can undergo antigenic variation (Webb *et al.*, 1997). This result clearly showed that the GPI-PLC is not required for the switch from metacyclic to bloodstream form VSG or for subsequent antigenic variation. On the other hand, it has been reported that GPI-PLC is necessary for the accelerated differentiation of pleomorphic trypanosomes that is induced by mild acid stress (Rolin *et al.*, 1998). In addition, since constitutive GPI-PLC-mediated VSG release is part of the parasite biology (Shapiro, 1986 & Black, 1982 #177) and improper control of the enzyme hampers GPI metabolism (Mensa-Wilmot *et al.*, 1994 & Garg, 1997 #181) it is anticipated that interference in GPI-PLC control could partially impair parasite viability.

The mechanism by which transferrin enters the cytoplasm of trypanosomes after binding to a GPI-anchored receptor is not clear. In particular it is not known whether the receptor is released from a membrane or how the occupancy of the receptor is signalled across the plasma membrane. It has been proposed that the GPI-PLC may be involved in the hydrolysis of the GPI-anchor of the transferrin receptor and therefore have a role in the endocytosis of transferrin into trypanosomes (Carrington *et al.*, 1998). The process of

endocytosis and exocytosis of both FITC labelled transferrin and FITC labelled anti-VSG IgG was examined in wild-type and GPI-PLC$^-$ mutant trypanosomes in this thesis. It was found that the GPI-PLC is not required for the process of endocytosis and subsequent exocytosis (Chapter 5).

The process of disaggregation in bloodstream form trypanosomes following aggregation with anti-VSG antibody was also investigated in the wild-type and GPI-PLC$^-$ mutant bloodstream form trypanosomes. The mechanism by which trypanosomes disaggregate is not known. The GPI-PLC$^-$ mutant trypanosomes disaggregated with the same time-course of disaggregation as the wild type cells, indicating that the GPI-PLC is not required for the process (Chapter 5). In addition, the VSG was not released from cells at any point during the process and the CRD did not become immunologically exposed. Furthermore, the C-terminal domain of the VSG did not become exposed following disaggregation, ruling out the possibility that another enzyme, the GPI-PLD, was responsible for the process.

The process of disaggregation in bloodstream form trypanosomes is intriguing and it was decided to delve further into the mechanism of disaggregation. The phenomenon of disaggregation has been investigated by many workers in the past (Laveran & Mesnil, 1900, 1901 & 1907; Francis, 1903 and O'Beirne 1998). As yet no satisfactory mechanism for the process has been established. While the evidence in the literature strengthens the case for a regulated physiological process (that leads to disaggregation) and has eliminated several possible mechanisms, it has not identified any specific protein or enzyme responsible for the process itself. It has been reported that disaggregation is not due to the separation of immunoglobulin chains and conversion to monomers by either disulphide reduction or disulphide exchange reactions (O'Beirne *et al.*, 1998). However, this work does not rule out the possibility of exchange of disulfides in the VSG molecule and hence, a substantial conformational change. This possibility was investigated using a sulfydryl blocking reagent, iodoacetamide. It was found that this reagent inhibited the process of disaggregation without affecting oxygen consumption. This result implies that an essential thiol group is involved in the disaggregation of bloodstream form trypanosomes. The specific location of this thiol group is as yet unknown but the preliminary results presented in this study suggest a location on the trypanosome rather than on the cross-linking immunoglobulin. The possibility exists that TbPDIs might have a role in the mechanism of disaggregation, perhaps by assisting in disulfide exchange reactions within the VSG molecule thereby scrambling the disulfide pairs and altering the conformation of the VSG,

and reducing the affinity of the VSG for the antibody (see chapter 5, Fig 5.18 & 5.19). The role of the protein disulphide isomerase (PDI), particularly the glycosylated enzyme, requires further study.

The PDIs are thiol-disulfide oxidoreductases that catalyse the formation, reduction and isomerization of disulfide bonds, depending on the redox environment. PDI itself contains two active site Cys residues, which must be in the –SH form for the isomerase to be active. The enzyme catalyses the random cleavage and reformation of a protein's disulfide bonds thereby interchanging them as the protein progressively attains thermodynamically more favourable conformations. Two PDIs have been well characterized in *T. brucei* (Rubotham *et al.*, 2005). These PDIs possess several unusual features that distinguish them from PDIs in other organisms. First, the expression of TbPDI-1 and –2 is restricted to the bloodstream forms of *T. brucei*. Both TbPDIs are post-translationally modified by N-glycosylation. N-glycosylation is rare among PDI enzymes, and the only previous example of a glycosylated PDI is a class 1 PDI from yeast (Mizunaga *et al.*, 1990). The extent of glycosylation of TbPDI-1 is modest and apparently contributes ~2-3 kDa to the mature form of the polypeptide (Rubotham *et al.*, 2005). In contrast, N-glycans account for a significant proportion of the apparent molecular mass of native TbPDI-2. The characterization of TbPDI-2 indicated that this PDI was modified by the addition of glycans containing linear repeats of poly-N-acetyllactosamine and this represents the first example of such a modification for any PDI (Rubotham *et al.*, 2005).

7.4 Future work.

This study has demonstrated a new location for the GPI-PLC in bloodstream forms of *T. brucei*, which in turn opens new doors for further investigation. In particular, it would be of great interest to establish whether the GPI-PLC changes its location when it is activated. Preliminary experiments have established that the GPI-PLC does not change its location when trypanosomes are incubated with 2-deoxyglucose. In this case, the VSG is released from the cell surface by GPI cleavage and the cells remain intact. Two additional procedures which are known to result in active GPI-PLC are 1: the treatment of trypanosomes with Ca^{2+} and the calcium ionophore, A23187 and 2: the preparation of plasma membranes from bloodstream forms of *T. brucei*. It would be of great interest to find out if the GPI-PLC alters its position in the cell under either of these treatments. Labelling trypanosomes with a plasma membrane marker prior to the preparation of

plasma membranes might allow clarification of whether the GPI-PLC remains associated with the flagellar membrane during this process. Furthermore, it would be interesting to establish what factor in the cell activates the GPI-PLC to cleave the GPI anchor of the VSG on the surface of bloodstream form trypanosomes.

The GPI-PLC was found not to be involved in the cycle of endo/exocytosis or the process of antibody-mediated disaggregation in *T. brucei*. However, while investigating the process of disaggregation it was discovered that the sulphydryl blocking reagent, iodoacetamide blocked the process of disaggregation. Conditional ablation of mRNAs through RNA interference has become a powerful method for investigating gene function (Fire *et al.*, 1998) and the technique has been extended to trypanosomes (Ngo *et al.*, 1998 & Bastin, 2000 #265). Using this technique it was found that neither of the PDIs of *T. brucei*, either individually or in combination, is essential for growth of bloodstream forms in culture (Rubotham *et al.*, 2005). It should be possible to determine, by the same technique, whether either of the PDIs is required for antibody-mediated disaggregation in bloodstream forms of *T. brucei*. This could potentially identify the enzyme or enzymes involved in the process of disaggregation. However, unequivocal results in this case may also require classic "knock-out" of these enzymes rather than simple "knock-down" if significant activity remains after the latter process.

This study found that the recombinant GPI-PLC did not react with the biotinylating reagent, sulfo-NHS-biotin. If all, or even the majority of the lysine residues, are involved in salt bridges in the hydrophobic core of the GPI-PLC this could explain their lack of reactivity. The reactivity of the lysine residues in the GPI-PLC with other ligands *e.g.* FITC, should be tested. Methylating or acetylating the GPI-PLC both before and after trypsin digestion would establish whether the lysine residues are blocked for reactivity in the whole molecule. In order to unequivocally establish the presence of salt bridges it may be necessary to await the crystal structure of the GPI-PLC. The MBP-TbGPI-PLC fusion protein purified in this study could be used for crystallization studies. The purified preparation contains just one contaminating protein. The identity of this contaminant was found to be Gro-EL (see (Thain *et al.*, 1996) for review). A method for removal of this co-purifying protein GST-fusion proteins has been reported (Thain *et al.*, 1996). This approach may lead to an essentially homogenous preparation of MBP-TbGPI-PLC. Crystal structures of fusion proteins containing MBP have been reported (Center *et al.*, 1998). Having the crystal structure of the GPI-PLC would inform us of the location of the

lysine residues in the protein, whether they are on the surface or in the hydrophobic core of the protein and if any or all of them exist in salt bridges.

7.5. Conclusion.

The GPI-PLC has been the topic of intense study for a long time. The location of the enzyme in bloodstream forms of *T. brucei* alone has caused much controversy with many different and conflicting reports being published. The cytoplasmic face of intracellular vesicles has been the preferred location for the enzyme in the past. However, this presented a topological problem – how does the GPI-PLC translocate across a membrane to gain access to the VSG? The GPI-PLC does not have an N-terminal signal sequence or any other overt hydrophobic domain therefore, crossing the plasma membrane to reach the VSG did not a seem viable hypothesis. With the new evidence presented in this study this issue is resolved. According to the results presented here the GPI-PLC resides in the flagellar membrane of bloodstream forms of *T. brucei*. The GPI-PLC is aligned along the flagellum in a patchy string-like fashion and it is shielded by the VSG. In addition, we have found that the GPI-PLC remains in the flagellar membrane upon activation.

The biological function of the GPI-PLC still remains a mystery. It is not required for any of the major VSG shedding events during the life cycle of the trypanosome. It does not play a role in the endocytosis and subsequent exocytosis of the VSG or transferrin and it is not required for the process of antibody-mediated disaggregation of bloodstream form trypanosomes. The viability of the null mutant indicates that the GPI-PLC is not essential. It does not make sense that bloodstream form trypanosomes contain such an abundant and active enzyme that is not required for any process. Further investigation is required to either establish or rule out the possibility that the GPI-PLC lies in the flagellar membrane in an inactive state *in vivo*.

Appendix

Introduction.

Quantitative evidence for the localization of the GPI-PLC in bloodstream form trypanosomes was the primary aim of the experiments described in this chapter. The ELISA assay system was used to detect total GPI-PLC, both active and inactive.

Enzyme-linked immunoabsorbent assay (ELISA) is a powerful tool for the detection of specific proteins and macromolecules in biological systems. Three principal types of ELISA are generally recognized: direct ELISA, indirect ELISA, and sandwich ELISA (Crowther, 1995). Each type has advantages and disadvantages, as described (Koenig and Paul, 1982). In addition, several ELISA protocols have been developed to meet the varying requirements for the detection of specific proteins or antigens (Crowther, 1995). ELISA has been widely used to detect antigenic proteins in biological samples.

An estimate of 3×10^4 molecules of GPI-PLC per cell has been reported in the literature (Hereld *et al.*, 1986). Three approaches have so far been taken for the quantitative detection of the total GPI-PLC in bloodstream form trypanosomes during this project. The first two approaches involved the use of a direct ELISA and a sandwich ELISA. However, these assays did not yield satisfactory results nor did they permit the sensitive detection of the GPI-PLC in whole cells. Firstly, the direct ELISA predicted a copy number for the GPI-PLC of 1.35×10^3 copies/cell, which differs by more than an order of magnitude from that reported in the literature (Hereld *et al.*, 1986). Because of the wide discrepancy between the copy number predicted by this direct ELISA assay and that obtained by measuring the GPI-PLC activity (Hereld *et al.*, 1986) a GPI-PLC $^-$ mutant cell line was examined with the same assay procedure. The results obtained when the direct ELISA was used to measure the copy number of the GPI-PLC in null mutant cells were almost identical to those obtained when assaying the GPI-PLC in wild-type cells (Fig 3). Therefore, this assay could not be used to quantitate the amount of GPI-PLC in bloodstream form trypanosomes because it did not possess sufficient specificity for the reliable detection of the GPI-PLC in whole cell extracts without unacceptable interference from other substances in the extract.

The sandwich (two-site) assay was the next approach tested for the detection of the GPI-PLC in bloodstream form trypanosomes. However, detection of the recombinant GPI-PLC in the standard assay produced very high background readings, 44 % compared to 5.5 % with the direct assay approach, and therefore, this assay could not be used to quantitate the amount of GPI-PLC in bloodstream form trypanosomes because it did not

have the specificity or reliability required to detect the recombinant GPI-PLC in the standard assay.

To improve the efficacy of the ELISA procedure for detecting the GPI-PLC, a cycling assay was introduced (Self *et al.*, 1985; Stanley *et al.*, 1988). Such assays, using enzyme amplification, have been devised to allow the development of highly sensitive and rapid immunoassays. The amplification is achieved by causing the enzyme to produce a catalytic activator for a secondary system, the activity of which is measured and used to quantify the enzyme. Amplification results from the combined catalytic effect of the enzyme producing the activator and the catalytic effect of that activator on the secondary system. Secondary systems may be based on enzymes, which require a specific activator or on cyclic systems in which the activator takes part in the cycle, being changed and then reformed, during which an irreversible change occurs in an associated reactant, such as the formation of a coloured product (Fig 2.11).

The use of the cycling assay in conjunction with the direct ELISA improved the sensitivity of detection of the GPI-PLC in bloodstream form trypanosomes. The number of cells required for the reliable detection of the GPI-PLC by the direct-cycling assay (3 x 10^4 cells) was found to be 100 times less then the number required to give the same absorbance readings in the non-cycling direct ELISA (3 x 10^6 cells). In addition, the background levels present in the direct-cycling assay were also found to be lower (4-5 fold) than those obtained in the non-cycling direct ELISA.

Results.

Quantitative detection of GPI-PLC in bloodstream form trypanosomes.

A standard assay procedure was developed that used the purified recombinant GPI-PLC as the antigen to coat the wells of microtitre plates and rabbit anti-GPI-PLC (1/1000 dilution) as the primary antibody. These conditions gave no background readings when recombinant antigen was used and the assay was very sensitive. The development time was 60 min. The optimum concentration of recombinant GPI-PLC for this assay was found to be between 0 – 1 μg/ml (Fig 1). The lowest reliable amount of recombinant GPI-PLC that could be detected with the assay was 0.05μg total/well, which, with a molecular weight of 37,000 – 39,800 daltons (Bulow and Overath, 1986; Fox *et al.*, 1986; Hereld *et al.*, 1986), corresponded to 8.13 x 10^{11} molecules. Consequently, in the

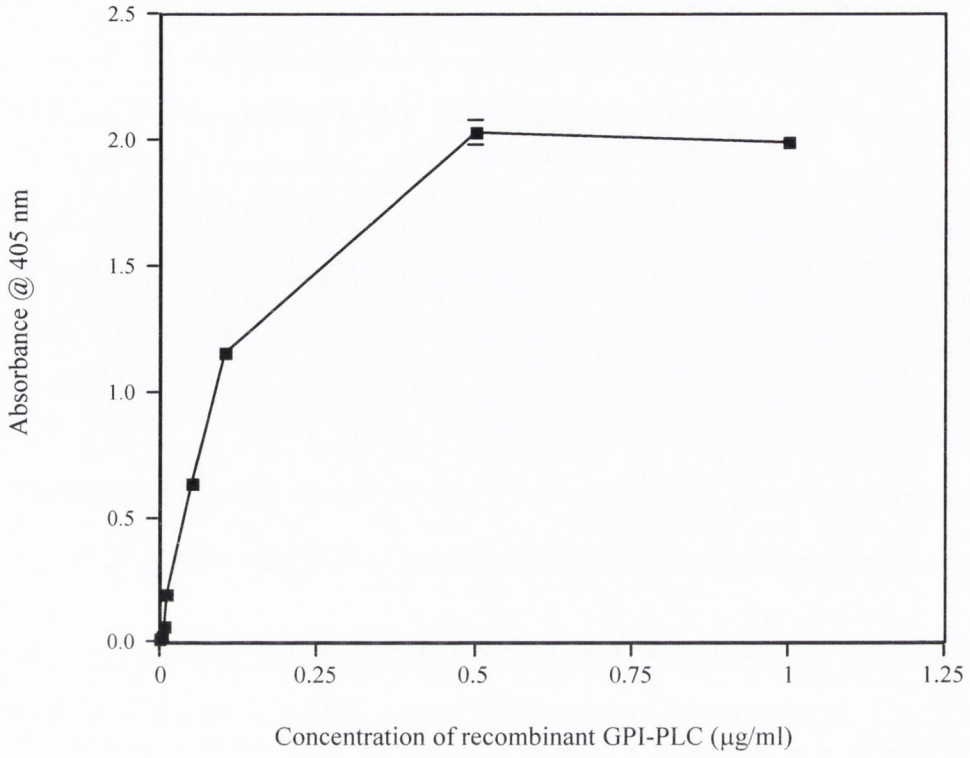

Fig 1. Quantitative detection of recombinant GPI-PLC by direct ELISA. Polystyrene high binding ELISA plates were coated with various concentrations of purified recombinant GPI-PLC (0.1 ml final volume / well) and incubated with anti-GPI-PLC antibody. Binding of the anti-GPI-PLC antibody was detected using an anti-rabbit IgG alkaline phosphatase conjugate (Section 2.1.54). The development was stopped after 60 min. Data are the mean +/- the standard deviation of quintriplicate measurements and where no error bar is shown, the error is smaller

absence of other problems, this assay could potentially detect the GPI-PLC in a sample containing 2.7×10^7 cells based on the copy number of 3×10^4 copies / cell as reported in the literature (Hereld *et al.*, 1986).

Once the conditions for the standard assay were established, an assay was developed for the detection of GPI-PLC in wild-type bloodstream form trypanosomes. Trypanosomes were solubilized in 0.1 M NaOH for 30 min at room temperature and then diluted in glycine buffer (pH 9.4). Originally, urea (8M) was used to solubilize the cells. However, it was found that the background readings were much higher using Urea than if NaOH (0.1M) was used. Up to 0.3M NaOH could be used to solubilize the cells without an increase in background readings (Fig 2). Consequently, the microtitre plate wells were coated with solubilized cells in the presence of 0.1 M NaOH. The optimum range of cell concentration for use in this assay was found to be between 1×10^4 cells/ml – 1×10^6 cells/ml. Cell concentrations higher than this range saturated the assay and eventually, absorbance readings actually decreased. Since this range is so far below the predicted number of cells required from the literature values, it appeared likely that the assay was mainly detecting some interfering substance in whole cells. In fact, assay of the GPI-PLC in whole cells with this method was found to give high background readings and the enzyme detecting assay had to be allowed to proceed for twelve times as long as the standard assay with pure recombinant GPI-PLC to obtain equivalent results. These results predicted a copy number for the GPI-PLC of 1.35×10^3 copies/cell, which differs by more than an order of magnitude from that reported in the literature (Hereld *et al.*, 1986).

Because of the wide discrepancy between the copy number predicted by this direct ELISA assay and that obtained by measuring the GPI-PLC activity (Hereld *et al.*, 1986) and because of the high backgrounds that I have found when using crude extracts of whole cells, a cell line of bloodstream form *T. brucei* that had a double "knock-out" for the GPI-PLC was examined. The double "knock-out" was required to eliminate completely the expression of the GPI-PLC in trypanosomes because of the necessity to remove both parental alleles in these diploid cells. This double deletion mutant was the kind gift of Drs. Helena Webb and Mark Carrington, Department of Biochemistry, University of Cambridge, Cambridge, UK. Proteins from cell lysates were immunoprecipitated using an anti-GPI-PLC antibody to confirm that the Null mutant no longer contained the GPI-PLC (see chapter 4). The results obtained when the direct ELISA was used to measure the copy number of the GPI-PLC in null mutant cells were

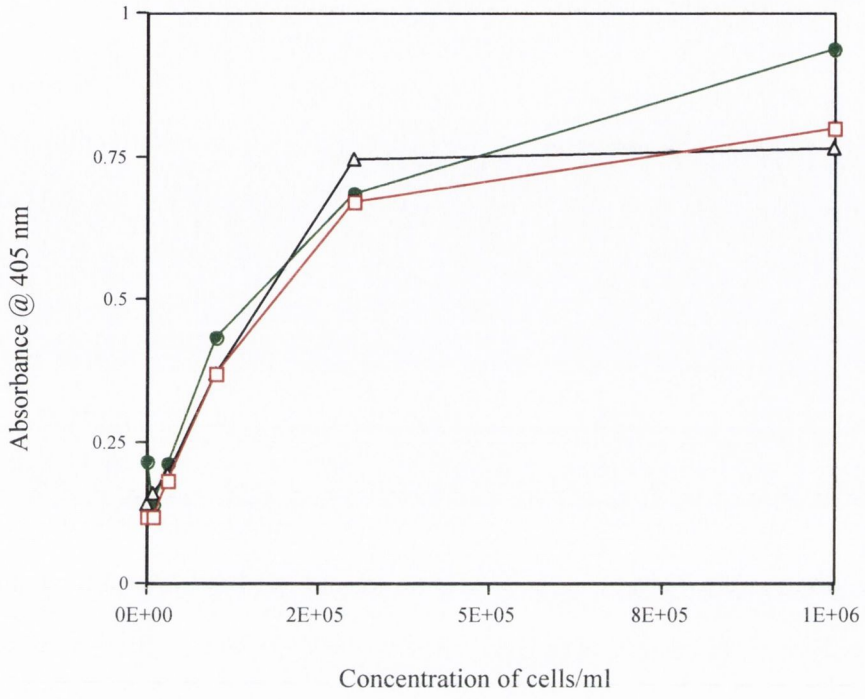

Fig 2. Concentration of NaOH required for solubilisation of bloodstream form trypanosomes in preparation for ELISA. NaOH (stock concentration 1M in Glycine buffer, pH 9.4) was used to solubilise cells for coating of high binding ELISA plates. Bloodstream form trypanosomes (1 x 10^8 cells/ml) were centrifuged (13,000 g, 1 min) and the pellet was resuspended in NaOH (0.1M (■), 0.2M (■) or 0.3M (■) to a final volume of 1 ml. The cells were left shaking gently for 30 min at room temperature and subsequently sampled for the coating of the plates. Binding of the anti-GPI-PLC antibody was detected using an anti-rabbit IgG alkaline phosphatase conjugate (Section 2.1.54). The development was stopped after 60 min. Data are the mean +/- the standard deviation of quintriplicate measurements and where no error bar is shown, the error is smaller than the symbol used.

almost identical to those obtained when assaying the GPI-PLC in wild-type cells (Fig 3). Therefore, this assay could not be used to quantitate the amount of GPI-PLC in bloodstream form trypanosomes because it did not possess sufficient specificity for the reliable detection of the GPI-PLC in whole cell extracts without unacceptable interference from other substances in the extract.

My next approach was to test the sandwich (two-site) ELISA for measuring the GPI-PLC (Fig 4). Purified recombinant GPI-PLC (0-2 μg/ml) was again used as the standard protein for detection of the GPI-PLC. It was found that the purified sheep anti-GPI-PLC as the capture antibody gave a better level of detection of the GPI-PLC than did the purified rabbit anti-GPI-PLC. Therefore, in the standard sandwich assay the sheep anti-GPI-PLC (1/600 dilution) was used to coat the plates in glycine buffer, pH 9.4. The recombinant GPI-PLC was added to the antibody coated plates at pH 9.4 and after washing a rabbit anti-GPI-PLC (1/1000 dilution) specific for the bound antigen was then added at pH 7.4. The GPI-PLC was detected using an alkaline phosphatase-anti-rabbit IgG conjugate. This assay produced higher background readings than the standard assay using the direct ELISA when assaying the pure recombinant GPI-PLC. When the alkaline phosphatase - anti IgG conjugate (tertiary antibody), which produces the absorbance to be detected, was omitted, the backgrounds were very low (0.081 +/- 0.002) and constant regardless of the amount of the antigen present. Consequently, this type of background must have been due mainly to machine noise and could be confidently subtracted from all readings. When just the rabbit anti – GPI-PLC IgG (secondary antibody) was omitted, the background readings (0.094 +/- 0.003) were very close to the machine noise and did not vary as the antigen concentration was increased. However, when just the sheep anti-GPI-PLC IgG (primary antibody) was omitted, the background readings at any antigen concentration below 0.1 μg/ml were low but significant (0.127 +/- 0.009) and did not vary with antigen concentration. Consequently, a small amount of the assay background must have been due to the inappropriate binding of the tertiary antibody-enzyme conjugate to the secondary antibody, which was detected in the absence of primary antibody. In addition, when the primary antibody was omitted but higher antigen concentrations were used, the backgrounds were found to be higher still and to vary with antigen concentration (0.140 +/- 0.015/μg antigen). Therefore, the majority of the background was due to specific binding of the tertiary antibody to the secondary antibody-antigen complex in the absence of the primary capture antibody, *i.e.* to non-specific binding of antigen to the wells at pH 7.4 and to a lesser extent to the non-specific

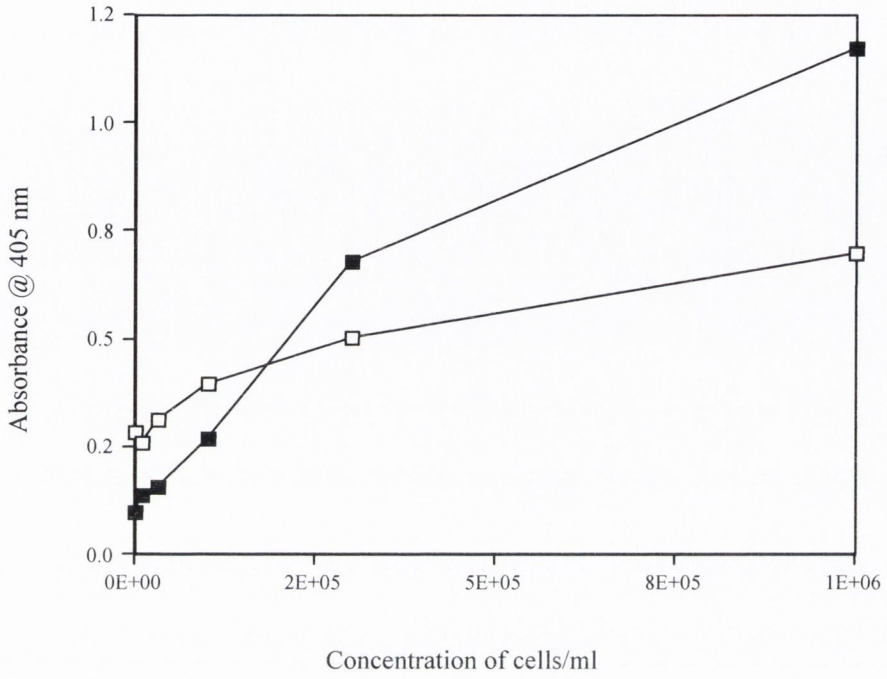

Fig 3. Detection of the GPI-PLC in wild type and GPI-PLC$^-$ mutant trypanosomes by direct ELISA. Polystyrene high binding ELISA plates were coated with wild-type (■) and GPI-PLC$^-$ mutant (□) trypanosomes that had been solubilized in 0.1 M NaOH for 30 min at room temperature. Binding of anti-GPI-PLC was detected using anti-rabbit IgG alkaline phosphatase conjugate (Section 2.1.54). The development was stopped after 60 min. Data are the mean +/- the standard deviation of quintriplicate measurements and where no error bar is shown, the error is smaller than the symbol used.

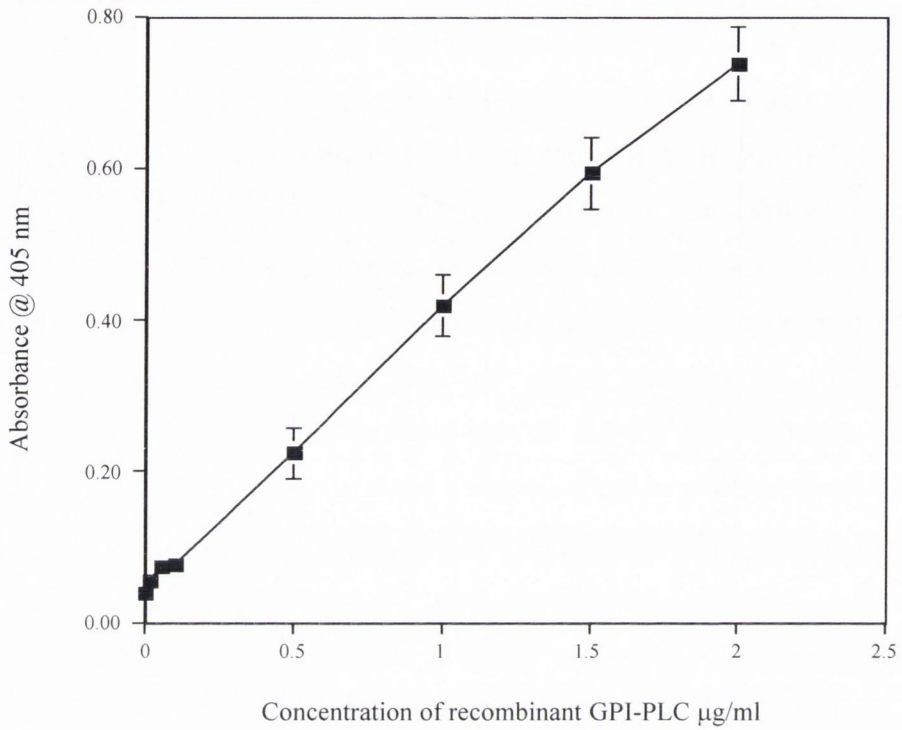

Fig 4. Quantitative detection of the recombinant GPI-PLC by Sandwich ELISA. Polystyrene high binding ELISA plates were coated with sheep anti-GPI-PLC antibody. Subsequently various concentrations of recombinant GPI-PLC were put onto the coated wells. Following this rabbit anti-GPI-PLC antibody was added. Binding of the antibodies to the recombinant GPI-PLC was detected using an anti-rabbit IgG alkaline phosphatase conjugate (Section 2.1.55). The development was stopped after 30 min. Data are the mean +/- the standard deviation of quintriplicate measurements and where no error bar is shown, the error is smaller than the symbol used.

binding of the secondary antibody to the wells. The total non-specific background (including the machine noise, antigen independent background and antigen dependent background) amounted to 44% of the final measurement at 0.2 μg of antigen/well. Increasing the bovine serum albumin (BSA) from 0.5 % to 5 % did not improve these backgrounds and substitution of Marvel (3%) for BSA only gave a minor reduction in background, from 44 % to 36 % of the final measurement at 0.2 μg of antigen/well. These results were disappointing when compared to the 5.5 % background in the direct ELISA, where the same measurements were obtained at only 0.01 μg of antigen/well, *i.e.* 20 times the sensitivity at 0.13 times the background. The sandwich assay can only be applied to the assay of the GPI-PLC in whole cells if the problems of sensitivity and specificity found when using recombinant GPI-PLC can be overcome. Therefore, the sandwich assay could not be used to quantitate the amount of GPI-PLC in bloodstream form trypanosomes because it did not have the specificity or reliability required to detect the recombinant GPI-PLC in the standard assay.

The cycling assay in conjunction with the direct ELISA was the method used to increase the sensitivity for the detection of the recombinant GPI-PLC (Fig 5). The first step undertaken in the development of a standard assay was to determine the lowest possible concentration of recombinant GPI-PLC that could be detected reliably. It was found that 0.01 μg of recombinant GPI-PLC /well was sufficient for reliable detection purposes. Furthermore, the cycling assay partnered with the direct ELISA (Fig 5) had no higher background readings than the direct ELISA when the recombinant antigen was being assayed. In addition, the cycling assay was found to be 4 times more sensitive than the non-cycling direct ELISA.

Assay of the GPI-PLC in whole cells with the cycling-direct ELISA was also found to be more sensitive than the non-cycling direct ELISA (Fig 6). The number of cells required for the reliable detection of the GPI-PLC by the direct-cycling assay (3 x 10^4 cells) was found to be 100 times less then the number required to give the same absorbance readings in the non-cycling direct ELISA (3 x 10^6 cells). The background levels present in the direct-cycling assay were also found to be lower (4-5 fold) than those obtained in the non-cycling direct ELISA, probably because of the reduction in interfering substances that results from reducing cell numbers in the assay. For example, the total non-specific background amounted to only 13 % of the final measurement at 3 x 10^4 cells/well in the direct-cycling ELISA, whereas the total non-specific background amounted to 44 % of the final measurement at 3 x 10^6 cells/well in the non-cycling direct

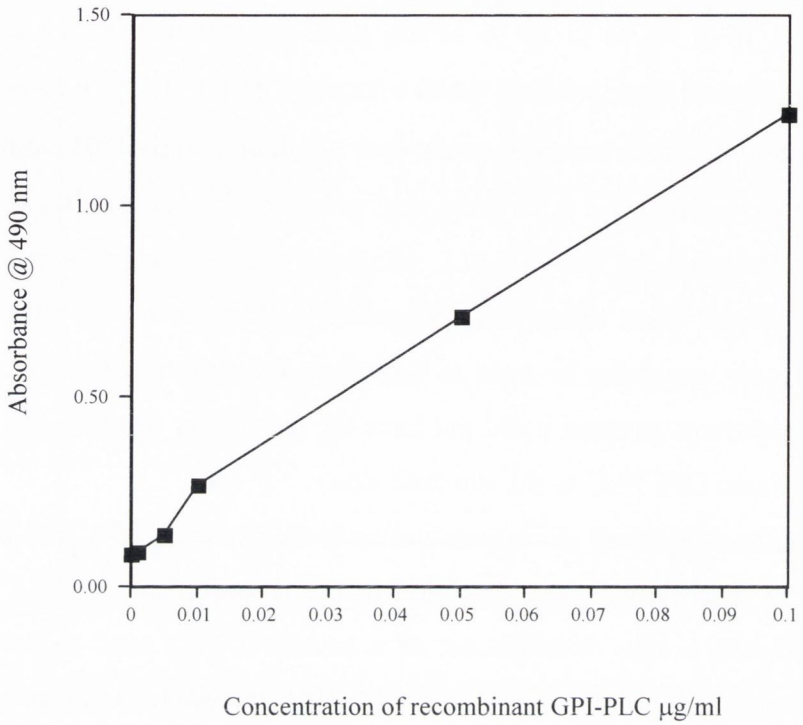

Fig 5. Quantitative detection of the recombinant GPI-PLC by direct ELISA followed by the cycling assay. Polystyrene high binding ELISA plates were coated with various concentrations of purified recombinant GPI-PLC and incubated with anti-GPI-PLC antibody. Binding of anti-GPI-PLC antibody was detected using an anti-rabbit IgG alkaline phosphatase conjugate followed by the cycling assay (Section 2.1.56). The development was stopped after 15 min. Data are mean +/- the standard deviation of quintriplicate measurements and where no error bar is shown, the error is smaller than the symbol used.

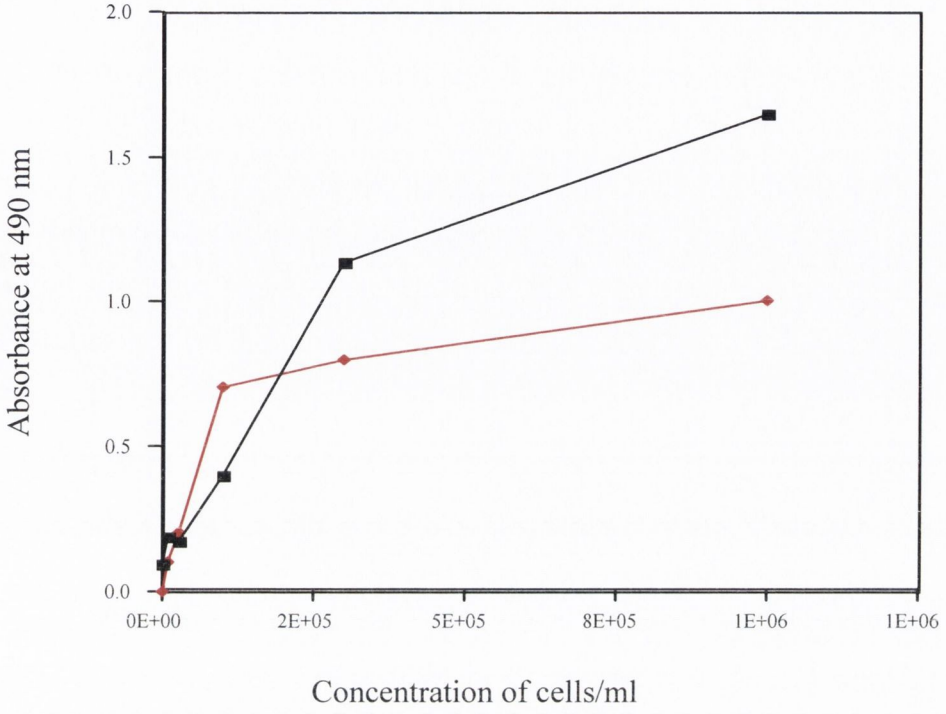

Fig 6. Detection of GPI-PLC in wild type and GPI-PLC$^-$ mutant trypanosomes by direct ELISA followed by cycling assay. Detection of GPI-PLC in wild type and GPI-PLC$^-$ mutant trypanosomes by direct ELISA. Polystyrene high binding ELISA plates were coated with wild-type (■) and GPI-PLC$^-$ mutant (◆) trypanosomes that had been solubilized in 0.1 M NaOH for 30 min at room temperature. Binding of anti-GPI-PLC was detected using anti-rabbit IgG alkaline phosphatase conjugate (Section 2.1.54) followed by the cycling assay (Section 2.1.56). The development was stopped after 20 min. Data are mean +/- the standard deviation of quintriplicate measurements and where no error bar is shown, the error is smaller than the symbol used.

ELISA. The results obtained when the direct-cycling ELISA was used to measure the copy number of the GPI-PLC in null mutant cells were disappointing. They were almost identical to those obtained when assaying the GPI-PLC in wild-type cells (Fig 6). Therefore, this assay could not be used to quantitate the amount of GPI-PLC in bloodstream form trypanosomes because it was not specific enough for the reliable detection of the GPI-PLC in whole cell extracts without unacceptable interference from other substances in the extract.

Further studies into the correct assay procedure where the backgrounds are low and there is no detectable level of GPI-PLC in the null mutant cells will be of great benefit in quantitating this enzyme in relation to its location on the surface of the trypanosome.

Bibliography

Abraham, J.M., Feagin, J.E., and Stuart, K. (1988). Characterization of cytochrome c oxidase III transcripts that are edited only in the 3' region. Cell *55*, 267-272.

Auffret, C.A., and Turner, M.J. (1981). Variant specific antigens of Trypanosoma brucei exist in solution as glycoprotein dimers. Biochem J *193*, 647-650.

Barry, J.D. (1979). Capping of variable antigen on Trypanosoma brucei, and its immunological and biological significance. J Cell Sci *37*, 287-302.

Barry, J.D., and Emergy, D.L. (1984). Parasite development and host responses during the establishment of Trypanosoma brucei infection transmitted by tsetse fly. Parasitology *88 (Pt 1)*, 67-84.

Bastin, P., Matthews, K.R., and Gull, K. (1996). The paraflagellar rod of kinetoplastida: solved and unsolved questions. Parasitol Today *12*, 302-307.

Bastin, P., Pullen, T.J., Moreira-Leite, F.F., and Gull, K. (2000). Inside and outside of the trypanosome flagellum:a multifunctional organelle. Microbes Infect *2*, 1865-1874.

Bastin, P., Pullen, T.J., Sherwin, T., and Gull, K. (1999). Protein transport and flagellum assembly dynamics revealed by analysis of the paralysed trypanosome mutant snl-1. J Cell Sci *112 (Pt 21)*, 3769-3777.

Bastin, P., Sherwin, T., and Gull, K. (1998). Paraflagellar rod is vital for trypanosome motility. Nature *391*, 548.

Becker, M., Aitcheson, N., Byles, E., Wickstead, B., Louis, E., and Rudenko, G. (2004). Isolation of the repertoire of VSG expression site containing telomeres of Trypanosoma brucei 427 using transformation-associated recombination in yeast. Genome Res *14*, 2319-2329.

Benne, R., Van den Burg, J., Brakenhoff, J.P., Sloof, P., Van Boom, J.H., and Tromp, M.C. (1986). Major transcript of the frameshifted coxII gene from trypanosome mitochondria contains four nucleotides that are not encoded in the DNA. Cell *46*, 819-826.

Berriman, M., Ghedin, E., Hertz-Fowler, C., Blandin, G., Renauld, H., Bartholomeu, D.C., Lennard, N.J., Caler, E., Hamlin, N.E., Haas, B., Bohme, U., Hannick, L., Aslett, M.A., Shallom, J., Marcello, L., Hou, L., Wickstead, B., Alsmark, U.C., Arrowsmith, C., Atkin, R.J., Barron, A.J., Bringaud, F., Brooks, K., Carrington, M., Cherevach, I., Chillingworth, T.J., Churcher, C., Clark, L.N., Corton, C.H., Cronin, A., Davies, R.M., Doggett, J., Djikeng, A., Feldblyum, T., Field, M.C., Fraser, A., Goodhead, I., Hance, Z., Harper, D., Harris, B.R., Hauser, H., Hostetler, J., Ivens, A., Jagels, K., Johnson, D., Johnson, J., Jones, K., Kerhornou, A.X., Koo, H., Larke, N., Landfear, S., Larkin, C., Leech, V., Line, A., Lord, A., Macleod, A., Mooney, P.J., Moule, S., Martin, D.M., Morgan, G.W., Mungall, K., Norbertczak, H., Ormond, D., Pai, G., Peacock, C.S., Peterson, J., Quail, M.A., Rabbinowitsch, E., Rajandream, M.A., Reitter, C., Salzberg, S.L., Sanders, M., Schobel, S., Sharp, S., Simmonds, M., Simpson, A.J., Tallon, L., Turner, C.M., Tait, A., Tivey, A.R., Van Aken, S., Walker, D., Wanless, D., Wang, S., White, B., White, O., Whitehead, S., Woodward, J., Wortman, J., Adams, M.D., Embley, T.M., Gull, K., Ullu, E., Barry, J.D., Fairlamb, A.H., Opperdoes, F., Barrell, B.G., Donelson, J.E., Hall, N., Fraser, C.M., Melville, S.E., and El-Sayed, N.M. (2005). The genome of the African trypanosome Trypanosoma brucei. Science *309*, 416-422.

Blose, S.H., Meltzer, D.I., and Feramisco, J.R. (1984). 10-nm filaments are induced to collapse in living cells microinjected with monoclonal and polyclonal antibodies against tubulin. J Cell Biol *98*, 847-858.

Bowles, D.J., and Voorheis, H.P. (1982). Release of the surface coat from the plasma membrane of intact bloodstream forms of Trypanosoma brucei requires Ca2+. FEBS Lett *139*, 17-21.

Bulow, R., Griffiths, G., Webster, P., Stierhof, Y.D., Opperdoes, F.R., and Overath, P. (1989). Intracellular localization of the glycosyl-phosphatidylinositol-specific phospholipase C of Trypanosoma brucei. J Cell Sci *93 (Pt 2)*, 233-240.

Bulow, R., Nonnengasser, C., and Overath, P. (1989). Release of the variant surface glycoprotein during differentiation of bloodstream to procyclic forms of Trypanosoma brucei. Mol Biochem Parasitol *32*, 85-92.

Bulow, R., and Overath, P. (1986). Purification and characterization of the membrane-form variant surface glycoprotein hydrolase of Trypanosoma brucei. J Biol Chem *261*, 11918-11923.

Bridgen, P.J., Cross, G.A., and Bridgen, J. (1976). N-terminal amino acid sequences of variant-specific surface antigens from Trypanosoma brucei. Nature *263*, 613-614.

Bridges, K., Harford, J., Ashwell, G., and Klausner, R.D. (1982). Fate of receptor and ligand during endocytosis of asialoglycoproteins by isolated hepatocytes. Proc Natl Acad Sci U S A *79*, 350-354.

Brumpt, M.E. (1906) Sur quelque especes nouvelles de Trypanosomes parasites des possons d'eau douce; leur mode d'evolution. *Comptes rendus de la Societe de Biologie, Paris 60*, 160-162.

Bulow, R., Nonnengasser, C., and Overath, P. (1989). Release of the variant surface glycoprotein during differentiation of bloodstream to procyclic forms of Trypanosoma brucei. Mol Biochem Parasitol *32*, 85-92.

Bulow, R., and Overath, P. (1985). Synthesis of a hydrolase for the membrane-form variant surface glycoprotein is repressed during transformation of Trypanosoma brucei. FEBS Lett *187*, 105-110.

Bulow, R., and Overath, P. (1986). Purification and characterization of the membrane-form variant surface glycoprotein hydrolase of Trypanosoma brucei. J Biol Chem *261*, 11918-11923.

Butikofer, P., Boschung, M., Brodbeck, U., and Menon, A.K. (1996). Phosphatidylinositol hydrolysis by Trypanosoma brucei glycosylphosphatidylinositol phospholipase C. J Biol Chem *271*, 15533-15541.

Buxbaum, L.U. (1994). Myristate exchange in glycolipid A and VSG of African trypanosomes. Braz J Med Biol Res *27*, 115-119.

Cachon, M., and Cosson, M.P. (1988). Ciliary and flagellar apparatuses and their associated structures. Biol Cell *63*, 115.

Cardoso de Almeida, M.L., and Turner, M.J. (1983). The membrane form of variant surface glycoproteins of Trypanosoma brucei. Nature *302*, 349-352.

Cardoso De Almeida, M.L., Geuskens, M., and Pays, E. (1999). Cell lysis induces redistribution of the GPI-anchored variant surface glycoprotein on both faces of the plasma membrane of Trypanosoma brucei. J Cell Sci *112 (Pt 23)*, 4461-4473.

Carnall, N., Webb, H., and Carrington, M. (1997). Mutagenesis study of the glycosylphosphatidylinositol phospholipase C of Trypanosoma brucei. Mol Biochem Parasitol *90*, 423-432.

Carrington, M., Miller, N., Blum, M., Roditi, I., Wiley, D., and Turner, M. (1991). Variant specific glycoprotein of Trypanosoma brucei consists of two domains each having an independently conserved pattern of cysteine residues. J Mol Biol *221*, 823-835.

Carrington, M., Bulow, R., Reinke, H., and Overath, P. (1989). Sequence and expression of the glycosyl-phosphatidylinositol-specific phospholipase C of Trypanosoma brucei. Mol Biochem Parasitol *33*, 289-296.

Carrington, M., Carnall, N., Crow, M.S., Gaud, A., Redpath, M.B., Wasunna, C.L., and Webb, H. (1998). The properties and function of the glycosylphosphatidylinositol-phospholipase C in Trypanosoma brucei. Mol Biochem Parasitol *91*, 153-164.

Carroll, M., and McCrorie, P. (1986). Lipid composition of bloodstream forms of Trypanosoma brucei brucei. Comp Biochem Physiol B *83*, 647-651.

Center, R.J., Kobe, B., Wilson, K.A., Teh, T., Howlett, G.J., Kemp, B.E., and Poumbourios, P. (1998). Crystallization of a trimeric human T cell leukemia virus type 1 gp21 ectodomain fragment as a chimera with maltose-binding protein. Protein Sci *7*, 1612-1619.

Chattopadhyay, A., Jones, N.G., Nietlispach, D., Nielsen, P.R., Voorheis, H.P., Mott, H.R., and Carrington, M. (2005). Structure of the C-terminal domain from Trypanosoma brucei variant surface glycoprotein MITat1.2. J Biol Chem *280*, 7228-7235.

Cohen, S.L., and Chait, B.T. (1996). Influence of matrix solution conditions on the MALDI-MS analysis of peptides and proteins. Anal Chem *68*, 31-37.

Coppens, I., Bastin, P., Courtoy, P.J., Baudhuin, P., and Opperdoes, F.R. (1991). A rapid method purifies a glycoprotein of Mr 145,000 as the LDL receptor of Trypanosoma brucei brucei. Biochem Biophys Res Commun *178*, 185-191.

Coppens, I., Baudhuin, P., Opperdoes, F.R., and Courtoy, P.J. (1988). Receptors for the host low density lipoproteins on the hemoflagellate Trypanosoma brucei: purification and involvement in the growth of the parasite. Proc Natl Acad Sci U S A *85*, 6753-6757.

Coppens, I., Opperdoes, F.R., Courtoy, P.J., and Baudhuin, P. (1987). Receptor-mediated endocytosis in the bloodstream form of Trypanosoma brucei. J Protozool *34*, 465-473.

Cross, G.A. (1975). Identification, purification and properties of clone-specific glycoprotein antigens constituting the surface coat of Trypanosoma brucei. Parasitology *71*, 393-417.

Cunningham, M.P., and Vickerman, K. (1962). Antigenic analysis in the Trypanosoma brucei group, using the agglutination reaction. Trans R Soc Trop Med Hyg *56*, 48-59.

Denny, P.W., Gokool, S., Russell, D.G., Field, M.C., and Smith, D.F. (2000). Acylation-dependent protein export in Leishmania. J Biol Chem *275*, 11017-11025.

Dixon, H., Ginger, C.D., and Williamson, J. (1971). The lipid metabolism of blood and culture forms of Trypanosoma lewisi and Trypanosoma rhodesiense. Comp Biochem Physiol B *39*, 247-266.

Dolan, M.T., Reid, C.G., and Voorheis, H.P. (1986). Calcium ions initiate the selective depolymerization of the pellicular microtubules in bloodstream forms of Trypanosoma brucei. J Cell Sci *80*, 123-140.

Dormeyer, M., Schoneck, R., Dittmar, G.A., and Krauth-Siegel, R.L. (1997). Cloning, sequencing and expression of ribonucleotide reductase R2 from Trypanosoma brucei. FEBS Lett *414*, 449-453.

Duchateau, P.N., Pullinger, C.R., Orellana, R.E., Kunitake, S.T., Naya-Vigne, J., O'Connor, P.M., Malloy, M.J., and Kane, J.P. (1997). Apolipoprotein L, a new human high density lipoprotein apolipoprotein expressed by the pancreas. Identification, cloning, characterization, and plasma distribution of apolipoprotein L. J Biol Chem *272*, 25576-25582.

Dyson, H.J., Wright, P.E., and Scheraga, H.A. (2006). The role of hydrophobic interactions in initiation and propagation of protein folding. Proc Natl Acad Sci U S A *103*, 13057-13061.

Engman, D.M., Krause, K.H., Blumin, J.H., Kim, K.S., Kirchhoff, L.V., and Donelson, J.E. (1989). A novel flagellar Ca2+-binding protein in trypanosomes. J Biol Chem *264*, 18627-18631.

Engstler, M., Thilo, L., Weise, F., Grunfelder, C.G., Schwarz, H., Boshart, M., and Overath, P. (2004). Kinetics of endocytosis and recycling of the GPI-anchored variant surface glycoprotein in Trypanosoma brucei. J Cell Sci *117*, 1105-1115.

Esser, K.M., and Schoenbechler, M.J. (1985). Expression of two variant surface glycoproteins on individual African trypanosomes during antigen switching. Science *229*, 190-193.

Fairlamb, A.H. (1990). Future prospects for the chemotherapy of human trypanosomiasis. 1. Novel approaches to the chemotherapy of trypanosomiasis. Trans R Soc Trop Med Hyg *84*, 613-617.

Ferguson, M.A., and Cross, G.A. (1984). Myristylation of the membrane form of a Trypanosoma brucei variant surface glycoprotein. J Biol Chem *259*, 3011-3015.

Ferguson, M.A., Haldar, K., and Cross, G.A. (1985). Trypanosoma brucei variant surface glycoprotein has a sn-1,2-dimyristyl glycerol membrane anchor at its COOH terminus. J Biol Chem *260*, 4963-4968.

Ferguson, M.A., Homans, S.W., Dwek, R.A., and Rademacher, T.W. (1988). The glycosylphosphatidylinositol membrane anchor of Trypanosoma brucei variant surface glycoprotein. Biochem Soc Trans *16*, 265-268.

Fernandez, A., and Scheraga, H.A. (2003). Insufficiently dehydrated hydrogen bonds as determinants of protein interactions. Proc Natl Acad Sci U S A *100*, 113-118.

Field, H., Farjah, M., Pal, A., Gull, K., and Field, M.C. (1998). Complexity of trypanosomatid endocytosis pathways revealed by Rab4 and Rab5 isoforms in Trypanosoma brucei. J Biol Chem *273*, 32102-32110.

Field, M.C., Menon, A.K., and Cross, G.A. (1991). A glycosylphosphatidylinositol protein anchor from procyclic stage Trypanosoma brucei: lipid structure and biosynthesis. Embo J *10*, 2731-2739.

Fire, A., Xu, S., Montgomery, M.K., Kostas, S.A., Driver, S.E., and Mello, C.C. (1998). Potent and specific genetic interference by double-stranded RNA in Caenorhabditis elegans. Nature 391, 806-811.

Fox, J.A., Duszenko, M., Ferguson, M.A., Low, M.G., and Cross, G.A. (1986). Purification and characterization of a novel glycan-phosphatidylinositol-specific phospholipase C from Trypanosoma brucei. J Biol Chem *261*, 15767-15771.

Freymann, D.M., Metcalf, P., Turner, M., and Wiley, D.C. (1984). 6 A-resolution X-ray structure of a variable surface glycoprotein from Trypanosoma brucei. Nature *311*, 167-169.

Gillett, M.P., and Owen, J.S. (1991). Trypanosoma brucei brucei: differences in the trypanocidal activity of human plasma and its relationship to the level of high density lipoproteins. Trans R Soc Trop Med Hyg *85*, 612-616.

Godsel, L.M., and Engman, D.M. (1999). Flagellar protein localization mediated by a calcium-myristoyl/palmitoyl switch mechanism. Embo J *18*, 2057-2065.

Goldstein, J.L., Brunschede, G.Y., and Brown, M.S. (1975). Inhibition of proteolytic degradation of low density lipoprotein in human fibroblasts by chloroquine, concanavalin A, and Triton WR 1339. J Biol Chem *250*, 7854-7862.

Grab, D.J., Shaw, M.K., Wells, C.W., Verjee, Y., Russo, D.C., Webster, P., Naessens, J., and Fish, W.R. (1993). The transferrin receptor in African trypanosomes: identification, partial characterization and subcellular localization. Eur J Cell Biol *62*, 114-126.

Grab, D.J., Webster, P., Ito, S., Fish, W.R., Verjee, Y., and Lonsdale-Eccles, J.D. (1987). Subcellular localization of a variable surface glycoprotein phosphatidylinositol-specific phospholipase-C in African trypanosomes. J Cell Biol *105*, 737-746.

Grab, D.J., Wells, C.W., Shaw, M.K., Webster, P., and Russo, D.C. (1992). Endocytosed transferrin in African trypanosomes is delivered to lysosomes and may not be recycled. Eur J Cell Biol *59*, 398-404.

Gray, A.R. (1962). The influence of antibody on serological variation in Trypanosoma brucei. Ann Trop Med Parasitol *56*, 4-13.

Grunfelder, C.G., Engstler, M., Weise, F., Schwarz, H., Stierhof, Y.D., Boshart, M., and Overath, P. (2002). Accumulation of a GPI-anchored protein at the cell surface requires sorting at multiple intracellular levels. Traffic *3*, 547-559.

Grunfelder, C.G., Engstler, M., Weise, F., Schwarz, H., Stierhof, Y.D., Morgan, G.W., Field, M.C., and Overath, P. (2003). Endocytosis of a glycosylphosphatidylinositol-anchored protein via clathrin-coated vesicles, sorting by default in endosomes, and exocytosis via RAB11-positive carriers. Mol Biol Cell *14*, 2029-2040.

Gruszynski, A.E., DeMaster, A., Hooper, N.M., and Bangs, J.D. (2003). Surface coat remodeling during differentiation of Trypanosoma brucei. J Biol Chem *278*, 24665-24672.

Gunzl, A., Bruderer, T., Laufer, G., Schimanski, B., Tu, L.C., Chung, H.M., Lee, P.T., and Lee, M.G. (2003). RNA polymerase I transcribes procyclin genes and variant surface glycoprotein gene expression sites in Trypanosoma brucei. Eukaryot Cell *2*, 542-551.

Hager, K.M., and Hajduk, S.L. (1997). Mechanism of resistance of African trypanosomes to cytotoxic human HDL. Nature *385*, 823-826.

Hajduk, S.L., Moore, D.R., Vasudevacharya, J., Siqueira, H., Torri, A.F., Tytler, E.M., and Esko, J.D. (1989). Lysis of Trypanosoma brucei by a toxic subspecies of human high density lipoprotein. J Biol Chem *264*, 5210-5217.

Hallak, H., Brass, L.F., and Manning, D.R. (1994). Failure to myristoylate the alpha subunit of Gz is correlated with an inhibition of palmitoylation and membrane attachment, but has no affect on phosphorylation by protein kinase C. J Biol Chem *269*, 4571-4576.

Han, K.K., and Martinage, A. (1992). Possible relationship between coding recognition amino acid sequence motif or residue(s) and post-translational chemical modification of proteins. Int J Biochem *24*, 1349-1363.

Hannaert, V., and Michels, P.A. (1994). Structure, function, and biogenesis of glycosomes in kinetoplastida. J Bioenerg Biomembr *26*, 205-212.

Heinz, D.W., Ryan, M., Bullock, T.L., and Griffith, O.H. (1995). Crystal structure of the phosphatidylinositol-specific phospholipase C from Bacillus cereus in complex with myo-inositol. Embo J *14*, 3855-3863.

Hereld, D., Krakow, J.L., Bangs, J.D., Hart, G.W., and Englund, P.T. (1986). A phospholipase C from Trypanosoma brucei which selectively cleaves the glycolipid on the variant surface glycoprotein. J Biol Chem *261*, 13813-13819.

Hereld, D., Hart, G.W., and Englund, P.T. (1988). cDNA encoding the glycosyl-phosphatidylinositol-specific phospholipase C of Trypanosoma brucei. Proc Natl Acad Sci U S A *85*, 8914-8918.

Hoare, C.A (1972) *In The Trypanosomes of Mammals*: 1st edition, Blackwell Scientific Publications, Oxford.

Holder, A.A. (1983). Characterisation of the cross-reacting carbohydrate groups on two variant surface glycoproteins of Trypanosoma brucei. Mol Biochem Parasitol *7*, 331-338.

Holder, A.A., and Cross, G.A. (1981). Glycopeptides from variant surface glycoproteins of Trypanosoma Brucei. C-terminal location of antigenically cross-reacting carbohydrate moieties. Mol Biochem Parasitol *2*, 135-150.

Ikeda, K., Inoue, S., Amasaki, C., Teshima, K., and Ikezawa, H. (1991). Kinetics of the hydrolysis of monodispersed and micellar phosphatidylcholines catalyzed by a phospholipase C from Bacillus cereus. J Biochem (Tokyo) *110*, 88-95.

Imboden, M., Muller, N., Hemphill, A., Mattioli, R., and Seebeck, T. (1995). Repetitive proteins from the flagellar cytoskeleton of African trypanosomes are diagnostically useful antigens. Parasitology *110 (Pt 3)*, 249-258.

Jackson, D.G., and Voorheis, H.P. (1985). Release of the variable surface coat glycoprotein from Trypanosoma brucei requires the cleavage of a phosphate ester. J Biol Chem *260*, 5179-5183.

Jackson, D.G., Windle, H.J., and Voorheis, H.P. (1993). The identification, purification, and characterization of two invariant surface glycoproteins located beneath the surface coat barrier of bloodstream forms of Trypanosoma brucei. J Biol Chem *268*, 8085-8095

Kanthak, A.A, Durham, H.E. & Bradford, W.F.H. (1898) On nagana or tsetse fly disease. Proceedings of the Royal Society *64*, 100-118.

Karas, M., and Hillenkamp, F. (1988). Laser desorption ionization of proteins with molecular masses exceeding 10,000 daltons. Anal Chem *60*, 2299-2301.

Kellermann, O.K., and Ferenci, T. (1982). Maltose-binding protein from Escherichia coli. Methods Enzymol *90 Pt E*, 459-463.

Kleisen, C.M., and Borst, P. (1975). Sequence heterogeneity of the mini-circles of kinetoplast DNA of Crithidia luciliae and evidence for the presence of a component more complex than mini-circle DNA in the kinetoplast network. Biochim Biophys Acta *407*, 473-478.

Kleisen, C.M., Weislogel, P.O., Fonck, K., and Borst, P. (1976). The structure of kinetoplast DNA. 2. Characterization of a novel component of high complexity present in the kinetoplast DNA network of Crithidia luciliae. Eur J Biochem *64*, 153-160.

Kohl, L., and Gull, K. (1998). Molecular architecture of the trypanosome cytoskeleton. Mol Biochem Parasitol *93*, 1-9.

Kohl, L., Sherwin, T., and Gull, K. (1999). Assembly of the paraflagellar rod and the flagellum attachment zone complex during the Trypanosoma brucei cell cycle. J Eukaryot Microbiol *46*, 105-109.

Kurecki, T., Kress, L.F., and Laskowski, M., Sr. (1979). Purification of human plasma alpha 2 macroglobulin and alpha 1 proteinase inhibitor using zinc chelate chromatography. Anal Biochem *99*, 415-420.

Laemmli, U.K. (1970). Cleavage of structural proteins during the assembly of the head of bacteriophage T4. Nature *227*, 680-685.

Lamont, G.S., Fox, J.A., and Cross, G.A. (1987). Glycosyl-sn-1,2-dimyristylphosphatidylinositol is the membrane anchor for Trypanosoma equiperdum and T. (Nannomonas) congolense variant surface glycoproteins. Mol Biochem Parasitol *24*, 131-136.

Langreth, S.G., and Balber, A.E. (1975). Protein uptake and digestion in bloodstream and culture forms of Trypanosoma brucei. J Protozool *22*, 40-53.

LaRochelle, W.J., and Froehner, S.C. (1986). Immunochemical detection of proteins biotinylated on nitrocellulose replicas. J Immunol Methods *92*, 65-71.

Legros, D., Ollivier, G., Gastellu-Etchegorry, M., Paquet, C., Burri, C., Jannin, J., and Buscher, P. (2002). Treatment of human African trypanosomiasis--present situation and needs for research and development. Lancet Infect Dis *2*, 437-440.

Linder, M.E., Middleton, P., Hepler, J.R., Taussig, R., Gilman, A.G., and Mumby, S.M. (1993). Lipid modifications of G proteins: alpha subunits are palmitoylated. Proc Natl Acad Sci U S A *90*, 3675-3679.

Lonsdale-Eccles, J.D., and Grab, D.J. (1987). Purification of African trypanosomes can cause biochemical changes in the parasites. J Protozool *34*, 405-408.

Low, M.G., Stiernberg, J., Waneck, G.L., Flavell, R.A., and Kincade, P.W. (1988). Cell-specific heterogeneity in sensitivity of phosphatidylinositol-anchored membrane antigens to release by phospholipase C. J Immunol Methods *113*, 101-111.

Maier, A., and Steverding, D. (1996). Low affinity of Trypanosoma brucei transferrin receptor to apotransferrin at pH 5 explains the fate of the ligand during endocytosis. FEBS Lett *396*, 87-89.

Masterson, W.J. (1990). Biosynthesis of the glycosyl phosphatidylinositol anchor of Trypanosoma brucei variant surface glycoprotein. Biochem Soc Trans *18*, 722-724.

Mengaud, J., Braun-Breton, C., and Cossart, P. (1991). Identification of phosphatidylinositol-specific phospholipase C activity in Listeria monocytogenes: a novel type of virulence factor? Mol Microbiol *5*, 367-372.

Mensa-Wilmot, K., LeBowitz, J.H., Chang, K.P., al-Qahtani, A., McGwire, B.S., Tucker, S., and Morris, J.C. (1994). GPI phospholipase C from Trypanosoma brucei causes a GPI-negative phenotype in Leishmania major: I. Implications for GPI-negative mammalian cells; II. Compartmentalization of two GPI biosynthetic pathways. Braz J Med Biol Res *27*, 177-184.

Miller, J.K. (1965). Variation of the soluble antigens of Trypanosoma brucei. Immunology *9*, 521-528.

Mizunaga, T., Katakura, Y., Miura, T., and Maruyama, Y. (1990). Purification and characterization of yeast protein disulfide isomerase. J Biochem (Tokyo) *108*, 846-851.

Mohanty, A.K., Simmons, C.R., and Wiener, M.C. (2003). Inhibition of tobacco etch virus protease activity by detergents. Protein Expr Purif *27*, 109-114.

.

Moore, D.R., Smith, A., Hager, K.M., Waldon, R., Esko, J.D., and Hajduk, S.L. (1995). Developmentally regulated sensitivity of Trypanosoma brucei brucei to the cytotoxic effects of human high-density lipoprotein. Exp Parasitol *81*, 216-226.

Morita, Y.S., Acosta-Serrano, A., Buxbaum, L.U., and Englund, P.T. (2000). Glycosyl phosphatidylinositol myristoylation in African trypanosomes. New intermediates in the pathway for fatty acid remodeling. J Biol Chem *275*, 14147-14154.

Mumby, S.M. (1997). Reversible palmitoylation of signaling proteins. Curr Opin Cell Biol *9*, 148-154.

Nagamune, K., Nozaki, T., Maeda, Y., Ohishi, K., Fukuma, T., Hara, T., Schwarz, R.T., Sutterlin, C., Brun, R., Riezman, H., and Kinoshita, T. (2000). Critical roles of glycosylphosphatidylinositol for Trypanosoma brucei. Proc Natl Acad Sci U S A *97*, 10336-10341.

Navarro, M., and Gull, K. (2001). A pol I transcriptional body associated with VSG mono-allelic expression in Trypanosoma brucei. Nature *414*, 759-763.

Ngo, H., Tschudi, C., Gull, K., and Ullu, E. (1998). Double-stranded RNA induces mRNA degradation in Trypanosoma brucei. Proc Natl Acad Sci U S A *95*, 14687-14692.

Nolan, D.P., Rolin, S., Rodriguez, J.R., Van Den Abbeele, J., and Pays, E. (2000). Slender and stumpy bloodstream forms of Trypanosoma brucei display a differential response to extracellular acidic and proteolytic stress. Eur J Biochem *267*, 18-27.

O'Beirne, C., Lowry, C.M., and Voorheis, H.P. (1998). Both IgM and IgG anti-VSG antibodies initiate a cycle of aggregation-disaggregation of bloodstream forms of Trypanosoma brucei without damage to the parasite. Mol Biochem Parasitol *91*, 165-193.

Opperdoes, F.R. (1985). Biochemical peculiarities of trypanosomes, African and South American. Br Med Bull *41*, 130-136.

Opperdoes, F.R., and Borst, P. (1977). Localization of nine glycolytic enzymes in a microbody-like organelle in Trypanosoma brucei: the glycosome. FEBS Lett *80*, 360-364.

Overath, P., and Engstler, M. (2004). Endocytosis, membrane recycling and sorting of GPI-anchored proteins: Trypanosoma brucei as a model system. Mol Microbiol *53*, 735-744.

Owen, M.J., and Voorheis, H.P. (1976). Active-site-directed inhibition of the plasma-membrane carrier transporting short-chain, neutral amino acids into Trypanosoma brucei. Eur J Biochem *62*, 619-624.

Paindavoine, P., Rolin, S., Van Assel, S., Geuskens, M., Jauniaux, J.C., Dinsart, C., Huet, G., and Pays, E. (1992). A gene from the variant surface glycoprotein expression site encodes one of several transmembrane adenylate cyclases located on the flagellum of Trypanosoma brucei. Mol Cell Biol *12*, 1218-1225.

Paturiaux-Hanocq, F., Hanocq-Quertier, J., de Almeida, M.L., Nolan, D.P., Pays, A., Vanhamme, L., Van den Abbeele, J., Wasunna, C.L., Carrington, M., and Pays, E. (2000). A role for the dynamic acylation of a cluster of cysteine residues in regulating the activity of the glycosylphosphatidylinositol-specific phospholipase C of Trypanosoma brucei. J Biol Chem *275*, 12147-12155.

Pays, E., Lips, S., Nolan, D., Vanhamme, L., and Perez-Morga, D. (2001). The VSG expression sites of Trypanosoma brucei: multipurpose tools for the adaptation of the parasite to mammalian hosts. Mol Biochem Parasitol *114*, 1-16.

Pays, E., Vanhollebeke, B., Vanhamme, L., Paturiaux-Hanocq, F., Nolan, D.P., and Perez-Morga, D. (2006). The trypanolytic factor of human serum. Nat Rev Microbiol *4*, 477-486.

Piper, R.C., Xu, X., Russell, D.G., Little, B.M., and Landfear, S.M. (1995). Differential targeting of two glucose transporters from Leishmania enriettii is mediated by an NH2-terminal domain. J Cell Biol *128*, 499-508.

Poelvoorde, P., Vanhamme, L., Van Den Abbeele, J., Switzer, W.M., and Pays, E. (2004). Distribution of apolipoprotein L-I and trypanosome lytic activity among primate sera. Mol Biochem Parasitol *134*, 155-157.

Porath, J., Carlsson, J., Olsson, I., and Belfrage, G. (1975). Metal chelate affinity chromatography, a new approach to protein fractionation. Nature *258*, 598-599.

Remak, A (1842) (referred to by Laveran & Mesnil, 1902). *Canstatts's Jahresbericht 10.*

Resh, M.D. (1993). Interaction of tyrosine kinase oncoproteins with cellular membranes. Biochim Biophys Acta *1155*, 307-322.

Richardson, J.P., Beecroft, R.P., Tolson, D.L., Liu, M.K., and Pearson, T.W. (1988). Procyclin: an unusual immunodominant glycoprotein surface antigen from the procyclic stage of African trypanosomes. Mol Biochem Parasitol *31*, 203-216.

Ridgley, E., Webster, P., Patton, C., and Ruben, L. (2000). Calmodulin-binding properties of the paraflagellar rod complex from Trypanosoma brucei. Mol Biochem Parasitol *109*, 195-201.

Rifkin, M.R. (1978). Identification of the trypanocidal factor in normal human serum: high density lipoprotein. Proc Natl Acad Sci U S A *75*, 3450-3454.

Rifkin, M.R. (1991). Trypanosoma brucei: cytotoxicity of host high-density lipoprotein is not mediated by apolipoprotein A-I. Exp Parasitol *72*, 216-218.

Robinson, D.R., Sherwin, T., Ploubidou, A., Byard, E.H., and Gull, K. (1995). Microtubule polarity and dynamics in the control of organelle positioning, segregation, and cytokinesis in the trypanosome cell cycle. J Cell Biol *128*, 1163-1172.

Robinson, N.P., Burman, N., Melville, S.E., and Barry, J.D. (1999). Predominance of duplicative VSG gene conversion in antigenic variation in African trypanosomes. Mol Cell Biol *19*, 5839-5846.

Roditi, I., Carrington, M., and Turner, M. (1987). Expression of a polypeptide containing a dipeptide repeat is confined to the insect stage of Trypanosoma brucei. Nature *325*, 272-274.

Roditi, I., Schwarz, H., Pearson, T.W., Beecroft, R.P., Liu, M.K., Richardson, J.P., Buhring, H.J., Pleiss, J., Bulow, R., Williams, R.O., and et al. (1989). Procyclin gene expression and loss of the variant surface glycoprotein during differentiation of Trypanosoma brucei. J Cell Biol *108*, 737-746.

Rohman, M., and Harrison-Lavoie, K.J. (2000). Separation of copurifying GroEL from glutathione-S-transferase fusion proteins. Protein Expr Purif *20*, 45-47.

Rolin, S., Hanocq-Quertier, J., Paturiaux-Hanocq, F., Nolan, D., Salmon, D., Webb, H., Carrington, M., Voorheis, P., and Pays, E. (1996). Simultaneous but independent activation of adenylate cyclase and glycosylphosphatidylinositol-phospholipase C under stress conditions in Trypanosoma brucei. J Biol Chem *271*, 10844-10852.

Rolin, S., Hancocq-Quertier, J., Paturiaux-Hanocq, F., Nolan, D.P., and Pays, E. (1998). Mild acid stress as a differentiation trigger in Trypanosoma brucei. Mol Biochem Parasitol *93*, 251-262.

Rubotham, J., Woods, K., Garcia-Salcedo, J.A., Pays, E., and Nolan, D.P. (2005). Characterization of two protein disulfide isomerases from the endocytic pathway of bloodstream forms of Trypanosoma brucei. J Biol Chem *280*, 10410-10418.

Russo, D.C., Grab, D.J., Lonsdale-Eccles, J.D., Shaw, M.K., and Williams, D.J. (1993). Directional movement of variable surface glycoprotein-antibody complexes in Trypanosoma brucei. Eur J Cell Biol *62*, 432-441.

Ryley, J.F. (1956). Studies on the metabolism of the Protozoa. 7. Comparative carbohydrate metabolism of eleven species of trypanosome. Biochem J *62*, 215-222.

Seed, J.R., Cornille, R.L., Risby, E.L., and Gam, A.A. (1969). The presence of agglutinating antibody in the IgM immunoglobulin fraction of rabbit antiserum during experimental African trypanosomiasis. Parasitology *59*, 283-292.

Self, C.H., Wimalawansa, S.J., Johannsson, A., Bates, D.L., Girgis, S.I., and Macintyre, I. (1985). A new sensitive and fast peptide immunoassay based on enzyme amplification used in the determination of CGRP and the demonstration of its presence in the thyroid. Peptides *6*, 627-630.

Seyfang, A., Mecke, D., and Duszenko, M. (1990). Degradation, recycling, and shedding of Trypanosoma brucei variant surface glycoprotein. J Protozool *37*, 546-552.

Shapiro, S.Z. (1986). Trypanosoma brucei: release of variant surface glycoprotein during the parasite life cycle. Exp Parasitol *61*, 432-437.

Shapiro, S.Z., and Webster, P. (1989). Coated vesicles from the protozoan parasite Trypanosoma brucei: purification and characterization. J Protozool *36*, 344-349.

Sherwin, T., and Gull, K. (1989). The cell division cycle of Trypanosoma brucei brucei: timing of event markers and cytoskeletal modulations. Philos Trans R Soc Lond B Biol Sci *323*, 573-588.

Shimamura, M., Hager, K.M., and Hajduk, S.L. (2001). The lysosomal targeting and intracellular metabolism of trypanosome lytic factor by Trypanosoma brucei brucei. Mol Biochem Parasitol *115*, 227-237.

Simpson, A.M., Suyama, Y., Dewes, H., Campbell, D.A., and Simpson, L. (1989). Kinetoplastid mitochondria contain functional tRNAs which are encoded in nuclear DNA and also contain small minicircle and maxicircle transcripts of unknown function. Nucleic Acids Res *17*, 5427-5445.

Stanley, C.J., Cox, R.B., Cardosi, M.F., and Turner, A.P. (1988). Amperometric enzyme-amplified immunoassays. J Immunol Methods *112*, 153-161.

Steiger, R.F., Opperdoes, F.R., and Bontemps, J. (1980). Subcellular fractionation of Trypanosoma brucei bloodstream forms with special reference to hydrolases. Eur J Biochem *105*, 163-175.

Steverding, D., Stierhof, Y.D., Chaudhri, M., Ligtenberg, M., Schell, D., Beck-

Sickinger, A.G., and Overath, P. (1994). ESAG 6 and 7 products of Trypanosoma brucei form a transferrin binding protein complex. Eur J Cell Biol *64*, 78-87.

Steverding, D., Stierhof, Y.D., Fuchs, H., Tauber, R., and Overath, P. (1995). Transferrin-binding protein complex is the receptor for transferrin uptake in Trypanosoma brucei. J Cell Biol *131*, 1173-1182.

Steverding, D. (1998). Bloodstream forms of Trypanosoma brucei require only small amounts of iron for growth. Parasitol Res *84*, 59-62.

Subramanya, S., and Mensa-Wilmot, K. (2006). Regulated cleavage of intracellular glycosylphosphatidylinositol in a trypanosome. Peroxisome-to-endoplasmic reticulum translocation of a phospholipase C. Febs J *273*, 2110-2126.

Takayanagi, T., Kawaguchi, H., Yabu, Y., Itoh, M., and Appawu, M.A. (1987). Contribution of the complement system to antibody-mediated binding of Trypanosoma gambiense to macrophages. J Parasitol *73*, 333-341.

Thain, A., Gaston, K., Jenkins, O., and Clarke, A.R. (1996). A method for the separation of GST fusion proteins from co-purifying GroEL. Trends Genet *12*, 209-210.

Turner, M.J. (1984). Antigenic variation in its biological context. Philos Trans R Soc Lond B Biol Sci *307*, 27-40.

Turner, C.M., and Barry, J.D. (1989). High frequency of antigenic variation in Trypanosoma brucei rhodesiense infections. Parasitology *99 Pt 1*, 67-75.

Van der Ploeg, L.H., Schwartz, D.C., Cantor, C.R., and Borst, P. (1984). Antigenic variation in Trypanosoma brucei analyzed by electrophoretic separation of chromosome-sized DNA molecules. Cell *37*, 77-84.

Vanhamme, L., Poelvoorde, P., Pays, A., Tebabi, P., Van Xong, H., and Pays, E. (2000). Differential RNA elongation controls the variant surface glycoprotein gene expression sites of Trypanosoma brucei. Mol Microbiol *36*, 328-340.

Vickerman, K. (1965). Polymorphism and mitochondrial activity in sleeping sickness trypanosomes. Nature *208*, 762-766.

Vickerman, K. (1969). On the surface coat and flagellar adhesion in trypanosomes. J Cell Sci *5*, 163-193.

Viitanen, P.V., Gatenby, A.A., and Lorimer, G.H. (1992). Purified chaperonin 60 (groEL) interacts with the nonnative states of a multitude of Escherichia coli proteins. Protein Sci *1*, 363-369

Voorheis, H.P., Gale, J.S., Owen, M.J., and Edwards, W. (1979). The isolation and partial characterization of the plasma membrane from Trypanosoma brucei. Biochem J *180*, 11-24.

Voorheis, H.P., Bowles, D.J., and Smith, G.A. (1982). Characteristics of the release of the surface coat protein from bloodstream forms of Trypanosoma brucei. J Biol Chem *257*, 2300-2304.

Webb, H., Carnall, N., Vanhamme, L., Rolin, S., Van Den Abbeele, J., Welburn, S., Pays, E., and Carrington, M. (1997). The GPI-phospholipase C of Trypanosoma brucei is nonessential but influences parasitemia in mice. J Cell Biol *139*, 103-114.

Webster, P., and Grab, D.J. (1988). Intracellular colocalization of variant surface glycoprotein and transferrin-gold in Trypanosoma brucei. J Cell Biol *106*, 279-288.

Webster, P., Russo, D.C., and Black, S.J. (1990). The interaction of Trypanosoma brucei with antibodies to variant surface glycoproteins. J Cell Sci *96 (Pt 2)*, 249-255.

Woods, A., Sherwin, T., Sasse, R., MacRae, T.H., Baines, A.J., and Gull, K. (1989). Definition of individual components within the cytoskeleton of Trypanosoma brucei by a library of monoclonal antibodies. J Cell Sci *93 (Pt 3)*, 491-500.

Wu, Y., Deford, J., Benjamin, R., Lee, M.G., and Ruben, L. (1994). The gene family of EF-hand calcium-binding proteins from the flagellum of Trypanosoma brucei. Biochem J *304* (*Pt 3*), 833-841.

Ziegelbauer, K., and Overath, P. (1990). Surface antigen change during differentiation of Trypanosoma brucei. Biochem Soc Trans *18*, 731-733.

Ziegelbauer, K., Stahl, B., Karas, M., Stierhof, Y.D., and Overath, P. (1993). Proteolytic release of cell surface proteins during differentiation of Trypanosoma brucei. Biochemistry *32*, 3737-3742.